National Laboratory for Scientific Computing

Computational Modeling Graduate Program

Numerical solution of inverse problems in computational neuroscience models

Jemy Alex Mandujano Valle

Petrópolis, RJ - Brazil

June, 2019

Jemy Alex Mandujano Valle

Numerical solution of inverse problems in computational neuroscience models

Thesis submitted to the examining committee in partial fulfillment of the requirements for the degree of Doctor of Sciences in Computational Modeling.

National Laboratory for Scientific Computing

Computational Modeling Graduate Program

Advisors: Alexandre Loureiro Madureira and Antonio Gardel Leitão

Petrópolis, RJ - Brazil

June, 2019

XXXX

Mandujano Valle, Jemy Alex
Numerical solution of inverse problems in computational neuroscience models / Jemy Alex Mandujano Valle. – Petrópolis, RJ - Brazil, June, 2019-
186 p. : il. ; 30 cm.

Advisors: Alexandre Loureiro Madureira and Antonio Gardel Leitão

Thesis (D.Sc.) – National Laboratory for Scientific Computing
Computational Modeling Graduate Program, June, 2019.

1. Passive Cable Model. 2. Hodgkin-Huxley Model. 3. Inverse Problems. 4. Iterative Regularization Methods. 5. Finite Difference Methods. I. Loureiro Madureira, Alexandre. II. LNCC/MCTIC. III. Title

CDD: XXX.XXX

Jemy Alex Mandujano Valle

Numerical solution of inverse problems in computational neuroscience models

Thesis submitted to the examining committee in partial fulfillment of the requirements for the degree of Doctor of Sciences in Computational Modeling.

Approved by:

Prof. Alexandre Loureiro Madureira, Ph.D.
(President)

Prof. Antonio Carlos Roque da Silva Filho, D.Sc.

Prof. Antônio André Novotny, D.Sc.

Prof. Roseli Suzi Wedemann, D.Sc.

Petrópolis, RJ - Brazil
June, 2019

Dedication

To my family and
Yeny Luz.

Acknowledgements

This thesis is a result of four years of hard work, that could not have been done without the support, guidance, patience, and dedication of the following people. I owe my deepest gratitude to them.

First and foremost, I would like to express my gratitude to God for his guidance and for having made everything possible.

I want to thank my academic teacher and advisor Alexandre L. Madureira, for the confidence in accepting to participate in this challenging project and for kindly receiving me as part of his research group, always finding time for discussions. I thank him for his attention, guidance and advice about my work and scientific career. Thank you for your fundamental role especially in my doctoral work. I express here my gratitude to my co-advisor Antonio Leitão as well.

I also would like to thank my family: Jhoel, Ana, Jhon, Abel, Rosy, Gaby, Estela, and my nephews, for their unconditional love, affection, and support.

I especially thank Yeny Luz, my partner, my friend, my love, my future wife. She supported me in innumerable ways and was always there throughout all the ups and downs of my doctoral journey.

Thanks to all the colleagues that, in a way or other, contributed to the making of this work and also to all my friends in and outside of LNCC.

“Mathematics is the alphabet with which God has written the universe.”
(Galileo Galilei)

Resumo

Nesta tese, estudamos três modelos matemáticos em neurociência computacional. Um modelo matemático para a iniciação e propagação de um potencial de ação em um neurônio foi nomeado após seus criadores em 1952. Desde então, o modelo Hodgkin-Huxley (H-H), ou modelo baseado em condutância, tem sido amplamente usado no mundo da fisiologia. Um sistema de quatro equações diferenciais ordinárias não-lineares acopladas, como o modelo H-H, é geralmente difícil de analisar. Nesse contexto, alguns novos modelos desenvolvidos parecem satisfatoriamente reduzi-lo de quatro para três ou duas equações diferenciais. Um dos modelos reduzidos, com um sistema de duas equações diferenciais ordinárias não-lineares acopladas, é o modelo FitzHugh-Nagumo (F-N).

Por outro lado, na matemática, é mais fácil trabalhar com equações diferenciais lineares do que com equações não lineares (modelos H-H e F-N). Por essa razão, iniciamos nossa pesquisa com a equação de cabo, uma equação diferencial parcial linear que descreve a voltagem em um cabo cilíndrico reto. Este modelo foi aplicado para modelar o potencial elétrico em dendritos e axônios. No entanto, às vezes, essa equação pode resultar em previsões incorretas para algumas geometrias realistas, especialmente quando o raio do cabo muda significativamente.

O principal objetivo deste trabalho foi, então, estimar parâmetros nos modelos mencionados anteriormente, dada a medição do potencial de membrana (problemas inversos). Para resolver os problemas inversos, consideramos os métodos de regularização iterativos, como o método de Landweber e o método de erro mínimo. Calculamos a adjunta da derivada de Gâteaux usando diferentes abordagens para cada um dos nossos problemas. Além disso, implementamos numericamente os métodos para mostrar sua eficiência, usando os métodos numéricos Euler explícito e Euler implícito.

Em seguida, descrevemos nossos problemas inversos. Na equação de cabo, determinamos condutâncias aproximadas com distribuição não uniforme, tanto em uma única ramificação quanto em uma árvore. Para obter os parâmetros desconhecidos na equação de cabo, usamos a iteração Landweber. Aplicamos o método de erro mínimo para encontrar uma função desconhecida aproximada no modelo FitzHugh-Nagumo. No modelo de Hodgkin-Huxley, estimamos as condutâncias máximas (três constantes), o número de partículas de ativação e inativação nos canais iônicos (três constantes) e também os parâmetros com distribuição não uniforme. Usamos o método do erro mínimo novamente, na equação H-H, para aproximar os parâmetros desconhecidos.

Palavras chaves: Modelo de Hodgkin-Huxley, Modelo FitzHugh–Nagumo, Equação do Cabo, Problema Inverso, Métodos de Regularização Iterativos.

Abstract

In this thesis, we studied three mathematical models in computational neuroscience. A mathematical model for the initiation and propagation of an action potential in a neuron was named after its creators in 1952. Since then, the Hodgkin-Huxley (H-H) model, or conductance-based model, has been used vastly in the world of physiology. A system of four coupled nonlinear ordinary differential equations, such as the H-H model is usually difficult to analyze. In this context, some new models developed appear to satisfactorily reduce it from four to three or two differential equations. One of the reduced models, with a system of two coupled nonlinear ordinary differential equations, is the FitzHugh–Nagumo (F-N) model.

On the other hand, in mathematics, it is easier to work with linear differential equations than with nonlinear equations (H-H and F-N models). For this reason, we begin our research with the cable equation, one linear partial differential equation that describes the voltage in a straight cylindrical cable. This model has been applied to model the electrical potential in dendrites and axons. However, sometimes this equation might result in incorrect predictions for some realistic geometries, in particular when the radius of the cable changes significantly.

The main goal of this work was then to estimate parameters in the previously mentioned models, given the membrane potential measurement (inverse problems). To solve the inverse problems we consider iterative regularization methods, as the Landweber and the minimal error methods. We compute the adjoint of the Gateaux derivative using different approaches for each one of our problems. Also, we numerically implement the methods in order to show their efficiency, using the forward Euler and backward Euler numerical methods.

Next, we describe our inverse problems. In the cable equation, we determine approximate conductances with non-uniform distribution, both in a single branch and in a tree. To obtain the unknown parameters in the cable equation we used the Landweber iteration. We apply the minimal error method to find an approximate unknown function in the FitzHugh-Nagumo model. In the Hodgkin-Huxley model, we estimate the maximal conductances (three constants), the number of activation and inactivation particles in the ion channels (three constants), and also parameters with non-uniform distribution. We use the minimal error method again, in the H-H equation, to approximate the unknown parameters.

Keywords: Hodgkin-Huxley Model, FitzHugh–Nagumo Model, Cable Equation, Inverse Problem, Iterative Regularization Methods.

List of Figures

List of Tables

Contents

1 Introduction

In this introductory chapter, we present the general aspects of the thesis, starting with the motivation and basic concepts of physiology. Next, we describe the mathematical models used in the thesis, followed by the objectives and contributions of the work. The chapter concludes with a description of the thesis structure.

1.1 Motivation

Neurodegenerative disease results from the progressive loss of structure or function of neurons, including the death of neurons. Examples of neurodegenerative diseases are Multiple Sclerosis (MS), Amyotrophic Lateral Sclerosis (ALS), Parkinson Disease (PD) and Alzheimer Disease (AD). The causes of their appearance and how such degradation can affect body movements and brain functioning, causing dementia, are not yet known. These diseases affect millions of people worldwide and presently represent the most important medical and socioeconomic problems (Ramanan e Saykin (2013)).

Nowadays, as a result of increased life expectancy and population demographics changes, neurodegenerative diseases are becoming more common. Neurodegenerative disorders account for a significant and increasing portion of morbidity and mortality rates in the world and cause a high economic burden.

Globally, neurological disorders are responsible for about 4% of all deaths and about 5% of disability-adjusted life years attributable to noncommunicable disease. The diagnosis of a neurological disease can be devastating, and in most instances there is no cure. A recent editorial by the Lancet pointed out that neurological diseases remain neglected and ignored: 'unlike cancer, stroke, and diabetes, which all have strategies and clinical champions, degenerative disorders are heterogeneous and complex' (Pearce e Kromhout (2014)).

The diagnosis of these diseases is not easy, and healthcare costs related to diseases are projected to rise drastically in the near future. In this context, accurate diagnosis increases the chance of an effective treatment and reduced disability over time, consequently also reducing direct and indirect healthcare costs (Batista e Pereira (2017)).

One way to learn about how a disease works is to develop a model system that recapitulates the hallmark characteristics of the disease. Powerful experimental model organisms such as the mouse, fruit fly, nematode worm, and even baker's yeast have been used for many years to study neurodegenerative diseases and have provided key insights into such disease mechanisms.

The need for improvements in the identification, understanding and treatment of neurodegenerative diseases is therefore of utmost importance. This serves as a motivation for the countless researches whose focus is the neuron, as in the present work.

1.2 Basic concepts of physiology

To motivate and better contextualize the mathematical models developed, this section highlights the most important physiological concepts developed in the thesis.

1.2.1 The Neuron

The nervous system is a complex network of nerves and cells that carry messages between the brain and spinal cord to various parts of the body.

A neuron is a nerve cell that is the basic building block of the nervous system. Neurons are similar to other cells in the human body in a number of ways, but there is one key difference between neurons and other cells: neurons are specialized in transmitting information throughout the body.

These highly specialized cells are responsible for communicating information in both chemical and electrical forms. There are also several different types of neurons responsible for different tasks in the human body. According to Azevedo et al. (2009), there are about 86 billion neurons in the human nervous system, and each one has on the order of 1000-10,000 connections to other neurons. A nerve cell (see Figure 1) has four basic parts: the dendrites, the cell body (also called the "soma"), the axon and the axon terminal.

- Dendrites - Extensions from the neuron cell body that takes information to the cell body. Dendrites usually branch close to the cell body.
- Cell body (soma) - the part of the cell that contains the nucleus.
- Axon - the extension from the neuron cell body that takes information away from the cell body. One single axon projects out of each cell body.
- Axon terminal - the ending part of an axon that makes synaptic contact with another cell.

1.2.2 Membrane potential

The membrane separates the extracellular space, outside of the cell, from the cytosol inside the cell. The plasma membrane is the border between the interior and exterior of a

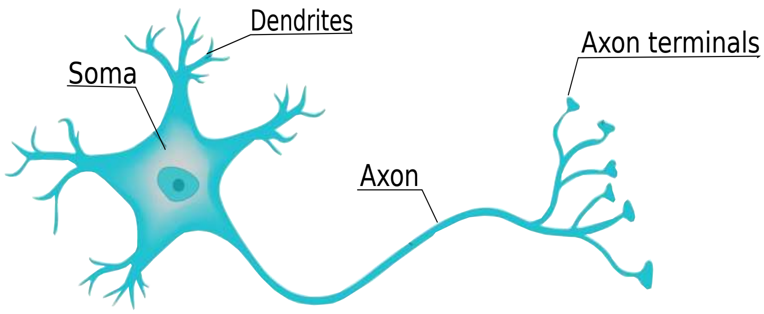

Figure 1 – Biological neuron. Adapted from link: Biological-neuron.

cell. The membrane potential (also voltage) is the difference in electric potential between the interior and the exterior of a biological cell, see Figure 2-A. The voltage (Ermentrout e Terman (2010)) is conventionally defined as

$$V = V_{\text{in}} - V_{\text{out}},$$

where V_{in} and V_{out} are the potentials inside and outside the cell, respectively.

A nerve impulse is an electrical signal that travels along an axon, see Figure 2-B. There is an electrical difference between the inside of the axon and its surroundings, like a tiny battery. When the nerve is activated, there is a sudden change in the voltage across the wall of the axon, caused by the movement of ions in and out of the neuron. This triggers a wave of electrical activity that passes from the cell body along the length of the axon to the synapse (Synapses are connections between neurons through which "information" flows from one neuron to another).

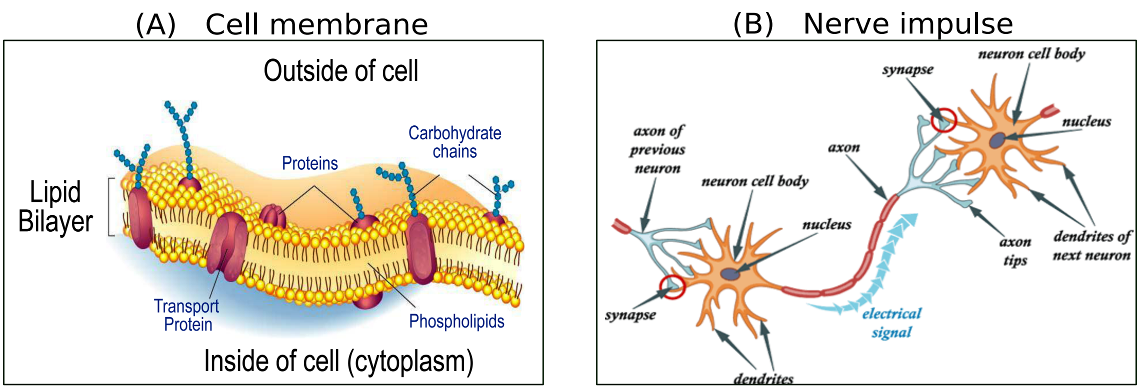

Figure 2 – Cell membrane and Nerve impulse. Adapted from links: Cell-Membrane and Nerve-Impulse, respectively.

The resting membrane potential, or simply the resting potential, refers to the potential across the membrane when the cell is at rest. A neuron at resting potential has a membrane with established amounts of sodium Na^+ and potassium K^+ ions on either side, leaving the inside of the neuron negatively charged relative to the outside. A typical neuron has a resting potential of about -70 mV.

An action potential occurs when the membrane potential of a specific cell location rapidly rises and falls. In order for a neuron to move from resting potential to action potential, the nerve cell must be stimulated by pressure, electricity, chemicals, or another form of stimuli. The level of stimulation that a neuron must receive to reach action potential is known as the threshold of excitation, and until it reaches that threshold, nothing will happen.

The action potential is characterized by three different steps: Depolarization, Repolarization and Hyperpolarization. These three steps are described below.

Step 1: Depolarization

A stimulus starts the depolarization of the membrane, and then sodium channels open in response to that stimulus. Na^+ rush into the cell through diffusion. The final potential difference is +30 mV.

Step 2: Repolarization

Na^+ channels close and K^+ channels open. K^+ rush out of the cell through diffusion. The potential difference is slightly below -70 mV.

Step 3: Hyperpolarization

The state of neuron in which more negative charge is developed inside the membrane is called Hyperpolarization. Sodium-Potassium exchange pump moves $Na+$ out and K^+ in. The potential difference is below $-70mV$.

In neuroscience, the threshold potential is the critical level to which a membrane potential must be depolarized in order to initiate an action potential. Threshold potentials are necessary to regulate and propagate signaling.

In Figure 3 we show the resting and action potentials. Number one is the resting potential, and numbers two, three and four represent the action potential.

1.3 Mathematical models in computational neuroscience

1.3.1 History of the Hodgkin–Huxley Equations

The initiation and propagation of electrical signals in nerves and other excitable tissues have fascinated physiologists for well over a century.

As early as 1902, the idea that the nervous impulse occurred as the result of a change in the permeability of the axonal membrane to ions was alive in the mainstream physiological literature. The German physiologist Julius Bernstein had proposed that K^+ ions were responsible for the resting potential of nerve and muscle cells and that during

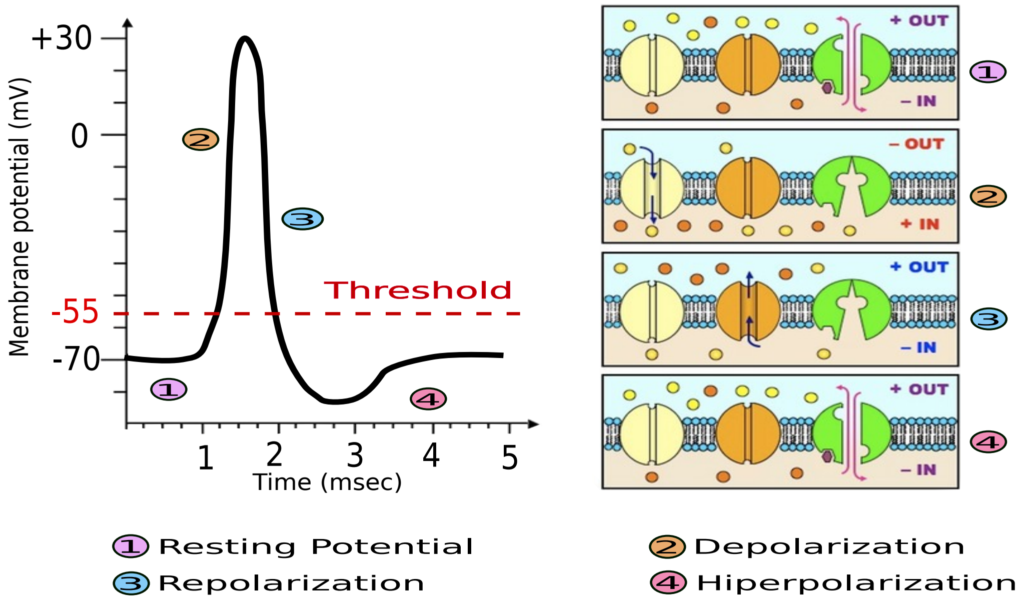

Figure 3 – Resting and action potentials. Adapted from link: Action-potential.

(what we would now call) an action potential, the membrane increased in permeability to other ions (Bernstein (1902), Bernstein (2013)). Bernstein was also the first to apply the Nernst equation to the problem of evaluating the resting potential across an excitable cell membrane, the generalization of which we now know as the Goldman-Hodgkin-Katz equation.

In 1907, the French physiologist Louis Lapicque investigated one of the earliest models of a neuron (integrate-and-fire model): as the inward current is applied to a neuron, the membrane voltage increases with time until it reaches the threshold voltage (Lapicque (1907)).

In 1939, Howard Curtis and Kenneth Cole managed to prove Bernstein's hypothesis. They applied both experimental and analytic techniques to measure the electrical properties of cell membranes (Cole e Curtis (1939)).

During his postdoctoral year in the U.S. in 1937-1938, Hodgkin established connections with Cole's group at Columbia and learned how to dissect squid axons. He returned to Cambridge in 1938 and in the following year started a collaboration with A. F. Huxley, (Keener e Sneyd (2009)).

Between 1946 and 1952, Hodgkin and Huxley, initially in collaboration with Bernard Katz, set about using the newly developed voltage-clamp technique to dissect the basis of the changes in selective permeability that occur during the propagation of action potentials in the squid giant axon. The goal was to determine the laws that govern the movement of ions in a nerve cell during an action potential. This culminated in the publication of five seminal papers in the Journal of Physiology in 1952, (Vandenberg e Waxman (2012)). The first paper examined the measurement of current-voltage relationships in the giant squid axon membrane (Hodgkin, Huxley e Katz (1952)). The second paper described the basic characteristics of the currents carried by sodium and potassium ions (Hodgkin e Huxley (1952a)). The third paper examined the effect of varying the time and duration of depolarization and repolarization steps on the different components of the membrane current (Hodgkin e Huxley (1952b)). The fourth paper outlined how the inactivation process gradually reduces sodium permeability after undergoing the initial rise associated with depolarization (Hodgkin e Huxley (1952c)). Finally, the fifth paper (Hodgkin e Huxley (1952d)) put together all of the information from the previous articles and turned them into a mathematical model (see Equation (1.8)).

In 1963, the Nobel Prize in Physiology or Medicine was awarded to Hodgkin and Huxley for their groundbreaking research on the squid giant axon.

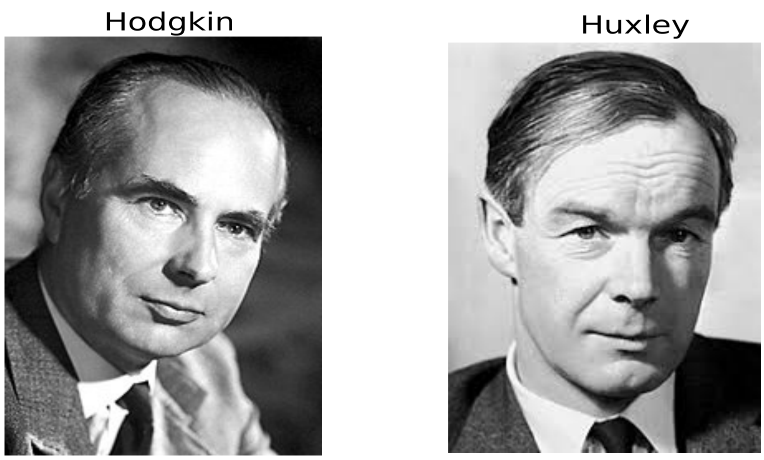

Figure 4 – Alan Lloyd Hodgkin and Andrew Fielding Huxley. Adapted from link: Hodgkin-Huxley.

1.3.2 The Hodgkin–Huxley Model

One of the most important models in computational neuroscience is the Hodgkin-Huxley model. Next, we describe it and finalize this section with the Hodgkin-Huxley equation (1.8).

1. The results obtained by Hodgkin-Huxley suggest (see, for example, table 1 from Hodgkin, Huxley e Katz (1952)) that the electrical behavior of the membrane may be represented by the network shown in Figure 5.

2. According to Kirchhoff's law, the total membrane current or external current I_{ext} is the sum of the capacitive current I_C and the ionic current I_{ion} (inward current positive). Thus

$$I_{\text{ext}} = I_C + I_{\text{ion}},$$

where

$$I_C = C_M \frac{\partial V}{\partial t},$$

the parameters C_M, t and $\partial V/\partial t$ are the membrane specific capacitance per unit area, the time and the derivative of the voltage with respect to time, respectively.

From the two equations above, we have

$$I_{\text{ext}} = C_M \frac{\partial V}{\partial t} + I_{\text{ion}}. \tag{1.1}$$

3. From Figure 5, the ionic current is the sum of three currents

$$I_{\text{ion}} = I_{Na} + I_K + I_L, \tag{1.2}$$

where I_{Na}, I_K and I_L are the potassium, sodium and leak ionic currents, respectively. The leak current consists mainly of Cl^- ions, and approximates the passive properties of the cell.

4. The sodium current (I_{Na}) is equal to the sodium conductance (g_{Na}) multiplied by the difference between the membrane potential (V) and the equilibrium potential (E_{Na}) for the sodium ion. Similar equations apply to the I_K and I_L currents (Hodgkin e Huxley (1952b)). Thus

$$I_{Na} = g_{Na}(V - E_{Na}), \quad I_K = g_K(V - E_K), \quad I_L = G_L(V - E_L), \tag{1.3}$$

where g_{Na}, g_K and G_L are the sodium, potassium and leak current conductances, respectively. The equilibrium potential of sodium, potassium and leak current is represented by E_{Na}, E_K and E_L, respectively. The experiments of Hodgkin and Huxley suggest that g_{Na} and g_K are functions of both time and potential membrane, but E_{Na}, E_K, E_L, C_M and G_L are constants (Hodgkin e Huxley (1952d)).

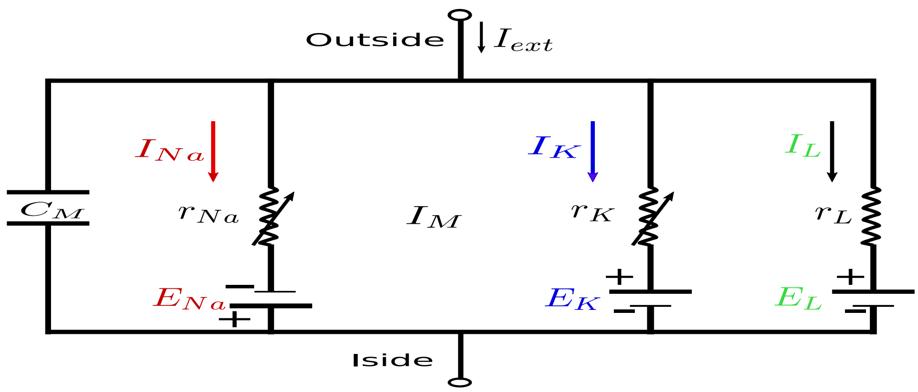

Figure 5 – Electrical circuit representing membrane. $r_{Na} = 1/g_{Na}$; $r_{Na} = 1/g_{Na}$; $r_L = 1/g_L$. r_{Na} and r_K vary with time and membrane potential; the other components are constant.

5. Using voltage-clamp data (see Figure 6), Hodgkin and Huxley derived expressions for K^+ and Na^+ conductances. They proposed that

$$g_{Na}(V,t) = G_{Na}n^4(V,t) \quad \text{and} \quad g_K = G_K m^3(V,t)h(V,t), \tag{1.4}$$

where G_{Na} and G_K are the maximal sodium and potassium conductances, respectively. The variable n describes the activation of the potassium channels, m describes the activation of the sodium channels, and h describes the inactivation of the sodium channels; these parameters take values between 0 and 1. The exponent of n signifies the number of gating particles on the channel. The exponents of m and h represent three activation gates and one inactivation gate, respectively (Gutkin, Pinto e Ermentrout (2003)).

In addition, m n and h satisfy the following differential equation:

$$\frac{\partial \mathcal{X}}{\partial t}(V,t) = \alpha_{\mathcal{X}}(V)(1-\mathcal{X}(V,t)) - \beta_{\mathcal{X}}(V)\mathcal{X}(V,t) \quad \text{where } \mathcal{X} = m,n,h. \tag{1.5}$$

The experiments performed by Hodgkin and Huxley suggest that:

$$\begin{aligned} \alpha_m(V) &= \frac{(25-V)/10}{\exp((25-V)/10)-1}, & \beta_m(V) &= 4\exp(-V/18), \\ \alpha_n(V) &= \frac{(10-V)/100}{\exp((10-V)/10)-1}, & \beta_n(V) &= 0.125\exp(-V/80), \\ \alpha_h(V) &= 0.07\exp(-V/20), & \beta_h(V) &= \frac{1}{\exp((30-V)/10)+1}. \end{aligned} \tag{1.6}$$

In this work, we add the following initial conditions to (1.1) and (1.5)

$$V(0) = V_0, \quad m(0) = m_0, \quad n(0) = n_0, \quad h(0) = h_0, \tag{1.7}$$

where the constants V_0, m_0, n_0 and h_0 are given data.

Then, from (1.1-1.7) we have the following ordinary differential equation (ODE):

$$\begin{cases} C_M \dfrac{\partial V}{\partial t} = I_{\text{ext}} - G_{Na}m^3h(V-E_{Na}) - G_K n^4(V-E_K) - G_L(V-E_L); \\ \dfrac{\partial m}{\partial t} = (1-m)\alpha_m(V) - m\beta_m(V); \\ \dfrac{\partial n}{\partial t} = (1-n)\alpha_n(V) - n\beta_n(V); \\ \dfrac{\partial h}{\partial t} = (1-h)\alpha_h(V) - h\beta_h(V); \\ V(0) = V_0, \quad m(0) = m_0, \quad n(0) = n_0, \quad h(0) = h_0. \end{cases} \tag{1.8}$$

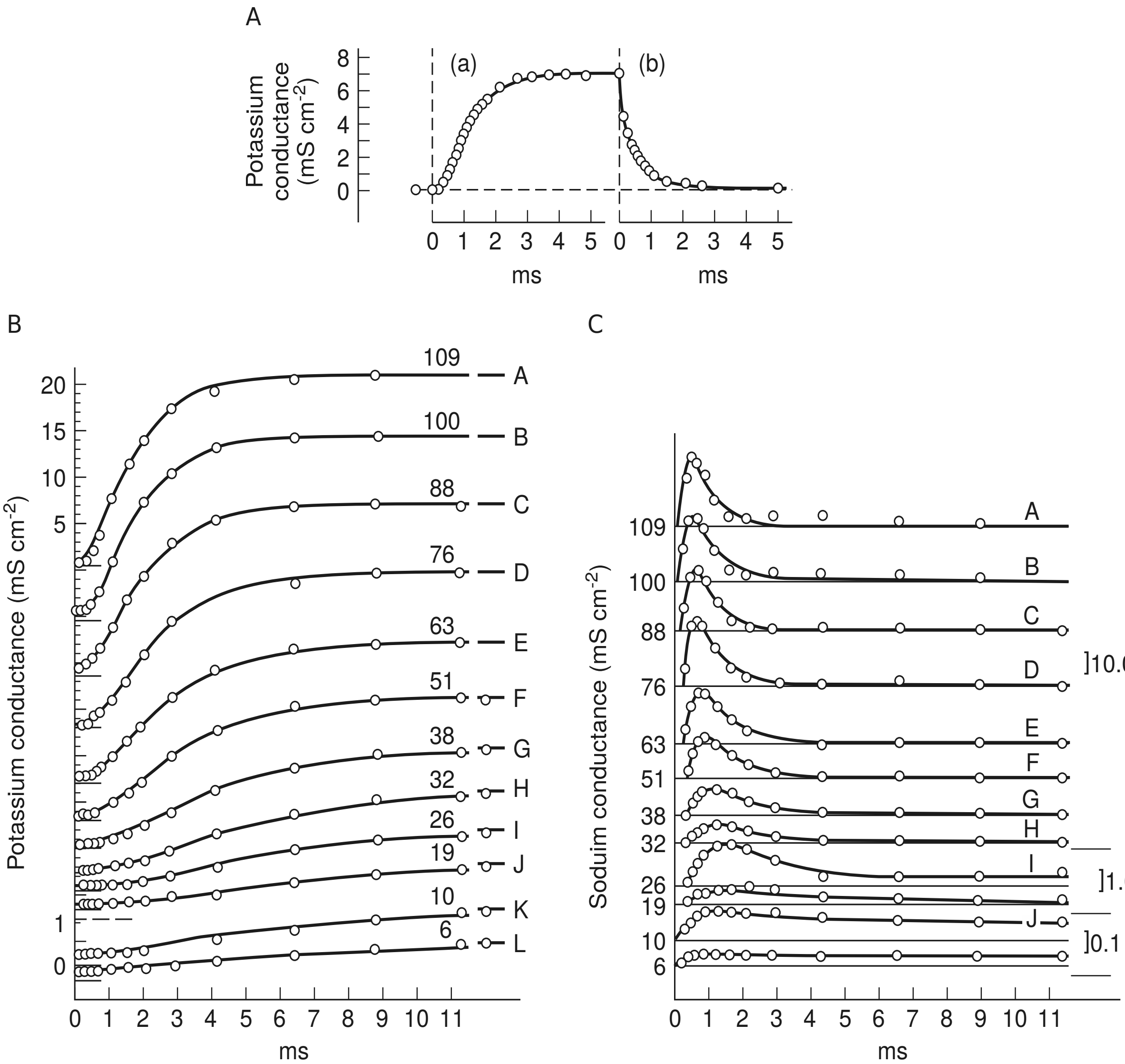

Figure 6 – Conductance changes as a function of time at different voltage clamps. A: The response of g_{K} to a step increase in V and then a step decrease. B: Responses of g_{K} to step increases in V of varying magnitudes. C: Responses of g_{Na} to step increases in V of magnitudes given by the numbers on the left, in mV. The smooth curves are the model solutions. Adapted from (Keener e Sneyd (2009)).

1.3.3 The FitzHugh-Nagumo Model

The four dimensional Hodgkin-Huxley equations are considered as the prototype for the description of neural pulse propagation. Their mathematical complexity and sophistication prompted the elaboration of a simplified two-dimensional model, the FitzHugh–Nagumo equations, which preserve many of the former's dynamical features. This model has been used to model many physiological systems from nerve to heart to muscle and is a favorite model for the study of excitability (Ermentrout e Terman (2010)).

The FitzHugh–Nagumo model has the form

$$\begin{cases} \dfrac{\partial V}{\partial t} = I + g(V) - \upsilon, \\ \dfrac{\partial \upsilon}{\partial t} = eV - f\upsilon, \end{cases} \tag{1.9}$$

where $g(V) = V(V-d)V$, V is the action potential, I is the stimulus current and υ is called recovery variable, which measures the cell excitability state (Phillipson e Schuster (2005)). The parameters d, e and f are dimensionless and positive. Note that, from (1.8), υ plays the role of all three variables m, n and h, also I plays the role of I_{ext}. In this Thesis, we add the initial conditions V_0 and υ_0. Thus, from (1.9) and the initial conditions we have

$$\begin{cases} \dfrac{\partial V}{\partial t} = I + g(V) - \upsilon, \\ \dfrac{\partial \upsilon}{\partial t} = eV - f\upsilon, \\ V(0) = V_0; \quad \upsilon(0) = \upsilon_0, \end{cases} \tag{1.10}$$

where the constants V_0 and υ_0 are given data.

Other choices for $g(V)$ include McKean model, for which

$$g(V) = H(V-d) - V,$$

where H is the Heaviside function (Keener e Sneyd (2009)). This choice is recommended because the model is piecewise linear, allowing explicit solutions for many interesting problems. Another example of piecewise linear model, also proposed by McKean, is

$$g(V) = \begin{cases} -V, & \text{for} \quad V < d/2 \\ V - d, & \text{for} \quad d/2 < V < (1+d)/2 \\ 1 - V, & \text{for} \quad V > (1+d)/2 \end{cases}$$

The FitzHugh–Nagumo equations can be derived from a simplified model of the cell membrane, Figure 7. Here, the cell consists of three components: a capacitor representing the membrane capacitance, a nonlinear current-voltage device for the fast current, and a resistor, inductor, and battery in series for the recovery current (see Keener e Sneyd (2009), pages 218-219).

1.3.4 The Cable Equation

We have discussed the effects of neurotransmitter-gated ion channels, leakage channels, and voltage-dependent ion channels on the membrane potential of a neuron. In order to get a comprehensive view of the state of a neuron, we must also include the conductance properties and the physical shape of the neuron. In contrast to axons with

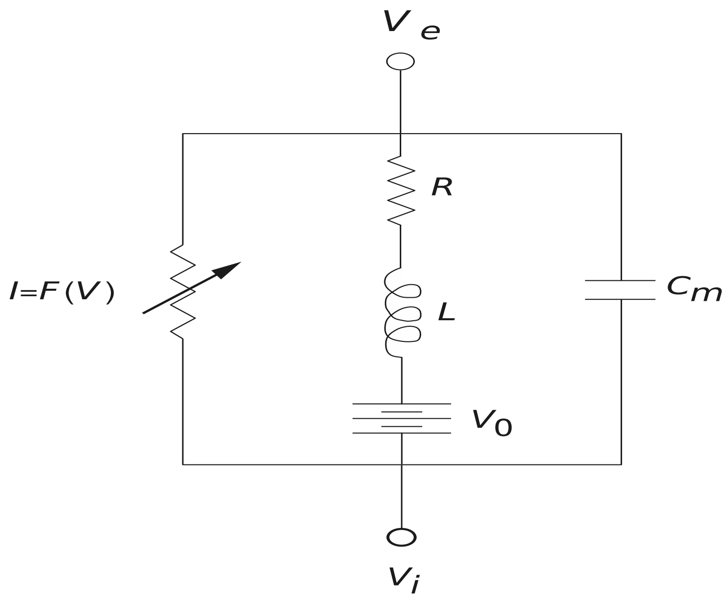

Figure 7 – Circuit diagram for the FitzHugh-Nagumo equations. Adapted from (Keener e Sneyd (2009)).

active membranes able to generate action potentials, dendrites have been seen historically more like passive conductors, analogous to long cables. The physics of conducting cables was worked out in the mid 19th century by Lord Kelvin, enabling the first transatlantic communication cables. Since then, many researchers have applied this theory to neural transmission. One example is Wilfrid Rall, who contributed to the theory and its applications (Trappenberg (2009)).

In the present subsection, we consider a cell shaped as a long cylinder, or cable, of radius a. We assume that the current flow is along a single spatial dimension, x, the distance along the cable. In particular, the membrane potential depends only on the x variable, not on the radial or angular components. The cable equation is a partial differential equation that describes how the membrane potential depends on currents entering, leaving, and flowing within the neuron. The equivalent circuit is shown in Figure 8. The cable equation is

$$C_M \frac{\partial V}{\partial t} = I_{\text{ext}} - I_{\text{ion}}, \tag{1.11}$$

while in Subsection 1.3.2 I_{ext} is a constant, in this Subsection

$$I_{\text{ext}} = \frac{1}{R_I + R_E} \frac{\partial^2 V}{\partial x^2}, \tag{1.12}$$

where R_I is the internal resistance, R_E is the external resistance and $\partial^2 V / \partial x^2$ second derivative of the voltage with respect to space.

In the squid giant axon, the ionic current I_{ion} is a function of m, n, h, and V as described in Subsection 1.3.2. This choice for I_{ion} allows waves that propagate along the axon at a constant speed and with a fixed profile. They require the input of energy from the axon, which must expend energy to maintain the necessary ionic concentrations, and thus they are often called active waves (Keener e Sneyd (2009)). For a passive cable and one ionic channel,

$$I_{\text{ion}} = G(V - E), \tag{1.13}$$

where G is the conductance and E is the equilibrium potential. There are some cables, primarily in neuronal dendritic networks, for which this is a good approximation in the range of normal activity. For other cells, activity is passive only if the membrane potential is sufficiently small.

From equations ((6.36)-(6.38)) we have the following partial differential equation (PDE)

$$C_M \frac{\partial V}{\partial t} = \frac{1}{R_I + R_E} \frac{\partial^2 V}{\partial x^2} - G(V - E). \tag{1.14}$$

To Equation (6.39) we add boundary and initial conditions given by

$$\frac{\partial V}{\partial x}(t, 0) = p(t), \qquad \frac{\partial V}{\partial x} V(t, L) = q(t), \qquad V(0, x) = r(x), \tag{1.15}$$

where the function p, q and r are given data. The time $t \in (0, T)$ and the space $x \in (0, L)$.

We next rewrite Equations (6.39) and (6.40) in a slightly more convenient form

$$\begin{cases} C_M \dfrac{\partial V}{\partial t} = \dfrac{1}{R_I + R_E} \dfrac{\partial^2 V}{\partial x^2} - G(V - E), \quad \text{for} \quad 0 < t < T,\, 0 < x < L, \\ V(0, x) = r(x) \quad \text{for} \;\; 0 < x < L, \\ \dfrac{\partial V}{\partial x}(t, 0) = p(t), \;\; \dfrac{\partial V}{\partial x}(t, L) = q(t) \quad \text{for} \quad 0 < t < T. \end{cases} \tag{1.16}$$

Madureira e Valle (2017) presents a mathematical modeling of the previous equation.

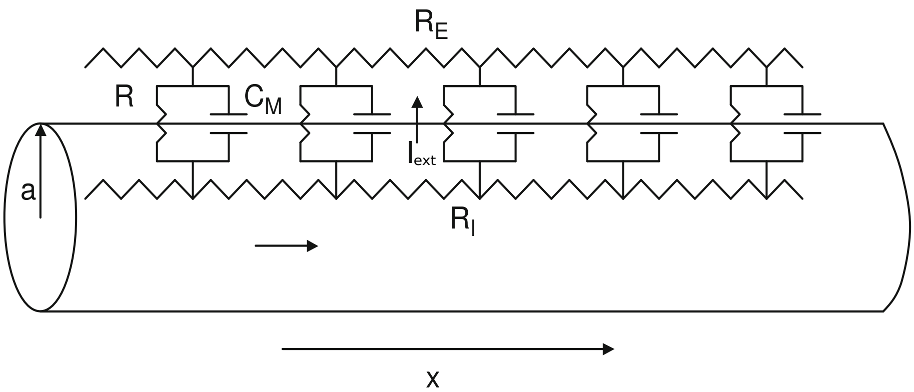

Figure 8 – Equivalent circuit for a uniform passive equation. I_{ext} is the current across the membrane, R_I is the internal resistance, R_E is the external resistance, and C_M is the membrane capacitance. Also, the resistance of the potassium channel is given by $R = 1/G$, where G is the conductance. In this figure we consider only one ionic channel. Adapted from (Ermentrout e Terman (2010)).

1.4 Objectives and contributions

In this work, we consider models (1.8), (1.10) and (6.41). We present now the objectives and contributions of this Thesis to these equations.

Objective

Given the measurement of membrane potential, this Thesis pursues three main goals: (i) to estimate unknown parameters in Hodgkin-Huxley model (ODE (1.8)); (ii) to obtain approximate values for unknown parameters in FitzHung-Nagumo model (ODE (1.10)); and (iii) to find approximate values for unknown parameters in cable equation (PDE (6.41)).

Naturally, the achievement of such objectives implies several activities and also specific goals, which are listed here:

1. Iterative regularization methods.

   Here we admit the existence of a single solution to the inverse problems. However, stability is not guaranteed. Stability is necessary if we want to ensure that small variations in the data lead to small changes in the solutions.

   To achieve our goals, the first step was to apply iterative regularization methods that controls the instability of the problems. With certain hypotheses and with a stopping criterion, the method guarantees an approximate solution to problem, and when the noise level is zero, the method converges to the exact solution. In this work, we utilize gradient-type methods which are iterative regularization methods.

2. Adjoint of the Gateaux derivative.

   The adjoint of the Gateaux derivative from the proposed methods are unknown. In all our problems, in a different way, we compute the unknown operator, this is one of our main results.

3. Numerical implementation.

   Another result of this work was the computational implementation, which was done through adequate and efficient numerical methods. The implementation was verified and validated through a series of known computational experiments and compared with literature data.

Contributions

During the preparation of this Thesis, relevant results were compiled in six manuscripts. Preliminary results were presented in the form of one poster, two articles in national and international conferences and three paper (two submitted for publication and one in preparation). Also, we presented five lecture: PROEX-LNCC 2016, CNMAC 2017, PROEX-LNCC 2017, CNMAC 2018 and PROEX-LNCC 2018.

1.5 Organization of work

This Thesis consists of a total of seven chapters that cover the multidisciplinary, mathematical and computational aspects considered in the work. Chapter 2 presents the concept of inverse problem, types of inverse problems and iterative regularization methods.

Chapter 3 describes the first paper. In this article, we tackle the inverse problem of determining approximately, given voltage measurement, conductances with non-uniform distribution in the simpler setting of a passive cable equation, both in a single branch and in a tree. To do so, we consider the Landweber iteration.

Chapter 4 presents the second paper. In this work, we consider two different inverse problems in Hodgkin and Huxley model. The first one is to estimate the maximum conductances G_{Na}, G_K and G_L. For the second problem, the goal is to obtain the exponents of the activation and inactivation variables a, b and c. To obtain the unknown parameters we apply the minimal error method.

Chapter 5 introduces the third paper. Here, we propose the minimal error method to estimate parameters with a non-uniform distribution in the FitzHugh-Nagumo and Hodgkin-Huxley models.

Chapter 6 describes the two articles presented at conferences. The three papers mentioned previously comprise inverse problems in continuous models. In these two articles, however, we determine parameters in discrete models. While the first work estimates unknown data in the discrete Hodgkin and Huxley model, the goal of the second work is to find approximate parameters in the discrete cable equation.

Finally, Chapter 7 presents the conclusions of this work, as well as some limitations and suggestions for future work.

2 About inverse problems

In this chapter, we describe the basic concepts of inverse problems. Also, we introduce the iterative methods of regularization for solving inverse problems. In particular, we have focused our attention on the methods of minimal error and Landweber, particular cases of the gradient method.

2.1 Basic concepts of inverse problem

There are several definitions for inverse problems. One definition can be stressed as: “Solving an inverse problem is to determine unknown causes from observed or desired effects” (Engl, Hanke e Neubauer (1996)). Direct problems have been studied extensively for some time, while inverse problems are more recent and not so well understood.

When studying Inverse Problems, there is an important definition which was introduced by Hadamard (2014):

Definition 2.1. *A problem is well-posed, in the Hadamard's sense, if the three following conditions are satisfied:*

1. *There exists a solution of the problem (existence)*
2. *There is at most one solution of the problem (uniqueness).*
3. *The solution depends continuously on the data (stability).*

If a problem does not satisfy any of the three above conditions, then it is an ill-posed problem. Inverse problems are typically ill-posed.

In this thesis, we admit the existence of a single solution to the problems. However, stability is not guaranteed. Stability is necessary if we want to ensure that small variations in the data lead to small changes in the solution. Then, our problems are ill-posed.

Let us give a mathematical description of the input, the output and the systems in functional analytic terms.

X : space of input quantities;

Y : space of output quantities;

F : operator from X into Y.

The operator F from a set X to a set Y is defined by $F(x) = y$.

- **The direct problem.** Given $x \in X$ (and F), find

$$y := F(x)$$

- **The inverse problem.** Given $y \in Y$ (and F), find

$$x \in X \quad \text{such that} \quad F(x) = y;$$

2.2 Iterative regularization methods

We consider the problem of determining some physical quantity x from data y, which are functionally related by

$$F(x) = y, \tag{2.1}$$

where $F : D(F) \subset X \to Y$ is a nonlinear operator between Hilbert spaces X and Y. The norms in X and Y will be denoted by $\|\cdot\|_X$ and $\|\cdot\|_Y$, respectively.

We are specially interested in the situation where the data is not exactly known, i.e., we have only an approximation y^δ of the exact data y, satisfying

$$\|y^\delta - y\|_Y \leq \delta, \tag{2.2}$$

where $\delta > 0$ is the noise level (assumed here to be known). Thus, the abstract formulation of the inverse problems (See figure 9) under consideration is to find x such that

$$F(x) = y^\delta. \tag{2.3}$$

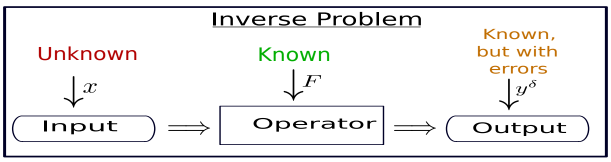

Figure 9 – Inverse problem.

Standard methods for obtaining stable solutions of the operator equation in (2.3) can be divided in two major groups, namely, Iterative type regularization methods and Tikhonov type regularization methods (Leitão e Svaiter (2015)). Some of the iterative regularization methods are the gradient type methods, Newton type methods and their variants. In this thesis, we apply the gradient type methods, more specifically, the Landweber method and the minimal error method.

Before writing the iterations of the methods, we will define the concept of the Gateaux derivative.

Definition 2.2.1. *Let X and Y normed vector spaces (for example, Hilbert spaces), $D(F) \subset X$ is open, $x_0 \in D(F)$, and $F : D(F) \subset X \longrightarrow Y$. The operator $F'(x_0) : X \longrightarrow Y$ defined by*

$$F'(x_0)(\boldsymbol{\theta}) = \lim_{\lambda \to 0} \frac{F(x_0 + \lambda \boldsymbol{\theta}) - F(x_0)}{\lambda} \; ; \quad \forall \, \boldsymbol{\theta} \in X$$

is the Gateaux derivative of F at x_0.

Consider equation (2.3). The gradient type iteration is defined by

$$x^{k+1,\delta} = x^{k,\delta} + w^{k,\delta} F'(x^{k,\delta})^* \left(y^\delta - F(x^{k,\delta}) \right) + \alpha^k \left(x^{1,\delta} - x^{k,\delta} \right), \tag{2.4}$$

where $F'(x^{k,\delta})$ is the Gateaux derivative of F computed at $x^{k,\delta}$, and $F'(x^{k,\delta})^*$ is its adjoint. We denote an initial guess $x^{1,\delta} = x^1 \in D(F)$. The coefficients $w^{k,\delta}$ and α^k are chosen as:

i) Classical Landweber method

$w^{k,\delta} = 1$ and $\alpha^k = 0$.

ii) Modified Landweber method

$w^{k,\delta} = 1$ and $\alpha^k \in (0, 1/2)$.

iii) Steepest descent method

$$w^{k,\delta} = \frac{\| F'(x^{k,\delta})^* \left(y^\delta - F(x^{k,\delta}) \right) \|_Y^2}{\| F'(x^{k,\delta}) F'(x^{k,\delta})^* \left(y^\delta - F(x^{k,\delta}) \right) \|_X^2} \quad \text{and} \quad \alpha^k = 0.$$

iv) Minimal error method

$$w^{k,\delta} = \frac{\| y^\delta - F(x^{k,\delta}) \|_Y^2}{\| F'(x^{k,\delta})^* (y^\delta - F(x^{k,\delta})) \|_X^2} \quad \text{and} \quad \alpha^k = 0.$$

In addition to *i)*, *ii)*, *iii)* and *iv)* there are other gradient type methods, for example the Landweber-Kaczmarz iteration. If the iteration (2.4) is applied to exact data, i.e., using y instead of y^δ, then we write x^k and w^k instead of $x^{k,\delta}$ and $w^{k,\delta}$, respectively.

In the case of noisy data, the iteration procedure has to be combined with a stopping rule in order to act as a regularization method. We will employ the discrepancy principle, i.e., the iteration is stopped after $k_* = k_*(\delta, y^\delta)$ steps with

$$\| y^\delta - F(x^{k_*,\delta}) \|_Y \le \tau \delta < \| y^\delta - F(x^{k,\delta}) \|_Y, \quad 0 \le k < k_*, \tag{2.5}$$

where $\tau > 2$ (Kaltenbacher, Neubauer e Scherzer (2008)).

It is possible to show that, under certain conditions (we assume that is the case), $x^{k_*,\delta}$ converges to a solution of $F(x) = y$ as $\delta \to 0$; (Kaltenbacher, Neubauer e Scherzer (2008), Baumeister e Leitao (2005), Engl, Hanke e Neubauer (1996), Neubauer (2000)).

In this thesis, from equation (2.3), we used the classical Landweber method (i) or the minimal error method (iv) to obtain an approximation of x, given y^δ.

From equation (2.4), the operator $F'(x^{k,\delta})^*$ is unknown. One of the essential contributions of this thesis is to calculate the unknown operator.

3 Inverse problem in cable equation

The cable equation is a mathematical equation derived from a circuit model of the membrane and its intracellular and extracellular space to provide a quantitative description of current flow and voltage change both within and between neurons, allowing a quantitative and qualitative understanding of how neurons function (Jaeger e Jung (2015)).

In this chapter, we investigate the inverse problem of recovering conductances in the passive cable equation, both in a single branch and on a tree. To estimate the unknown parameters, we apply the Landweber method with the membrane potential measurement given.

Throughout the study on the estimation of conductances in the passive cable equation, we presented some preliminary results in the following conferences:

- XXXVI Congresso Nacional de Matemática Aplicada e Computacional (CNMAC-2016), complete work (Madureira e Mandujano (2017b)).
- X Encontro Acadêmico de Modelagem Computacional (EAMC-2017), complete work (Madureira e Mandujano (2017a)).
- Programa de Excelência Acadêmica (PROEX-LNCC-2016), presentation of work.
- Programa de Excelência Acadêmica (PROEX-LNCC-2017), presentation of work.

Moreover, we submitted an article for publication (Valle, Madureira e Leitão (2018)). The paper is shown in Appendix A, and here, we present a summary.

3.1 Inverse problem for a single branch

In this section, we consider that the spatial variable $\mathbf{x}$ is defined in a single branch, represented by the interval $[0, L]$. Moreover, we generalize equation (6.39) as

$$C_M \frac{\partial V}{\partial t} = \frac{1}{R_I + R_E} \frac{\partial^2 V}{\partial \mathbf{x}^2} - \sum_{i \in \text{Ion}} G_i(t, \mathbf{x}) \Big(V(t, \mathbf{x}) - E_i \Big) \quad \text{for } 0 < t < T,\ 0 < \mathbf{x} < L, \tag{3.1}$$

where $\text{Ion} = \{1, 2, \cdots, N_{\text{ion}}\}$ is the set of ions of the model, G_i is the conductance for the ion $i \in \text{Ion}$, E_i is the equilibrium potential for the ion $i \in I_{\text{ion}}$ and N_{ion} is the number of ions of the set Ion. Thus, from (6.40) and (3.1) we have the following passive cable model

$$\begin{cases} c\dfrac{\partial V}{\partial t}(t,\mathbf{x}) = \dfrac{\partial^2 V}{\partial \mathbf{x}^2}(t,\mathbf{x}) - \sum\limits_{i\in Ion} g_i(t,\mathbf{x})[V(t,\mathbf{x}) - E_i] \quad \text{for} \quad t\in(0,T), \mathbf{x}\in(0,L), \\ V(0,\mathbf{x}) = r(\mathbf{x}) \quad \text{for } \ 0<\mathbf{x}<L, \\ \dfrac{\partial V}{\partial \mathbf{x}}(t,0) = p(t), \quad \dfrac{\partial V}{\partial \mathbf{x}}(t,L) = q(t) \quad \text{for} \quad 0<t<T. \end{cases} \tag{3.2}$$

where $c = C_M(R_I + R_E)$ and $g_i(t,\mathbf{x}) = G_i(t,\mathbf{x})(R_I + R_E)$. The new unknown parameters g_i are unitless, but still positive. We assume that the constants c, E_i, T, and L, and the functions p, q and r are known parameters.

Let $\boldsymbol{g} = (g_1, g_2, \cdots, g_{N_{\text{ion}}})$ be the conductance of the set Ion, and $V|_\Gamma = \{V(t,\mathbf{x});\ \ (t,\mathbf{x}) \in \Gamma\}$ the membrane potential, where

$$\Gamma = [0,T]\times[0,L] = \{(t,\mathbf{x}),\ t\in[0,T] \text{ and } x\in[0,L]\}, \tag{3.3}$$

or

$$\Gamma = [0,T]\times\{0,L\} = \{(t,\mathbf{x}),\ t\in[0,T] \text{ and } x\in\{0,L\}\}. \tag{3.4}$$

We assume that the membrane potential $V|_\Gamma : \Gamma \to \mathbb{R}$ is unknown, but its measurement $V^\delta|_\Gamma$ is known.

Consider the nonlinear operator

$$F : \Big(L^2\left([0,T]\times[0,L]\right)\Big)^{N_{\text{ion}}} \longrightarrow L^2(\Gamma), \tag{3.5}$$

defined by $F(\boldsymbol{g}) = V|_\Gamma$, where V solves (3.2). We consider the inverse problem of finding an approximation for $\boldsymbol{g}$ given the noisy data $V^\delta|_\Gamma$.

From iteration (2.4), for $x = \boldsymbol{g}$, $w^{k,\delta} = 1$ and $\alpha^k = 0$, we have

$$\boldsymbol{g}^{k+1,\delta} = \boldsymbol{g}^{k,\delta} + F'(\boldsymbol{g}^{k,\delta})^*(V^\delta|_\Gamma - F(\boldsymbol{g}^{k,\delta})). \tag{3.6}$$

Computing the adjoint of the Gateaux derivative $F'(\boldsymbol{g}^{k,\delta})^*$ (see Theorem 3.1.1), from previous iteration, we have

$$\boldsymbol{g}^{k+1,\delta} = \boldsymbol{g}^{k,\delta} - \Big((V^{k,\delta} - E_1)U^k, (V^{k,\delta} - E_2)U^k, \cdots, (V^{k,\delta} - E_{N_{\text{ion}}})U^k\Big), \tag{3.7}$$

where $V^{k,\delta}$ solves equation (3.2) replacing $\boldsymbol{g}$ by $\boldsymbol{g}^{k,\delta}$, and U^k solves equation (3.8).

To obtain an approximation for $\boldsymbol{g}$, given an initial guess $\boldsymbol{g}^{1,\delta}$, we used the Landweber iteration (3.7).

In the next Theorem, we compute the adjoint of the Gateaux derivative.

Theorem 3.1.1. *Consider the nonlinear operator F defined in (3.5) and iteration (3.6). Then,*

$$F'(\boldsymbol{g}^{k,\delta})^*(V^\delta|_\Gamma - F(\boldsymbol{g}^{k,\delta})) = -\Big((V^{k,\delta} - E_1)U^k, (V^{k,\delta} - E_2)U^k, \cdots, (V^{k,\delta} - E_{N_{ion}})U^k\Big),$$

where $V^{k,\delta}$ *solves* (3.2)*, given* $\boldsymbol{g} = \boldsymbol{g}^{k,\delta}$*. Finally, given* $\boldsymbol{g}^{k,\delta}$ *and* $V^{k,\delta}$*, the parameter* U^k *solves*

$$\begin{cases} -\dfrac{\partial^2 U^k}{\partial \mathbf{x}^2}(t,\mathbf{x}) - c\dfrac{\partial U^k}{\partial t}(t,\mathbf{x}) + \sum\limits_{i\in Ion} g_i^{k,\delta}(t,\mathbf{x})U^k(t,\mathbf{x}) = \\ \qquad\qquad\qquad\qquad \alpha_1\left(V^\delta(t,\mathbf{x}) - V^{k,\delta}(t,\mathbf{x})\right), \\ U^k(T,\mathbf{x}) = 0, \quad 0 < \mathbf{x} < L, \\ \dfrac{\partial U^k}{\partial \mathbf{x}}(t,0) = -\alpha_2\left(V^\delta(t,0) - V^{k,\delta}(t,0)\right), \quad 0 < t < T, \\ \dfrac{\partial U^k}{\partial \mathbf{x}}(t,L) = \alpha_2\left(V^\delta(t,L) - V^{k,\delta}(t,L)\right), \quad 0 < t < T. \end{cases} \tag{3.8}$$

The constants α_1*,* α_2 *depend on the set* Γ *as follows:*

$$(\alpha_1, \alpha_2) = \begin{cases} (1,0) & \text{if} \quad \Gamma = [0,T]\times[0,L], \\ (0,1) & \text{if} \quad \Gamma = [0,T]\times\{0,L\}. \end{cases} \tag{3.9}$$

Proof. See Section 3.4. ∎

We next describe the computational scheme.

Data: $V^\delta|_\Gamma$, δ, τ.
Result: Compute an approximation for $\boldsymbol{g}$ using Landweber Iteration Scheme
Choose $\boldsymbol{g}^{1,\delta}$ as an initial approximation for $\boldsymbol{g}$;
Compute $V^{1,\delta}$ from equation (3.2), replacing $\boldsymbol{g}$ by $\boldsymbol{g}^{1,\delta}$;
k=1;
while $\tau\delta \leq \|V^\delta - V^{k,\delta}\|_{L^2(\Gamma)}$ **do**
  Compute U^k from Eq. (3.8);
  Compute $\boldsymbol{g}^{k+1,\delta}$ using Eq. (3.7);
  Compute $V^{k+1,\delta}$ from Eq. (3.2), replacing $\boldsymbol{g}$ by $\boldsymbol{g}^{k+1,\delta}$;
  $k \leftarrow k+1$;
end

Algorithm 1: Landweber iteration to obtain conductances defined in a single branch.

3.2 Inverse problem for a tree

In this case, the spatial variable "$\mathbf{x}$" is defined on a tree. We consider that the tree has three edges(branches), the general case where the tree has more of three edges is in Appendix A.

Let $\mathbf{x} \in \Theta = \mathcal{E} \cup \mathcal{V}$, where $\mathcal{E} = \{e_1, e_2, e_3\}$ is a set of edges, and $\mathcal{V} = \{\nu_1, \nu_2, \nu_3, \nu_4\}$ is a set of vertices, and the edges are connected at the vertices ν_j. The points ν_1, ν_3 and ν_4 are boundary vertices, and ν_2 is the bifurcation point, see Figure 10.

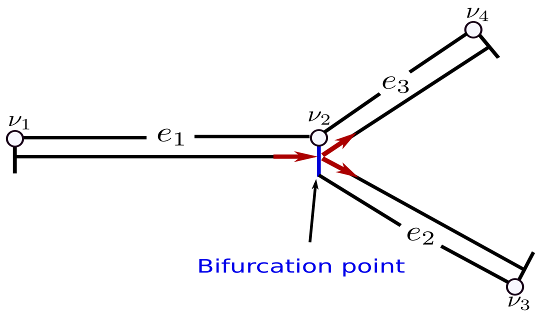

Figure 10 – Tree with three branches.

We denote $\partial V_{e_j}(t,\nu_2)/\partial \mathbf{x}$ as the derivative of V at the vertex ν_2, taken along the edge e_j in the direction towards the vertex. Our cable equation model defined on a tree with three branches is given by

$$\begin{cases} c\dfrac{\partial V}{\partial t}(t,\mathbf{x}) = \dfrac{\partial^2 V}{\partial \mathbf{x}^2}(t,\mathbf{x}) - \displaystyle\sum_{i\in Ion} g_i(t,\mathbf{x})\left[V(t,\mathbf{x}) - E_i\right], \qquad \text{in} \quad (0,T)\times\mathcal{E}, \\ V(0,\mathbf{x}) = r(\mathbf{x}), \qquad \text{in } \mathbf{x}\in\Theta, \\ \dfrac{\partial V}{\partial \mathbf{x}}(t,\nu_1) = f_1(t), \quad \dfrac{\partial V}{\partial \mathbf{x}}(t,\nu_3) = f_3(t), \quad \dfrac{\partial V}{\partial \mathbf{x}}(t,\nu_4) = f_4(t), \qquad t\in[0,T], \\ \dfrac{\partial V_{e_1}}{\partial \mathbf{x}}(t,\nu_2) - \dfrac{\partial V_{e_2}}{\partial \mathbf{x}}(t,\nu_2) - \dfrac{\partial V_{e_3}}{\partial \mathbf{x}}(t,\nu_2) = 0, \qquad t\in[0,T]. \end{cases} \tag{3.10}$$

Let

$$\Omega = (0,T)\times\Theta, \tag{3.11}$$

and define the nonlinear operator

$$F : \left(L^2(\Omega)\right)^{N_{\text{ion}}} \longrightarrow L^2(\Omega)$$

such that $F(\boldsymbol{g}) = V(\cdot,\cdot)$, where V solves Equation (3.10) and $\boldsymbol{g} = (g_1, g_2, \cdots, g_{N_{\text{ion}}})$. From (3.10), our goal is to estimate $\boldsymbol{g}$, given V^δ.

Here, we also compute the adjoint of the Gateaux derivative, from (3.6), and we obtain the iteration (3.7), where $V^{k,\delta}$ solves (3.10) replacing $\boldsymbol{g}$ by $\boldsymbol{g}^{k,\delta}$, and U^k solves the following PDE

$$\begin{cases} -\dfrac{\partial^2 U^k}{\partial x^2}(t,\mathbf{x}) - c\dfrac{\partial U^k}{\partial t}(t,\mathbf{x}) + \sum\limits_{i\in \text{Ion}} g_i^{k,\delta}(t,\mathbf{x})U^k(t,\mathbf{x}) \\ \qquad\qquad = V^\delta(t,\mathbf{x}) - V^{k,\delta}(t,\mathbf{x}), \quad (t,\mathbf{x}) \in (0,T)\times\mathcal{E}, \\ U^k(T,\mathbf{x}) = 0, \quad \text{in } x \in \Theta, \\ \dfrac{\partial U^k}{\partial \mathbf{x}}(t,\nu_1) = 0, \quad \dfrac{\partial U^k}{\partial \mathbf{x}}(t,\nu_3) = 0, \quad \dfrac{\partial U^k}{\partial \mathbf{x}}(t,\nu_4) = 0, \qquad t\in[0,T], \\ \dfrac{\partial U_{e_1}}{\partial \mathbf{x}}(t,\nu_2) - \dfrac{\partial U_{e_2}}{\partial \mathbf{x}}(t,\nu_2) - \dfrac{\partial U_{e_3}}{\partial \mathbf{x}}(t,\nu_2) = 0, \qquad t\in[0,T]. \end{cases} \tag{3.12}$$

To estimate $\boldsymbol{g}$, we apply the iteration (3.7), given $\boldsymbol{g}^{1,\delta}$.

We next describe the computational scheme.

Data: V^δ, δ, τ.
Result: Compute an approximation for $\boldsymbol{g}$ using Landweber Iteration Scheme
Choose $\boldsymbol{g}^{1,\delta}$ as an initial approximation for $\boldsymbol{g}$;
Compute $V^{1,\delta}$ from equation (3.10),replacing $\boldsymbol{g}$ by $\boldsymbol{g}^{1,\delta}$;
k=1;
while $\tau\delta \le \|V^\delta - V^{k,\delta}\|_{L^2(\Omega)}$ **do**
  Compute U^k from Eq. (3.12);
  Compute $\boldsymbol{g}^{k+1,\delta}$ using Eq. (3.7);
  Compute $V^{k+1,\delta}$ from Eq. (3.10), replacing $\boldsymbol{g}$ by $\boldsymbol{g}^{k+1,\delta}$;
  $k \leftarrow k+1$;
end
Algorithm 2: Landweber iteration to obtain conductances defined on a tree.

3.3 Numerical simulations

To design our numerical experiments, we first choose $\boldsymbol{g}$ and compute V from equation (3.2) or (3.10), then we calculate, given δ,

$$V^\delta(t,\mathbf{x}) = V(t,\mathbf{x}) + V(t,\mathbf{x})\text{rand}_\Delta(t,\mathbf{x}), \quad (t,\mathbf{x}) \in S, \tag{3.13}$$

where $S = \Gamma$ (see equation (3.3) or (3.4)) or $S = \Omega$ (see equation (3.11)). The uniformly distributed random variable,

$$\text{rand}_\Delta(t,\mathbf{x}) \in [-\Delta, \Delta]$$

where $\Delta = \delta/\|V\|_{L^2(S)}$. Next, given the initial guess $\boldsymbol{g}^{1,\delta}$, the data $V^\delta|_S$, and the noise threshold δ, we approximate $\boldsymbol{g}$ using either the Algorithm 1 or Algorithm 2. Note that $V^\delta|_S = \{V(t,\mathbf{x});\ (t,\mathbf{x}) \in S\}$.

In practice, after discretizing the equations and the unknown functions, only nodal values are known. Consider the space-time discretization $t_n = (n-1)T/(N-1)$ for $n = 1, 2\cdots, N$ and $\mathbf{x}_j = (j-1)L/(J-1)$ for $j = 1, 2\cdots, J$. Thus, the relative error introduced above relates to the *the mean absolute percentage error*

$$\text{Error}_k = \frac{1}{N_{\text{ion}}}\frac{T}{N}\frac{L}{J}\sum_{i\in\text{Ion}}\sum_{n=1}^{J}\sum_{j=1}^{N}\left|\frac{g_i(t_n,\mathbf{x}_j) - g_i^{k,\delta}(t_n,\mathbf{x}_j)}{g_i(t_n,\mathbf{x}_j)}\right| \times 100\%. \qquad (3.14)$$

In this Section, we present two numerical tests. In the first example the geometry is defined by a segment. In the second example, we consider the case where the geometry is defined by a tree.

Example 3.1. *Consider a particular instance from PDE (3.2), where $c = 1$ $[\Omega F/cm^2]$, $Ion = \{1\}$ $(N_{ion} = 1)$, $g_1 = \boldsymbol{g}$, $E_1 = 1$ $[mV]$, $L = 1$ $[cm]$, $T = 1$ $[ms]$, and*

$$r(\mathbf{x}) = \mathbf{x}/2, \qquad p(t) = \exp(t), \qquad q(t) = -\exp(-t).$$

In this test, we consider $\Gamma = [0,T]\times[0,L]$ and $N = J = 50$. The goal is to estimate

$$\boldsymbol{g}(t,\mathbf{x}) = \frac{1}{1+\exp(-15\mathbf{x}+4)} + t + 1,$$

given $V^\delta|_\Gamma$, $\boldsymbol{g}^{1,\delta}(t,\mathbf{x}) = 0$ and $\tau = 2.01$.

In Table 1 we present the results for various levels of noise. In Figures 11 and 12 we plot numerical results for $\Delta = 0.01\%$ (see Table 1, line 6)

Δ	k_*	Error_{k_*}	*Time (s)*
100%	1	100%	1×10^{-2}
10%	68	18%	5×10^{-1}
1%	532	7%	4×10^{0}
0.1%	6485	2%	52×10^{0}
0.01%	88340	0.7%	727×10^{0}

Table 1 – Numerical results for Example 3.1. The first column describes the noise level Δ, as in equation(3.13). The second column contains the number of iterations according to equation (2.5). The third column lists the error according to equation (3.14). Finally, The last column is the running time of the algorithm, in seconds.

Example 3.2. *We consider the domain defined by a tree with three branches, see Figure 10. The length of the edges are $|e_1| = 1$, $|e_2| = 1$ and $|e_3| = 3$, and the numerical values of the vertices are $\nu_1 = 0$, $\nu_2 = 1$, $\nu_3 = 2$ and $\nu_4 = 4$. The values for equation (3.10) are: $c = 5$ $[\Omega F/cm^2]$, $Ion = \{1\}$ $(N_{ion} = 1)$, $g_1(t,\mathbf{x}) = \boldsymbol{g}(\mathbf{x})$, $E_5 = 0$ $[mV]$, $T = 1$ $[ms]$, and the boundary conditions $f_1(t) = \exp(t)$, $f_2(t) = t$ and $f_3(t) = \sin(t)$. For a point $x \in \Theta$ we define the initial condition $V(0,\mathbf{x}) = r(\mathbf{x}) = 0$.*

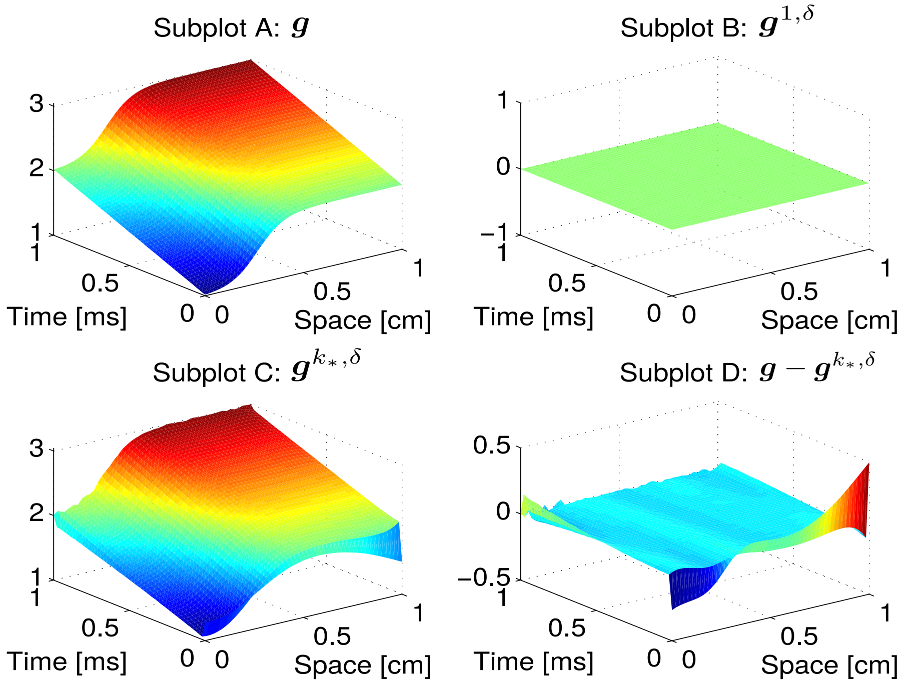

Figure 11 – Plots for Example 3.1. Subplots A, B and C are the exact solution, the initial guess, and the approximate solution for $\Delta = 0.01\%$, respectively. Finally, in D we display the difference between $\boldsymbol{g}$ and its approximation $\boldsymbol{g}^{k_*,\delta}$.

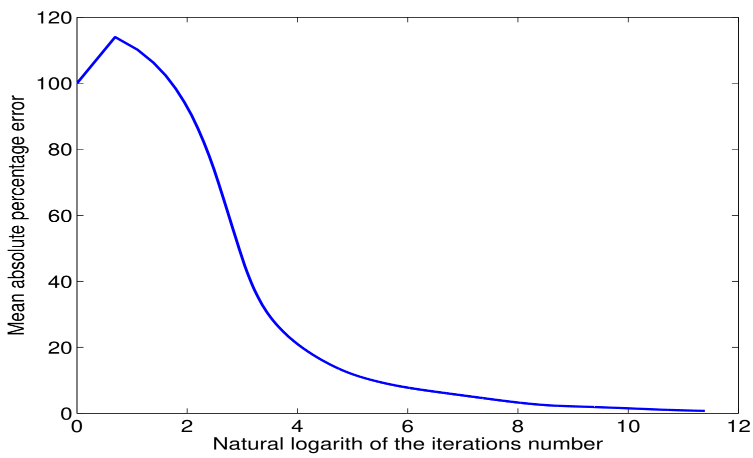

Figure 12 – Convergence results for Example 3.1. This figure shows the mean absolute percentage error between $\boldsymbol{g}$ and $\boldsymbol{g}^{k,\delta}$ as a function of the iteration k according to (3.14).

Given $V^\delta(t, \mathbf{x})$, the goal of this example is to estimate

$$\boldsymbol{g}(\mathbf{x}) = \begin{cases} \dfrac{1}{1 + \exp(-3\,\mathrm{dist}(\mathbf{x}, \nu_1) + 4)} & \text{if } \mathbf{x} \in e_1, \\ \dfrac{1}{1 + \exp(-3\,\mathrm{dist}(\mathbf{x}, \nu_2) + 1)} & \text{if } \mathbf{x} \in e_2 \cup e_3, \end{cases}$$

where $\mathrm{dist}(a, b)$ *is the distance between the points a and b. Note that the function $\boldsymbol{g}(\cdot)$ is continuous.*

We consider the initial guess $\boldsymbol{g}^{1,\delta}(\mathbf{x}) = 0$ for $\mathbf{x} \in \Theta$ and $\tau = 2.01$. In this example, *we discretize the edges* e_1*,* e_2 *and* e_3 *using* 16*,* 16 *and* 45 *points. Then, for equation* (3.14) $N = 500$*,* $J = 77$ *and* $L = 1$*.*

Δ	k_*	Error_{k_*}	*Time* (*s*)
100%	1	100%	1×10^{-4}
10%	6	23%	8×10^{-2}
1%	16	6%	3×10^{-1}
0.1%	44	2%	7×10^{-1}
0.01%	478	0.5%	6×10^{0}

Table 2 – Numerical results for Example 3.2. See Table 1 for a description of the contents .

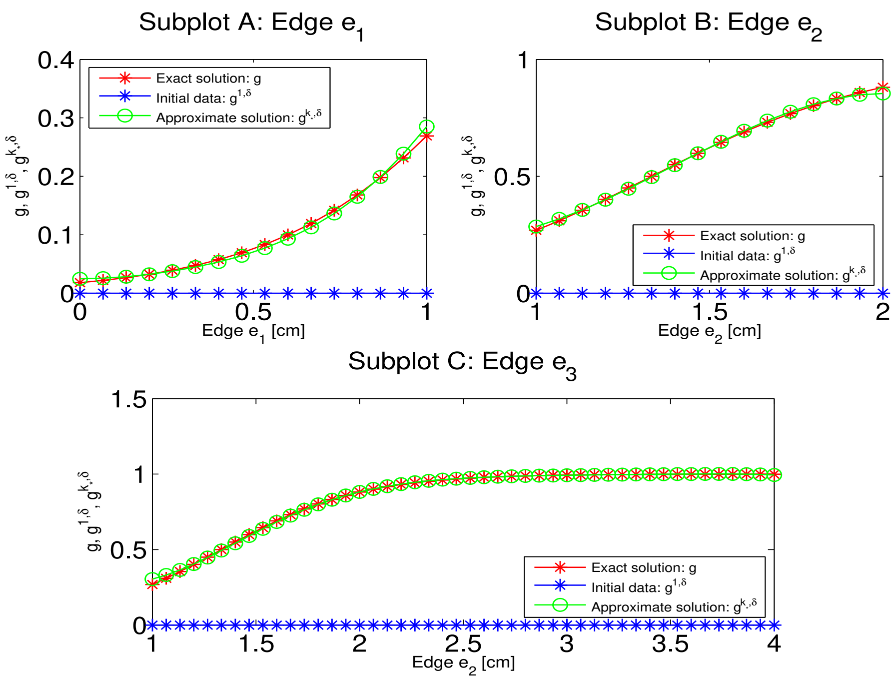

Figure 13 – For Example 3.2, in all the Subplots, the red line is the exact solution, the blue line is the initial guess, and the green line is the approximate solution for $\Delta = 0.1\%$ of noise, these figures shows the conductances as functions of the spatial variable. The subplots A, B, and C correspond to the edges e_1, e_2 and e_3, respectively.

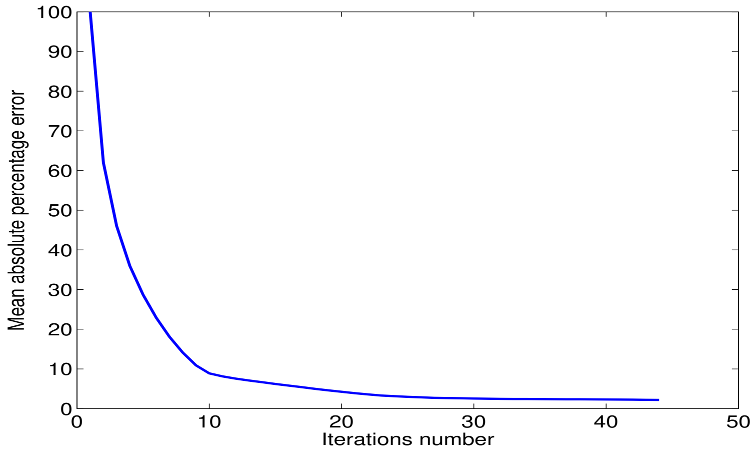

Figure 14 – Convergence results for Example 3.1. This figure shows the mean absolute percentage error between $\boldsymbol{g}$ and $\boldsymbol{g}^{k,\delta}$ as a function of the iteration k according to (3.14).

3.4 Detailed proof of Theorem 3.1.1

Before demonstrating the Theorem, we defined the following sets

$$\begin{aligned} \Omega &= \{(t,x); 0 \le t \le T, 0 \le x \le L\} \\ H(F) &= \left(L^2(\Omega)\right)^{N_{ion}} = \left\{ f:\Omega \to \mathbb{R}^{N_{ion}}; \int_\Omega |f(\xi)|^2 d\xi < \infty \right\} \\ R(F) &= L^2(\Gamma) = \left\{ f:\Gamma \to \mathbb{R}; \int_\Gamma |f(\xi)|^2 d\xi < \infty \right\}. \end{aligned}$$

It is well-known that $H(F)$ and $R(F)$ become Hilbert spaces under the inner products

$$\langle f,h\rangle_{H(F)} = \int_\Omega f(\xi)h(\xi)d\xi, \qquad \langle f,h\rangle_{R(F)} = \int_\Gamma f(\xi)h(\xi)d\xi,.$$

and the associated norms $\|f\|_{H(F)} = \langle f,f\rangle_{H(F)}^{1/2}$, $\|f\|_{R(F)} = \langle f,f\rangle_{R(F)}^{1/2}$. Note that the inner product on $R(F)$ depends on Γ (see Equation (3.3) or (3.4)) as follows:

$$\langle f,h\rangle_{R(F)} = \alpha_1 \int_0^L \int_0^T f(t,x)h(t,x)\,dt\,dx + \alpha_2 \int_0^T f(t,0)h(t,0)dt + \alpha_2 \int_0^T f(t,L)g(t,L)\,dt, \quad (3.15)$$

where α_1, α_2 are as in Eq. (3.9).

Proof. Given $\boldsymbol{g}^{k,\delta} \in D(F)$ and $\boldsymbol{\theta} = (\theta_1,\dots,\theta_{N_{\text{ion}}}) \in \left(L^\infty(\Omega)\right)^{N_{ion}}$, the Gâteux derivative of F at $\boldsymbol{g}^{k,\delta}$ in the direction $\boldsymbol{\theta}$ is given by

$$F'(\boldsymbol{g}^{k,\delta})(\boldsymbol{\theta}) = \lim_{\lambda\to 0} \frac{F(\boldsymbol{g}^{k,\delta} + \lambda\boldsymbol{\theta}) - F(\boldsymbol{g}^{k,\delta})}{\lambda} = W^k|_\Gamma, \quad (3.16)$$

where W^k solves

$$\begin{cases} W^k_{xx}(t,x) - cW^k_t(t,x) - \sum_{i\in\text{Ion}} g_i^{k,\delta}(t,x)W^k(t,x) \\ \qquad\qquad\qquad = \sum_{i\in\text{Ion}} \theta_i(V^{k,\delta}(t,x) - E_i) \quad \text{in } \Omega, \\ W^k(0,x) = 0 \qquad\qquad \text{for } \ 0 < x < L, \\ W^k_x(t,0) = W^k_x(t,L) = 0 \quad \text{for } \ 0 < t < T, \end{cases} \tag{3.17}$$

and $V^{k,\delta}$ solves Eq. (3.2) with g_i replaced by $g_i^{k,\delta}$. To obtain Eq. (3.17) from Eq. (3.16), it is enough to consider the difference between problem in Eq. (3.2) with coefficients $\boldsymbol{g}^{k,\delta} + \lambda\boldsymbol{\theta}$ and $\boldsymbol{g}^{k,\delta}$, divide by λ and take the limit $\lambda \to 0$.

Let $V^{k,\delta}|_\Gamma = F(\boldsymbol{g}^{k,\delta})$. From the Landweber iteration in Eq. (3.6), we gather that

$$\begin{aligned} \langle \boldsymbol{g}^{k+1,\delta} - \boldsymbol{g}^{k,\delta}, \boldsymbol{\theta}\rangle_{H(F)} &= \langle F'(\boldsymbol{g}^{k,\delta})^*(V^\delta|_\Gamma - F(\boldsymbol{g}^{k,\delta})), \boldsymbol{\theta}\rangle_{H(F)} \\ &= \langle F'(\boldsymbol{g}^{k,\delta})^*(V^\delta|_\Gamma - V^{k,\delta}|_\Gamma), \boldsymbol{\theta}\rangle_{H(F)}. \end{aligned}$$

By definition of adjoint operator,

$$\langle \boldsymbol{g}^{k+1,\delta} - \boldsymbol{g}^{k,\delta}, \boldsymbol{\theta}\rangle_{H(F)} = \langle V^\delta|_\Gamma - V^{k,\delta}|_\Gamma, F'(\boldsymbol{g}^{k,\delta})(\boldsymbol{\theta})\rangle_{R(F)} = \langle V^\delta|_\Gamma - V^{k,\delta}|_\Gamma, W^k|_\Gamma\rangle_{R(F)}, \tag{3.18}$$

from Eq. (3.16).

Although Eq. (3.18) yields an interesting relation, it carries an impeding dependence on $\boldsymbol{\theta}$ through W^k. It is possible to avoid that by performing some "trick" manipulations.

Multiplying the first equation of (3.8) by $-W^k$, and integrating in the intervals $[0,T]$ and $[0,L]$ we gather that

$$\begin{aligned} \int_0^L \int_0^T U^k_{xx}(t,x)W^k(t,x)\,dt\,dx + \int_0^L \int_0^T c\,U^k_t(t,x)W^k(t,x)\,dt\,dx \\ - \int_0^L \int_0^T \sum_{i\in ion} g_i^{k,\delta}(t,x)\,U^k(t,x)W^k(t,x)\,dt\,dx = \\ - \alpha_1 \int_0^L \int_0^T \Big(V^\delta(t,x) - V^{k,\delta}(t,x)\Big)\, W^k(t,x)\,dt\,dx. \end{aligned} \tag{3.19}$$

Integrating by parts twice the first term from Eq. (3.19) with respect to the space variable, and using the boundary conditions for W^k we have

$$\begin{aligned} \int_0^L \int_0^T U^k_{xx}(t,x)W^k(t,x)\,dt\,dx = \int_0^L \int_0^T U^k(t,x)W^k_{xx}(t,x)\,dt\,dx \\ + \int_0^T U^k_x(t,x)W^k(t,x)|_0^L\,dt, \end{aligned} \tag{3.20}$$

where we denote $U^k_x(t,x)W^k(t,x)|_0^L = U^k(t,L)W^k(t,L) - U^k(t,0)W^k(t,0)$. Similarly, integrating by parts the second term of Eq. (3.19) with respect to time and using the initial condition of W^k and the final condition of U^k, we gather that

$$\int_0^L \int_0^T c\,U^k_t(t,x)W^k(t,x)\,dt\,dx = - \int_0^L \int_0^T cU^k(t,x)W^k_t(t,x)\,dt\,dx. \tag{3.21}$$

Substituting Eqs. (3.20) and (3.21) in Eq. (3.19), it follows that

$$\int_0^L \int_0^T \Big(W_{xx}^k(t,x) - cW_t^k(t,x) - \sum_{i\in ion} g_i^{k,\delta}(t,x)W^k(t,x)\Big)U^k(t,x)\,dtdx =$$
$$-\alpha_1 \int_0^L \int_0^T \Big(V^\delta(t,x) - V^{k,\delta}(t,x)\Big)W^k(t,x)\,dt\,dx - \int_0^T U_x^k(t,x)W^k(t,x)|_0^L\,dt.$$

Substituting the first equation from (3.17) in the previous equation, we obtain

$$\int_0^L \int_0^T \sum_{i\in ion} \theta_i(V^{k,\delta}(t,x) - E_i)U^k(t,x)\,dt\,dx$$
$$= -\alpha_1 \int_0^L \int_0^T \Big(V^\delta(t,x) - V^{k,\delta}(t,x)\Big)\,W^k(t,x)\,dtdx - \int_0^T U_x^k(t,x)W^k(t,x)|_0^L\,dt.$$

From the boundary conditions from Eq. (3.8), the following expression holds:

$$\int_0^L \int_0^T \sum_{i\in ion} \theta_i(V^{k,\delta}(t,x) - E_i)U^k(t,x)\,dtdx$$
$$= -\alpha_1 \int_0^L \int_0^T \Big(V^\delta(t,x) - V^{k,\delta}(t,x)\Big)\,W^k(t,x)\,dtdx$$
$$-\alpha_2 \int_0^T \Big(V^\delta(t,0) - V^{k,\delta}(t,0)\Big)\,W^k(t,0) - \alpha_2 \int_0^T \Big(V^\delta(t,L) - V^{k,\delta}(t,L)\Big)\,W^k(t,L)\,dt.$$

From the previous equation and the definition of the inner product in Eq. (3.15), we have

$$\int_0^L \int_0^T \sum_{i\in ion} \theta_i(V^{k,\delta}(t,x) - E_i)U^k(t,x)\,dtdx = -\langle V^\delta|_\Gamma - V^{k,\delta}|_\Gamma, W^k|_\Gamma\rangle_{R(F)}. \tag{3.22}$$

From Eqs. (3.18) and (3.22) we have

$$\int_0^L \int_0^T \sum_{i\in \text{Ion}} \theta_i \left(g_i^{k+1,\delta}(t,x) - g_i^{k,\delta}(t,x)\right)\,dtdx$$
$$= -\int_0^L \int_0^T \sum_{i\in \text{Ion}} \theta_i(V^{k,\delta}(t,x) - E_i)U^k(t,x)\,dtdx.$$

Since $\boldsymbol{\theta} \in \left(L^\infty(\Omega)\right)^{N_{ion}}$ is arbitrary and $L^\infty(\Omega)$ is dense in $L^2(\Omega)$, we gather that the following iteration holds:

$$g_i^{k+1,\delta}(t,x) = g_i^{k,\delta}(t,x) - (V^{k,\delta}(t,x) - E_i)U^k(t,x) \quad \text{for all } i \in \text{Ion}.$$

■

4 Inverse problem in Hodgkin-Huxley model

One of the most important models in computational neuroscience is the Hodgkin-Huxley model for the squid giant axon. Using pioneering experimental techniques at that time, Hodgkin e Huxley (1952d) determined that the squid axon carries three major currents: a potassium current K^+ with four activation gates (n^4); a sodium current $Na+$ with three activation gates and one inactivation gate (m^3h), and a leak current, I_l, which is carried mostly by Cl^- ions (Izhikevich (2007)). The complete set of Hodgkin-Huxley equations is shown in Equation (1.8).

In this chapter, we solve two inverse problems utilizing the minimal error method. In the first problem, we obtain approximate maximum conductances, given the membrane potential measurement. For the second problem, the goal is to estimate the inactivation and activation gates, given the membrane potential measurement.

Throughout the study on the estimation of parameters in the Hodgkin-Huxley model, we presented some preliminary results in the following conferences:

- XXXVII Congresso Nacional de Matemática Aplicada e Computacional (CNMAC-2017), conference or lecture of work.
- Programa de Excelência Acadêmica (PROEX-LNCC-2017), presentation of work.
- Programa de Excelência Acadêmica (PROEX-LNCC-2018), presentation of work.

Moreover, we submitted an article for publication (Valle e Madureira (2019)). In this chapter, we present a summary of this Paper, shown in Appendix B.

4.1 Inverse problem for determining conductances

In this section we consider that, in Equation (1.8), the vector $\boldsymbol{G} = (G_{Na}, G_K, G_L) \in \mathbb{R}^3$ is unknown and the parameters C_M, I_M, E_{Na}, E_K, E_L, V_0, m_0, n_0 and h_0 are known. Also, the membrane potential $V : [0,T] \to \mathbb{R}$ is unknown, but its measurement V^δ is known.

Consider the set of functions $L^2[0,T]$, and the nonlinear operator

$$F : \mathbb{R}^3 \to L^2[0,T], \tag{4.1}$$

defined by $F(\boldsymbol{G}) = V$, where V solves (1.8). The goal of this Section is to obtain $\boldsymbol{G}$, given V^δ. From iteration (2.4), for $x = \boldsymbol{G}$ and $w^{k,\delta} \geq 0$, we have

$$\boldsymbol{G}^{k+1,\delta} = \boldsymbol{G}^{k,\delta} + w^{k,\delta} F'(\boldsymbol{G}^{k,\delta})^*(V^\delta - F(\boldsymbol{G}^{k,\delta})), \tag{4.2}$$

where

$$w^{k,\delta} = \frac{\|V^\delta - V^{k,\delta}\|^2_{L^2[0,T]}}{\left\|F'(\boldsymbol{G}^{k,\delta})^*(V^\delta - F(\boldsymbol{G}^{k,\delta}))\right\|^2_{\mathbb{R}^3}}.$$

From equation (4.2), we compute the adjoint of the Gateaux derivative $F'(\boldsymbol{G}^{k,\delta})^*$ (see Theorem 4.1.1), and we obtain the iteration

$$\boldsymbol{G}^{k+1,\delta} = \boldsymbol{G}^{k,\delta} + w^{k,\delta}\left(X^{k,\delta}_{Na}, X^{k,\delta}_{K}, X^{k,\delta}_{L}\right), \tag{4.3}$$

where $w^{k,\delta}$, $X^{k,\delta}_{Na}$, $X^{k,\delta}_{K}$ and $X^{k,\delta}_{L}$ satisfy equations (4.10), (4.5), (4.6) and (4.7), respectively.

To estimate $\boldsymbol{G}$, given $\boldsymbol{G}^{1,\delta}$, we used the minimal error iteration (4.3).

In the next theorem, we compute the adjoint of the Gateaux derivative $F'(\boldsymbol{G}^{k,\delta})^*$.

Theorem 4.1.1. *It follows from* (4.1) *and* (4.2) *that*

$$F'(\boldsymbol{G}^{k,\delta})^*(V^\delta - F(\boldsymbol{G}^{k,\delta})) = \left(X^{k,\delta}_{Na}, X^{k,\delta}_{K}, X^{k,\delta}_{L}\right), \tag{4.4}$$

where

$$X^{k,\delta}_{Na} = \int_0^T \left(m^{k,\delta}\right)^a \left(h^{k,\delta}\right)^b (V^{k,\delta} - E_{Na}) U^{k,\delta}\, dt, \tag{4.5}$$

$$X^{k,\delta}_{K} = \int_0^T \left(n^{k,\delta}\right)^c (V^{k,\delta} - E_{K}) U^{k,\delta}\, dt, \tag{4.6}$$

$$X^{k,\delta}_{L} = \int_0^T \left(n^{k,\delta}\right)^c (V^{k,\delta} - E_{K}) U^{k,\delta}\, dt. \tag{4.7}$$

The functions $m^{k,\delta}$, $n^{k,\delta}$, $h^{k,\delta}$ and $V^{k,\delta}$ solve, given $G^{k,\delta}_{Na}$, $G^{k,\delta}_{K}$ and $G^{k,\delta}_{L}$,

$$\begin{cases} C_M\dot{V}^{k,\delta} = I_{ext} - G^{k,\delta}_{Na}\left(m^{k,\delta}\right)^3\left(h^{k,\delta}\right)(V^{k,\delta} - E_{Na}) - G^{k,\delta}_{K}\left(n^{k,\delta}\right)^4(V^{k,\delta} - E_K) \\ \qquad\qquad -G^{k,\delta}_{L}(V^{k,\delta} - E_L), \\ \dot{\mathcal{X}} = (1-\mathcal{X})\alpha_{\mathcal{X}}(V^{k,\delta}) - \mathcal{X}\beta_{\mathcal{X}}(V^{k,\delta}) \quad \text{for } \mathcal{X} = m^{k,\delta}, n^{k,\delta}, h^{k,\delta}, \\ V^{k,\delta}(0) = V_0, \quad m^{k,\delta}(0) = m_0, \quad n^{k,\delta}(0) = n_0, \quad h^{k,\delta}(0) = h_0. \end{cases} \tag{4.8}$$

Finally, $U^{k,\delta}$ solves, given $m^{k,\delta}$, $n^{k,\delta}$, $h^{k,\delta}$ and $V^{k,\delta}$,

$$\begin{cases} C_M\dot{U}^{k,\delta} - \left(G^{k,\delta}_{Na}\left(m^{k,\delta}\right)^3\left(h^{k,\delta}\right) + G^{k,\delta}_{K}\left(n^{k,\delta}\right)^c + G^{k,\delta}_{L}\right)U^{k,\delta} \\ -[(1-m^{k,\delta})\alpha'_{m^{k,\delta}}(V^{k,\delta}) - m^{k,\delta}\beta'_{m^{k,\delta}}(V^{k,\delta})]P^{k,\delta} \\ -[(1-n^{k,\delta})\alpha'_{n^{k,\delta}}(V^{k,\delta}) - n^{k,\delta}\beta'_{n^{k,\delta}}(V^{k,\delta})]Q^{k,\delta} \\ -[(1-h^{k,\delta})\alpha'_{h^{k,\delta}}(V^{k,\delta}) - h^{k,\delta}\beta'_{h^{k,\delta}}(V^{k,\delta})]R^{k,\delta} = V^\delta - V^{k,\delta}, \\ \dot{P}^{k,\delta} - [\alpha_{m^{k,\delta}}(V^{k,\delta}) + \beta_{m^{k,\delta}}(V^{k,\delta})]P^{k,\delta} = -3G^{k,\delta}_{Na}\left(m^{k,\delta}\right)^2\left(h^{k,\delta}\right)(V^{k,\delta} - E_{Na})U^{k,\delta}, \\ \dot{Q}^{k,\delta} - [\alpha_{n^{k,\delta}}(V^{k,\delta}) + \beta_{n^{k,\delta}}(V^{k,\delta})]Q^{k,\delta} = -4G^{k,\delta}_{K}\left(n^{k,\delta}\right)^3(V^{k,\delta} - E_K)U^{k,\delta}, \\ \dot{R}^{k,\delta} - [\alpha_{h^{k,\delta}}(V^{k,\delta}) + \beta_{h^{k,\delta}}(V^{k,\delta})]R^{k,\delta} = -G^{k,\delta}_{Na}\left(m^{k,\delta}\right)^3(V^{k,\delta} - E_{Na})U^{k,\delta}, \\ U^{k,\delta}(T) = 0, \quad P^{k,\delta}(T) = 0, \quad Q^{k,\delta}(T) = 0, \quad R^{k,\delta}(T) = 0. \end{cases} \tag{4.9}$$

Note that,

$$w^{k,\delta} = \frac{\|V^\delta - V^{k,\delta}\|^2_{L^2[0,T]}}{\left\|\left(X^{k,\delta}_{Na}, X^{k,\delta}_{K}, X^{k,\delta}_{L}\right)\right\|^2_{\mathbb{R}^3}}. \tag{4.10}$$

Proof. See Subsection 4.4.1. ∎

We next describe the computational scheme.

Data: V^δ, δ and τ
Result: Compute an approximation for $\boldsymbol{G}$ using Minimal Error Iteration Scheme
Choose $\boldsymbol{G}^{1,\delta}$ as an initial approximation for $\boldsymbol{G}$;
Compute $m^{1,\delta}$, $n^{1,\delta}$, $h^{1,\delta}$ and $V^{1,\delta}$ from (4.8), replacing $\boldsymbol{G}^{k,\delta}$ by $\boldsymbol{G}^{1,\delta}$;
k=1;
while $\tau\delta \leq \|V^\delta - V^{k,\delta}\|_{L^2[0,T]}$ **do**
  Compute $U^{k,\delta}$ from (4.9);
  Compute $\boldsymbol{G}^{k+1,\delta}$ using (4.3);
  Compute $m^{k+1,\delta}$, $n^{k+1,\delta}$, $h^{k+1,\delta}$ and $V^{k+1,\delta}$ from (4.8), replacing $\boldsymbol{G}^{k,\delta}$ by $\boldsymbol{G}^{k+1,\delta}$;
  $k \leftarrow k+1$;
end

Algorithm 3: Minimal error iteration to obtain maximal conductances

4.2 Inverse problem for determining exponents

Here, we consider that the inactivation and activation gates (a, b and c) are unknown. Then, from (1.8) we have the following ODE

$$\begin{cases} C_M \dfrac{\partial V}{\partial t} = I_M - G_{Na} m^a h^b (V - E_{Na}) - G_K n^c (V - E_K) - G_L (V - E_L); \\ \dfrac{\partial m}{\partial t} = (1-m)\alpha_m(V) - m\beta_m(V); \\ \dfrac{\partial n}{\partial t} = (1-n)\alpha_n(V) - n\beta_n(V); \\ \dfrac{\partial h}{\partial t} = (1-h)\alpha_h(V) - h\beta_h(V); \\ V(0) = V_0, \quad m(0) = m_0, \quad n(0) = n_0, \quad h(0) = h_0. \end{cases} \tag{4.11}$$

The constants C_M, I_M, G_{Na}, G_{K}, G_L E_{Na}, E_{K}, E_L, V_0, m_0, n_0 and h_0 are known. We denote $\boldsymbol{a} = (a, b, c)$, and we assume the operator F defined in (4.1) and the iteration (4.2), where $\boldsymbol{G} = \boldsymbol{a}$. The goal of this Section is to estimate $\boldsymbol{a}$, given V^δ. Computing the adjoint of the Gateaux derivative $F'(\boldsymbol{a})^*$ (see Theorem 4.2.1), from (4.2), we have the iteration

$$\boldsymbol{a}^{k+1,\delta} = \boldsymbol{a}^{k,\delta} + w^{k,\delta}\left(X^{k,\delta}_a, X^{k,\delta}_b, X^{k,\delta}_c\right), \tag{4.12}$$

where $w^{k,\delta}$, $X_a^{k,\delta}$, $X_b^{k,\delta}$ and $X_c^{k,\delta}$ satisfy equations (4.19), (4.14), (4.15) and (4.16), respectively.

Given an initial guess $\boldsymbol{a}^{1,\delta}$, we obtain a regularizing approximation $\boldsymbol{a}^{k_*,\delta}$ for $\boldsymbol{a}$, from minimal error iteration (4.12).

In the next Theorem, we compute the adjoint of the Gateaux derivative $F'(\boldsymbol{a}^{k,\delta})^*$ from (4.2).

Theorem 4.2.1. *Consider the nonlinear operator F defined in (4.1) and iteration (4.2), replacing $\boldsymbol{G}$ by $\boldsymbol{a}$. It follows then that*

$$F'(\boldsymbol{a}^{k,\delta})^* \left(V^\delta - F(\boldsymbol{a}^{k,\delta})\right) = \left(X_a^{k,\delta}, X_b^{k,\delta}, X_c^{k,\delta}\right), \tag{4.13}$$

where

$$X_a^{k,\delta} = \int_0^T G_{Na}(V^{k,\delta} - E_{Na})\left(m^{k,\delta}\right)^{a^{k,\delta}} \left(h^{k,\delta}\right)^{b^{k,\delta}} U^{k,\delta} \ln(m^{k,\delta})\, dt, \tag{4.14}$$

$$X_b^{k,\delta} = \int_0^T G_{Na}(V^{k,\delta} - E_{Na})\left(m^{k,\delta}\right)^{a^{k,\delta}} \left(h^{k,\delta}\right)^{b^{k,\delta}} U^{k,\delta} \ln(h^{k,\delta})\, dt, \tag{4.15}$$

$$X_c^{k,\delta} = \int_0^T G_K(V^{k,\delta} - E_K)\left(n^{k,\delta}\right)^{c^{k,\delta}} U^{k,\delta} \ln(n^{k,\delta})\, dt. \tag{4.16}$$

The functions $m^{k,\delta}$, $n^{k,\delta}$, $h^{k,\delta}$ and $V^{k,\delta}$ solve

$$\begin{cases} C_M \dot{V}^{k,\delta} = I_{ext} - G_{Na}\left(m^{k,\delta}\right)^{a^{k,\delta}} \left(h^{k,\delta}\right)^{b^{k,\delta}} (V^{k,\delta} - E_{Na}) \\ \qquad -G_K\left(n^{k,\delta}\right)^{c^{k,\delta}} (V^{k,\delta} - E_K) - G_L(V^{k,\delta} - E_L), \\ \dot{\mathcal{X}} = (1-\mathcal{X})\alpha_{\mathcal{X}}(V^{k,\delta}) - \mathcal{X}\beta_{\mathcal{X}}(V^{k,\delta}); \quad \mathcal{X} = m^{k,\delta}, n^{k,\delta}, h^{k,\delta}, \\ V^{k,\delta}(0) = V_0; \quad m^{k,\delta}(0) = m_0; \quad n^{k,\delta}(0) = n_0; \quad h^{k,\delta}(0) = h_0, \end{cases} \tag{4.17}$$

where $a^{k,\delta}$, $b^{k,\delta}$ and $c^{k,\delta}$ are given. Also, $U^{k,\delta}$ solves

$$\begin{cases} C_M \dot{U}^{k,\delta} - \left(G_{Na}\left(m^{k,\delta}\right)^{a^{k,\delta}} \left(h^{k,\delta}\right)^{b^{k,\delta}} + G_K\left(n^{k,\delta}\right)^{c^{k,\delta}} + G_L\right) U^{k,\delta} \\ \qquad -[(1-m^{k,\delta})\alpha'_{m^{k,\delta}}(V^{k,\delta}) - m^{k,\delta}\beta'_{m^{k,\delta}}(V^{k,\delta})]P^{k,\delta} \\ \qquad -[(1-n^{k,\delta})\alpha'_{n^{k,\delta}}(V^{k,\delta}) - n^{k,\delta}\beta'_{n^{k,\delta}}(V^{k,\delta})]Q^{k,\delta} \\ \qquad -[(1-h^{k,\delta})\alpha'_{h^{k,\delta}}(V^{k,\delta}) - h^{k,\delta}\beta'_{h^{k,\delta}}(V^{k,\delta})]R^{k,\delta} = V^\delta - V^{k,\delta}, \\ \dot{P}^{k,\delta} - [\alpha_{m^{k,\delta}}(V^{k,\delta}) + \beta_{m^{k,\delta}}(V^{k,\delta})]P^{k,\delta} = \\ \qquad -a^{k,\delta}G_{Na}\left(m^{k,\delta}\right)^{a^{k,\delta}-1}\left(h^{k,\delta}\right)^{b^{k,\delta}}(V^{k,\delta} - E_{Na})U^{k,\delta}, \\ \dot{Q}^{k,\delta} - [\alpha_{n^{k,\delta}}(V^{k,\delta}) + \beta_{n^{k,\delta}}(V^{k,\delta})]Q^{k,\delta} = \\ \qquad -c^{k,\delta}G_K\left(n^{k,\delta}\right)^{c^{k,\delta}-1}(V^{k,\delta} - E_K)U^{k,\delta}, \\ \dot{R}^{k,\delta} - [\alpha_{h^{k,\delta}}(V^{k,\delta}) + \beta_{h^{k,\delta}}(V^{k,\delta})]R^{k,\delta} = \\ \qquad -b^{k,\delta}G_{Na}\left(m^{k,\delta}\right)^{a^{k,\delta}}\left(h^{k,\delta}\right)^{b^{k,\delta}-1}(V^{k,\delta} - E_{Na})U^{k,\delta}, \\ U^{k,\delta}(T) = 0; \quad P^{k,\delta}(T) = 0; \quad R^{k,\delta}(T) = 0; \quad Q^{k,\delta}(T) = 0, \end{cases} \tag{4.18}$$

given $m^{k,\delta}$, $n^{k,\delta}$, $h^{k,\delta}$ and $V^{k,\delta}$.

Note that $w^{k,\delta}$ satisfies

$$w^{k,\delta} = \frac{\|V^{\delta} - V^{k,\delta}\|^2_{L^2[0,T]}}{\left\|\left(X_a^{k,\delta}, X_b^{k,\delta}, X_c^{k,\delta}\right)\right\|^2_{\mathbb{R}^3}}. \tag{4.19}$$

Proof. See Subsection 4.4.2. ■

We next describe the computational scheme.

Data: V^{δ}, δ and τ
Result: Compute an approximation for $\boldsymbol{a}$ using Minimal Error Iteration Scheme
Choose $\boldsymbol{a}^{1,\delta}$ as an initial approximation for $\boldsymbol{a}$;
Compute $m^{1,\delta}$, $n^{1,\delta}$, $h^{1,\delta}$ and $V^{1,\delta}$ from (4.17), replacing $\boldsymbol{a}^{k,\delta}$ by $\boldsymbol{a}^{1,\delta}$;
k=1;
while $\tau\delta \le \|V^{\delta} - V^{k,\delta}\|_{L^2[0,T]}$ **do**
  Compute $U^{k,\delta}$ from (4.18);
  Compute $\boldsymbol{a}^{k+1,\delta}$ using (4.12);
  Compute $m^{k+1,\delta}$, $n^{k+1,\delta}$, $h^{k+1,\delta}$ and $V^{k+1,\delta}$ from (4.17), replacing $\boldsymbol{a}^{k,\delta}$ by $\boldsymbol{a}^{k+1,\delta}$;
  $k \leftarrow k+1$;
end

Algorithm 4: Minimal error iteration to obtain inactivation and activation gates.

4.3 Numerical simulations

To design our numerical experiments, we first choose x ($x = \boldsymbol{G}$ or $x = \boldsymbol{a}$) and compute V from (1.8) or (4.11). In our examples, for a given δ, the noisy V^{δ} is obtained from

$$V^{\delta}(t) = V(t) + V(t)\text{rand}_{\varepsilon}(t), \quad \text{for all } t \in [0,T] \tag{4.20}$$

where $\text{rand}_{\varepsilon}(t)$ is a uniformly distributed random variable taking values in the range $[-\varepsilon, \varepsilon]$, and $\varepsilon = \delta/\|V\|_{L^2[0,T]}$.

Given the initial guess $x^{1,\delta}$, the data V^{δ} and δ, we estimate x using either Algorithm 3 (for $x = \boldsymbol{G}$) or Algorithm 4 (for $x = \boldsymbol{a}$). Note that the exact value for x is known, and we use this to measure the algorithm performance.

The percent error of vector $x \in \mathbb{R}^3$ is defined by

$$\text{Error}_k = \frac{\|x - x^{k,\delta}\|_{\mathbb{R}^3}}{\|x\|_{\mathbb{R}^3}} \times 100\%, \quad k = 1, 2, \cdots, k_*. \tag{4.21}$$

In this section we will present two numerical simulations. In Example 4.1 we estimate the conductances (G_{Na}, G_{K} and G_L), and in Example 4.2 we estimate the inactivation and activation gates (a, b and c).

Example 4.1. *This example is a particular case from* (1.8)*, with values:* $C_M = 1$ $[\mu F/cm^2]$*,* $E_{Na} = 110$ $[mV]$*,* $E_K = -12$ $[mV]$*,* $E_L = 10$ $[mV]$*,* $G_{Na} = 100$ $[mS/cm^2]$*,* $G_K = 30$ $[mS/cm^2]$*,* $G_L = 1$ $[mS/cm^2]$*, and* $I_{ext} = 10$ $[\mu A/cm^2]$*. Let the initial conditions* $V(0) = -50$ $[mV]$*,* $m(0) = 0.5$*,* $n(0) = 0.2$ *and* $h(0) = 0.4$*. We consider* $T = 10$ $[ms]$ *and* $\Delta t = 0.01$*. Given* V^δ*, the goal of this example is to approximate* $\boldsymbol{G} = (G_{Na}, G_K, G_L)$ $[mS/cm^2]$*.*

First, given $\boldsymbol{G} = (100, 30, 1)$ $[mS/cm^2]$*, we compute* V *from* (1.8)*. Then, we calculate* V^δ *from* (4.20) *given* ε *(see table 3). Next, we consider* V *and* $\boldsymbol{G}$ *unknown.*

In this test we consider the initial guess $\boldsymbol{G}^{1,\delta} = (0, 0, 0)$ $[mS/cm^2]$ *and* $\tau = 2.01$*. Table 3 presents the results for various levels of noise. When* ε *decreases, the number of iterations grows resulting in a better approximation for* $\boldsymbol{G} = (G_{Na}, G_K, G_L)$ $[mS/cm^2]$*.*

In Figures 15 and 16, we plot some results for $\varepsilon = 0.1\%$ *(Table 2, line 5).*

ε	k_*	$G_{\text{Na}}^{k_*,\delta}$	$G_{\text{K}}^{k_*,\delta}$	$G_L^{k_*,\delta}$	$Error_{k_*}$	$Time\ (s)$
100%	1	0	0	0	100 %	2×10^{-2}
10%	640	50	16	1.866	50 %	4×10^0
1%	26804	91	27	1.080	9 %	179×10^0
0.1%	97405	99	29	1.004	1 %	653×10^0
0.01%	181526	100	30	1.000	0 %	1216×10^0

Table 3 – Numerical results for Example 4.1 for various values of ε, as in (4.20). The second column contains the number of iterations according to (1.10). The third, fourth and fifth columns are the approximations for G_{Na}, G_{K} and G_L respectively. The sixth column is the relative error of $\boldsymbol{G} = (G_{\text{Na}}, G_{\text{K}}, G_L)$ according to (4.21). The last column is the running time of the algorithm, in seconds.

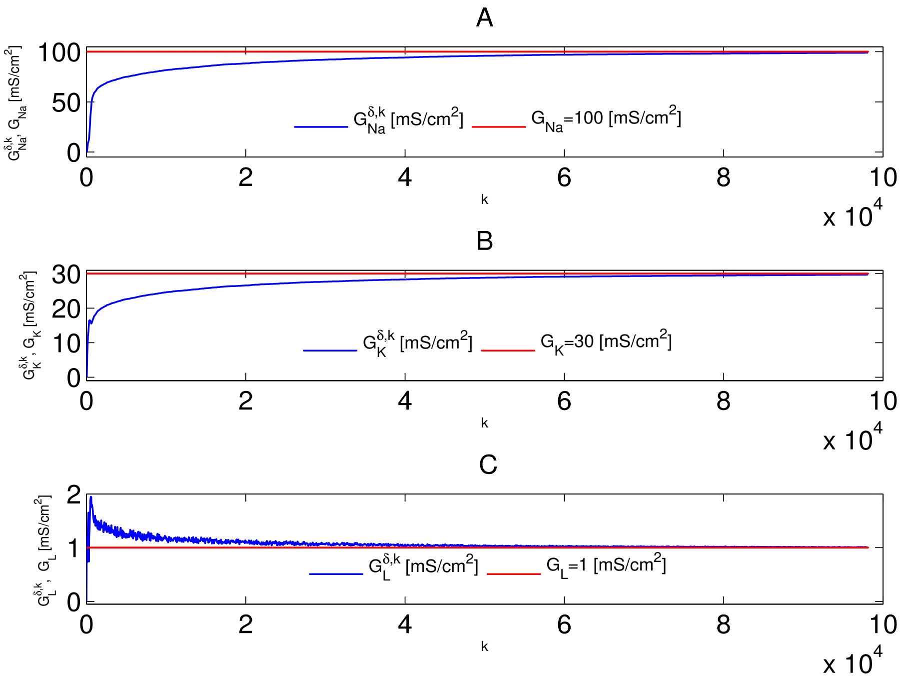

Figure 15 – Figures for Example 4.1 (estimation of the conductances) with $\varepsilon = 0.1\%$. The x-axis gives the number of iterations (k) and the y-axis gives the conductance. The red lines are the exact solutions, and blue lines are the approximations. The figures 15-A, 15-B and 15-C display the estimates of the maximum conductances of sodium, potassium and leakage, respectively.

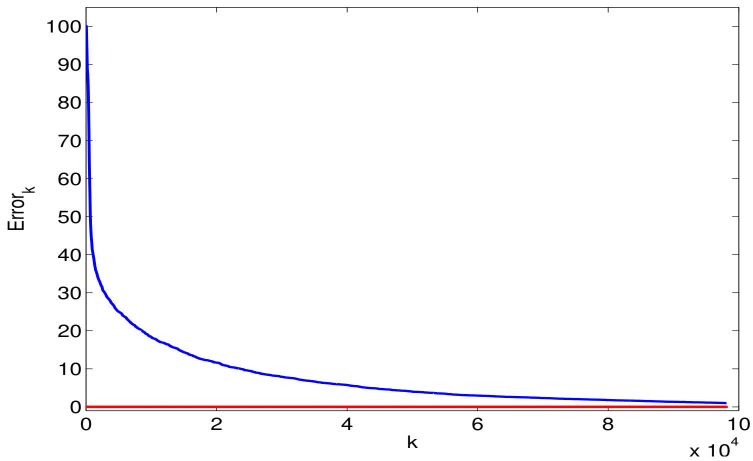

Figure 16 – Convergence results for Example 4.1. This figure displays the percentage error between $x = \boldsymbol{G}$ and $x^{k,\delta} = \boldsymbol{G}^{k,\delta}$ as a function of the iteration k according to (4.21).

Example 4.2. *This example is another particular case from* (4.11) *with values:* $C_M = 1\ [\mu F/cm^2]$, $E_{Na} = 115\ [mV]$, $E_K = -12\ [mV]$, $E_L = 10\ [mV]$, $G_{Na} = 120\ [mS/cm^2]$, $G_K = 36\ [mS/cm^2]$, $G_L = 0.3\ [mS/cm^2]$ *and* $I_{ext} = 10\ [\mu A/cm^2]$. *Let the initial conditions* $V(0) = -10\ [mV]$, $m(0) = 0.5$, $n(0) = 0.6$ *and* $h(0) = 0.8$. *We consider the time* $T = 10\ [ms]$ *with* $\Delta t = 0.01$. *Given* V^δ, *our goal is to approximate* $\boldsymbol{a} = (a, b, c) = (2, 2, 2)$.

First we calculate V *from* (4.11) *given* $\boldsymbol{a}$. *Then, we calculate* V^δ *from* (4.20) *given*

ε *(see table 4). We then consider V and $\boldsymbol{a}$ unknown.*

In this example we consider the initial guess $\boldsymbol{a}^{1,\delta} = (0,0,0)$ and $\tau = 2.01$. Table 4 presents the results for various levels of noise. In figures 17, and 18, we plot some results for a level of noise $\varepsilon = 1\%$ (Table 4, line 4).

ε	k_*	$a^{k_*,\delta}$	$b^{k_*,\delta}$	$c^{k_*,\delta}$	$Error_{k_*}$	$Time\ (s)$
100 %	76	0.02	0.58	−0.02	92 %	0.6
10 %	306	1.24	1.65	0.38	53 %	2.4
1 %	533	1.92	1.96	1.84	5 %	4.1
0.1 %	762	1.99	1.99	1.99	0.5 %	6.0
0.01 %	991	2.00	2.00	2.00	0 %	7.8

Table 4 – Numerical results for Example 4.2. See Table 3 for a description of the contents.

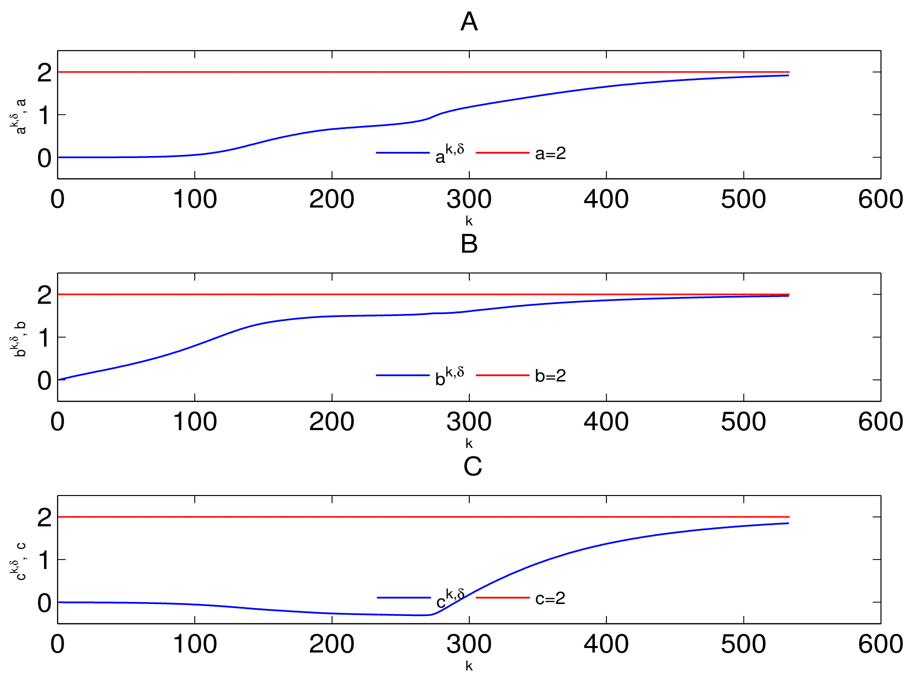

Figure 17 – Figures for Example 4.2 (estimation of the inactivation and activation gates) with $\varepsilon = 1\%$. The x-axis is the number of iterations (k). In y-axis, the red lines are the exact solutions, and blue lines are the approximations. The figures 17-A, 17-B and 17-C are the estimates of a, b and c, respectively.

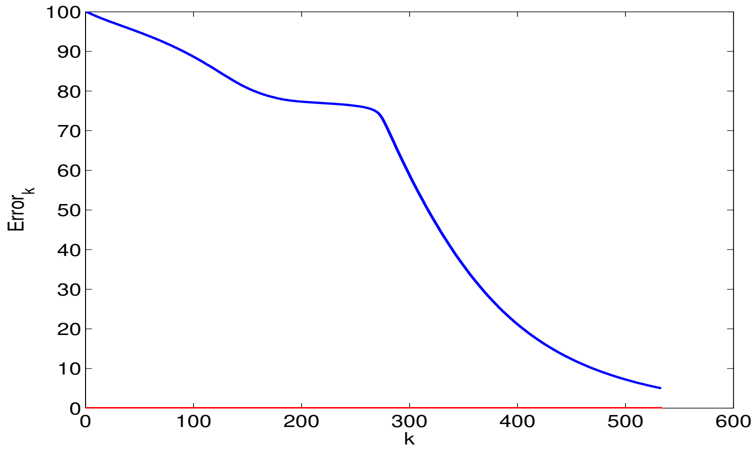

Figure 18 – Convergence results for Example 4.2 with 1 %. This figure shows the percentage error between $x = \boldsymbol{a}$ and $x^{k,\delta} = \boldsymbol{a}^{k,\delta}$ as a function of the iteration k according to (4.21).

4.4 Detailed proofs of Theorems 4.1.1 and 4.2.1

4.4.1 Proof of Theorem 4.1.1

Proof. Consider the operator F defined in (4.1). Evaluating $\boldsymbol{G}^{k,\delta}$ in F , we have $F(\boldsymbol{G}^{k,\delta}) = V^{k,\delta}$, where $V^{k,\delta}$, $m^{k,\delta}$, $n^{k,\delta}$ and $h^{k,\delta}$ solve the ODE (4.17).

Let vector $\boldsymbol{\theta} = (\theta_{\text{Na}}, \theta_{\text{K}}, \theta_L) \in \mathbb{R}^3$ and $\lambda \in \mathbb{R}$, then evaluating $\boldsymbol{G}^{k,\delta} + \lambda\boldsymbol{\theta}$ in the operator F, we have $F(\boldsymbol{G}^{k,\delta} + \lambda\boldsymbol{\theta}) = V_\lambda^{k,\delta}$, where $V_\lambda^{k,\delta}$, $m_\lambda^{k,\delta}$, $n_\lambda^{k,\delta}$ and $h_\lambda^{k,\delta}$ solve

$$\begin{cases} C_M \dot{V}_\lambda^{k,\delta} = I_{\text{ext}} - \left(G_{\text{Na}}^{k,\delta} + \lambda\theta_{\text{Na}}\right)\left(m_\lambda^{k,\delta}\right)^a\left(h_\lambda^{k,\delta}\right)^b\left(V_\lambda^{k,\delta} - E_{\text{Na}}\right) \\ \quad - \left(G_{\text{K}}^{k,\delta} + \lambda\theta_K\right)\left(n_\lambda^{k,\delta}\right)^c\left(V_\lambda^{k,\delta} - E_{\text{K}}\right) - \left(G_L^{k,\delta} + \lambda\theta_L\right)\left(V_\lambda^{k,\delta} - E_L\right), \\ \dot{\mathcal{X}} = (1-\mathcal{X})\alpha_{\mathcal{X}}(V^{k,\delta}) - \mathcal{X}\beta_{\mathcal{X}}(V^{k,\delta}); \qquad \mathcal{X} = m_\lambda^{k,\delta}, n_\lambda^{k,\delta}, h_\lambda^{k,\delta}, \\ V_\lambda^{k,\delta}(0) = V_0; \quad m_\lambda^{k,\delta}(0) = m_0; \quad n_\lambda^{k,\delta}(0) = n_0; \quad n_\lambda^{k,\delta}(0) = n_0. \end{cases} \tag{4.22}$$

The Gateaux derivative of F at $\boldsymbol{G}^{k,\delta}$ in the direction $\boldsymbol{\theta}$ is given by

$$W^{k,\delta} = F'(\boldsymbol{G}^{k,\delta})(\boldsymbol{\theta}) = \lim_{\lambda\to 0} \frac{F(\boldsymbol{G}^{k,\delta} + \lambda\boldsymbol{\theta}) - F(\boldsymbol{G}^{k,\delta})}{\lambda}. \tag{4.23}$$

Also, we denote the following limits

$$M^{k,\delta} = \lim_{\lambda\to 0} \frac{m_\lambda^{k,\delta} - m^{k,\delta}}{\lambda}, \qquad N^{k,\delta} = \lim_{\lambda\to 0} \frac{n_\lambda^{k,\delta} - n^{k,\delta}}{\lambda}, \qquad H^{k,\delta} = \lim_{\lambda\to 0} \frac{h_\lambda^{k,\delta} - h^{k,\delta}}{\lambda}, \tag{4.24}$$

where $M^{k,\delta}$, $N^{k,\delta}$ and $H^{k,\delta}$ are the Gateaux derivatives of $m^{k,\delta}$, $n^{k,\delta}$ and $h^{k,\delta}$, respectively.

Considering the difference between ODEs (4.22) and (4.17), dividing by λ and taking the limit $\lambda \to 0$, we have the following ODE

$$\begin{cases} C_M \dot{W}^{k,\delta} + \left(G_{\text{Na}}^{k,\delta}\left(m^{k,\delta}\right)^a\left(h^{k,\delta}\right)^b + G_{\text{K}}^{k,\delta}\left(n^{k,\delta}\right)^c + G_L^{k,\delta}\right) W^{k,\delta} = \\ -aG_{\text{Na}}^{k,\delta}\left(m^{k,\delta}\right)^{a-1} M^{k,\delta}\left(h^{k,\delta}\right)^b (V^{k,\delta} - E_{\text{Na}}) \\ -bG_{\text{Na}}^{k,\delta}\left(m^{k,\delta}\right)^a\left(h^{k,\delta}\right)^{b-1} H^{k,\delta}(V^{k,\delta} - E_{\text{Na}}) - cG_{\text{K}}^{k,\delta}\left(n^{k,\delta}\right)^{c-1} N^{k,\delta}(V^{k,\delta} - E_{\text{K}}) \\ -\theta_{\text{Na}}\left(m^{k,\delta}\right)^a\left(h^{k,\delta}\right)^b (V^{k,\delta} - E_{\text{Na}}) - \theta_K\left(n^{k,\delta}\right)^c (V^{k,\delta} - E_{\text{K}}) - \theta_L(V^{k,\delta} - E_L), \\ \dot{\mathcal{X}} + [\alpha_{\mathcal{Y}}(V^{k,\delta}) + \beta_{\mathcal{Y}}(V^{k,\delta})]\mathcal{X} = [(1-\mathcal{Y})\alpha'_{\mathcal{Y}}(V^{k,\delta}) - \mathcal{Y}\beta'_{\mathcal{Y}}(V^{k,\delta})]W^{k,\delta}; \\ (\mathcal{X}, \mathcal{Y}) = (M^{k,\delta}, m^{k,\delta}), (N^{k,\delta}, n^{k,\delta}), (H^{k,\delta}, h^{k,\delta}), \\ W^{k,\delta}(0) = 0; \quad M^{k,\delta}(0) = 0; \quad N^{k,\delta}(0) = 0; \quad H^{k,\delta}(0) = 0. \end{cases} \tag{4.25}$$

This last equation is yet another system of coupled nonlinear differential equations, depending on the parameter $\boldsymbol{\theta} = (\theta_{\text{Na}}, \theta_K, \theta_L)$, representing an arbitrary point in $\mathbb{R}^3$.

From minimal error iteration (4.2) and $\boldsymbol{\theta} \in \mathbb{R}^3$ arbitrary, we have

$$\begin{aligned} \langle \boldsymbol{G}^{k+1,\delta} - \boldsymbol{G}^{k,\delta}, \boldsymbol{\theta} \rangle_{\mathbb{R}^3} &= w^{k,\delta}\langle F'(\boldsymbol{G}^{k,\delta})^*(V^\delta - F(\boldsymbol{G}^{k,\delta})), \boldsymbol{\theta} \rangle_{\mathbb{R}^3}, \\ &= w^{k,\delta}\langle F'(\boldsymbol{G}^{k,\delta})^*(V^\delta - V^{k,\delta}), \boldsymbol{\theta} \rangle_{\mathbb{R}^3}. \end{aligned}$$

By definition of adjoint operator

$$\langle \boldsymbol{G}^{k+1,\delta} - \boldsymbol{G}^{k,\delta}, \boldsymbol{\theta} \rangle_{\mathbb{R}^3} = w^{k,\delta}\langle V^\delta - V^{k,\delta}, F'(x_k)(\boldsymbol{\theta}) \rangle_{L^2[0,T]},$$

where the internal product in $L^2[0,T]$ is given by $\Phi = \int_0^T (V^\delta - V^{k,\delta})W^{k,\delta} \; dt$, and from (4.23) and the previous equation,

$$\langle \boldsymbol{G}^{k+1,\delta} - \boldsymbol{G}^{k,\delta}, \boldsymbol{\theta} \rangle_{\mathbb{R}^3} = w^{k,\delta}\langle V^\delta - V^{k,\delta}, W^{k,\delta}\rangle_{L^2[0,T]}.$$

Denoting the last equality by Φ, we gather that

$$\Phi = \frac{\langle \boldsymbol{G}^{k+1,\delta} - \boldsymbol{G}^{k,\delta}, \boldsymbol{\theta} \rangle_{\mathbb{R}^3}}{w^{k,\delta}} = \langle V^\delta - V^{k,\delta}, W^{k,\delta}\rangle_{L^2[0,T]}. \tag{4.26}$$

From the previous equation and the first equality from ODE (5.10), we obtain

$$\begin{aligned} \Phi = \int_0^T \left(C_M \dot{U}^{k,\delta} W^{k,\delta} - \left(G_{\text{Na}}^{k,\delta}\left(m^{k,\delta}\right)^a\left(h^{k,\delta}\right)^b + G_{\text{K}}^{k,\delta}\left(n^{k,\delta}\right)^c + G_L^{k,\delta}\right) U^{k,\delta} W^{k,\delta} \right) dt \\ - \int_0^T \left[(1-m^{k,\delta})\alpha'_{m^{k,\delta}}(V^{k,\delta}) - m^{k,\delta}\beta'_{m^{k,\delta}}(V^{k,\delta})\right] P^{k,\delta} W^{k,\delta}\, dt \\ - \int_0^T \left[(1-n^{k,\delta})\alpha'_{n^{k,\delta}}(V^{k,\delta}) - n^{k,\delta}\beta'_{n^{k,\delta}}(V^{k,\delta})\right] Q^{k,\delta} W^{k,\delta}\, dt \\ - \int_0^T \left[(1-h^{k,\delta})\alpha'_{h^{k,\delta}}(V^{k,\delta}) - h^{k,\delta}\beta'_{h^{k,\delta}}(V^{k,\delta})\right] R^{k,\delta} W^{k,\delta}\, dt. \end{aligned} \tag{4.27}$$

Integrating the first term from (4.27) by parts, and from the initial ($W^{k,\delta}(0) = 0$) and final ($U^{k,\delta}(T) = 0$) conditions, we obtain

$$\int_0^T C_M \dot{U}^{k,\delta} W^{k,\delta} = - \int_0^T C_M U^{k,\delta} \dot{W}^{k,\delta}. \tag{4.28}$$

Replacing equation (4.28) in (4.27), we have

$$\begin{aligned}
\Phi \;=\; & -\int_0^T \left(C_M \dot{W}^{k,\delta} + \left(G_{\mathrm{Na}}^{k,\delta} \left(m^{k,\delta}\right)^a \left(h^{k,\delta}\right)^b + G_{\mathrm{K}}^{k,\delta} \left(n^{k,\delta}\right)^c + G_L^{k,\delta} \right) W^{k,\delta} \right) U^{k,\delta}\, dt \\
& - \int_0^T \left[(1-m^{k,\delta}) \alpha'_{m^{k,\delta}}(V^{k,\delta}) - m^{k,\delta} \beta'_{m^{k,\delta}}(V^{k,\delta}) \right] P^{k,\delta} W^{k,\delta}\, dt \\
& - \int_0^T \left[(1-n^{k,\delta}) \alpha'_{n^{k,\delta}}(V^{k,\delta}) - n^{k,\delta} \beta'_{n^{k,\delta}}(V^{k,\delta}) \right] Q^{k,\delta} W^{k,\delta}\, dt \\
& - \int_0^T \left[(1-h^{k,\delta}) \alpha'_{h^{k,\delta}}(V^{k,\delta}) - h^{k,\delta} \beta'_{h^{k,\delta}}(V^{k,\delta}) \right] R^{k,\delta} W^{k,\delta}\, dt.
\end{aligned}$$

Replacing, the first equality from the ODE (4.25), in the first integral from the previous equation, we gather

$$\begin{aligned}
\Phi = & \int_0^T a G_{\mathrm{Na}}^{k,\delta} (m^{k,\delta})^{a-1} M^{k,\delta} \left(h^{k,\delta}\right)^b (V^{k,\delta} - E_{\mathrm{Na}}) U^{k,\delta}\, dt \\
& + \int_0^T b G_{\mathrm{Na}}^{k,\delta} \left(m^{k,\delta}\right)^a (h^{k,\delta})^{b-1} H^{k,\delta} (V^{k,\delta} - E_{\mathrm{Na}}) U^{k,\delta}\, dt \\
& + \int_0^T c G_{\mathrm{K}}^{k,\delta} (n^{k,\delta})^{c-1} N^{k,\delta} (V^{k,\delta} - E_{\mathrm{K}}) U^{k,\delta}\, dt \\
& + \int_0^T \left(m^{k,\delta}\right)^a \left(h^{k,\delta}\right)^b (V^{k,\delta} - E_{\mathrm{Na}}) \alpha U^{k,\delta}\, dt \\
& + \int_0^T \left(n^{k,\delta}\right)^c (V^{k,\delta} - E_{\mathrm{K}}) \beta U^{k,\delta}\, dt + \int_0^T (V^{k,\delta} - E_L) \gamma U^{k,\delta}\, dt \\
& - \int_0^T \left[(1-m^{k,\delta}) \alpha'_{m^{k,\delta}}(V^{k,\delta}) - m^{k,\delta} \beta'_{m^{k,\delta}}(V^{k,\delta}) \right] P^{k,\delta} W^{k,\delta}\, dt \\
& - \int_0^T \left[(1-n^{k,\delta}) \alpha'_{n^{k,\delta}}(V^{k,\delta}) - n^{k,\delta} \beta'_{n^{k,\delta}}(V^{k,\delta}) \right] Q^{k,\delta} W^{k,\delta}\, dt \\
& - \int_0^T \left[(1-h^{k,\delta}) \alpha'_{h^{k,\delta}}(V^{k,\delta}) - h^{k,\delta} \beta'_{h^{k,\delta}}(V^{k,\delta}) \right] R^{k,\delta} W^{k,\delta}\, dt.
\end{aligned} \tag{4.29}$$

Multiplying the second equation from (4.18) by $M^{k,\delta}$, and integrating in the interval $[0, T]$ it follows that

$$\begin{aligned}
& \int_0^T P_t^{k,\delta} M^{k,\delta} - \left[\alpha_{m^{k,\delta}}(V^{k,\delta}) + \beta_{m^{k,\delta}}(V^{k,\delta}) \right] P^{k,\delta} M^{k,\delta}\, dt = \\
& \qquad - \int_0^T a G_{\mathrm{Na}}^{k,\delta} \left(m^{k,\delta}\right)^{a-1} \left(h^{k,\delta}\right)^b (V^{k,\delta} - E_{\mathrm{Na}}) U^{k,\delta} M^{k,\delta}\, dt.
\end{aligned}$$

Integrating by parts the first term from the previous equation, and using the initial ($M^{k,\delta}(0) = 0$) and final ($P^{k,\delta}(T) = 0$) conditions, we have

$$\begin{aligned}
& \int_0^T \left(\dot{M}^{k,\delta} + \left[\alpha_{m^{k,\delta}}(V^{k,\delta}) + \beta_{m^{k,\delta}}(V^{k,\delta}) \right] M^{k,\delta} \right) P^{k,\delta}\, dt = \\
& \qquad \int_0^T a G_{\mathrm{Na}}^{k,\delta} \left(m^{k,\delta}\right)^{a-1} \left(h^{k,\delta}\right)^b (V^{k,\delta} - E_{\mathrm{Na}}) U^{k,\delta} M^{k,\delta}\, dt.
\end{aligned}$$

Then, from the previous equation and the second equation from ODE (4.25), for $(\mathcal{X}, \mathcal{Y}) = (M^{k,\delta}, m^{k,\delta})$,

$$\int_0^T aG_{\mathrm{K}}^{k,\delta}\left(m^{k,\delta}\right)^{a-1}\left(h^{k,\delta}\right)^{b}(V^{k,\delta} - E_{\mathrm{Na}})U^{k,\delta}M^{k,\delta}\,dt = \int_0^T \left[(1 - m^{k,\delta})\alpha'_{m^{k,\delta}}(V^{k,\delta}) - m^{k,\delta}\beta'_{m^{k,\delta}}(V^{k,\delta})\right] W^{k,\delta}P^{k,\delta}\,dt. \quad (4.30)$$

Multiplying the third equation from (4.18) by $N^{k,\delta}$, and integrating in the interval $[0, T]$ we gather that

$$\int_0^T \dot{Q}^{k,\delta}N^{k,\delta} - \left[\alpha_{n^{k,\delta}}(V^{k,\delta}) + \beta_{n^{k,\delta}}(V^{k,\delta})\right] Q^{k,\delta}N^{k,\delta}\,dt = -\int_0^T cG_{\mathrm{K}}^{k,\delta}\left(n^{k,\delta}\right)^{c-1}(V^{k,\delta} - E_{\mathrm{K}})U^{k,\delta}\,dt.$$

Integrating by parts the first term from previous equation, and using the initial $(N^{k,\delta}(0) = 0)$ and final $(Q^{k,\delta}(T) = 0)$ conditions, we have

$$\int_0^T \left(\dot{N}^{k,\delta} + \left[\alpha_{n^{k,\delta}}(V^{k,\delta}) + \beta_{n^{k,\delta}}(V^{k,\delta})\right] N^{k,\delta}\right) Q^{k,\delta}\,dt = \int_0^T cG_{\mathrm{K}}^{k,\delta}\left(n^{k,\delta}\right)^{c-1}(V^{k,\delta} - E_{\mathrm{K}})U^{k,\delta}\,dt.$$

Then, from the previous equation and the second equation from ODE (4.25), for $(\mathcal{X}, \mathcal{Y}) = (N^{k,\delta}, n^{k,\delta})$, we have

$$\int_0^T cG_{\mathrm{K}}^{k,\delta}\left(n^{k,\delta}\right)^{c-1}(V^{k,\delta} - E_{\mathrm{K}})U^{k,\delta}\,dt = \int_0^T \left[(1 - n^{k,\delta})\alpha a'_{n^{k,\delta}}(V^{k,\delta}) - n^{k,\delta}\beta'_{n^{k,\delta}}(V^{k,\delta})\right] WQ^{k,\delta}\,dt. \quad (4.31)$$

Multiplying the fourth equation from (4.18) by $H^{k,\delta}$, and integrating in the interval $[0, T]$ we gather that

$$\int_0^T \dot{R}^{k,\delta}H^{k,\delta} - \left[\alpha_{h^{k,\delta}}(V^{k,\delta}) + \beta_{h^{k,\delta}}(V^{k,\delta})\right] R^{k,\delta}H^{k,\delta}\,dt = -\int_0^T bG_{\mathrm{Na}}^{k,\delta}\left(m^{k,\delta}\right)^{a}\left(h^{k,\delta}\right)^{b-1}(V^{k,\delta} - E_{\mathrm{Na}})U^{k,\delta}\,dt.$$

Integrating by parts the first term from the previous equation, and using the initial $(H^{k,\delta}(0) = 0)$ and final $(R^{k,\delta}(T) = 0)$ conditions, we have

$$\int_0^T \left(\dot{H}^{k,\delta} + \left[\alpha_{h^{k,\delta}}(V^{k,\delta}) + \beta_{h^{k,\delta}}(V^{k,\delta})\right] H^{k,\delta}\right) R^{k,\delta}\,dt = \int_0^T bG_{\mathrm{Na}}^{k,\delta}\left(m^{k,\delta}\right)^{a}\left(h^{k,\delta}\right)^{b-1}(V^{k,\delta} - E_{\mathrm{Na}})U^{k,\delta}\,dt.$$

Then, from the previous equation and the second equation from ODE (4.25), for $(\mathcal{X}, \mathcal{Y}) = (H^{k,\delta}, h^{k,\delta})$, we have

$$\int_0^T bG_{\text{Na}}^{k,\delta}\left(m^{k,\delta}\right)^a\left(h^{k,\delta}\right)^{b-1}(V^{k,\delta} - E_{\text{Na}})U^{k,\delta}\,dt = \int_0^T \left[(1-h^{k,\delta})\alpha'_{h^{k,\delta}}(V^{k,\delta}) - h^{k,\delta}\beta'_{h^{k,\delta}}(V^{k,\delta})\right] W^{k,\delta}R^{k,\delta}\,dt. \quad (4.32)$$

Substituting equations (4.30), (4.31), and (4.32) in (4.29), we have

$$\Phi = \int_0^T \left(m^{k,\delta}\right)^a\left(h^{k,\delta}\right)^b(V^{k,\delta} - E_{\text{Na}})\theta_{\text{Na}}U^{k,\delta}\,dt + \int_0^T \left(n^{k,\delta}\right)^c(V^{k,\delta} - E_{\text{K}})\theta_{\text{K}}U^{k,\delta}\,dt + \int_0^T (V^{k,\delta} - E_L)\theta_L U^{k,\delta}\,dt. \quad (4.33)$$

Substituting equations (4.5), (4.6) and (4.7) in equation (4.33) we gather that

$$\Phi = X_{\text{Na}}^{k,\delta}\,\theta_{\text{Na}} + X_K^{k,\delta}\,\theta_{\text{K}} + X_L^{k,\delta}\,\theta_L = \left\langle\left(X_{\text{Na}}^{k,\delta}, X_K^{k,\delta}, X_L^{k,\delta}\right), (\theta_{\text{Na}}, \theta_{\text{K}}, \theta_L)\right\rangle_{\mathbb{R}^3}. \quad (4.34)$$

From (4.26) and (4.34)

$$\frac{\langle \boldsymbol{G}^{k+1,\delta} - \boldsymbol{G}^{k,\delta}, \boldsymbol{\theta}\,\rangle_{\mathbb{R}^3}}{w^{k,\delta}} = \left\langle\left(X_{\text{Na}}^{k,\delta}, X_K^{k,\delta}, X_L^{k,\delta}\right), \boldsymbol{\theta}\right\rangle_{\mathbb{R}^3}.$$

Since $\boldsymbol{\theta} \in \mathbb{R}^3$ is arbitrary, we obtain (4.4). ■

4.4.2 Proof of Theorem 4.2.1

Proof. Consider the operator F defined in (4.3). Evaluating $\boldsymbol{a}^{k,\delta}$ in F, we have $F(\boldsymbol{a}^{k,\delta}) = V^{k,\delta}$, where $V^{k,\delta}$, $m^{k,\delta}$, $n^{k,\delta}$ and $h^{k,\delta}$ solve ODE (4.17). Let $\boldsymbol{\theta} = (\theta_a, \theta_b, \theta_c) \in \mathbb{R}^3$ and $\lambda \in \mathbb{R}$, then $F(\boldsymbol{a}^{k,\delta} + \lambda\boldsymbol{\theta}) = V_\lambda^{k,\delta}$, where $V_\lambda^{k,\delta}$, $m_\lambda^{k,\delta}$, $n_\lambda^{k,\delta}$ and $h_\lambda^{k,\delta}$ solve

$$\begin{cases} C_M\dot{V}_\lambda^{k,\delta} = I_{\text{ext}} - G_{\text{Na}}\left(m_\lambda^{k,\delta}\right)^{a^{k,\delta}+\lambda\theta_a}\left(h_\lambda^{k,\delta}\right)^{b^{k,\delta}+\lambda\theta_b}\left(V_\lambda^{k,\delta} - E_{\text{Na}}\right) \\ \quad -G_{\text{K}}^{k,\delta}\left(n_\lambda^{k,\delta}\right)^{c^{k,\delta}+\lambda\theta_c}\left(V_\lambda^{k,\delta} - E_{\text{K}}\right) - G_L\left(V_\lambda^{k,\delta} - E_L\right), \\ \dot{\mathcal{X}} = (1-\mathcal{X})\alpha_{\mathcal{X}}(V^{k,\delta}) - \mathcal{X}\beta_{\mathcal{X}}(V^{k,\delta}), \quad \text{for } \mathcal{X} = m_\lambda^{k,\delta}, n_\lambda^{k,\delta}, h_\lambda^{k,\delta}, \\ V_\lambda^{k,\delta}(0) = V_0, \quad m_\lambda^{k,\delta}(0) = m_0, \quad n_\lambda^{k,\delta}(0) = n_0, \quad n_\lambda^{k,\delta}(0) = n_0. \end{cases} \quad (4.35)$$

Considering the difference between the ODEs (4.35) and (4.17), dividing by λ and taking the limit $\lambda \to 0$, we have the ODE

$$
\begin{cases}
C_M \dot{W}^{k,\delta} + \left(G_{\mathrm{Na}} \left(m^{k,\delta}\right)^{a^{k,\delta}} \left(h^{k,\delta}\right)^{b^{k,\delta}} + G_{\mathrm{K}} \left(n^{k,\delta}\right)^{c^{k,\delta}} + G_L \right) W^{k,\delta} = \\
\quad -a^{k,\delta} G_{\mathrm{Na}} \left(m^{k,\delta}\right)^{a^{k,\delta}-1} M^{k,\delta} \left(h^{k,\delta}\right)^{b^{k,\delta}} (V^{k,\delta} - E_{\mathrm{Na}}) \\
\quad -\mathsf{b} G_{\mathrm{Na}} \left(m^{k,\delta}\right)^{a^{k,\delta}} \left(h^{k,\delta}\right)^{b^{k,\delta}-1} H^{k,\delta} (V^{k,\delta} - E_{\mathrm{Na}}) \\
\quad -c^{k,\delta} G_{\mathrm{K}} \left(n^{k,\delta}\right)^{c^{k,\delta}-1} N^{k,\delta} (V^{k,\delta} - E_{\mathrm{K}}) \\
\quad -G_{\mathrm{Na}} \left(m^{k,\delta}\right)^{a^{k,\delta}} \ln(m^{k,\delta}) \left(h^{k,\delta}\right)^{b^{k,\delta}} (V^{k,\delta} - E_{\mathrm{Na}}) \theta_a \\
\quad -G_{\mathrm{Na}} \left(m^{k,\delta}\right)^{a^{k,\delta}} \left(h^{k,\delta}\right)^{b^{k,\delta}} \ln(h^{k,\delta}) (V^{k,\delta} - E_{\mathrm{Na}}) \theta_b \\
\quad -G_k \left(n^{k,\delta}\right)^{\mathsf{c}} \ln(n^{k,\delta}) (V^{k,\delta} - E_{\mathrm{K}}) \theta_c, \\
\dot{\mathcal{X}} + [\alpha_{\mathcal{Y}}(V^{k,\delta}) + \beta_{\mathcal{Y}}(V^{k,\delta})] \mathcal{X} = [(1 - \mathcal{Y}) \alpha'_{\mathcal{Y}}(V^{k,\delta}) - \mathcal{Y} \beta'_{\mathcal{Y}}(V^{k,\delta})] W^{k,\delta}, \\
\quad (\mathcal{X}, \mathcal{Y}) = (M^{k,\delta}, m^{k,\delta}), (N^{k,\delta}, n^{k,\delta}), (H^{k,\delta}, h^{k,\delta}), \\
W^{k,\delta}(0) = 0, \quad M^{k,\delta}(0) = 0, \quad N^{k,\delta}(0) = 0, \quad H^{k,\delta}(0) = 0.
\end{cases}
\tag{4.36}
$$

where $W^{k,\delta}$ is defined in equation (4.23) by replacing $\boldsymbol{G}^{k,\delta}$ by $\boldsymbol{a}^{k,\delta}$. Also, $M^{k,\delta}$, $N^{k,\delta}$ and $H^{k,\delta}$ are defined in equation (4.24).

This last equation is again a system of coupled nonlinear differential equations, parametrized by $\boldsymbol{\theta} = (\theta_a, \theta_b, \theta_c)$, where $\boldsymbol{\theta} \in \mathbb{R}^3$ is arbitrary. Considering (4.18), and proceeding as in Theorem 4.1.1, we gather (4.13). ■

5 Inverse problem of distributed parameters

The model (1.8) was originally used to explain the action potential in the long giant axon of a squid nerve cell, but the ideas have since been extended and applied to a wide variety of excitable cells. Hodgkin–Huxley theory is remarkable, not only for its influence on electrophysiology, but also for its influence, after some filtering, on applied mathematics. FitzHugh (in particular) showed how the essentials of the excitable process could be distilled into a simpler model on which mathematical analysis could make some progress. Because this simplified model turned out to be of such great theoretical interest, it contributed enormously to the formation of a new field of applied mathematics, the study of excitable systems, a field that continues to stimulate a vast amount of research Keener e Sneyd (2009).

In this chapter, we obtain approximate parameters with non-uniform distribution in the Hodgkin-Huxley and FitzHugh–Nagumo models.

Throughout the study on the estimation of parameters in Hodgkin-Huxley and FitzHugh–Nagumo models, we presented some preliminary results in the following conference:

- XXXVIII Congresso Nacional de Matemática Aplicada e Computacional (CNMAC-2018), conference or lecture of work.

In this chapter, we present a summary of Appendix C (Paper 3), this article has not yet been submitted.

5.1 Inverse problem in Hodgkin-Huxley model

In this section, we work with the Hodgkin-Huxley model, and rewriting the system of equations we have

$$\begin{cases} C_M \dfrac{\partial V}{\partial t} = I_M - G_{Na} m^3 h (V - E_{Na}) - G_K n^4 (V - E_K) - G_L (V - E_L); \\ \dfrac{\partial m}{\partial t} = (1-m)\alpha_m(V) - m\beta_m(V); \\ \dfrac{\partial n}{\partial t} = (1-n)\alpha_n(V) - n\beta_n(V); \\ \dfrac{\partial h}{\partial t} = (1-h)\alpha_h(V) - h\beta_h(V); \\ V(0) = V_0, \quad m(0) = m_0, \quad n(0) = n_0, \quad h(0) = h_0, \end{cases} \tag{5.1}$$

where the parameters C_M, I_{ext}, G_{Na}, G_K, G_L, E_{Na}, E_{K}, E_L, m_0, n_0 and h_0 are assumed to be known. Let $\boldsymbol{\alpha} = (\alpha_m \circ V, \beta_m \circ V, \alpha_n \circ V, \beta_n \circ V, \alpha_h \circ V, \beta_h \circ V)$, where $(\alpha \circ V)(t) = \alpha(V(t))$.

Here, our goal is to estimate $\boldsymbol{\alpha}$, given the membrane potential measurement, such that

$$F(\boldsymbol{\alpha}) = V, \tag{5.2}$$

where $F : (L^2[0,T])^6 \to L^2[0,T]$ is the nonlinear operator. Note that V solves equation (5.1).

From equation (2.4), for $x = \boldsymbol{\alpha}$ and $w^{k,\delta} \geq 0$, we have

$$\boldsymbol{\alpha}^{k+1,\delta} = \boldsymbol{\alpha}^{k,\delta} + w^{k,\delta} F'(\boldsymbol{\alpha}^{k,\delta})^*(V^\delta - F(\boldsymbol{\alpha}^{k,\delta})), \tag{5.3}$$

where

$$w^{k,\delta} = \frac{\|V^\delta - V^{k,\delta}\|^2_{L^2[0,T]}}{\|F'(\boldsymbol{\alpha}^{k,\delta})^*(V^\delta - F(\boldsymbol{\alpha}^{k,\delta}))\|^2_{(L[0,T])^6}}.$$

Here, we also compute the adjoint of the Gateaux derivative. Then, from iteration (5.3) and Theorem (5.1.1), we gather that

$$\boldsymbol{\alpha}^{k+1,\delta} = \boldsymbol{\alpha}^{k,\delta} + w^{k,\delta} \left(X^{k,\delta}_{\alpha_m}, X^{k,\delta}_{\beta_m}, X^{k,\delta}_{\alpha_n}, X^{k,\delta}_{\beta_n}, X^{k,\delta}_{\alpha_h}, X^{k,\delta}_{\beta_h} \right), \tag{5.4}$$

where $X^{k,\delta}_{\alpha_m}$, $X^{k,\delta}_{\beta_m}$, $X^{k,\delta}_{\alpha_n}$, $X^{k,\delta}_{\beta_n}$, $X^{k,\delta}_{\alpha_h}$ and $X^{k,\delta}_{\beta_h}$ satisfy equations (5.6), (5.7) and (5.8).

To estimate $\boldsymbol{\alpha}$, given $\boldsymbol{\alpha}^{1,\delta}$, we consider the minimal error iteration (5.4).

In the next theorem, we compute the adjoint of the Gateaux derivative from iteration (5.3).

Theorem 5.1.1. *Consider the iteration (5.3). It follows then that*

$$F'(\boldsymbol{\alpha}^{k,\delta})^*(V^\delta - F(\boldsymbol{\alpha}^{k,\delta})) = \left(X^{k,\delta}_{\alpha_m}, X^{k,\delta}_{\beta_m}, X^{k,\delta}_{\alpha_n}, X^{k,\delta}_{\beta_n}, X^{k,\delta}_{\alpha_h}, X^{k,\delta}_{\beta_h} \right), \tag{5.5}$$

where

$$X^{k,\delta}_{\alpha_m} = \left(1 - m^{k,\delta}\right) P^{k,\delta} \quad ; \quad X^{k,\delta}_{\beta_m} = -m^{k,\delta} P^{k,\delta}; \tag{5.6}$$

$$X^{k,\delta}_{\alpha_n} = \left(1 - n^{k,\delta}\right) Q^{k,\delta} \quad ; \quad X^{k,\delta}_{\beta_n} = -n^{k,\delta} Q^{k,\delta}; \tag{5.7}$$

$$X^{k,\delta}_{\alpha_h} = \left(1 - h^{k,\delta}\right) R^{k,\delta} \quad ; \quad X^{k,\delta}_{\beta_h} = -h^{k,\delta} R^{k,\delta}. \tag{5.8}$$

Given $\alpha_{\mathcal{X}}(V^{k,\delta})$ and $\beta_{\mathcal{X}}(V^{k,\delta})$ for $\mathcal{X} = m^{k,\delta}, n^{k,\delta}, h^{k,\delta}$, the functions $m^{k,\delta}$, $n^{k,\delta}$ and $h^{k,\delta}$ solve

$$\begin{cases} C_M \dot{V}^{k,\delta} = I_{ext} - G_{Na}\left(m^{k,\delta}\right)^3 \left(h^{k,\delta}\right)(V^{k,\delta} - E_{Na}) - G_K\left(n^{k,\delta}\right)^4 (V^{k,\delta} - E_K) \\ \qquad\qquad -G_L(V^{k,\delta} - E_L), \\ \dot{\mathcal{X}} = (1 - \mathcal{X})\alpha_{\mathcal{X}}(V^{k,\delta}) - \mathcal{X}\beta_{\mathcal{X}}(V^{k,\delta}) \quad \text{for } \mathcal{X} = m^{k,\delta}, n^{k,\delta}, h^{k,\delta}, \\ V^{k,\delta}(0) = V_0, \quad m^{k,\delta}(0) = m_0, \quad n^{k,\delta}(0) = n_0, \quad h^{k,\delta}(0) = h_0. \end{cases} \tag{5.9}$$

Finally, the functions $P^{k,\delta}$, $Q^{k,\delta}$ and $R^{k,\delta}$ solve, given $m^{k,\delta}$, $n^{k,\delta}$, $h^{k,\delta}$ and $V^{k,\delta}$,

$$\begin{cases} C_M\dot{U}^{k,\delta} - \Big(G_{Na}\big(m^{k,\delta}\big)^3\big(h^{k,\delta}\big) + G_K\big(n^{k,\delta}\big)^4 + G_L\Big)U^{k,\delta} \\ -[(1-m^{k,\delta})\alpha'_{m^{k,\delta}}(V^{k,\delta}) - m^{k,\delta}\beta'_{m^{k,\delta}}(V^{k,\delta})]P^{k,\delta} \\ -[(1-n^{k,\delta})\alpha'_{n^{k,\delta}}(V^{k,\delta}) - n^{k,\delta}\beta'_{n^{k,\delta}}(V^{k,\delta})]Q^{k,\delta} \\ -[(1-h^{k,\delta})\alpha'_{h^{k,\delta}}(V^{k,\delta}) - h^{k,\delta}\beta'_{h^{k,\delta}}(V^{k,\delta})]R^{k,\delta} = V^\delta - V^{k,\delta}, \\ \dot{P}^{k,\delta} - [\alpha_{m^{k,\delta}}(V^{k,\delta}) + \beta_{m^{k,\delta}}(V^{k,\delta})]P^{k,\delta} = -3G_{Na}\big(m^{k,\delta}\big)^2\big(h^{k,\delta}\big)(V^{k,\delta} - E_{Na})U^{k,\delta}, \\ \dot{Q}^{k,\delta} - [\alpha_{n^{k,\delta}}(V^{k,\delta}) + \beta_{n^{k,\delta}}(V^{k,\delta})]Q^{k,\delta} = -4G_K\big(n^{k,\delta}\big)^3(V^{k,\delta} - E_K)U^{k,\delta}, \\ \dot{R}^{k,\delta} - [\alpha_{h^{k,\delta}}(V^{k,\delta}) + \beta_{h^{k,\delta}}(V^{k,\delta})]R^{k,\delta} = -G_{Na}\big(m^{k,\delta}\big)^3(V^{k,\delta} - E_{Na})U^{k,\delta}, \\ U^{k,\delta}(T) = 0, \quad P^{k,\delta}(T) = 0, \quad Q^{k,\delta}(T) = 0, \quad R^{k,\delta}(T) = 0. \end{cases} \tag{5.10}$$

As previously mentioned, we assume that the constants C_M, I_{ext}, m_0, n_0, h_0, G_{Na}, G_K, G_L, E_{Na} ,E_K and E_L are known data. Note that $\alpha'_m(V)$ is the derivative of α_m with respect to voltage V.

Proof. See Subsection 5.4.1. ■

We next describe the computational scheme.

Data: V^δ, δ and τ
Result: Compute an approximation for $\boldsymbol{\alpha}$ using Iteration Scheme (5.4)
Choose $\boldsymbol{\alpha}^{1,\delta}$ as an initial approximation for $\boldsymbol{\alpha}$;
Compute $m^{1,\delta}$, $n^{1,\delta}$, $h^{1,\delta}$ and $V^{1,\delta}$ from (5.9), replacing $\boldsymbol{\alpha}^{k,\delta}$ by $\boldsymbol{\alpha}^{1,\delta}$;
k=1;
while $\tau\delta \leq \|V^\delta - V^{k,\delta}\|_{L^2[0,T]}$ **do**
  Compute $P^{k,\delta}$, $Q^{k,\delta}$ and $R^{k,\delta}$ from (5.10);
  Compute $\boldsymbol{\alpha}^{k+1,\delta}$ using (5.4);
  Compute $m^{k+1,\delta}$, $n^{k+1,\delta}$, $h^{k+1,\delta}$ and $V^{k+1,\delta}$ from (5.9), replacing $\boldsymbol{\alpha}^{k,\delta}$ by $\boldsymbol{\alpha}^{k+1,\delta}$;
  $k \leftarrow k+1$;
end
Algorithm 5: Minimal error iteration to obtain functions in the H-H model

5.2 Inverse problem in FitzHugh–Nagumo model

In this Section, we consider FitzHugh–Nagumo equation (1.10). Then, rewriting this model we obtain

$$\begin{cases} \dfrac{\partial V}{\partial t} = I + g(V) - \upsilon, \\ \dfrac{\partial \upsilon}{\partial t} = bV - c\upsilon, \\ V(0) = V_0; \quad \upsilon(0) = \upsilon_0, \end{cases} \tag{5.11}$$

where the constants I, b, c, V_0 and υ_0 are known, and the function $\boldsymbol{g} = g(V)$ is unknown. Consider the nonlinear operator $F : L^2[0,T] \to L^2[0,T]$ defined by

$$F(\boldsymbol{g}) = V, \tag{5.12}$$

where V solves (5.11). The current goal is to estimate $\boldsymbol{g}$, given V^δ. From iteration (2.4), for $x = \boldsymbol{g}$ and $w^{k,\delta} \geq 0$, we have

$$\boldsymbol{g}^{k+1,\delta} = \boldsymbol{g}^{k,\delta} + w^{k,\delta} F'(\boldsymbol{g}^{k,\delta})^*(V^\delta - F(\boldsymbol{g}^{k,\delta})), \tag{5.13}$$

where

$$w^{k,\delta} = \frac{\|V^\delta - V^{k,\delta}\|^2_{L^2[0,T]}}{\|F'(\boldsymbol{g}^{k,\delta})^*(V^\delta - F(\boldsymbol{g}^{k,\delta}))\|^2_{(L[0,T])^6}}.$$

From equation (5.13) and Theorem 5.2.1, we have the following iteration

$$\boldsymbol{g}^{k+1,\delta} = \boldsymbol{g}^{k,\delta} + w^{k,\delta} U^{k,\delta}, \tag{5.14}$$

where $U^{k,\delta}$ solves equation (5.17).

To obtain an approximation for $\boldsymbol{g}$, given $\boldsymbol{g}^{1,\delta}$, we used the minimal error method (5.14).

In the next theorem, we compute the adjoint of the Gateaux derivative from algorithm (5.13).

Theorem 5.2.1. *Consider the iteration* (5.13)*. It follows then that*

$$F'(\boldsymbol{g}^{k,\delta})^*(V^\delta - F(\boldsymbol{g}^{k,\delta})) = U^{k,\delta}. \tag{5.15}$$

Given $\boldsymbol{g}^{k,\delta}$, the functions $V^{k,\delta}$ and $\upsilon^{k,\delta}$ solve

$$\begin{cases} \dot{V}^{k,\delta} = I + \boldsymbol{g}^{k,\delta} - \upsilon^{k,\delta}; \\ \dot{\upsilon}^{k,\delta} = bV^{k,\delta} - c\upsilon^{k,\delta}; \\ V(0) = V_0, \quad \upsilon(0) = \upsilon_0. \end{cases} \tag{5.16}$$

Finally, $U^{k,\delta}$ solves, given $V^{k,\delta}$ and $\boldsymbol{g}^{k,\delta}$,

$$\begin{cases} \dot{U}^{k,\delta} + \boldsymbol{g}^{k,\delta\prime} U^{k,\delta} - bP^{k,\delta} = V^{\delta} - V^{k,\delta}, \\ \dot{P}^{k,\delta} - cP^{k,\delta} = -U^{k,\delta}, \\ U^{k,\delta}(T) = 0; \quad P^{k,\delta}(T) = 0, \end{cases} \tag{5.17}$$

where $\boldsymbol{g}^{k,\delta\prime}$ is the derivative of $g^{k,\delta}$ with respect to $V^{k,\delta.}$.

As previously mentioned, we assume that the constants b, c, V_0, v_0 and I are known data.

Proof. See Subsection 5.4.2. ■

We next describe the computational scheme.

Data: V^{δ}, δ and τ
Result: Compute an approximation for $\boldsymbol{g}$ using Iteration Scheme (5.14)
Choose $\boldsymbol{g}^{1,\delta}$ as an initial approximation for $\boldsymbol{g}$;
Compute $r^{1,\delta}$ and $V^{1,\delta}$ from (5.16), replacing $\boldsymbol{g}^{k,\delta}$ by $\boldsymbol{g}^{1,\delta}$;
k=1;
while $\tau\delta \leq \|V^{\delta} - V^{k,\delta}\|_{L^2[0,T]}$ **do**
  Compute $U^{k,\delta}$ from (5.17);
  Compute $\boldsymbol{g}^{k+1,\delta}$ using (5.14);
  Compute $r^{k+1,\delta}$ and $V^{k+1,\delta}$ from (5.16), replacing $\boldsymbol{g}^{k,\delta}$ by $\boldsymbol{g}^{k+1,\delta}$;
  $k \leftarrow k+1$;
end

Algorithm 6: Minimal error iteration to obtain one function in the F-N model

5.3 Numerical simulations

In Section 5.1, we consider and obtain analytical results for six unknown functions. In computational experiments, we estimate only one function $\boldsymbol{\alpha} = \alpha_n(V)$, from equation (5.1).

In this section, we consider two examples. The first one is to estimate $x = \boldsymbol{\alpha}$ from (5.1), given V^{δ}. For the second example, the goal is to estimate $x = \boldsymbol{g}$ from (5.11), given V^{δ}.

To design our numerical experiments, we first choose x ($x = \boldsymbol{\alpha}$ or $x = \boldsymbol{g}$) and compute V from (5.1) or (5.11), obtaining then V. In our examples, for a given δ, the noisy V^{δ} is obtained by

$$V^{\delta}(t) = V(t) + V(t)\text{rand}_{\varepsilon}(t), \quad \text{for all } t \in [0,T] \tag{5.18}$$

where $\text{rand}_{\varepsilon}$ is a uniformly distributed random variable in the interval $[-\varepsilon, \varepsilon]$, and $\varepsilon = \delta/\|V\|_{L^2[0,T]}$. Now, we consider V and x unknown.

Next, given the initial guess $x^{1,\delta}$, V^δ and δ, we start to recover x using either Algorithm 5 (for $x = \boldsymbol{\alpha}$) or Algorithm 6 (for $x = \boldsymbol{g}$).

In practice, after discretizing the equations and the unknown functions, only nodal values are know. Consider the space-time discretization $t_n = (n-1)T/(N-1)$ for $n = 1, 2, \cdots, N$. Thus, the relative error introduced above relates to the the mean absolute percentage error

$$Error_k = \frac{T}{N} \sum_{n=1}^{N} \left| \frac{x(t_n) - x^{k,\delta}(t_n)}{x(t_n)} \right| \times 100\%, \quad k = 1, 2 \cdots, k_*. \tag{5.19}$$

Example 5.1. *This example is a particular case from (5.1), where the fixed parameters are:* $T = 4$ $[ms]$, $C = 1$ $[\mu F/cm^2]$, $I_{ext} = 5$ $[\mu A/cm^2]$, $E_{Na} = 115$ $[mV]$, $E_K = -12$ $[mV]$, $E_L = 10.6$ $[mV]$, $G_{Na} = 120$ $[mS/cm^2]$, $G_K = 36$ $[mS/cm^2]$, $G_L = 0.3$ $[mS/cm^2]$ *and* $N = 100$. *The initial conditions are:* $V(0) = -20$ $[mV]$, $m(0) = 0.1$, $n(0) = 0.2$ *and* $h(0) = 0.5$. *Given* V^δ, *the goal of this example is to estimate*

$$\beta_n(V) = 0.125 \exp(V/80).$$

In this test, we consider the initial guess $\beta_n^{1,\delta} = 0$ *and* $\tau = 2.01$. *Table 5 presents the results for various levels of noise. In Figures 19 and 20 we show the convergence of the method* ($\epsilon = 0.0001\%$ *of noise*).

ε	k_*	$Error_{k_*}$	$Time$ (s)
100%	1	100 %	4×10^{-5}
10%	11	35 %	1×10^{-2}
1%	43	31 %	3×10^{-2}
0.1%	1030	15 %	8×10^{-1}
0.01%	11498	6.6 %	9×10^{0}
0.001%	84045	1.8 %	66×10^{0}
0.0001%	412201	0.7 %	323×10^{0}

Table 5 – Numerical results for Example 5.1, for various values of ε, as in (4.20). The second column contains the number of iterations according to (2.5). The third column is the mean absolute percentage error of $x = \beta_n$ according to (5.19). The last column is the running time of the algorithm, in seconds.

Example 5.2. *This example is a particular case from (5.11), where the fixed parameters are:* $T = 10$, $N = 1000$, $I_{ext} = 5$, $b = 0.05$ *and* $c = 0.01$. *The initial conditions are:* $V(0) = -5$ *and* $\upsilon(0) = 10$. *Given* V^δ, *the goal of this example is to find* $\boldsymbol{g} = V(a-V)(V-1)$ *for* $a = 0.5$.

In this test, we consider the initial guess $\boldsymbol{g}^{1,\delta} = 0$ *and* $\tau = 2.01$. *Table 6 presents the results for various levels of noise. In Figures (21) and (22), we plot results to show the convergence of the method (*$\epsilon = 0.01\%$ *of noise).*

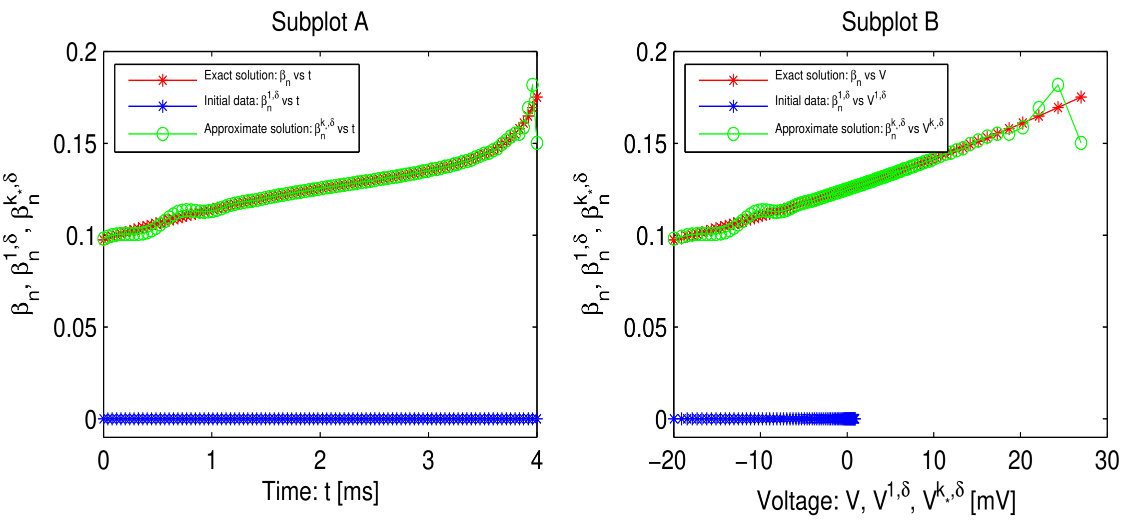

Figure 19 – Example 5.1. For the Subplots A and B, the red lines are the exact solution, the blue lines are the initial guesses and the green lines are the approximation for $\varepsilon = 0.0001\%$. In Subplot A, we present the parameters β_n, $\beta_n^{1,\delta}$ and $\beta_n^{k_*,\delta}$ as a function of time. In Subplot B, we show the parameters β_n, $\beta_n^{1,\delta}$ and $\beta_n^{k_*,\delta}$ as a function of V, $V^{1,\delta}$ and $V^{k_*,\delta}$, respectively.

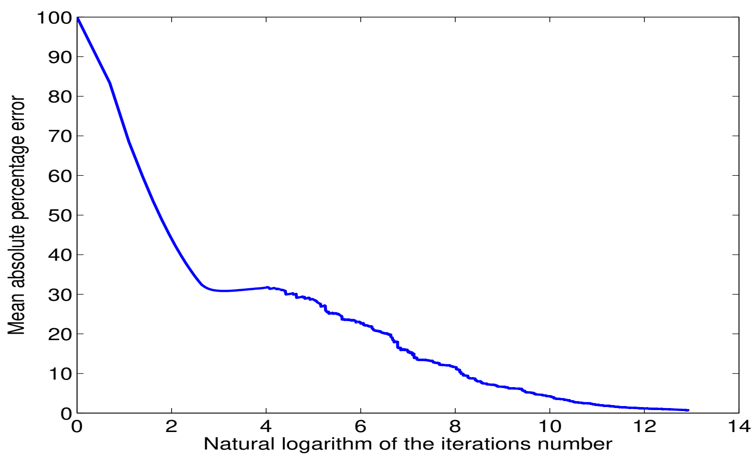

Figure 20 – Convergence results for Example 5.1. This figure displays the mean absolute percentage error between β_n and $\beta_n^{k,\delta}$ as a function of the natural logarithm of the iteration k.

ε	k_*	$Error_{k_*}$	$Time\ \ (s)$
100%	4	20 %	3×10^{-3}
10%	212	6 %	2×10^{-1}
1%	12224	3 %	9×10^{0}
0.1%	133134	1 %	94×10^{0}
0.01%	658496	0.02 %	464×10^{0}

Table 6 – Numerical results for Example 5.2. See Table 5 for a description of the contents.

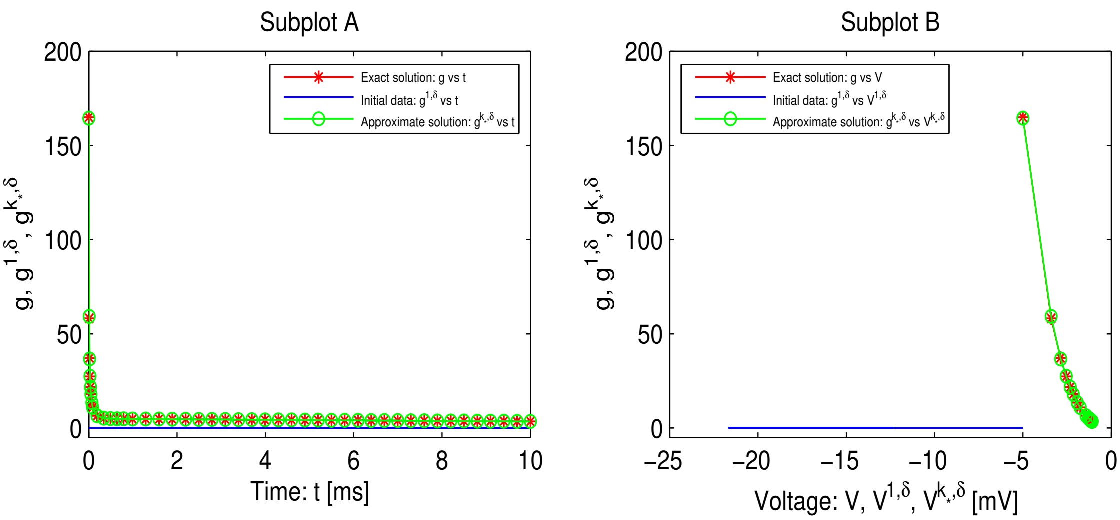

Figure 21 – Example 5.2. For the Subplots A and B, the red lines are the exact solution, the blue lines are the initial guesses and the green lines are the approximation for $\varepsilon = 0.01\%$. In Subplot A, we present the parameters $\boldsymbol{g}$, $\boldsymbol{g}^{1,\delta}$ and $\boldsymbol{g}^{k_*,\delta}$ as a function of time. In Subplot B, we show the parameters $\boldsymbol{g}$, $\boldsymbol{g}^{1,\delta}$ and $\boldsymbol{g}^{k_*,\delta}$ as a function of V, $V^{1,\delta}$ and $V^{k_*,\delta}$, respectively.

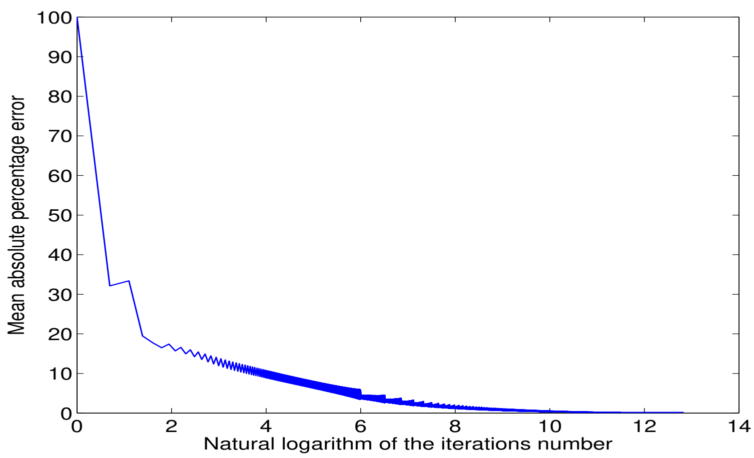

Figure 22 – Convergence results for Example 5.2. This figure displays the mean absolute percentage error between $\boldsymbol{g}$ and $\boldsymbol{g}^{k,\delta}$ as a function of the natural logarithm of the iteration k.

5.4 Detailed proofs of Theorems 5.1.1 and 5.2.1

5.4.1 Proof of Theorem 5.1.1

Proof. Consider the operator F defined in (5.2). Evaluating $\boldsymbol{\alpha}^{k,\delta}$ in F, we have $F(\boldsymbol{\alpha}^{k,\delta}) = V^{k,\delta}$, where $V^{k,\delta}$, $m^{k,\delta}$, $n^{k,\delta}$ and $h^{k,\delta}$ solve the ODE (5.9).

Let the vector $\boldsymbol{\theta} = (\theta_{\alpha_m}, \theta_{\beta_m}, \theta_{\alpha_n}, \theta_{\beta_n}, \theta_{\alpha_h}, \theta_{\beta_h}) \in (L^2[0,T])^6$ and $\lambda \in \mathbb{R}$, then evaluating $\boldsymbol{\alpha} + \lambda\boldsymbol{\theta}$ in the operator F, we have $F(\boldsymbol{\alpha} + \lambda\boldsymbol{\theta}) = V_\lambda^{k,\delta}$, where $V_\lambda^{k,\delta}$ solves

$$\begin{cases} C\dot{V}_\lambda^{k,\delta} = I_{ext} - G_{Na}\Big(m_\lambda^{k,\delta}\Big)^3\Big(h_\lambda^{k,\delta}\Big)(V_\lambda^{k,\delta} - E_{Na}) \\ \qquad\qquad -G_K\Big(n_\lambda^{k,\delta}\Big)^4(V_\lambda^{k,\delta} - E_K) - G_L(V_\lambda^{k,\delta} - E_L), \\ \dot{m}_\lambda^{k,\delta} = (1 - m_\lambda^{k,\delta})\left[\alpha_{m_\lambda^{k,\delta}}(V_\lambda^{k,\delta}) + \lambda\theta_{\alpha_m}\right] - \left[m_\lambda^{k,\delta}\beta_{m_\lambda^{k,\delta}}(V_\lambda^{k,\delta}) + \lambda\theta_{\beta_m}\right], \\ \dot{n}_\lambda^{k,\delta} = (1 - n_\lambda^{k,\delta})\left[\alpha_{n_\lambda^{k,\delta}}(V_\lambda^{k,\delta}) + \lambda\theta_{\alpha_n}\right] - \left[n_\lambda^{k,\delta}\beta_{n_\lambda^{k,\delta}}(V_\lambda^{k,\delta}) + \lambda\theta_{\beta_n}\right], \\ \dot{h}_\lambda^{k,\delta} = (1 - h_\lambda^{k,\delta})\left[\alpha_{h_\lambda^{k,\delta}}(V_\lambda^{k,\delta}) + \lambda\theta_{\alpha_h}\right] - \left[h_\lambda^{k,\delta}\beta_{h_\lambda^{k,\delta}}(V_\lambda^{k,\delta}) + \lambda\theta_{\beta_h}\right], \\ V_\lambda^{k,\delta}(0) = V_0; \quad m_\lambda^{k,\delta}(0) = m_0; \quad n_\lambda^{k,\delta}(0) = n_0; \quad h_\lambda^{k,\delta}(0) = h_0. \end{cases} \tag{5.20}$$

The Gateaux derivative of F at $\boldsymbol{\alpha}^{k,\delta}$ in the direction $\boldsymbol{\theta}$ is given by

$$F'(\boldsymbol{\alpha}^{k,\delta})(\boldsymbol{\theta}) = \lim_{\lambda\to 0}\frac{F(\boldsymbol{\alpha}^{k,\delta} + \lambda\boldsymbol{\theta}) - F(\boldsymbol{\alpha}^{k,\delta})}{\lambda} = W^{k,\delta}. \tag{5.21}$$

Also, we denote the following limits

$$M^{k,\delta} = \lim_{\lambda\to 0}\frac{m_\lambda^{k,\delta} - m^{k,\delta}}{\lambda}, \qquad N^{k,\delta} = \lim_{\lambda\to 0}\frac{n_\lambda^{k,\delta} - n^{k,\delta}}{\lambda}, \qquad H^{k,\delta} = \lim_{\lambda\to 0}\frac{h_\lambda^{k,\delta} - h^{k,\delta}}{\lambda}, \tag{5.22}$$

where $M^{k,\delta}$, $N^{k,\delta}$ and $H^{k,\delta}$ are the Gateaux derivatives of $m^{k,\delta}$, $n^{k,\delta}$ and $h^{k,\delta}$, respectively.

Considering the difference between the ODEs (5.20) and (5.9), dividing by λ and taking the limit $\lambda \to 0$, we have the following ODE

$$\begin{cases} C\dot{W}^{k,\delta} + \left(G_{Na}\Big(m^{k,\delta}\Big)^3\Big(h^{k,\delta}\Big) + G_K\Big(n^{k,\delta}\Big)^4 + G_L\right)W^{k,\delta} = \\ \qquad -3G_{Na}\Big(m^{k,\delta}\Big)^2 M^{k,\delta}h^{k,\delta}(V^{k,\delta} - E_{Na}) \\ \qquad -G_{Na}\Big(m^{k,\delta}\Big)^3 H^{k,\delta}(V^{k,\delta} - E_{Na}) \\ \qquad -4G_K\Big(n^{k,\delta}\Big)^3 N^{k,\delta}(V^{k,\delta} - E_K), \\ \dot{M}^{k,\delta} + [\alpha_{m^{k,\delta}}(V^{k,\delta}) + \beta_{m^{k,\delta}}(V^{k,\delta})]M^{k,\delta} = \\ \left[(1 - m^{k,\delta})\alpha'_{m^{k,\delta}}(V^{k,\delta}) - m^{k,\delta}\beta'_{m^{k,\delta}}(V^{k,\delta})\right]W^{k,\delta} + (1 - m^{k,\delta})\theta_{\alpha_m} - m^{k,\delta}\theta_{\beta_m}, \\ \dot{N}^{k,\delta} + [\alpha_{n^{k,\delta}}(V^{k,\delta}) + \beta_{n^{k,\delta}}(V^{k,\delta})]N^{k,\delta} = \\ \left[(1 - n^{k,\delta})\alpha'_{n^{k,\delta}}(V^{k,\delta}) - n^{k,\delta}\beta'_{n^{k,\delta}}(V^{k,\delta})\right]W^{k,\delta} + (1 - n^{k,\delta})\theta_{\alpha_n} - n^{k,\delta}\theta_{\beta_n}, \\ \dot{H}^{k,\delta} + [\alpha_{h^{k,\delta}}(V^{k,\delta}) + \beta_{h^{k,\delta}}(V^{k,\delta})]H^{k,\delta} = \\ \left[(1 - h^{k,\delta})\alpha'_{h^{k,\delta}}(V^{k,\delta}) - h^{k,\delta}\beta'_{h^{k,\delta}}(V^{k,\delta})\right]W^{k,\delta} + (1 - h^{k,\delta})\theta_{\alpha_h} - h^{k,\delta}\theta_{\beta_h}, \\ W^{k,\delta}(0) = 0; \quad M^{k,\delta}(0) = 0; \quad N^{k,\delta}(0) = 0; \quad H^{k,\delta}(0) = 0. \end{cases} \tag{5.23}$$

This last equation is yet another system of coupled nonlinear differential equations, depending on the parameter $\boldsymbol{\theta}$. Note that the variable $\boldsymbol{\theta}$ represent any point in space $\left(L^2[0,T]\right)^6$.

From Landweber iteration (5.3) and $\boldsymbol{\theta} \in (L^2[0,T])^6$ arbitrary, we have

$$\begin{aligned}\langle \boldsymbol{\alpha}^{k+1,\delta} - \boldsymbol{\alpha}^{k,\delta}, \boldsymbol{\theta} \rangle_{(L^2[0,T])^6} &= w^{k,\delta} \langle F'(\boldsymbol{\alpha}^{k,\delta})^*(V^\delta - F(\boldsymbol{\alpha}^{k,\delta})), \boldsymbol{\theta} \rangle_{(L^2[0,T])^6}, \\ &= w^{k,\delta} \langle F'(\boldsymbol{\alpha}^{k,\delta})^*(V^\delta - V^{k,\delta}), \boldsymbol{\theta} \rangle_{(L^2[0,T])^6}.\end{aligned}$$

By the definition of adjunct operator

$$\langle \boldsymbol{\alpha}^{k+1,\delta} - \boldsymbol{\alpha}^{k,\delta}, \boldsymbol{\theta} \rangle_{(L^2[0,T])^6} = w^{k,\delta} \langle V^\delta - V^{k,\delta}, F'(\boldsymbol{\alpha}^{k,\delta}).(\boldsymbol{\theta}) \rangle_{L^2[0,T]}.$$

From (5.21) and the previous equation,

$$\langle \boldsymbol{\alpha}^{k+1,\delta} - \boldsymbol{\alpha}^{k,\delta}, \boldsymbol{\theta} \rangle_{(L^2[0,T])^6} = w^{k,\delta} \langle V^\delta - V^{k,\delta}, W^{k,\delta} \rangle_{L^2[0,T]}.$$

We denote the last equality by Φ, then

$$\Phi = \frac{\langle \boldsymbol{\alpha}^{k+1,\delta} - \boldsymbol{\alpha}^{k,\delta}, \boldsymbol{\theta} \rangle_{(L^2[0,T])^6}}{w^{k,\delta}} = \langle V^\delta - V^{k,\delta}, W^{k,\delta} \rangle_{L^2[0,T]}. \tag{5.24}$$

By the definition of inner product in $L^2[0,T]$

$$\Phi = \int_0^T (V^\delta - V^{k,\delta}) W^{k,\delta} \, dt.$$

From the previous equation and the first equality from ODE (5.10), we obtain the following expression

$$\begin{aligned}\Phi &= \int_0^T \left(C_M \dot{U}^{k,\delta} W^{k,\delta} - \left(G_{Na} \left(m^{k,\delta} \right)^3 \left(h^{k,\delta} \right) + G_K \left(n^{k,\delta} \right)^4 + G_L \right) U^{k,\delta} W^{k,\delta} \right) \, dt \\ &\quad - \int_0^T \left[(1 - m^{k,\delta}) \alpha'_{m^{k,\delta}}(V^{k,\delta}) - m^{k,\delta} \beta'_{m^{k,\delta}}(V^{k,\delta}) \right] P^{k,\delta} W^{k,\delta} \, dt \\ &\quad - \int_0^T \left[(1 - n^{k,\delta}) \alpha'_{n^{k,\delta}}(V^{k,\delta}) - n^{k,\delta} \beta'_{n^{k,\delta}}(V^{k,\delta}) \right] Q^{k,\delta} W^{k,\delta} \, dt \\ &\quad - \int_0^T \left[(1 - h^{k,\delta}) \alpha'_{h^{k,\delta}}(V^{k,\delta}) - h^{k,\delta} \beta'_{h^{k,\delta}}(V^{k,\delta}) \right] R^{k,\delta} W^{k,\delta} \, dt.\end{aligned} \tag{5.25}$$

Integrating by parts the first term from equation (5.25), and initial (see (5.23), $W^{k,\delta}(0) = 0$) and final (see (5.10), $U^{k,\delta}(T) = 0$) conditions, we obtain

$$\int_0^T C_M \dot{U}^{k,\delta} W^{k,\delta} dt = - \int_0^T C_M U^{k,\delta} \dot{W}^{k,\delta} dt. \tag{5.26}$$

Replacing equation (5.26) in (5.25), we have the following equality

$$\begin{aligned}\Phi &= - \int_0^T \left(C \dot{W}^{k,\delta} + \left(G_{Na} \left(m^{k,\delta} \right)^3 \left(h^{k,\delta} \right) + G_K \left(n^{k,\delta} \right)^4 + G_L \right) W^{k,\delta} \right) U^{k,\delta} \, dt \\ &\quad - \int_0^T \left[(1 - m^{k,\delta}) \alpha'_{m^{k,\delta}}(V^{k,\delta}) - m^{k,\delta} \beta'_{m^{k,\delta}}(V^{k,\delta}) \right] P^{k,\delta} W^{k,\delta} \, dt \\ &\quad - \int_0^T \left[(1 - n^{k,\delta}) \alpha'_{n^{k,\delta}}(V^{k,\delta}) - n^{k,\delta} \beta'_{n^{k,\delta}}(V^{k,\delta}) \right] Q^{k,\delta} W^{k,\delta} \, dt \\ &\quad - \int_0^T \left[(1 - h^{k,\delta}) \alpha'_{h^{k,\delta}}(V^{k,\delta}) - h^{k,\delta} \beta'_{h^{k,\delta}}(V^{k,\delta}) \right] R^{k,\delta} W^{k,\delta} \, dt.\end{aligned}$$

Replacing the first equality from ODE (5.23) in the first integral from the previous equation, we obtain

$$\begin{aligned}\Phi \;=\; & \int_0^T 3G_{Na}\Big(m^{k,\delta}\Big)^2 M^{k,\delta}\left(h^{k,\delta}\right)(V^{k,\delta}-E_{Na})U^{k,\delta}\,dt \\ & + \int_0^T G_{Na}\Big(m^{k,\delta}\Big)^3 H^{k,\delta}(V^{k,\delta}-E_{Na})U^{k,\delta}\,dt \\ & + \int_0^T 4G_K\Big(n^{k,\delta}\Big)^3 N^{k,\delta}(V^{k,\delta}-E_K)U^{k,\delta}\,dt \\ & - \int_0^T \Big[(1-m^{k,\delta})\alpha'_{m^{k,\delta}}(V^{k,\delta}) - m^{k,\delta}\beta'_{m^{k,\delta}}(V^{k,\delta})\Big] P^{k,\delta}W^{k,\delta}\,dt \\ & - \int_0^T \Big[(1-n^{k,\delta})\alpha'_{n^{k,\delta}}(V^{k,\delta}) - n^{k,\delta}\beta'_{n^{k,\delta}}(V^{k,\delta})\Big] Q^{k,\delta}W^{k,\delta}\,dt \\ & - \int_0^T \Big[(1-h^{k,\delta})\alpha'_{h^{k,\delta}}(V^{k,\delta}) - h^{k,\delta}\beta'_{h^{k,\delta}}(V^{k,\delta})\Big] R^{k,\delta}W^{k,\delta}\,dt.\end{aligned} \tag{5.27}$$

Multiplying the second equation from (5.10) by $M^{k,\delta}$, and integrating in the interval $[0,T]$ we gather that

$$\begin{aligned}\int_0^T \Big(\dot{P}^{k,\delta}M^{k,\delta} - \Big[\alpha_{m^{k,\delta}}(V^{k,\delta}) + \beta_{m^{k,\delta}}(V^{k,\delta})\Big] P^{k,\delta}M^{k,\delta}\Big)\,dt = \\ -\int_0^T \Big(3G_{Na}\Big(m^{k,\delta}\Big)^2\left(h^{k,\delta}\right)(V^{k,\delta}-E_{Na})U^{k,\delta}M^{k,\delta}\Big)\,dt.\end{aligned}$$

Integrating by parts the first term from the previous equation, and initial (see (5.23), $M^{k,\delta}(0)=0$) and final (see (5.10), $P^{k,\delta}(T)=0$) conditions, we have

$$\begin{aligned}\int_0^T \Big(\dot{M}^{k,\delta} + \Big[\alpha_{m^{k,\delta}}(V^{k,\delta}) + \beta_{m^{k,\delta}}(V^{k,\delta})\Big] M^{k,\delta}\Big) P^{k,\delta}\,dt = \\ \int_0^T 3G_{Na}\Big(m^{k,\delta}\Big)^2\left(h^{k,\delta}\right)(V^{k,\delta}-E_{Na})U^{k,\delta}M^{k,\delta}\,dt,\end{aligned}$$

Then, from the previous equation and the second equation from ODE (5.23), we have

$$\begin{aligned}\int_0^T 3G_{Na}\Big(m^{k,\delta}\Big)^2\left(h^{k,\delta}\right)(V^{k,\delta}-E_{Na})U^{k,\delta}M^{k,\delta}\,dt = \\ \int_0^T \Big[(1-m^{k,\delta})\alpha'_{m^{k,\delta}}(V^{k,\delta}) - m^{k,\delta}\beta'_{m^{k,\delta}}(V^{k,\delta})\Big] W^{k,\delta}P^{k,\delta}\,dt \\ + \int_0^T (1-m^{k,\delta})\theta_{\alpha_m}P^{k,\delta}dt - \int_0^T m^{k,\delta}\theta_{\beta_m}P^{k,\delta}dt.\end{aligned} \tag{5.28}$$

Multiplying the third equation from (5.10) by $N^{k,\delta}$, and integrating in the interval $[0,T]$ we gather that

$$\begin{aligned}\int_0^T \dot{Q}^{k,\delta}N^{k,\delta} - \Big[\alpha_{n^{k,\delta}}(V^{k,\delta}) + \beta_{n^{k,\delta}}(V^{k,\delta})\Big] Q^{k,\delta}N^{k,\delta}\,dt = \\ -\int_0^T 4G_K\Big(n^{k,\delta}\Big)^3(V^{k,\delta}-E_K)U^{k,\delta}N^{k,\delta}\,dt.\end{aligned}$$

Integrating for parts the first term of the previous equation, and initial (see (5.23), $N^{k,\delta}(0) = 0$) and final (see (5.10), $Q^{k,\delta}(T) = 0$) conditions, we have

$$\int_0^T \left(\dot{N}^{k,\delta} + \left[\alpha_{n^{k,\delta}}(V^{k,\delta}) + \beta_{n^{k,\delta}}(V^{k,\delta})\right] N^{k,\delta}\right) Q^{k,\delta}\, dt = \int_0^T 4G_K\left(n^{k,\delta}\right)^3 (V^{k,\delta} - E_K) U^{k,\delta}\, dt$$

Then, from the previous equation and the third equation from ODE (5.23), we gather

$$\int_0^T 4G_K\left(n^{k,\delta}\right)^3 (V^{k,\delta} - E_K) U^{k,\delta}\, dt = \int_0^T \left[(1-n^{k,\delta})\alpha'_{n^{k,\delta}}(V^{k,\delta}) - n^{k,\delta}\beta'_{n^{k,\delta}}(V^{k,\delta})\right] W Q^{k,\delta}\, dt. + \int_0^T (1-n^{k,\delta})\theta_{\alpha_n} Q^{k,\delta} dt - \int_0^T n^{k,\delta}\theta_{\beta_n} Q^{k,\delta} dt. \quad (5.29)$$

Multiplying the fourth equation from (5.10) by $H^{k,\delta}$, and integrating in the interval $[0, T]$ we gather that

$$\int_0^T \dot{R}^{k,\delta} H^{k,\delta} - \left[\alpha_{h^{k,\delta}}(V^{k,\delta}) + \beta_{h^{k,\delta}}(V^{k,\delta})\right] R^{k,\delta} H^{k,\delta}\, dt = -\int_0^T G_{Na}^{k,\delta}\left(m^{k,\delta}\right)^3 (V^{k,\delta} - E_{Na}) U^{k,\delta}\, dt$$

Integrating for parts the first term of the previous equation, and using the initial conditions $H^{k,\delta}(0) = 0$ and $R^{k,\delta}(0) = 0$ we have,

$$\int_0^T \left(\dot{H}^{k,\delta} + \left[\alpha_{h^{k,\delta}}(V^{k,\delta}) + \beta_{h^{k,\delta}}(V^{k,\delta})\right] H^{k,\delta}\right) R^{k,\delta}\, dt = \int_0^T G_{Na}\left(m^{k,\delta}\right)^3 (V^{k,\delta} - E_{Na}) U^{k,\delta}\, dt,$$

Then, from the previous equation and the fourth equation from ODE (5.23), we have

$$\int_0^T G_{Na}\left(m^{k,\delta}\right)^3 (V^{k,\delta} - E_{Na}) U^{k,\delta}\, dt = \int_0^T \left[(1-h^{k,\delta})\alpha'_{h^{k,\delta}}(V^{k,\delta}) - h^{k,\delta}\beta'_{h^{k,\delta}}(V^{k,\delta})\right] W^{k,\delta} R^{k,\delta}\, dt. + \int_0^T (1-h^{k,\delta})\theta_{\alpha_h} R^{k,\delta} dt - \int_0^T h^{k,\delta}\theta_{\beta_h} R^{k,\delta} dt. \quad (5.30)$$

Substituting the equations (5.28), (5.29), and (5.30) in the equation (5.27), leads to

$$\Phi = \int_0^T (1-m^{k,\delta})\theta_{\alpha_m} P^{k,\delta} dt - \int_0^T m^{k,\delta}\theta_{\beta_m} P^{k,\delta} dt + \int_0^T (1-n^{k,\delta})\theta_{\alpha_n} Q^{k,\delta} dt - \int_0^T n^{k,\delta}\theta_{\beta_n} Q^{k,\delta} dt + \int_0^T (1-h^{k,\delta})\theta_{\alpha_h} R^{k,\delta} dt - \int_0^T h^{k,\delta}\theta_{\beta_h} R^{k,\delta} dt. \quad (5.31)$$

Replacing equations (5.6), (5.7) and (5.8) into (5.31) we gather that

$$\Phi = \int_0^T X^{k,\delta}_{\alpha_m}\theta_{\alpha_m} dt + \int_0^T X^{k,\delta}_{\beta_m}\theta_{\beta_m} dt + \int_0^T X^{k,\delta}_{\alpha_n}\theta_{\alpha_n} dt + \int_0^T X^{k,\delta}_{\beta_n}\theta_{\beta_n} dt + \int_0^T X^{k,\delta}_{\alpha_h}\theta_{\alpha_h} dt + \int_0^T X^{k,\delta}_{\beta_h}\theta_{\beta_h} dt.$$

Then from previous equation, we have

$$\Phi = \left\langle \left(X^{k,\delta}_{\alpha_m}, X^{k,\delta}_{\beta_m}, X^{k,\delta}_{\alpha_n}, X^{k,\delta}_{\beta_n}, X^{k,\delta}_{\alpha_h}, X^{k,\delta}_{\beta_h}\right), \boldsymbol{\theta} \right\rangle_{(L^2[0,T])^6}. \tag{5.32}$$

From (5.24) and (5.32)

$$\frac{\langle \boldsymbol{\alpha}^{k+1,\delta} - \boldsymbol{\alpha}^{k,\delta}, \boldsymbol{\theta} \rangle_{(L^2[0,T])^6}}{w^{k,\delta}} = \left\langle \left(X^{k,\delta}_{\alpha_m}, X^{k,\delta}_{\beta_m}, X^{k,\delta}_{\alpha_n}, X^{k,\delta}_{\beta_n}, X^{k,\delta}_{\alpha_h}, X^{k,\delta}_{\beta_h}\right), \boldsymbol{\theta} \right\rangle_{(L^2[0,T])^6}.$$

Since $\boldsymbol{\theta} \in (L^2[0,T])^6$ is arbitrary, we have (5.5) ∎

5.4.2 Proof of Theorem 5.2.1

Proof. As in Subsection 5.4.2, the operator F is defined in (5.12). Evaluating $\boldsymbol{g}^{k,\delta}$ in F, we have $F(\boldsymbol{g}^{k,\delta}) = V^{k,\delta}$, where $V^{k,\delta}$ and $\upsilon^{k,\delta}$ solve ODE (5.16). Let $\boldsymbol{\theta} \in L^2[0,T]$ and $\lambda \in \mathbb{R}$, then $F(\boldsymbol{g}^{k,\delta} + \lambda\boldsymbol{\theta}) = V^{k,\delta}_\lambda$, where $V^{k,\delta}_\lambda$ and $\upsilon^{k,\delta}_\lambda$ solve

$$\begin{cases} \dot{V}^{k,\delta}_\lambda = I_{ext} + g^{k,\delta}(V^{k,\delta}_\lambda) + \lambda\boldsymbol{\theta} - \upsilon^{k,\delta}_\lambda, \\ \dot{\upsilon}^{k,\delta}_\lambda = bV^{k,\delta}_\lambda - c\upsilon^{k,\delta}_\lambda, \\ V^{k,\delta}_\lambda(0) = V_0; \quad \upsilon^{k,\delta}_\lambda(0) = \upsilon_0. \end{cases} \tag{5.33}$$

The Gateaux derivative of F at $\boldsymbol{g}^{k,\delta}$ in the direction $\boldsymbol{\theta}$ is given by

$$W^{k,\delta} = F'(\boldsymbol{g}^{k,\delta})(\boldsymbol{\theta}) = \lim_{\lambda\to 0} \frac{F(\boldsymbol{g}^{k,\delta} + \lambda\boldsymbol{\theta}) - F(\boldsymbol{g}^{k,\delta})}{\lambda}. \tag{5.34}$$

Also, we denote the following limit

$$R^{k,\delta} = \lim_{\lambda\to 0} \frac{\upsilon^{k,\delta}_\lambda - \upsilon^{k,\delta}}{\lambda}, \tag{5.35}$$

where $R^{k,\delta}$ is the Gateaux derivative of $\upsilon^{k,\delta}$.

Considering the difference between ODEs (5.33) and (5.16), dividing by λ and taking the limit $\lambda \to 0$, we have the following ODE

$$\begin{cases} \dot{W}^{k,\delta} - g^{k,\delta\prime}(V^{k,\delta})W^{k,\delta} = \boldsymbol{\theta} - R^{k,\delta}, \\ \dot{R}^{k,\delta} + cR^{k,\delta} = bW^{k,\delta}, \\ W^{k,\delta}(0) = 0; \quad R^{k,\delta}(0) = 0. \end{cases} \tag{5.36}$$

This last equation is yet another system of coupled nonlinear differential equations, depending on the parameter $\boldsymbol{\theta}$, representing an arbitrary function in $L^2[0,T]$.

From Landweber iteration (5.13) and $\boldsymbol{\theta} \in L^2[0,T]$ arbitrary, we have

$$\begin{aligned} \langle \boldsymbol{g}^{k+1,\delta} - \boldsymbol{g}^{k,\delta}, \boldsymbol{\theta} \rangle_{L^2[0,T]} &= w^{k,\delta} \langle F'(\boldsymbol{g}^{k,\delta})^* (V^\delta - F(\boldsymbol{g}^{k,\delta})), \boldsymbol{\theta} \rangle_{L^2[0,T]}, \\ &= w^{k,\delta} \langle F'(\boldsymbol{g}^{k,\delta})^* (V^\delta - V^{k,\delta}), \boldsymbol{\theta} \rangle_{L^2[0,T]}. \end{aligned}$$

By the definition of adjoint operator

$$\langle \boldsymbol{g}^{k+1,\delta} - \boldsymbol{g}^{k,\delta}, \boldsymbol{\theta} \rangle_{L^2[0,T]} = w^{k,\delta} \langle V^\delta - V^{k,\delta}, F'(x_k)(\boldsymbol{\theta}) \rangle_{L^2[0,T]},$$

Combining the previous equation and (5.34) gives

$$\langle \boldsymbol{g}^{k+1,\delta} - \boldsymbol{g}^{k,\delta}, \boldsymbol{\theta} \rangle_{L^2[0,T]} = w^{k,\delta} \langle V^\delta - V^{k,\delta}, W^{k,\delta} \rangle_{L^2[0,T]}.$$

We denote the last equality by Φ, then

$$\Phi = \frac{\langle \boldsymbol{g}^{k+1,\delta} - \boldsymbol{g}^{k,\delta}, \boldsymbol{\theta} \rangle_{L^2[0,T]}}{w^{k,\delta}} = \langle V^\delta - V^{k,\delta}, W^{k,\delta} \rangle_{L^2[0,T]}. \tag{5.37}$$

By the definition of internal product in $L^2[0,T]$

$$\Phi = \int_0^T (V^\delta - V^{k,\delta}) W^{k,\delta} dt.$$

From the previous equation and the first equality from ODE (5.17), we obtain

$$\Phi = \int_0^T \left(\dot{U}^{k,\delta} W^{k,\delta} + g'(V^{k,\delta}) U^{k,\delta} W^{k,\delta} - b P^{k,\delta} W^{k,\delta} \right) dt. \tag{5.38}$$

Integrating by parts the first term from equation (5.38), and from initial (see (5.36), $W^{k,\delta}(0) = 0$) and final (see (5.17), $U^{k,\delta}(T) = 0$) conditions, we obtain

$$\int_0^T \dot{U}^{k,\delta} W^{k,\delta} dt = -\int_0^T \dot{W}^{k,\delta} U^{k,\delta} dt. \tag{5.39}$$

Replacing equation (5.39) into (5.38), we have

$$\Phi = -\int_0^T \left(\dot{W}^{k,\delta} - g'(V^{k,\delta}) W^{k,\delta} \right) U^{k,\delta} dt - \int_0^T b P^{k,\delta} W^{k,\delta} dt.$$

Replacing, the first equality from ODE (5.36), in the first integral from the previous equation, we gather

$$\Phi = -\int_0^T \boldsymbol{\theta} U^{k,\delta} dt + \int_0^T R^{k,\delta} U^{k,\delta} dt - \int_0^T b P^{k,\delta} W^{k,\delta} dt. \tag{5.40}$$

Multiplying the second equation from (5.17) by $R^{k,\delta}$, and integrating in the interval $[0,T]$ we gather that

$$\int_0^T \dot{P}^{k,\delta} R^{k,\delta} dt - \int_0^T c P^{k,\delta} R^{k,\delta} dt = -\int_0^T U^{k,\delta} R^{k,\delta} dt.$$

Integrating by parts the first term from the previous equation, and from initial (see (5.36), $M^{k,\delta}(0) = 0$) and final (see (5.17), $P^{k,\delta}(T) = 0$) conditions, we obtain

$$\int_0^T \left(\dot{R}^{k,\delta} + cR^{k,\delta}\right) P^{k,\delta} dt = \int_0^T U^{k,\delta} R^{k,\delta} dt.$$

Then, from the previous equation and the second equation from ODE (5.36)

$$\int_0^T bP^{k,\delta} W^{k,\delta} dt = \int_0^T U^{k,\delta} R^{k,\delta} dt. \tag{5.41}$$

Substituting equation (5.41) into (5.40), we gather

$$\Phi = -\int_0^T \boldsymbol{\theta} U^{k,\delta} dt = -\left\langle U^{k,\delta}, \boldsymbol{\theta} \right\rangle_{L^2[0,T]}.$$

Combining the previous equation and (5.37), we obtain

$$\frac{\left\langle \boldsymbol{g}^{k+1,\delta} - \boldsymbol{g}^{k,\delta}, \boldsymbol{\theta} \right\rangle_{L^2[0,T]}}{w^{k,\delta}} = -\left\langle U^{k,\delta}, \boldsymbol{\theta} \right\rangle_{L^2[0,T]}.$$

Since $\boldsymbol{\theta} \in L^2[0,T]$ is arbitrary, we have (5.15). ■

6 Discrete inverse problems

The main difference between the discrete inverse problem and the continuous inverse problem is whether x and y data, from (2.1), are treated as continuous functions or discrete parameters (Menke (2018), Hansen (2010)). Particularly, in numerical implementations, the x and y parameters are necessarily discrete. In this context, we study the discrete inverse problem in cable equation and in Hodgkin-Huxley model.

Throughout the study on the estimation of parameters in discrete models, we presented two complete work in the following conferences:

- XII Encontro Acadêmico de Modelagem Computacional (EAMC-2019).
- V International Symposium on Inverse Problems, Design and Optimization (IPDO-2019).

In the first work, Section 6.1, we estimate conductances in the discrete cable model. For our second work, in Section 6.2, we also obtain approximate conductances, but in discrete Hodgkin-Huxley model. In Sections 6.1 and 6.2 we present a summary of works, and in Appendix D we present the articles.

6.1 Discrete inverse problem in cable equation

In this Section, we consider the Subsection 1.3.4. Let the space-time discretization $t_n = (n-1)\Delta t$ for $n = 1, 2, \cdots, N$ and $x_j = (j-1)\Delta x$ for $j = 1, 2, \cdots, nx$, where $\Delta t = T/(nt-1)$ and $\Delta x = L/(nx-1)$. The points V_j^n and G_j represent the numerical approximation of $V(t_n, x_j)$ and $G(x_j)$, respectively.

For simplicity we denote

$$a = \frac{\Delta t}{(R_I + R_E)\Delta x^2 C_M}, \quad b = -2a + 1, \quad c = \frac{\Delta t}{C_M}.$$

Then, applying finite differences in equation (6.41), we have the following discrete cable model

$$\begin{cases} V_j^{n+1} = aV_{j-1}^n + bV_j^n + aV_{j+1}^n - cG_j\left(V_j^n - E\right), \\ V_j^1 = r_j; \quad j = 1, 2, \cdots, nx, \\ V_0^n = V_1^n - \Delta x p^n, \quad V_{nx+1}^n = \Delta x q^n + V_{nx}^n; \quad n = 1, 2, \cdots, nt. \end{cases} \tag{6.1}$$

We denote

$$\boldsymbol{G} = (G_1, \cdots, G_{nx}) \in \mathbb{R}^{nx} \quad \text{and} \quad \boldsymbol{V} = \begin{bmatrix} V_1^1 & V_{nx}^1 \\ \vdots & \vdots \\ V_1^{nt} & V_{nx}^{nt} \end{bmatrix} \in \mathbb{R}^{nt\times 2}$$

Let $F : \mathbb{R}^{nx} \to \mathbb{R}^{nt\times 2}$ be a non-linear operator defined by

$$F(\boldsymbol{G}) = \boldsymbol{V} \tag{6.2}$$

The discrete inverse problem is to determinate $\boldsymbol{G}$ approximately, given the noisy data $\boldsymbol{V}^{\delta}$. Considering minimal error iteration (2.4), for $x = \boldsymbol{G}$ and $w^{k,\delta} \geq 0$, we have

$$\boldsymbol{G}^{k+1,\delta} = \boldsymbol{G}^{k,\delta} + w^{k,\delta} F'(\boldsymbol{G}^{k,\delta})^* \left(\boldsymbol{V}^{\delta} - F(\boldsymbol{G}^{k,\delta})\right), \tag{6.3}$$

where

$$w^{k,\delta} = \frac{\|\boldsymbol{V}^{\delta} - \boldsymbol{V}^{k,\delta}\|^2_{\mathbb{R}^{nt\times 2}}}{\left\|F'(\boldsymbol{G}^{k,\delta})^*(\boldsymbol{V}^{\delta} - F(\boldsymbol{G}^{k,\delta}))\right\|^2_{\mathbb{R}^{nx}}}.$$

From equation (6.3), we compute the adjoint of the Gateaux derivative $F'(\boldsymbol{G}^{k,\delta})^*$ (see Theorem 6.1.1), and we obtain the iteration

$$\boldsymbol{G}^{k+1,\delta} = \boldsymbol{G}^{k,\delta} - w^{k,\delta} \left(X_1^{k,\delta}, X_2^{k,\delta}, \cdots, X_{nx}^{k,\delta}\right), \tag{6.4}$$

where $X_i^{k,\delta}$, for $i = 1, 2, \cdots, nx$, satisfies equation (6.5).

We used the minimal error method (6.4) to estimate $\boldsymbol{G}$, given $\boldsymbol{G}^{1,\delta}$.

In the next theorem, we calculate, from (6.3), the adjoint of the directional derivative.

Theorem 6.1.1. *Consider the nonlinear operator F defined in (6.2) and the iteration (4.2). Then*

$$F'(\boldsymbol{G}^{k,\delta})^* \left(\boldsymbol{V}^{\delta} - F(\boldsymbol{G}^{k,\delta})\right) = -\left(X_1^{k,\delta}, X_2^{k,\delta}, \cdots, X_{nx}^{k,\delta}\right),$$

where

$$X_j^{k,\delta} = \frac{1}{a\Delta x} \sum_{n=1}^{nt} \left((V_j^n)^{k,\delta} - E\right) (U_j^n)^{k,\delta}; \quad \text{for } i = 1, 2, \cdots, nx. \tag{6.5}$$

The parameter $(V_j^n)^{k,\delta}$ solves, given $\boldsymbol{G}^{k,\delta}$,

$$\begin{cases} (V_j^{n+1})^{k,\delta} = a(V_{j-1}^n)^{k,\delta} + b(V_j^n)^{k,\delta} + a(V_{j+1}^n)^{k,\delta} - cG_j^{k,\delta}\left((V_j^n)^{k,\delta} - E\right), \\ (V_j^1)^{k,\delta} = r_j; \quad j = 1, 2, \cdots, nx, \\ (V_0^n)^{k,\delta} = (V_1^n)^{k,\delta} - \Delta x p^n, \quad (V_{nx+1}^n)^{k,\delta} = \Delta x q^n + (V_{nx}^n)^{k,\delta}; \quad n = 1, 2, \cdots, nt. \end{cases} \tag{6.6}$$

Given $(V_j^n)^{k,\delta}$ and $\boldsymbol{G}^{k,\delta}$, $(U_j^n)^{k,\delta}$ solves

$$\begin{cases} (U_j^n)^{k,\delta} = a(U_{j-1}^{n+1})^{k,\delta} + b(U_j^{n+1})^{k,\delta} + a(U_{j+1}^{n+1})^{k,\delta} - cG_j^{k,\delta}(U_j^{n+1})^{k,\delta}; \\ (U_j^{nt})^{k,\delta} = 0; \\ (U_0^{n+1})^{k,\delta} = (U_1^1)^{k,\delta} + \Delta x \left((V_1^{n+1})^{\delta} - (V_{nx}^{n+1})^{k,\delta}\right); \\ (U_{nx+1}^{n+1})^{k,\delta} = (U_{nx}^{n+1})^{k,\delta} + \Delta x \left((V_{nx}^{n+1})^{\delta} - (V_{nx}^{n+1})^{k,\delta}\right). \end{cases} \tag{6.7}$$

Proof. See Appendix D. ■

We next describe the computational scheme.

Data: $\boldsymbol{V}^{\delta}$, δ and τ
Result: Compute an approximation for $\boldsymbol{G}$ using Iteration Scheme (6.4)
Choose $\boldsymbol{G}^{1,\delta}$ as an initial approximation for $\boldsymbol{G}$;
Compute $(V_j^n)^{1,\delta}$ from (6.6), replacing $\boldsymbol{G}^{k,\delta}$ by $\boldsymbol{G}^{1,\delta}$;
k=1;
while $\tau\delta \le \|\boldsymbol{V}^{\delta} - \boldsymbol{V}^{k,\delta}\|_{\mathbb{R}^{nt\times 2}}$ **do**
  Compute $(U_j^n)^{k,\delta}$ from (6.7);
  Compute $\boldsymbol{G}^{k+1,\delta}$ using (6.4);
  Compute $(V_j^n)^{k+1,\delta}$ from (6.6), replacing $\boldsymbol{G}^{k,\delta}$ by $\boldsymbol{G}^{k+1,\delta}$;
  $k \leftarrow k+1$;
end

Algorithm 7: Minimal error iteration in the discrete cable model

6.2 Discrete inverse problem in Hodgkin-Huxley model

We partition the domain in time ($[0,T]$) using a mesh $t_1, t_2, \cdots, t_{nt}$. The point V_i represents the numerical approximation of $V(t_i)$. Here $t_i = (i-1)\Delta t$, for $i = 1, 2, \cdots, nt$, where $\Delta t = T/(nt-1)$. Applying finite differences in equation (1.8), we have the following discrete Hodgkin-Huxley model,

$$\begin{cases} C\dfrac{V_{i+1}-V_i}{\Delta t} = I_{\text{ext}} - G_{Na}{m_i}^3 h_i(V_i - E_{Na}) - G_K n_i^4(V_i - E_K) - G_L(V_i - E_L); \\ \dfrac{\mathcal{X}_{i+1}-\mathcal{X}_i}{\Delta t} = (1-\mathcal{X}_i)\alpha_{\mathcal{X}_i}(V_i) - \mathcal{X}_i\beta_{\mathcal{X}_i}(V_i); \qquad \mathcal{X} = m, n, h; \\ V_1 = V_0, \quad m_1 = m_0, \quad n_1 = n_0, \quad h_1 = h_0. \end{cases} \tag{6.8}$$

Functions $\alpha_{\mathcal{X}_i}$ and $\beta_{\mathcal{X}_i}$ satisfy the following equations:

$$\alpha_{m_i} = \tfrac{(25-V_i)/10}{\exp((25-V_i)/10)-1}; \quad \alpha_{h_i} = 0.07\exp(-V_i/20); \quad \alpha_{n_i} = \tfrac{(10-V_i)/100}{\exp((10-V_i)/10)-1};$$

$$\beta_{m_i} = 4\exp(-V_i/18); \quad \beta_{h_i} = \tfrac{1}{\exp((30-V_i)/10)+1}; \quad \beta_{n_i} = 0.125\exp(-V_i/80).$$

We denote $\boldsymbol{V} = (V_1, \cdots, V_{nt})$, $\boldsymbol{m} = (m_1, \cdots, m_{nt})$, $\boldsymbol{n} = (n_1, \cdots, n_{nt})$, $\boldsymbol{h} = (h_1, \cdots, h_{nt})$ and $\boldsymbol{G} = (G_{Na}, G_K, G_L)$.

Consider the nonlinear operator $F : \mathbb{R}^3 \to \mathbb{R}^{nt}$, defined by

$$F(\boldsymbol{G}) = \boldsymbol{V}, \tag{6.9}$$

where $\boldsymbol{V}$ solves (6.8). The goal of this Section is to estimate $\boldsymbol{G}$, from (6.8), given $\boldsymbol{V}^\delta$.

From iteration (2.4), for $x = \boldsymbol{G}$ and $w^{k,\delta} = 1$, we have

$$\boldsymbol{G}^{k+1,\delta} = \boldsymbol{G}^{k,\delta} + F'(\boldsymbol{G}^{k,\delta})^*(\boldsymbol{V}^\delta - F(\boldsymbol{G}^{k,\delta})). \tag{6.10}$$

From previous equation and theorem 6.2.1, we have the following iteration

$$\boldsymbol{G}^{k+1,\delta} = \boldsymbol{G}^{k,\delta} + \left(X_{\text{Na}}^{k,\delta}, X_K^{k,\delta}, X_L^{k,\delta}\right), \tag{6.11}$$

where $X_{\text{Na}}^{k,\delta}$, $X_K^{k,\delta}$ and $X_L^{k,\delta}$ satisfy equations (6.12), (6.13) and (6.14), respectively.

To obtain an approximation for $\boldsymbol{G}$, we used Landweber iteration (6.11).

In the next theorem, we calculate the adjoint of the directional derivative.

Theorem 6.2.1. *Consider the nonlinear operator F defined in (6.9) and iteration (2.4). Then*

$$F'(\boldsymbol{G}^{k,\delta})^*(\boldsymbol{V}^\delta - F(\boldsymbol{G}^{k,\delta})) = \left(X_{Na}^{k,\delta}, X_K^{k,\delta}, X_L^{k,\delta}\right),$$

where

$$X_{\text{Na}}^{k,\delta} = \Delta t^3 \sum_{i=1}^{nt} \left(m_i^{k,\delta}\right)^3 \left(h_i^{k,\delta}\right) (V_i^{k,\delta} - E_{Na}) U_i^{k,\delta}, \tag{6.12}$$

$$X_K^{k,\delta} = \Delta t^3 \sum_{i=1}^{nt} \left(n_i^{k,\delta}\right)^4 (V_i^{k,\delta} - E_K) U_i^{k,\delta}, \tag{6.13}$$

$$X_L^{k,\delta} = \Delta t^3 \sum_{i=1}^{nt} (V_i^{k,\delta} - E_L) U_i^{k,\delta}. \tag{6.14}$$

The parameters $\boldsymbol{V}^{k,\delta}$, $\boldsymbol{m}^{k,\delta}$, $\boldsymbol{n}^{k,\delta}$ and $\boldsymbol{h}^{k,\delta}$ solve, given $\boldsymbol{G}^{k,\delta}$,

$$\begin{cases} C\dfrac{V_{i+1}^{k,\delta} - V_i^{k,\delta}}{\Delta t} = I_{\text{ext}} - G_{Na}^{k,\delta}\left(m_i^{k,\delta}\right)^3 \left(h_i^{k,\delta}\right)(V_i^{k,\delta} - E_{Na}) \\ \qquad\qquad -G_K^{k,\delta}\left(n_i^{k,\delta}\right)^4 (V_i^{k,\delta} - E_K) - G_L^{k,\delta}(V_i^{k,\delta} - E_L), \\ \dfrac{\mathcal{X}_{i+1} - \mathcal{X}_i}{\Delta t} = (1 - \mathcal{X}_i)\alpha_{\mathcal{X}_i}(V_i^{k,\delta}) - \mathcal{X}_i \beta_{\mathcal{X}_i}(V_i^{k,\delta}); \qquad \mathcal{X} = m^{k,\delta}, n^{k,\delta}, h^{k,\delta}, \\ V_1 = V_0; \quad m_1 = m_0; \quad n_1 = n_0; \quad h_1 = h_0. \end{cases} \tag{6.15}$$

Finally, $U_i^{k,\delta}$ solves the following ODE

$$\begin{cases} C\dfrac{U_i^{k,\delta}-U_{i-1}^{k,\delta}}{\Delta t} - \left(G_{Na}^{k,\delta}\left(m_i^{k,\delta}\right)^3\left(h_i^{k,\delta}\right) + G_K^{k,\delta}\left(n_i^{k,\delta}\right)^4 + G_L^{k,\delta}\right)U_i^{k,\delta} \\ -\left[\left(1-m_i^{k,\delta}\right)\alpha'_{m_i^{k,\delta}}(V_i^{k,\delta}) - \left(m_i^{k,\delta}\right)\beta'_{m_i^{k,\delta}}(V_i^{k,\delta})\right]P_i^{k,\delta} \\ -\left[\left(1-n_i^{k,\delta}\right)\alpha'_{n_i^{k,\delta}}(V_i^{k,\delta}) - \left(n_i^{k,\delta}\right)\beta'_{n_i^{k,\delta}}(V_i^{k,\delta})\right]Q_i^{k,\delta} \\ -\left[\left(1-h_i^{k,\delta}\right)\alpha'_{h_i^{k,\delta}}(V_i^{k,\delta}) - \left(h_i^{k,\delta}\right)\beta'_{h_i}(V_i^{k,\delta})\right]R_i^{k,\delta} = V_i^\delta - V_i^{k,\delta}, \\ \dfrac{P_i^{k,\delta}-P_{i-1}^{k,\delta}}{\Delta t} - [\alpha_{m_i^{k,\delta}}(V_i^{k,\delta}) + \beta_{m_i^{k,\delta}}(V_i^{k,\delta})]P_i^{k,\delta} = \\ \qquad -3G_{Na}^{k,\delta}\left(m_i^{k,\delta}\right)^2\left(h_i^{k,\delta}\right)(V_i^{k,\delta}-E_{Na})U_i^{k,\delta}, \\ \dfrac{Q_i^{k,\delta}-Q_{i-1}^{k,\delta}}{\Delta t} - [\alpha_{n_i^{k,\delta}}(V_i^{k,\delta}) + \beta_{n_i^{k,\delta}}(V_i^{k,\delta})]Q_i^{k,\delta} = \\ \qquad -4G_K^{k,\delta}\left(n_i^{k,\delta}\right)^3(V_i^{k,\delta}-E_K)U_i^{k,\delta}, \\ \dfrac{R_i^{k,\delta}-R_{i-1}^{k,\delta}}{\Delta t} - [\alpha_{h_i^{k,\delta}}(V_i^{k,\delta}) + \beta_{h_i^{k,\delta}}(V_i^{k,\delta})]R_i^{k,\delta} = \\ \qquad -G_{Na}^{k,\delta}\left(m_i^{k,\delta}\right)^3(V_i^{k,\delta}-E_{Na})U_i^{k,\delta}, \\ U_{nt}^{k,\delta}=0; \quad P_{nt}^{k,\delta}=0; \quad Q_{nt}^{k,\delta}=0; \quad R_{nt}=0. \end{cases} \tag{6.16}$$

Proof. See Appendix D. ■

We next describe the computational scheme.

Data: $\boldsymbol{V}^\delta$, δ and τ
Result: Compute an approximation for $\boldsymbol{G}$ using Iteration Scheme (6.11)
Choose $\boldsymbol{G}^{1,\delta}$ as an initial approximation for $\boldsymbol{G}$;
Compute $\boldsymbol{V}^{1,\delta}$ from (6.15), replacing $\boldsymbol{G}^{k,\delta}$ by $\boldsymbol{G}^{1,\delta}$;
k=1;
while $\tau\delta \le \|\boldsymbol{V}^\delta - \boldsymbol{V}^{k,\delta}\|_{\mathbb{R}^{nt}}$ **do**
  Compute $U_i^{k,\delta}$ from (6.16);
  Compute $\boldsymbol{G}^{k+1,\delta}$ using (6.11);
  Compute $\boldsymbol{V}^{k+1,\delta}$ from (6.15), replacing $\boldsymbol{G}^{k,\delta}$ by $\boldsymbol{G}^{k+1,\delta}$;
  $k \leftarrow k+1$;
end

Algorithm 8: Landweber iteration in the discrete Hodgkin-Huxley model

6.3 Numerical simulations

To compare the results obtained, first we calculate $\boldsymbol{V}$ from (6.1), given $\boldsymbol{G} = (G_1, G_2, \cdots, G_{nt})$, or from (6.8), given $\boldsymbol{G} = (G_{\text{Na}}, G_K, G_L)$. We obtain $\boldsymbol{V}^\delta$, given δ, from the following equation

$$\boldsymbol{V}^\delta = \boldsymbol{V} + \text{rand}_\epsilon \boldsymbol{V}, \tag{6.17}$$

where $\text{rand}_\epsilon \in H_{\boldsymbol{V}}$ ($H_{\boldsymbol{V}} = \mathbb{R}^{nt\times 2}$ for $\boldsymbol{G} = (G_1, G_2, \cdots, G_{nt})$ or $H_{\boldsymbol{V}} = \mathbb{R}^{nt}$ for $\boldsymbol{G} = (G_1, G_2, G_3)$) is a uniformly distributed random variable in the interval $[-\epsilon, \epsilon]$, and $\epsilon = \delta/\|\boldsymbol{V}\|_{H_{\boldsymbol{V}}}$. The matrix $\text{rand}_\delta \in S$ generates uniformly distributed numbers in the interval $[-\delta, \delta]$. The relative error of x is defined as

$$\text{Error}_k = \frac{\|x - x^{k,\delta}\|_{H_x}}{\|x\|_{H_x}} \times 100\%, \quad k = 1, 2, \cdots, k_*, \tag{6.18}$$

where $H_x = \mathbb{R}^{nx}$ or $H_x = \mathbb{R}^3$.

We present two numerical tests. In the first example, we determine conductances in cable equation. In the second example, we also estimate conductances, but in Hodgkin-Huxley model.

Example 6.1. *This example is a particular case from (6.1), with values:* $\Delta t = 5.0025 \times 10^{-4}$ $[ms]$*,* $\Delta x = 0.0339$ $[cm]$*,* $R_I + R_E = 1$ $[\Omega]$*,* $C_M = 5$ $[F/cm^2]$*,* $E = 10$ $[mV]$*. The boundary conditions are* $p^n = \exp((n-1)\Delta t)$ $[mV/cm]$ *and* $q^n = 0$ $[mV/cm]$ *for* $n = 1, 2, \cdots, 2000$*, and the initial condition is* $r_j = 0$ $[mV]$ *for* $j = 1, 2, \cdots 60$*. Given* $\boldsymbol{V}^\delta$*,* $\boldsymbol{G}^{1,\delta} = (0, 0, \cdots, 0)$ *and* $\tau = 2.01$*, the goal of this example is to estimate*

$$\begin{aligned} G_j &= 1 \quad j \in \{1, 2, \cdots, 10\} \cup \{21, 22, \cdots, 40\} \cup \{51, 22, \cdots, 60\}, \\ G_j &= 2 \quad j \in \{11, 12, \cdots, 20\} \cup \{41, 22, \cdots, 60\}. \end{aligned}$$

Table 7 presents the results for various levels of noise. In figure 23, we plot results for $\epsilon = 0.001\%$ *of noise.*

ε	k_*	$Error_{k_*}$	$Time$ (s)
100%	1	100 %	0.03
10%	3	73 %	0.08
1%	23	33 %	0.6
0.1%	78	21 %	2
0.01%	1057	16 %	28
0.001%	11799	14 %	312

Table 7 – Numerical results for Example 6.1 for various values of ε, as in (4.20). The second column contains the number of iterations according to (2.5). The third column is the relative error of $\boldsymbol{G}$ according to (6.18). The last column is the running time of the algorithm, in seconds.

Example 6.2. *The parameters for the discrete H-H model (6.8) are:* $C = 1$ $[\mu F/cm^2]$*,* $I_{ext} = 10$ $[\mu A/cm^2]$*,* $E_{Na} = 50$ $[mV]$*,* $E_K = -77$ $[mV]$*,* $E_L = -54$ $[mV]$*,* $V_0 = -15$ $[mV]$*,* $m_0 = 0.6$*,* $n_0 = 0.4$*,* $h_0 = 0.4$*,* $\Delta t = 0.01$ *and* $nt = 500$*. The goal of this section is to find approximate values for* $G_{Na} = 90$ mS/cm^2*,* $G_K = 25$ mS/cm^2 *and* $G_L = 0.5$ mS/cm^3*.*

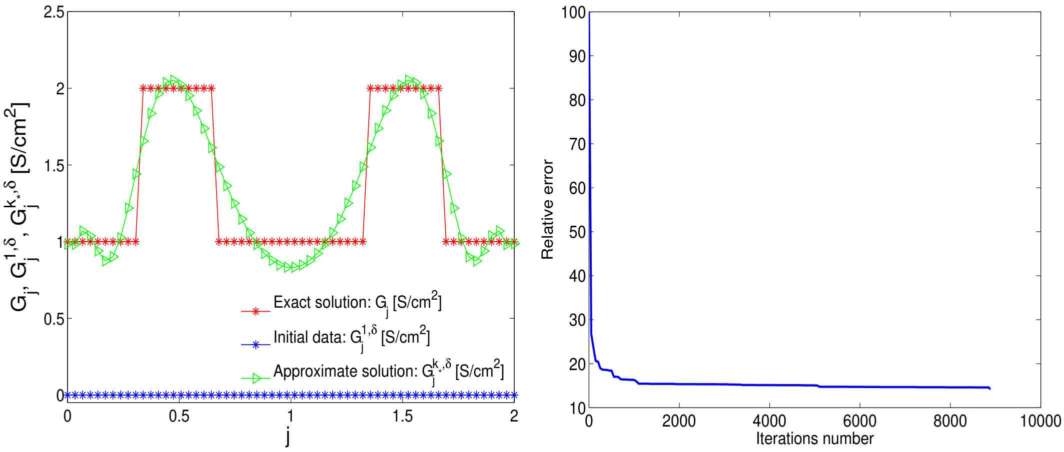

Figure 23 – Example 6.1. The plot on the left represents the exact solution (red line), the approximated solution (green line), and the initial guess (blue line). The plot to the right displays the relative error between $\boldsymbol{G}$ and $\boldsymbol{G}^{k,\delta}$ as a function of the iteration k.

To estimate $\boldsymbol{G}$ *we use* (6.11)*, given* $\boldsymbol{V}^{\delta}$*,* $\boldsymbol{G}^{1,\delta} = (0,0,0)$ *and* $\tau = 2.01$*. In Table 8 we present the results for various levels of noise. In figure 24, we plot results for* $\epsilon = 0.1\%$ *of noise.*

ε	k_*	$G_{\mathrm{Na}}^{k_*,\delta}$	$G_{\mathrm{K}}^{k_*,\delta}$	$G_L^{k_*,\delta}$	$Error_{k_*}$	$Time\ (s)$
100%	1	0	0	0	100 %	1.2×60^{-1}
10%	172	0.02	0.01	1.11	99.98 %	0.6×60^{0}
1%	1163726	81.09	21.20	0.56	10.37 %	1.1×60^{2}
0.1%	1985621	89.14	24.63	0.51	1.01 %	1.9×60^{2}
0.01%	2764712	89.91	24.96	0.50	0.10 %	2.6×60^{2}

Table 8 – Numerical results for Example 6.2 for various values of ε, as in (4.20). The second column contains the number of iterations according to (1.10). The third, fourth and fifth columns are the approximations for G_{Na}, G_{K} and G_L respectively. The sixth column is the relative error of $\boldsymbol{G} = (G_{\mathrm{Na}}, G_{\mathrm{K}}, G_L)$ according to (4.21). The last column is the running time of the algorithm, in seconds.

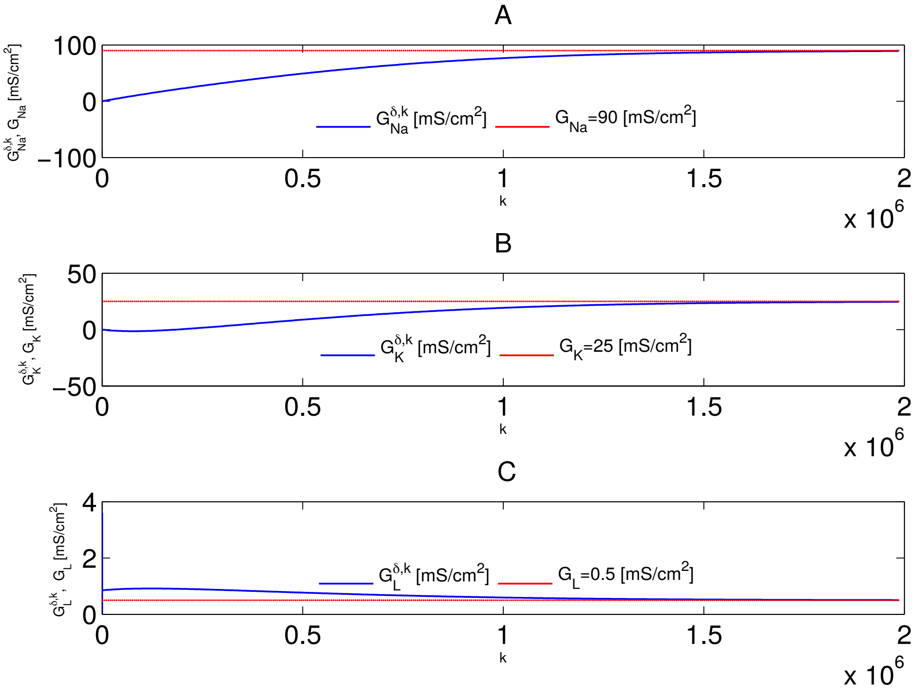

Figure 24 – Estimation of the conductances G_{Na} (Subplot-A), G_{K} (Subplot-B) and G_L (Subplot-C), for Example 6.2 with $\epsilon = 0.1\%$.

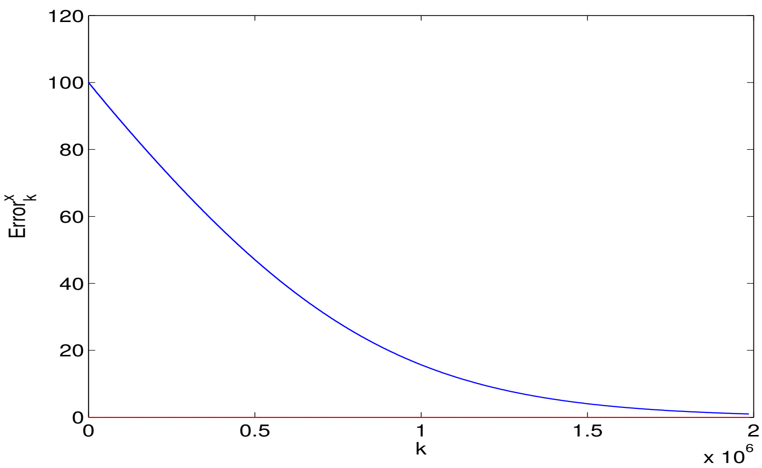

Figure 25 – The relative error between $x = (G_{\text{Na}}, G_K, G_L)$ and $x^{k,\delta} = (G_{\text{Na}}^{k,\delta}, G_K^{k,\delta}, G_L^{k,\delta})$ as a function of the iteration k according to (6.18), for Example 6.2 with $\epsilon = 0.1\%$.

6.4 Detailed proofs of Theorems 6.1.1 and 6.2.1

6.4.1 Proof of Theorem 6.1.1

Proof. Consider the operator F defined in (6.2). Evaluating $\boldsymbol{G}^{k,\delta}$ in the operator F, we have $F(\boldsymbol{G}^{k,\delta}) = \boldsymbol{V}^{k,\delta}$, where $\left(V_j^n\right)^{k,\delta} = \mathcal{V}_j^n$ solves Equation (6.6).

Let the vector $\boldsymbol{\theta} = (\theta_1, \theta_1, \cdots, \theta_{nx}) \in \mathbb{R}^{nx}$ and $\lambda \in \mathbb{R}$, then evaluating $\boldsymbol{G}^{k,\delta} + \lambda\boldsymbol{\theta}$ in the operator F, we have $F(\boldsymbol{G}^{k,\delta} + \lambda\boldsymbol{\theta}) = \boldsymbol{V}^{k,\delta} + \lambda\boldsymbol{W}^{k,\delta}$, where $\left(V_j^n\right)^{k,\delta} + \lambda\left(W_j^n\right)^{k,\delta} = \mathcal{V}^{\lambda}{}_j^n$ solves

$$\begin{cases} \mathcal{V}^{\lambda}{}_j^{n+1} = a\mathcal{V}^{\lambda}{}_{j-1}^n + b\mathcal{V}^{\lambda}{}_j^n + a\mathcal{V}^{\lambda}{}_{j+1}^n - \left(cG_j^{k,\delta} + \lambda\theta_j\right)\left(\mathcal{V}^{\lambda}{}_j^n - E\right), \\ \mathcal{V}^{\lambda}{}_j^1 = r_j; \quad j = 1, 2, \cdots, nx, \\ \mathcal{V}^{\lambda}{}_0^n = \mathcal{V}^{\lambda}{}_1^n - \Delta x\, p^n; \qquad n = 1, 2, \cdots, nt. \\ \mathcal{V}^{\lambda}{}_{nx+1}^n = \Delta x q^n + \mathcal{V}^{\lambda}{}_{nx}^n; \quad n = 1, 2, \cdots, nt. \end{cases} \tag{6.19}$$

The directional derivative of F at $\boldsymbol{G}^{k,\delta}$ in the direction $\boldsymbol{\theta}$ is given by

$$\boldsymbol{W}^{k,\delta} = F'(\boldsymbol{G}^{k,\delta}).(\boldsymbol{\theta}) = \lim_{\lambda\to 0} \frac{F(\boldsymbol{G}^{k,\delta} + \lambda\boldsymbol{\theta}) - F(\boldsymbol{G}^{k,\delta})}{\lambda}. \tag{6.20}$$

Considering the difference between (6.6) and (6.19), dividing by λ and taking limit $\lambda \to 0$, we have the equation (6.21), where $\left(W_j^n\right)^{k,\delta} = \mathcal{W}_j^n$.

$$\begin{cases} \mathcal{W}_j^{n+1} = a\mathcal{W}_{j-1}^n + b\mathcal{W}_j^n + a\mathcal{W}_{j+1}^n - cG_j^{k,\delta}\mathcal{W}_j{}^n - \theta_j\left(\mathcal{V}_j^n - E\right), \\ \mathcal{W}_j^1 = 0, \\ \mathcal{W}_1{}^n = \mathcal{W}_0^n; \quad \mathcal{W}_{nx+1}^n = \mathcal{W}_{nx}^n. \end{cases} \tag{6.21}$$

Note that the variable θ_j, from (6.21), represents any point in $\mathbb{R}$.

By definition of adjoint operator, we have

$$\left\langle F'(\boldsymbol{G}^{k,\delta})^{*}.\left(\boldsymbol{V}^{\delta} - F(\boldsymbol{G}^{k,\delta})\right), \boldsymbol{\theta}\right\rangle_{\mathbb{R}^{nx}} = \left\langle \boldsymbol{V}^{\delta} - F(\boldsymbol{G}^{k,\delta})\ ,\ F'(\boldsymbol{G}^{k,\delta}).\,(\boldsymbol{\theta})\right\rangle_{\mathbb{R}^{nt\times 2}}.$$

From the previous equation and from (6.20), we obtain

$$\left\langle F'(\boldsymbol{G}^{k,\delta})^{*}.\left(\boldsymbol{V}^{\delta} - F(\boldsymbol{G}^{k,\delta})\right), \boldsymbol{\theta}\right\rangle_{\mathbb{R}^{nx}} = \left\langle \boldsymbol{V}^{\delta} - \boldsymbol{V}^{k,\delta}\ , \boldsymbol{W}^{k,\delta}\right\rangle_{\mathbb{R}^{nt\times 2}}.$$

From the previous equation and by definition of inner product, we have

$$\left\langle F'(\boldsymbol{G}^{k,\delta})^{*}.\left(\boldsymbol{V}^{\delta} - F(\boldsymbol{G}^{k,\delta})\right), \boldsymbol{\theta}\right\rangle_{\mathbb{R}^{nx}} = \sum_{n=1}^{nt}\left(V_1^{n\delta} - V_1^{n k,\delta}\right)\mathcal{W}_1^n + \sum_{n=1}^{nt}\left(V_{nx}^{n\,\delta} - V_{nx}^{n\,k,\delta}\right)\mathcal{W}_{nx}^n. \tag{6.22}$$

We denote $\left(U_j^n\right)^{k,\delta} = \mathcal{U}_j^n$ for differential equation (6.7). Multiplying the first equation from (6.7) by $\mathcal{W}_j^{n+1}$, and summing at points $n = 0, 1, \cdots, nt-1$ and $j = 1, 2, \cdots, nx$ we gather

$$\sum_{n=0}^{nt-1}\sum_{j=1}^{nx}\mathcal{U}_j^n\mathcal{W}_j^{n+1} = \sum_{n=0}^{nt-1}\sum_{j=1}^{nx}\left(a\mathcal{U}_{j-1}^{n+1} + a\mathcal{U}_{j+1}^{n+1}\right)\mathcal{W}_j^{n+1}$$
$$\sum_{n=0}^{nt-1}\sum_{j=1}^{nx}\left(b\mathcal{U}_j^{n+1} - cG_j^{k,\delta}\mathcal{U}_j^{n+1}\right)\mathcal{W}_j^{n+1}. \quad (6.23)$$

From equation (6.7), $\mathcal{U}_j^{nt} = 0$, and from equation (6.21), $\mathcal{W}_j^1 = 0$, then we gather

$$\sum_{n=0}^{nt-1}\sum_{j=1}^{nx}\mathcal{U}_j^n\mathcal{W}_j^{n+1} = \sum_{n=1}^{nt}\sum_{j=1}^{nx}\mathcal{U}_j^n\mathcal{W}_j^{n+1}. \quad (6.24)$$

Substituting equation (6.24) into (6.23), we have

$$\sum_{n=0}^{nt-1}\sum_{j=1}^{nx}\mathcal{U}_j^n\mathcal{W}_j^{n+1} = \sum_{n=0}^{nt-1}\sum_{j=1}^{nx}\left(a\mathcal{U}_{j-1}^{n+1} + a\mathcal{U}_{j+1}^{n+1}\right)\mathcal{W}_j^{n+1}$$
$$\sum_{n=0}^{nt-1}\sum_{j=1}^{nx}\left(b\mathcal{U}_j^{n+1} - cG_j^{k,\delta}\mathcal{U}_j^{n+1}\right)\mathcal{W}_j^{n+1}. \quad (6.25)$$

From the second double summation from equation (6.25), leads to

$$\sum_{j=1}^{nx}\left(a\mathcal{U}_{j-1}^{n+1} + a\mathcal{U}_{j+1}^{n+1}\right)\mathcal{W}_j^{n+1} = a\mathcal{U}_0^{n+1}\mathcal{W}_1^{n+1} + a\mathcal{U}_1^{n+1}\mathcal{W}_2^{n+1}$$
$$+\sum_{j=2}^{nx-1}\left(a\mathcal{W}_{j-1}^{n+1} + a\mathcal{W}_{j+1}^{n+1}\right)\mathcal{U}_j^{n+1}a\mathcal{U}_{nx}^{n+1}\mathcal{W}_{nx-1}^{n+1} + a\mathcal{U}_{nx+1}^{n+1}\mathcal{W}_{nx}^{n+1}. \quad (6.26)$$

From equation (6.7)

$$\mathcal{U}_0^{n+1} = \mathcal{U}_1^{n+1} + \Delta x\left(V_1^{n+1^\delta} - \mathcal{V}_{nx}^{n+1}\right) \text{ and } \mathcal{U}_{nx+1}^{n+1} = \mathcal{U}_{nx}^{n+1} + \Delta x\left(V_{nx}^{n+1^\delta} - \mathcal{V}_{nx}^{n+1}\right). \quad (6.27)$$

From equation (6.21)

$$\mathcal{W}_1^{n+1} = \mathcal{W}_0^{n+1} \quad\text{and}\quad \mathcal{W}_{nx+1}^{n+1} = \mathcal{W}_{nx}^{n+1}. \quad (6.28)$$

Replacing equations (6.27) and (6.28) in equation (6.26), we obtain

$$\sum_{j=1}^{nx}\left(a\mathcal{U}_{j-1}^{n+1} + a\mathcal{U}_{j+1}^{n+1}\right)\mathcal{W}_j^{n+1} = \sum_{j=1}^{nx}\left(a\mathcal{W}_{j-1}^{n+1} + a\mathcal{W}_{j+1}^{n+1}\right)\mathcal{U}_j^{n+1} +$$
$$a\Delta x\left(V_1^{n+1^\delta} - V_1^{n+1^{k,\delta}}\right)\mathcal{W}_1^{n+1} + a\Delta x\left(V_{nx}^{n+1^\delta} - V_{nx}^{n+1^{k,\delta}}\right)\mathcal{W}_{nx}^{n+1}.$$

Summing the previous equation at point $n = 1, 2, \cdots, nt-1$, it follows that

$$\sum_{n=0}^{nt-1}\sum_{j=1}^{nx}\left(a\mathcal{U}_{j-1}^{n+1} + a\mathcal{U}_{j+1}^{n+1}\right)\mathcal{W}_j^{n+1} = \sum_{n=0}^{nt-1}\sum_{j=1}^{nx}\left(a\mathcal{W}_{j-1}^{n+1} + a\mathcal{W}_{j+1}^{n+1}\right)\mathcal{U}_j^{n+1} +$$
$$a\Delta x\sum_{n=0}^{nt-1}\left(V_1^{n+1^{\delta}} - V_1^{n+1^{k,\delta}}\right)\mathcal{W}_1^{n+1} + a\Delta x\sum_{n=0}^{nt-1}\left(V_{nx}^{n+1^{\delta}} - V_{nx}^{n+1^{k,\delta}}\right)\mathcal{W}_{nx}^{n+1}. \quad (6.29)$$

We consider

$$\sum_{n=0}^{nt-1}\alpha^{n+1} = \sum_{n=1}^{nt}\alpha^n,$$

and from equation (6.29), we obtain

$$\sum_{n=0}^{nt-1}\sum_{j=1}^{nx}\left(a\mathcal{U}_{j-1}^{n+1} + a\mathcal{U}_{j+1}^{n+1}\right)\mathcal{W}_j^{n+1} = \sum_{n=1}^{nt}\sum_{j=1}^{nx}\left(a\mathcal{W}_{j-1}^{n} + a\mathcal{W}_{j+1}^{n}\right)\mathcal{U}_j^{n} +$$
$$a\Delta x\sum_{n=1}^{nt}\left(V_1^{n^{\delta}} - aV_1^{n^{k,\delta}}\right)\mathcal{W}_1^{n} + a\Delta x\sum_{n=1}^{nt}\left(V_{nx}^{n\ \delta} - aV_{nx}^{n\ k,\delta}\right)\mathcal{W}_{nx}^{n}. \quad (6.30)$$

From the third double summation from equation (6.25), leads to

$$\sum_{n=0}^{nt-1}\sum_{j=1}^{nx}\left(b\mathcal{U}_j^{n+1} - cG_j^{k,\delta}\mathcal{U}_j^{n+1}\right)W_j^{n+1} = \sum_{n=1}^{nt}\sum_{j=1}^{nx}\left(b\mathcal{W}_j^{n} - cG_j^{k,\delta}\mathcal{W}_j^{n}\right)\mathcal{U}_j^{n}. \quad (6.31)$$

Replacing (6.30) and (6.31) into (6.25), we have

$$\sum_{n=1}^{nt}\sum_{j=1}^{nx}\mathcal{U}_j^n\mathcal{W}_j^{n+1} = \sum_{n=1}^{nt}\sum_{j=1}^{nx}\left(a\mathcal{W}_{j-1}^{n} + a\mathcal{W}_{j+1}^{n}\right)\mathcal{U}_j^{n} +$$
$$a\Delta x\sum_{n=1}^{nt}\left(V_1^{n^{\delta}} - aV_1^{n^{k,\delta}}\right)\mathcal{W}_1^{n} + a\Delta x\sum_{n=1}^{nt}\left(V_{nx}^{n\ \delta} - V_{nx}^{n\ k,\delta}\right)\mathcal{W}_{nx}^{n} +$$
$$\sum_{n=1}^{nt}\sum_{j=1}^{nx}\left(b\mathcal{W}_j^{n} - cG_j^{k,\delta}\mathcal{W}_j^{n}\right)\mathcal{U}_j^{n}. \quad (6.32)$$

Multiplying the first equation from (6.21) by $\mathcal{U}_j^n$, and summing at points $n = 1, 2, \cdots, nt$ and $j = 1, 2, \cdots, nx$, we gather

$$\sum_{n=1}^{nt}\sum_{j=1}^{nx}\mathcal{U}_j^n\mathcal{W}_j^{n+1} = \sum_{n=1}^{nt}\sum_{j=1}^{nx}\left(a\mathcal{W}_{j-1}^{n} + a\mathcal{W}_{j+1}^{n}\right)\mathcal{U}_j^{n} +$$
$$\sum_{n=1}^{nt}\sum_{j=1}^{nx}\left(b\mathcal{W}_j^{n} - cG_j^{k,\delta}\mathcal{W}_j^{n}\right)\mathcal{U}_j^{n} + -\sum_{n=1}^{nt}\sum_{j=1}^{nx}\theta_j\left(\mathcal{V}_j^{\ n} - E\right)\mathcal{U}_j^{n}. \quad (6.33)$$

Replacing the equation (6.32) into (6.33), we obtain

$$\sum_{n=1}^{nt}\left(V_1^{n^{\delta}} - V_1^{n^{k,\delta}}\right)\mathcal{W}_1^{n} + \sum_{n=1}^{nt}\left(V_{nx}^{n\ \delta} - V_{nx}^{n\ k,\delta}\right)\mathcal{W}_{nx}^{n} =$$
$$-\frac{1}{a\Delta x}\sum_{j=1}^{nx}\sum_{n=1}^{nt}\theta_j(\mathcal{V}_j^n - E)\mathcal{U}_j^n. \quad (6.34)$$

From equations (6.34) and (6.22), we gather

$$\left\langle F'(\boldsymbol{G}^{k,\delta})^{*}.\left(\mathcal{V}^{\delta}-F(\boldsymbol{G}^{k,\delta})\right),\boldsymbol{\theta}\right\rangle_{\mathbb{R}^{nx}}=-\frac{1}{a\Delta x}\sum_{j=1}^{nx}\sum_{n=1}^{nt}\theta_j(\mathcal{V}_j^n-E)\mathcal{U}_j^n.$$

From the previous equation

$$\left\langle F'(\boldsymbol{G}^{k,\delta})^{*}.\left(\mathcal{V}^{\delta}-F(\boldsymbol{G}^{k,\delta})\right),\boldsymbol{\theta}\right\rangle_{\mathbb{R}^{nx}}= \\ -\frac{1}{a\Delta x}\left\langle\sum_{n=1}^{nt}\left((\mathcal{V}_1^n-E)\mathcal{U}_1^n,\cdots,(\mathcal{V}_{nx}^n-E)\mathcal{U}_{nx}^n\right),\boldsymbol{\theta}\right\rangle_{\mathbb{R}^{nx}}.$$

Since $\boldsymbol{\theta}\in\mathbb{R}^{nx}$ is arbitrary, we gather that the following equation holds:

$$F'(\boldsymbol{G}^{k,\delta})^{*}.\left(\mathcal{V}^{\delta}-F(\boldsymbol{G}^{k,\delta})\right)=-\frac{1}{a\Delta x}\sum_{n=1}^{nt}\left((\mathcal{V}_1^n-E)\mathcal{U}_1^n,\cdots,(\mathcal{V}_{nx}^n-E)\mathcal{U}_{nx}^n\right).$$

■

6.4.2 Proof of Theorem 6.2.1

Proof. Evaluating $\boldsymbol{G}$ in the operator F and from (1.2) we have $\boldsymbol{V}$, $\boldsymbol{m}$, $\boldsymbol{n}$ and $\boldsymbol{h}$.

Let the vector $\boldsymbol{\theta}=(\theta_{Na},\theta_K,\theta_L)\in\mathbb{R}^3$ and $\lambda\in\mathbb{R}$, then evaluating $\boldsymbol{G}+\lambda\boldsymbol{\theta}$ in the operator F, we have $F(\boldsymbol{G}+\lambda\boldsymbol{\theta})=\boldsymbol{V}^{\lambda}$, where $\boldsymbol{V}^{\lambda}$, $\boldsymbol{m}^{\lambda}$, $\boldsymbol{n}^{\lambda}$ and $\boldsymbol{h}^{\lambda}$ solve

$$\begin{cases} C\dfrac{V_{i+1}^{\lambda}-V_i^{\lambda}}{\Delta t}=I_{ext}-(G_{Na}+\lambda\theta_{Na})\left(m_i^{\lambda}\right)^3\left(h_i^{\lambda}\right)\left(V_i^{\lambda}-E_{Na}\right) \\ \qquad -(G_K+\lambda\theta_K)\left(n_i^{\lambda}\right)^4\left(V_i^{\lambda}-E_K\right)-(G_L+\lambda\theta_L)\left(V_i^{\lambda}-E_L\right), \\ \dfrac{\mathcal{X}_{i+1}-\mathcal{X}_i}{\Delta t}=(1-\mathcal{X}_i)\alpha_{\mathcal{X}_i}(V_i)-\mathcal{X}_i\beta_{\mathcal{X}_i}(V_i); \qquad \mathcal{X}=m^{\lambda},n^{\lambda},h^{\lambda}, \\ V_1^{\lambda}(0)=V_0;\quad m_1^{\lambda}(0)=m_0;\quad n_1^{\lambda}(0)=n_0;\quad n_1^{\lambda}(0)=n_0. \end{cases} \tag{6.35}$$

We denote $\boldsymbol{W}=(W_1,\cdots,W_{nt})$, $\boldsymbol{M}=(M_1,\cdots,M_{nt})$, $\boldsymbol{N}=(N_1,\cdots,N_{nt})$ and $\boldsymbol{H}=(H_1,\cdots,H_{nt})$. The directional derivative of F at $\boldsymbol{G}$ in the direction $\boldsymbol{\theta}$ is given by

$$\boldsymbol{W}=F'(\boldsymbol{G}).(\boldsymbol{\theta})=\lim_{\lambda\to0}\frac{F(\boldsymbol{G}+\lambda\boldsymbol{\theta})-F(\boldsymbol{G})}{\lambda}=\langle\nabla F,\boldsymbol{\theta}\rangle. \tag{6.36}$$

Also, we denote the following limits

$$\boldsymbol{M}=\lim_{\lambda\to0}\frac{\boldsymbol{m}^{\lambda}-\boldsymbol{m}}{\lambda},\qquad \boldsymbol{N}=\lim_{\lambda\to0}\frac{\boldsymbol{n}^{\lambda}-\boldsymbol{n}}{\lambda},\qquad \boldsymbol{H}=\lim_{\lambda\to0}\frac{\boldsymbol{h}^{\lambda}-\boldsymbol{h}}{\lambda}, \tag{6.37}$$

where $\boldsymbol{M}$, $\boldsymbol{N}$ and $\boldsymbol{H}$ are the directional derivatives of $\boldsymbol{m}$, $\boldsymbol{n}$ and $\boldsymbol{h}$, respectively.

Considering the difference between (1.2) and (6.35), dividing by λ and taking the limit $\lambda \to 0$, we have the following equation

$$\begin{cases} C\dfrac{W_{i+1}-W_i}{\Delta t} + \left(G_{Na}m_i^3h_i + G_Kn_i^4 + G_L\right)W_i = -3G_{Na}m_i^2M_ih_i(V_i-E_{Na}) \\ \quad -G_{Na}m_i^3H_i(V_i-E_{Na}) - 4G_Kn_i^3N_i(V_i-E_K) \\ \quad -\theta_{Na}m_i^3h_i(V_i-E_{Na}) - \theta_Kn_i^4(V_i-E_K) - \theta_L(V_i-E_L), \\ \dfrac{\mathcal{Y}_{i+1}-\mathcal{Y}_i}{\Delta t} + [\alpha_{\mathcal{X}_i}(V_i)+\beta_{\mathcal{X}_i}(V_i)]\mathcal{Y}_i = [(1-\mathcal{X}_i)\alpha'_{\mathcal{X}_i}(V_i) - \mathcal{X}_i\beta'_{\mathcal{X}_i}(V_i)]W_i; \\ (\mathcal{X},\mathcal{Y}) = (m,M),(n,N),(h,H), \\ W_1 = 0; \quad M_1 = 0;; \quad N_1 = 0; \quad H_1 = 0. \end{cases} \tag{6.38}$$

This last equation is another system of coupled nonlinear differential equations, depending on the parameter $\boldsymbol{\theta} = (\theta_{Na}, \theta_K, \theta_L)$. Note that the variable $\boldsymbol{\theta}$ represents any point in space $\mathbb{R}^3$.

We define the following system of equations

$$\begin{cases} C\dfrac{U_i-U_{i-1}}{\Delta t} - \left(G_{Na}m_i^3h_i + G_Kn_i^4 + G_L\right)U_i \\ -[(1-m_i)\alpha'_{m_i}(V_i) - m_i\beta'_{m_i}(V_i)]P_i \\ -[(1-n_i)\alpha'_{n_i}(V_i) - n_i\beta'_{n_i}(V_i)]Q_i \\ -[(1-h_i)\alpha'_{h_i}(V_i) - h_i\beta'_{h_i}(V_i)]R_i = V_i^\delta - V_i \\ \dfrac{P_i-P_{i-1}}{\Delta t} - [\alpha_{m_i}(V_i)+\beta_{m_i}(V_i)]P_i = -3G_{Na}m_i^2h_i(V_i-E_{Na})U_i \\ \dfrac{Q_i-Q_{i-1}}{\Delta t} - [\alpha_{n_i}(V_i)+\beta_{n_i}(V_i)]Q_i = -4G_Kn_i^3(V_i-E_K)U_i \\ \dfrac{R_i-R_{i-1}}{\Delta t} - [\alpha_{h_i}(V_i)+\beta_{h_i}(V_i)]R_i = -G_{Na}m_i^3(V_i-E_{Na})U_i \\ U_{nt} = 0; \quad P_{nt} = 0; \quad Q_{nt} = 0; \quad R_{nt} = 0. \end{cases} \tag{6.39}$$

We denote $\boldsymbol{U} = (U_1, \cdots, U_{nt})$, $\boldsymbol{P} = (P_1, \cdots, P_{nt})$, $\boldsymbol{Q} = (Q_1, \cdots, Q_{nt})$ and $\boldsymbol{R} = (R_1, \cdots, R_{nt})$.

By the definition of adjoint operator, we have

$$\left\langle F'(\boldsymbol{G})^*\left(\boldsymbol{V}^\delta - F(\boldsymbol{G})\right), \boldsymbol{\theta}\right\rangle_{\mathbb{R}^3} = \left\langle \boldsymbol{V}^\delta - F(\boldsymbol{G})\ ,\ F'(\boldsymbol{G}).\,(\boldsymbol{\theta})\right\rangle_{\mathbb{R}^{nt}}.$$

Combining the previous equation and (6.36) gives

$$\left\langle F'(\boldsymbol{G})^*\left(\boldsymbol{V}^\delta - F(\boldsymbol{G})\right), \boldsymbol{\theta}\right\rangle_{\mathbb{R}^3} = \left\langle \boldsymbol{V}^\delta - F(\boldsymbol{G})\ ,\ \boldsymbol{W}\right\rangle_{\mathbb{R}^{nt}}.$$

By the definition of inner product (**??**), we have

$$\left\langle F'(\boldsymbol{G})^* \left(\boldsymbol{V}^\delta - F(\boldsymbol{G})\right), \boldsymbol{\theta}\right\rangle_{\mathbb{R}^3} = \Delta t^3 \sum_{i=1}^{nt} \left(V_i^\delta - V_i\right) W_i.$$

We denote the last equality by Φ, then

$$\Phi = \frac{1}{\Delta t^3} \left\langle F'(\boldsymbol{G})^* \left(V^\delta - F(\boldsymbol{G})\right), \boldsymbol{\theta}\right\rangle_{\mathbb{R}^3} = \sum_{i=1}^{nt} \left(V_i^\delta - V_i\right) W_i. \tag{6.40}$$

From the previous equation and the first equality from (6.39), we obtain the following expression

$$\begin{aligned}\Phi = \sum_{i=1}^{nt} C\frac{U_i - U_{i-1}}{\Delta t} W_i - \sum_{i} \left(G_{Na} m_i^3 h_i + G_K n_i^4 + G_L\right) U_i W_i \\ - \sum_{i=1}^{nt} [(1-m_i)\alpha'_{m_i}(V_i) - m_i \beta_{m_i}(V_i)] P_i - \sum_{i=1}^{nt} [(1-n_i)\alpha'_{n_i}(V_i) - n_i \beta'_{n_i}(V_i)] Q_i \\ - \sum_{i=1}^{nt} [(1-h)\alpha'_{h_i}(V_i) - h\beta'_{h_i}(V_i)] R_i.\end{aligned} \tag{6.41}$$

From equations (6.38) and (6.39), the vector (W_1, U_{nt}) is equal to $(0,0)$. Then, we obtain

$$\sum_{i=1}^{nt} C\frac{U_i - U_{i-1}}{\Delta t} W_i = -\sum_{i=1}^{nt} C\frac{W_{i+1} - W_i}{\Delta t} U_i. \tag{6.42}$$

Substituting (6.42) into (6.41), we have the following equality

$$\begin{aligned}\Phi = -\sum_{i=1}^{nt} \left(C\frac{W_{i+1} - W_i}{\Delta t} + \left(G_{Na} m_i^3 h_i + G_K n_i^4 + G_L\right) W_i\right) U_i \\ - \sum_{i=1}^{nt} [(1-m_i)\alpha'_{m_i}(V_i) - m_i \beta_{m_i}(V_i)] P_i W_i - \sum_{i=1}^{nt} [(1-n_i)\alpha'_{n_i}(V_i) - n_i \beta'_{n_i}(V_i)] Q_i W_i \\ - \sum_{i=1}^{nt} [(1-h)\alpha'_{h_i}(V_i) - h\beta'_{h_i}(V_i)] R_i W_i.\end{aligned}$$

Replacing the first equality from (6.38) in the previous equation, leads to

$$\begin{aligned}\Phi = \sum_{i=1}^{nt} 3G_{Na} m_i^2 M_i h_i (V_i - E_{Na}) U_i + \sum_{i=1}^{nt} G_{Na} m_i^3 H_i (V_i - E_{Na}) U_i \\ + \sum_{i=1}^{nt} 4G_K n_i^3 N_i (V_i - E_K) U_i + \sum_{i=1}^{nt} \theta_{Na} m_i^3 h_i (V_i - E_{Na}) U_i \\ + \sum_{i=1}^{nt} \theta_K n_i^4 (V_i - E_K) U_i + \sum_{i=1}^{nt} \theta_L (V_i - E_L) U_i \\ - \sum_{i=1}^{nt} [(1-m_i)\alpha'_{m_i}(V_i) - m_i \beta_{m_i}(V_i)] P_i W_i - \sum_{i=1}^{nt} [(1-n_i)\alpha'_{n_i}(V_i) - n_i \beta'_{n_i}(V_i)] Q_i W_i \\ - \sum_{i=1}^{nt} [(1-h)\alpha'_{h_i}(V_i) - h\beta'_{h_i}(V_i)] R_i W_i.\end{aligned} \tag{6.43}$$

Let $(\mathcal{X}_i, \mathcal{Y}_i, \mathcal{Z}_i) \in \{(m_i, M_i, P_i), (n_i, N_i, Q_i), (h_i, H_i, R_i)\}$. Then, multiplying the second equation from (6.38) by $\mathcal{Z}_i$,

$$\sum_{i=1}^{nt}\left(\frac{\mathcal{Y}_{i+1}-\mathcal{Y}_i}{\Delta t} + [\alpha_{\mathcal{X}_i}(V_i)+\beta_{\mathcal{X}_i}(V_i)]\mathcal{Y}_i\right)\mathcal{Z}_i = \sum_{i=1}^{nt}[(1-\mathcal{X}_i)\alpha'_{\mathcal{X}_i}(V_i) - \mathcal{X}_i\beta'_{\mathcal{X}_i}(V_i)]W_i\mathcal{Z}_i. \quad (6.44)$$

From equations (6.38) and (6.39), the vector $(\mathcal{Y}_1, \mathcal{Z}_{nt}) \in \{(M_1, P_{nt}), (N_1, Q_{nt}), (H_1, R_{nt})\}$ equals $(0,0)$. Then, we have

$$\sum_{i=1}^{nt}\frac{\mathcal{Y}_{i+1}-\mathcal{Y}_i}{\Delta t}\mathcal{Z}_i = -\sum_{i=1}^{nt}\frac{\mathcal{Z}_i-\mathcal{Z}_{i-1}}{\Delta t}\mathcal{Y}_i. \quad (6.45)$$

Replacing equation (6.45) in (6.44), we obtain

$$-\sum_{i=1}^{nt}\left(\frac{\mathcal{Z}_i-\mathcal{Z}_{i-1}}{\Delta t} - [\alpha_{\mathcal{X}_i}(V_i)+\beta_{\mathcal{X}_i}(V_i)]\mathcal{Z}_i\right)\mathcal{X}_i = \sum_{i=1}^{nt}[(1-\mathcal{X}_i)\alpha'_{\mathcal{X}_i}(V_i) - \mathcal{X}_i\beta'_{\mathcal{X}_i}(V_i)]W_i\mathcal{Z}_i. \quad (6.46)$$

For $(\mathcal{X}_i, \mathcal{Y}_i, \mathcal{Z}_i) = (m_i, M_i, P_i)$ into (6.46), leads to

$$-\sum_{i=1}^{nt}\left(\frac{P_i-P_{i-1}}{\Delta t} - [\alpha_{m_i}(V_i)+\beta_{m_i}(V_i)]P_i\right)M_i = \sum_{i=1}^{nt}[(1-m_i)\alpha'_{m_i}(V_i) - m_i\beta'_{m_i}(V_i)]W_iP_i. \quad (6.47)$$

Substituting the second equation from (6.39) into (6.47),

$$\sum_{i=1}^{nt}3G_{Na}m_i^2h_i(V_i-E_{Na})U_iM_i = \sum_{i=1}^{nt}[(1-m_i)\alpha'_{m_i}(V_i) - m_i\beta'_{m_i}(V_i)]W_iP_i. \quad (6.48)$$

For $(\mathcal{X}_i, \mathcal{Y}_i, \mathcal{Z}_i) = (n_i, N_i, Q_i)$ into (6.46), we have

$$-\sum_{i=1}^{nt}\left(\frac{Q_i-Q_{i-1}}{\Delta t} - [\alpha_{n_i}(V_i)+\beta_{n_i}(V_i)]Q_i\right)N_i = \sum_{i=1}^{nt}[(1-n_i)\alpha'_{n_i}(V_i) - n_i\beta'_{n_i}(V_i)]W_iQ_i. \quad (6.49)$$

Substituting the third equation from (6.39) into (6.49),

$$\sum_{i=1}^{nt}4G_Kn_i^3(V_i-E_K)U_iN_i = \sum_{i=1}^{nt}[(1-n_i)\alpha'_{n_i}(V_i) - n_i\beta'_{n_i}(V_i)]W_iQ_i. \quad (6.50)$$

For $(\mathcal{X}_i, \mathcal{Y}_i, \mathcal{Z}_i) = (h_i, H_i, R_i)$ into (6.46), we obtain

$$-\sum_{i=1}^{nt}\left(\frac{R_i - R_{i-1}}{\Delta t} - [\alpha_{h_i}(V_i) + \beta_{h_i}(V_i)]R_i\right) H_i = \sum_{i=1}^{nt}[(1-h_i)\alpha'_{h_i}(V_i) - h_i\beta'_{h_i}(V_i)]W_i R_i. \quad (6.51)$$

Substituting the fourth equation from (6.39) into (6.51),

$$\sum_{i=1}^{nt} G_{Na} m_i^3 (V_i - E_{Na}) U_i H_i = \sum_{i=1}^{nt}[(1-h_i)\alpha'_{h_i}(V_i) - h_i\beta'_{h_i}(V_i)]W_i R_i. \quad (6.52)$$

Substituting equations (6.48), (6.50) and (6.52) in (6.43), we have

$$\Phi = \sum_{i=1}^{nt} \theta_{Na} m_i^3 h_i (V_i - E_{Na}) U_i + \sum_{i=1}^{nt} \theta_K n_i^4 (V_i - E_K) U_i + \sum_{i=1}^{nt} \theta_L (V_i - E_L) U_i.$$

By the definition of inner product

$$\Phi = \left\langle \left(\sum_{i=1}^{nt} m_i^3 h_i (V_i - E_{Na}) U_i, \sum_{i=1}^{nt} n_i^4 (V_i - E_K) U_i, \sum_{i=1}^{nt} (V_i - E_L) U_i \right), \boldsymbol{\theta} \right\rangle_{\mathbb{R}^3}. \quad (6.53)$$

From equations (6.40) and (6.53), since $\boldsymbol{\theta} \in \mathbb{R}^3$ is arbitrary, we obtain

$$F'(\boldsymbol{G})^* \left(\boldsymbol{V}^\delta - F(\boldsymbol{G}) \right) = \Delta t^3 \left(\sum_{i=1}^{nt} m_i^3 h_i (V_i - E_{Na}) U_i, \sum_{i=1}^{nt} n_i^4 (V_i - E_K) U_i, \sum_{i=1}^{nt} (V_i - E_L) U_i \right).$$

■

7 Conclusions

In this thesis, we studied models based on conductances of single neurons, in particular, the Hodgkin-Huxley, FitzHung-Nagumo, and cable models. These differential equations depend on parameters that are difficult to estimate. Thus, our main goal was to calculate the unknown parameters in the models previously mentioned. In this chapter, we will review the main contributions of our thesis and a list of future works.

7.1 Thesis contributions

In Chapter 3, we estimated conductances in the passive cable equation, both in a single branch and in a tree. To determine the unknown parameters we applied the Landweber method. The adjoint of the Gateaux derivative of this iteration is unknown, and in that chapter, we calculated it. The performance of the iterative method depends on i) the amount of unknown data, ii) the difficulty of the problem, iii) the initial guess and iv) the measurements on the data. For instance, determining two conductances is harder than determining one, finding conductances that depend on time and space is harder than finding conductances that depend only on space. If the initial guess is far from the solution, the algorithm will need many iterations to get an approximation or, in the worst cases, the algorithm may diverge. Having data at all points is better than if the data is available at isolated points only. Also, if the noise level in the measurements increases, the method provides reasonable approximations, but these approximations cannot be qualitatively better than those available.

In Chapter 4, we propose the minimal error method to estimate parameters in the Hodgkin-Huxley model. This iterative method is more efficient than the Landweber method. Furthermore, in many numerical tests, such as examples 5.1 and 5.2, the Landweber iteration diverges from the exact solution. Here, we also calculate the adjoint of the Gateaux derivative.

In Chapter 5, we estimated parameters with non-uniform distribution in the Hodgkin-Huxley model. To find approximate values for the unknown parameters we applied the minimal error method. The analytical results for the six unknown functions, such as calculating the adjoint of the Gateaux derivative, are satisfactory, but in the numerical results the method was only able to estimate one unknown function. Here we also test the Landweber iteration and note that the iterative method diverges for almost every example. To show that the method works for simplified models, we applied the proposed iteration in the FitzHugh-Nagumo model and obtained satisfactory analytical and numerical results. The work presents an essential contribution because we determine the unknown adjoint operator. Perhaps, using another iterative method in which the adjoint operator is defined, such as the Landweber-Kaczmarz and steepest descent methods, we will be able to obtain more than one unknown function.

Finally, in chapter 6, we worked with two discrete inverse problems. For the first problem, in the discrete cable equation, we estimated the conductance with nonuniform distribution. To determine these parameters, we used the minimal error method. In the second problem, in the Hodgkin-Huxley model, we applied the Landweber method to determine approximate values for the maximal conductances. In this chapter, we showed that it is possible to calculate the adjoint of the Gateaux derivative in discrete models.

7.2 Future Work

Although the iterative regularization methods proposed in this thesis provide reasonable estimates for the unknown parameters, some improvements can still be made.

In this context, we will survey some of the provided results which can be improved or extended further. Here are these points:

- We used the finite difference method to solve the differential equations. In this sense, we can apply more efficient computational methods to solve these equations.
- To estimate more than one function with non-uniform distribution, in the Hodgkin-Huxley equation, we can apply another iterative regularization method, for example, the Landweber-Kaczmarz iteration.
- We can show the convergence conditions of the proposed iterative methods for each inverse problem.
- We can apply other regularization methods to estimate parameters in the proposed problems.
- We can apply the proposed iterative methods in neuron population models, for example the Wilson-Cowan model.

Bibliography

AZEVEDO, F. A. et al. Equal numbers of neuronal and nonneuronal cells make the human brain an isometrically scaled-up primate brain. *Journal of Comparative Neurology*, Wiley Online Library, v. 513, n. 5, p. 532–541, 2009. Cited on page 16.

BATISTA, P.; PEREIRA, A. Impact and prevention of neurodegenerative diseases in society: Alzheimer and parkinson. 2017. Cited on page 15.

BAUMEISTER, J.; LEITAO, A. *Topics in inverse problems*. [S.l.]: IMPA, 2005. Cited on page 31.

BERNSTEIN, J. Untersuchungen zur thermodynamik der bioelektrischen ströme. *Pflügers Archiv European Journal of Physiology*, Springer, v. 92, n. 10, p. 521–562, 1902. Cited on page 19.

BERNSTEIN, J. *Elektrobiologie: die Lehre von den elektrischen Vorgängen im Organismus auf moderner Grundlage dargestellt*. [S.l.]: Springer-Verlag, 2013. Cited on page 19.

COLE, K. S.; CURTIS, H. J. Electric impedance of the squid giant axon during activity. *The Journal of general physiology*, Rockefeller University Press, v. 22, n. 5, p. 649–670, 1939. Cited on page 19.

ENGL, H. W.; HANKE, M.; NEUBAUER, A. *Regularization of inverse problems*. [S.l.]: Springer Science & Business Media, 1996. v. 375. Cited 2 times on pages 29 and 31.

ERMENTROUT, G. B.; TERMAN, D. H. *Mathematical foundations of neuroscience*. [S.l.]: Springer Science & Business Media, 2010. v. 35. Cited 4 times on pages 9, 17, 23, and 26.

GUTKIN, B.; PINTO, D.; ERMENTROUT, B. Mathematical neuroscience: from neurons to circuits to systems. *Journal of Physiology-Paris*, Elsevier, v. 97, n. 2-3, p. 209–219, 2003. Cited on page 22.

HADAMARD, J. *Lectures on Cauchy's problem in linear partial differential equations*. [S.l.]: Courier Corporation, 2014. Cited on page 29.

HANSEN, P. C. *Discrete inverse problems: insight and algorithms*. [S.l.]: Siam, 2010. v. 7. Cited on page 73.

HODGKIN, A. L.; HUXLEY, A. F. The components of membrane conductance in the giant axon of loligo. *The Journal of physiology*, Wiley Online Library, v. 116, n. 4, p. 473–496, 1952. Cited on page 20.

HODGKIN, A. L.; HUXLEY, A. F. Currents carried by sodium and potassium ions through the membrane of the giant axon of loligo. *The Journal of physiology*, Wiley Online Library, v. 116, n. 4, p. 449–472, 1952. Cited 2 times on pages 20 and 21.

HODGKIN, A. L.; HUXLEY, A. F. The dual effect of membrane potential on sodium conductance in the giant axon of loligo. *The Journal of physiology*, Wiley Online Library, v. 116, n. 4, p. 497–506, 1952. Cited on page 20.

HODGKIN, A. L.; HUXLEY, A. F. A quantitative description of membrane current and its application to conduction and excitation in nerve. *The Journal of physiology*, Wiley-Blackwell, v. 117, n. 4, p. 500–544, 1952. Cited 3 times on pages 20, 21, and 44.

HODGKIN, A. L.; HUXLEY, A. F.; KATZ, B. Measurement of current-voltage relations in the membrane of the giant axon of loligo. *The Journal of physiology*, Wiley Online Library, v. 116, n. 4, p. 424–448, 1952. Cited on page 20.

IZHIKEVICH, E. M. *Dynamical systems in neuroscience*. [S.l.]: MIT press, 2007. Cited on page 44.

JAEGER, D.; JUNG, R. *Encyclopedia of computational neuroscience*. [S.l.]: Springer Publishing Company, Incorporated, 2015. Cited on page 33.

KALTENBACHER, B.; NEUBAUER, A.; SCHERZER, O. *Iterative regularization methods for nonlinear ill-posed problems*. [S.l.]: Walter de Gruyter, 2008. v. 6. Cited on page 31.

KEENER, J.; SNEYD, J. *Mathematical Phsiology I: Cellular Physiology*. [S.l.]: Springer, 2009. v. 2. Cited 7 times on pages 9, 19, 23, 24, 25, 26, and 58.

LAPICQUE, L. Recherches quantitatives sur l'excitation electrique des nerfs traitee comme une polarization. *Journal de Physiologie et de Pathologie Generalej*, v. 9, p. 620–635, 1907. Cited on page 19.

LEITÃO, A.; SVAITER, B. Projective acceleration of the nonlinear landweber method under the tangential cone condition. *Numerische Mathematik*, v. 130, 2015. Cited on page 30.

MADUREIRA, A. L.; MANDUJANO, J. A. Determinação de parâmetros com distribuição espacial não uniforme num modelo de neurociência via o método de landweber não linear. *X Encontro Acadêmico de Modelagem Computacional*, X-EAMC, v. 1, n. 1, p. 1–7, 2017. Cited on page 33.

MADUREIRA, A. L.; MANDUJANO, J. A. Solução numérica de um problema inverso em neurociência via o método de landweber não linear. *Proceedings Series of the Brazilian Society of Computational and Applied Mathematics*, SBMAC, v. 5, n. 1, p. 10487–1–10487–7, 2017. Cited on page 33.

MADUREIRA, A. L.; VALLE, J. A. M. Solução numérica de um problema inverso em neurociência via o método de landweber não linearlinear. *Proceeding Series of the Brazilian Society of Computational and Applied Mathematics*, v. 5, n. 1, 2017. Cited on page 26.

MENKE, W. *Geophysical data analysis: Discrete inverse theory*. [S.l.]: Academic press, 2018. Cited on page 73.

NEUBAUER, A. On landweber iteration for nonlinear ill-posed problems in hilbert scales. *Numerische Mathematik*, Springer, v. 85, n. 2, p. 309–328, 2000. Cited on page 31.

PEARCE, N.; KROMHOUT, H. *Neurodegenerative disease: The next occupational disease epidemic?* [S.l.]: BMJ Publishing Group Ltd, 2014. Cited on page 15.

PHILLIPSON, P. E.; SCHUSTER, P. A comparative study of the hodgkin–huxley and fitzhugh–nagumo models of neuron pulse propagation. *International Journal of Bifurcation and Chaos*, World Scientific, v. 15, n. 12, p. 3851–3866, 2005. Cited on page 24.

RAMANAN, V.; SAYKIN, A. *Pathways to neurodegeneration: mechanistic insights from GWAS in Alzheimer's disease, Parkinson's disease, and related disorders*. [S.l.]: American Journal of Neurodegenerative Disease, 2013. v. 2. 145-175 p. Cited on page 15.

TRAPPENBERG, T. *Fundamentals of computational neuroscience*. [S.l.]: OUP Oxford, 2009. Cited on page 25.

VALLE, J. A. M.; MADUREIRA, A. L. Parameter identification problem in the hodgkin and huxley model. *arXiv preprint arXiv:1903.10286*, 2019. Cited on page 44.

VALLE, J. A. M.; MADUREIRA, A. L.; LEITÃO, A. A computational approach for the inverse problem of neuronal conductances determination. *arXiv preprint arXiv:1810.05887*, 2018. Cited on page 33.

VANDENBERG, J. I.; WAXMAN, S. G. Hodgkin and huxley and the basis for electrical signalling: a remarkable legacy still going strong. *The Journal of physiology*, Wiley Online Library, v. 590, n. 11, p. 2569–2570, 2012. Cited on page 19.

APPENDIX A – Paper 1

A Computational Approach for the Inverse Problem of Neuronal Conductances Determination

A COMPUTATIONAL APPROACH FOR THE INVERSE PROBLEM OF NEURONAL CONDUCTANCES DETERMINATION

JEMY A. MANDUJANO VALLE, ALEXANDRE L. MADUREIRA, ANTONIO LEITÃO

Abstract. The derivation by Alan Hodgkin and Andrew Huxley of their famous neuronal conductance model relied on experimental data gathered using the squid giant axon. It becomes clear that determining experimentally the conductances of neurons is difficult, in particular under the presence of spatial and temporal heterogeneities. Moreover, it is reasonable to expect variations between species or even between different types of neurons of the same species. Determining conductances from one type of neuron is no guarantee that it would work for all types.

We tackle the inverse problem of determining, given voltage data, conductances with non-uniform distribution in the simpler setting of a passive cable equation, both in a single branch or in a tree. To do so, we consider the Landweber iteration, a computational technique used to solve inverse problems. We provide several numerical results showing that the method is able to provide reasonable approximations for the conductances, given enough information on the voltages, even for noisy data.

1. Introduction.

The seminal model of Hodgkin and Huxley [22] of neuronal voltage conductance describes how action potential occurs and propagate. It is a landmark model and presents an outstanding combination of modeling based on physical arguments and experimental data, needed to determine the behavior of ion channels. As a part of their work, they modeled the conductances by designing several mathematical functions (the α's and β's) that make the computed voltage to behave as the data. In this paper we propose a numerical procedure to approximate the conductances of the ion channels. To obtain the unknown parameters we use an iterative method.

Finding the conductances is crucial if one wants to emulate the neuronal voltage propagation using computational models, since the conductances *are part of the data required by the models*. Mimicking the work of Hodgkin and Huxley for every single neuron and or experimental condition is very demanding. Using other, simpler models might be an alternative, but it is always necessary to find out what are the physiological parameters. What we would

Date: April 16, 2019.

like to offer is a computational way to determine the conductances based on experimental data, and we consider our method a step towards that final goal. The method can also be extended to accommodate excitatory and inhibitory synapses, and could be used, in principle, in several nonlinear models, such as the FitzHugh-Nagumo, Morris-Lecar, Hodgkin-Huxley, etc, with varying degrees of difficulty.

We use a simplified neuronal model, the passive cable equation [4, 19, 40], given by a parabolic partial differential equation (PDE). We consider first the case of a single branch of length L, represented by the interval $[0, L]$. The more general case of a branched tree is described in the Section 2.1. In the cable model the membrane electrical potential $V : [0, T] \times [0, L] \to \mathbb{R}$ solves

$$C_M \frac{\partial V}{\partial t} = \frac{1}{R_I + R_E} \frac{\partial^2 V}{\partial x^2} - I_{\text{ion}}(t, x) \quad \text{for } 0 < t < T,\ 0 < x < L, \tag{1}$$

where the potential V is in millivolt (mV); the internal and external neuronal resistance R_I, R_E are in ohm (Ω) ; C_M represents membrane specific capacitance in farad per square centimeter (F/cm^2); the specific ionic current I_{ion} is in milliampere per square centimeter (mA/cm^2). For the passive cable models, the ionic current is given by

$$I_{\text{ion}}(t, x) = \sum_{i \in \text{Ion}} G_i(t, x)\big(V(t, x) - E_i\big),$$

where Ion is the set of ions of the model, e.g., Ion $= \{\text{K}, \text{Na}, \text{Leak}\}$. Also, the membrane specific conductance G_i for the ion $i \in$ Ion is in siemen per square centimeter (S/cm^2), and it might depend on spatial and temporal variables, as indicated in the notation. In this paper, these functions are not known. Finally, the Nerst potential E_i for each ion $i \in$ Ion is given in millivolt (mV).

To Eq. (1) we add boundary and initial conditions given by

$$\frac{\partial V}{\partial x}(t, 0) = p(t), \qquad \frac{\partial V}{\partial x}(t, L) = q(t), \qquad V(0, x) = r(x), \quad \text{for } 0 < t < T, \quad 0 < x < L. \tag{2}$$

We assume that the constants C_M, R_I, R_E and E_i, and the functions p, q and r are given data.

We next rewrite Eqs. (1) and (2) in a slightly more convenient form. Consider the positive quantities $c = C_M(R_I + R_E)$ and $g_i(t, x) = G_i(t, x)(R_I + R_E)$, and then

$$\begin{cases} cV_t(t, x) = V_{xx}(t, x) - \sum_{i \in Ion} g_i(t, x)[V(t, x) - E_i] & \text{for} \quad 0 < t < T,\ 0 < x < L, \\ V(0, x) = r(x) \quad \text{for } 0 < x < L, \\ V_x(t, 0) = p(t), \quad V_x(t, L) = q(t) \quad \text{for} \quad 0 < t < T. \end{cases} \tag{3}$$

Note that the new unknowns g_i are unitless but still positive.

Let N_{ion} be the number of ions of the set Ion, and $\boldsymbol{g}(t,x) = (g_1(t,x),\dots,g_{N_{\text{ion}}}(t,x))$. The inverse problem of finding the "correct" $\boldsymbol{g}$ given measurements of the voltage is highly nontrivial, in the sense that it leads to ill-posed problems [45], and that it becomes even harder in the presence of *spatially dependent parameters*. There are different approaches to deal with the problem in hand, but certainly no panacea.

Hodgkin and Huxley [22] tackled such problem by a highly nontrivial data fitting, in a wonderful achievement made possible only due to an ingenious combination of experiments and biophysical insight. Wilfrid Rall and co-authors considered several related questions for the cable equation [34, 35, 36, 37, 38, 23]. See also [41, 24, 7, 17, 16, 39, 26]. In [46] there is an interesting attempt to introduce heterogeneity into the Hodgkin and Huxley model.

In terms of biologically inclined references, in [48] the authors consider the branched cable equation with the chemical synapses, and convert somatic conductances into dendritic conductances. There are several other articles [3, 28, 43, 44, 47] dealing with the issue of determining conductances and pre-synaptic inputs with different techniques, ranging from deterministic to statistical and stochastic. However, it is far from clear if their approach can be mathematically justified and if it is possible at all to extend those ideas for spatially distributed conductances.

We consider next references with a stronger mathematical flavor. Uniqueness of solutions for finding constant parameters in the cable equation, and related methods, are considered in [10, 13, 15], and [12] for a nonlinear model; see also [1, 33] for further considerations related to existence and uniqueness. In [14] a related problem was tackled based on the FitzHugh–Nagumo and Morris–Lecar models, where nonlinear functions modeling the conductances are sought. The method is based on fixed point arguments, and despite its ingenuity, it is not clear how to extend it to more involved models or to accommodate for spatially distributed ions channels.

In [5, 42, 11, 1, 2], the question of determining spatially distributed conductances is investigated through different techniques and algorithms. They differ considerably from our method, and seem harder to generalize for other situations, as, for instance, when the domain is given by trees (with the obvious exception of [1, 2]), for time dependent conductances, and for general nonlinear equations, our ultimate goal.

We would like to stress that although neuroscience models based on ordinary differential equations are, and will always be, of paramount importance, it is our belief that spatially distributed equations will grow in importance. And spatially distributed data will become easier to gather, in particular due to techniques as *voltage-sensitive dye imaging* (VSDI) [8, 20].

CASE I	$\Gamma = [0,T] \times [0,L] = \{(t,x);\ \ 0 \le t \le T,\ \ 0 \le x \le L\}$
CASE II	$\Gamma = [0,T] \times \{0,L\} = \{(t,x);\ \ 0 \le t \le T,\ \ x \in \{0,L\}\}$

TABLE 1. Summary of the two different cases considered in this paper. We seek the unknowns g_i assuming that Eq. (3) holds and that a perturbation of the voltage V is known at the space-time domain Γ defined above. In case I, the data is known at all points and at all times; in case II, the data is known at two end-points and at all times.

Inverse problems like the present one are ill-posed, and, under certain conditions, the *Landweber method* [30] provides convergent iterative scheme. The main goal of the present paper is to develop the *Nonlinear Landweber method* [21, 6, 32, 9] to solve the inverse problem of recovering the conductances in the cable equation. We also test the scheme under different scenarios.

The Landweber method is one among several iterative regularization methods for obtaining stable solutions for ill-posed problems. It has the advantage of each iteration being "cheap" (it avoids inversions of Newton-like methods) at the possible price of taking more iterations to converge. See [31] for a nice review and comparison among the methods.

We next outline the contents of the paper. In Section 2 we present the method, detailing how it should be applied in the cases of a non-branched and branched cable, where the geometry is given by a tree. Section 3 presents the related numerical results. In Section 4 we draw some concluding remarks, and the Appendix provide some technical details regarding the method and the mathematics behind it.

2. Method: The Landweber scheme applied to the conductance determination

Here we consider an application of the Landweber method to the problem at hand. Knowing the voltage V at the time-space domain Γ, we want to determine $\boldsymbol{g}$ assuming that Eq. (3) holds. We consider two different cases, depending on where the voltage is measured. In the first case, we assume that V is known at all time-space points, i.e., $\Gamma = [0,T] \times [0,L]$ (Table 1, Case I). In the second case, we assume that the voltage is known at all end points and all the time. Thus $\Gamma = [0,T] \times \{0,L\}$ (Table 1, Case II).

Let

$$V|_\Gamma = \{V(t,x),\ \ (t,x) \in \Gamma\},$$

and consider the nonlinear operator

$$F : D(F) \to R(F) \tag{4}$$

that associates for a given $\boldsymbol{g} \in D(F)$ the resulting voltage, i.e., $F(\boldsymbol{g}) = V|_\Gamma$, where V solves Eq. (3). The domain $D(F)$ and the image $R(F) = L^2(\Gamma)$ (the space of square integrable functions) are properly defined in the Appendix A. Given a smooth enough function f, we define its L^2 norm $\|\cdot\|_{L^2(\Gamma)}$ such that

$$\|f\|^2_{L^2(\Gamma)} = \int_\Gamma |f(\xi)|^2 d\,\xi.$$

We consider the inverse problem of finding an approximation for $\boldsymbol{g}$ given the noisy data $V^\delta|_\Gamma$, where

$$\|V - V^\delta\|_{L^2(\Gamma)} \leq \delta, \tag{5}$$

for some known noise threshold $\delta > 0$. That makes sense since, in practice, the data $V|_\Gamma$ are never known exactly. In section 3 we detail the type of noise introduced.

Given an initial guess $\boldsymbol{g}^{1,\delta}$, the Landweber approximation for $\boldsymbol{g}$ is defined by the sequence

$$\boldsymbol{g}^{k+1,\delta} = \boldsymbol{g}^{k,\delta} + F'(\boldsymbol{g}^{k,\delta})^*(V^\delta|_\Gamma - F(\boldsymbol{g}^{k,\delta})), \tag{6}$$

for $k = 1, 2, \ldots,$ where $F'(\cdot)^*$ is adjoint of the Gâteux derivative. The Landweber iteration is a gradient method, as is the steepest descent method. Although the steps of both methods follow the same direction (the gradient), they differ on their step size [25].

As a stopping criteria we use the *discrepancy principle* [25] with $\tau > 2$, i.e., we define the stopping iteration step k_* such that

$$\|V^\delta - F(\boldsymbol{g}^{k_*,\delta})\|_{L^2(\Gamma)} \leq \tau\delta \leq \|V^\delta - F(\boldsymbol{g}^{k,\delta})\|_{L^2(\Gamma)}, \tag{7}$$

for all $1 \leq k < k_*$. In practice, stopping criteria are needed for all iterative methods, otherwise the scheme might stop before it is accurate enough, or might diverge, or might waste computing time without significantly improving the solution. For inverse problems with noisy data this is even more crucial since running regularization iterative methods beyond certain threshold forces the method to "fit the noise". It is possible to show that, under certain conditions (we assume that is the case), $\boldsymbol{g}^{k_*,\delta}$ converges to a solution of $F(\boldsymbol{g}) = V$ as $\delta \to 0$; see [25], Theorem 2.6.

From Eqs. (6) and (7) we obtain an approximation $\boldsymbol{g}^{k_*,\delta}$ for $\boldsymbol{g}$. Although the adjoint $F'(\boldsymbol{g}^{k,\delta})^*$ is not known, it is possible to show that Eq. (6) is actually

$$g_i^{k+1,\delta}(t,x) = g_i^{k,\delta}(t,x) - (V^{k,\delta}(t,x) - E_i)U^k(t,x) \quad \text{for all } i \in \text{Ion}, \tag{8}$$

where $V^{k,\delta}$ solves Eq. (3) replacing $\boldsymbol{g}$ by $\boldsymbol{g}^{k,\delta}$, and U^k solves the following PDE with *final condition*:

$$\begin{cases} -U^k_{xx}(t,x) - cU^k_t(t,x) + \sum_{i\in\text{Ion}} g_i^{k,\delta}(t,x)U^k(t,x) = \alpha_1\left(V^\delta(t,x) - V^{k,\delta}(t,x)\right), \\ U^k(T,x) = 0, & 0 < x < L, \\ U^k_x(t,0) = -\alpha_2\left(V^\delta(t,0) - V^{k,\delta}(t,0)\right), & 0 < t < T, \\ U^k_x(t,L) = \alpha_2\left(V^\delta(t,L) - V^{k,\delta}(t,L)\right), & 0 < t < T. \end{cases} \tag{9}$$

The constants α_1, α_2 depend on the set Γ as follows:

$$(\alpha_1, \alpha_2) = \begin{cases} (1,0) & \text{if } \Gamma = [0,T]\times[0,L], \\ (0,1) & \text{if } \Gamma = [0,T]\times\{0,L\}. \end{cases} \tag{10}$$

In Theorem A.1 of the Appendix, we show how we obtain Eq. (8) from Eq. (6).

Remark 1. *Note from Eq.* (8) *that* $g_i^{k+1,\delta}(T,x) = g_i^{k,\delta}(T,x)$ *for all* $x \in [0,1]$ *and every* $k \in \mathbb{N}$, *since, from Eq.* (9), $U^k(T,x) = 0$. *Thus,* $g_i^{k,\delta}$ *is* never corrected at the final time T. *To recover* g_i *at time* T, *one could perform the computations up to* $T + \delta t$, *for some given* $\delta t > 0$, *and then consider only the values up to* T.

The numerical scheme of our method is as follows. Check Table 1 for notation. Note from Algorithm 1 that solutions of two PDEs are needed for each iteration.

Data: $V^\delta|_\Gamma$, r, p, q, δ, τ
Result: Compute an approximation for $\boldsymbol{g}$ using Landweber Iteration Scheme
Choose $\boldsymbol{g}^{1,\delta}$ as an initial approximation for $\boldsymbol{g}$;
Compute $V^{1,\delta}$ from Eq. (3), replacing $\boldsymbol{g}$ by $\boldsymbol{g}^{1,\delta}$;
k=1;
while $\tau\delta \le \|V^\delta - V^{k,\delta}\|_{L^2(\Gamma)}$ **do**
    Compute U^k from Eq. (9);
    Compute $\boldsymbol{g}^{k+1,\delta}$ using Eq. (8);
    Compute $V^{k+1,\delta}$ from Eq. (3), replacing $\boldsymbol{g}$ by $\boldsymbol{g}^{k+1,\delta}$;
    $k \leftarrow k+1$;
end

Algorithm 1: Nonlinear Landweber Iteration

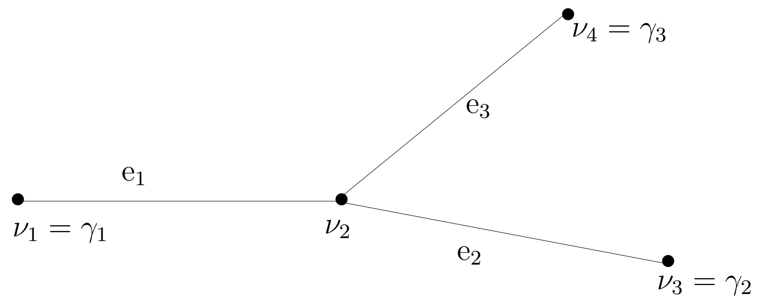

Figure 1. Example of a tree with one bifurcation point.

Remark 2. *A modification to Algorithm 1 would be to consider the Landweber-Kaczmarcz method* [25]*, where multiple experiments are performed sequentially or in parallel, and used to update* $\boldsymbol{g}$*.*

Remark 3. *Whenever* $\boldsymbol{g}$ *is time independent, and in this case we write* $\boldsymbol{g}(t,x) = \boldsymbol{g}(x)$*, the interaction is defined by*

$$g_i^{k+1,\delta} = g_i^{k,\delta} - \frac{1}{T}\int_0^T (V^{k,\delta} - E_i)U^k\,dt \quad \textit{for } i \in Ion. \tag{11}$$

2.1. **The Landweber Method applied to the conductance determination defined on a tree.** Following the notation of [1, 2], we let $\Theta = \mathcal{E} \cup \mathcal{V}$ be a tree, where $\mathcal{E} = \{e_1, e_2, \cdots, e_N\}$ is a set of edges, $\mathcal{V} = \{\nu_1, \nu_2, \cdots, \nu_M\}$ is a set of vertices, and the edges are connected at the vertices ν_j. Let $\{\gamma_1, \gamma_2, \cdots, \gamma_m\} = \partial\Theta \subset \mathcal{V}$, i.e. if the index of a vertex, $\mathrm{id}(\nu)$, is the number of edges incident to it, then $\partial\Theta = \{\nu \in \mathcal{V} : \mathrm{id}(\nu) = 1\}$. Hence $\mathcal{V} \setminus \partial\Theta = \{\nu \in \mathcal{V} : \mathrm{id}(\nu) > 2\}$. In Figure 1 we depict a simple example of a tree with one bifurcation point.

Our cable equation model defined on a tree is given by

$$\begin{cases} V_{xx}(t,x) = cV_t(t,x) + \displaystyle\sum_{i \in Ion} g_i(t,x)\left[V(t,x) - E_i\right], & \text{in} \quad (0,T) \times \mathcal{E}, \\ V(0,x) = r(x), & \text{in } x \in \Theta, \\ V_x(t,\gamma_k) = f_k(t), & \text{at each vertex } \gamma_k \in \partial\Theta \text{ and } t \in [0,T], \\ \displaystyle\sum_{e_j \sim \nu} V_j'(t,\nu) = 0, & \text{at each vertex } \nu \in \mathcal{V} \setminus \partial\Theta \text{ and } t \in [0,T], \end{cases} \tag{12}$$

where c, r, f_k and $\boldsymbol{g} = (g_1, \ldots, g_{N_{\text{ion}}})$ are the given data; cf. Eq. (3).

In the last equation of the PDE (12), $V_j'(\nu)$ denotes the derivative of V at the vertex ν taken along the edge e_j in the direction towards the vertex. Also, $e_j \sim \nu$ means edge e_j is incident to vertex ν, and the sum is taken over all edges incident to ν. Since $\partial\Theta$ consists of m vertices, f_k can be naturally identified with a function acting from $[0,T]$ to $\mathbb{R}^m$.

Let $\Omega = (0,T)\times\Theta$ and define the operator

$$F : \left(L^2(\Omega)\right)^{N_{\text{ion}}} \to L^2(\Omega)$$

such that $F(\boldsymbol{g}) = V(\cdot,\cdot)$, where V solves Eq. (12). The objective of this section is to, given V^δ, obtain an approximation to $\boldsymbol{g}$, using the method Eq. (6). To compute the adjoint operator $F'(\cdot)^*$, we define the following PDE:

(13)
$$\begin{cases} -U^k_{xx}(t,x) - cU^k_t(t,x) + \sum\limits_{i\in Ion} g_i(t,x)U^k(t,x) = V^\delta(t,x) - V^{k,\delta}(t,x), & \text{in } (0,T)\times\mathcal{E}, \\ U^k(T,x) = 0, & \text{in } x\in\Theta, \\ U^k_x(t,\gamma_k) = 0, & \text{at each vertex } \gamma_k\in\partial\Theta \text{ and } t\in[0,T], \\ \sum\limits_{e_j\sim\nu} U'_j(t,\nu) = 0, & \text{at each vertex } \nu\in\mathcal{V}\setminus\partial\Theta \text{ and } t\in[0,T]. \end{cases}$$

We then compute $g_i^{k+1,\delta}$ according to (8). Remarks 1–3 also hold for this problem.

3. Results: Numerical Simulation

In this section we test the method under different scenarios. Of course, the solutions are obtained numerically, and for that we use finite difference scheme in space coupled with backward Euler in time. To compute the integral in Eq. (11) we use the trapezoidal rule. In what follows we assume that the numerical approximations are accurate enough. All the experiments were performed using Matlab®, and the codes are available at `https://github.com/MandujanoValle/Inverse-Problem-in-the-Cable-Equation`

To design our *in silico* experiments, we first choose $\boldsymbol{g}$ and compute V from Eq. (3), obtaining then $V|_\Gamma$. Of course, in practice, only the values of $V^\delta|_\Gamma$ are given by some experimental measures, and thus subject to experimental/measurement errors. In our examples, $V^\delta|_\Gamma$ is obtained by considering linear-multiplicative noise

$$V^\delta(t,x) = V(t,x) + (aV+b)\text{rand}_\Delta(t,x) \quad \text{for all } (t,x)\in\Gamma, \tag{14}$$

for scalars a, b, and rand_Δ is a uniformly distributed random variable taking values in the range $[-\Delta,\Delta]$. The threshold δ is such that (cf. Eq. (5)) $\|(aV+b)\text{rand}_\Delta\|_{L^2(\Gamma)} \le \delta$, and we impose then

$$\|(aV+b)\|_{L^2(\Gamma)}\Delta = \delta. \tag{15}$$

In our numerical examples, we use multiplicative error, i.e., $a = 1$ and $b = 0$ at Eq. (14). Thus, δ and Δ are related by $\|V\|_{L^2(\Gamma)}\Delta = \delta$.

Remark 4. *In general it is not possible to predict how the added noise will affect the conductances since the operator F defined in Eq.* (4) *is not bounded, meaning that small perturbation of the data might lead to large perturbation of the conductances. That is why inverse problems are so hard to approximate.*

Next, given the initial guess $\boldsymbol{g}^{1,\delta}$, the data $V^\delta|_\Gamma$, and the noise threshold δ, we approximate $\boldsymbol{g}$ using the Algorithm 1. Unlike in "direct" PDE problems where the exact solution usually has to be computed by numerical over-kill, here we have the exact $\boldsymbol{g}$ and we use that to gauge the algorithm performance. We introduce for $k = 1, 2, \dots,$

$$\text{Res}_k = \|V^\delta - F(\boldsymbol{g}^{k,\delta})\|_{L^2(\Gamma)}, \qquad \text{Error}_k = \frac{1}{N_{ion}} \sum_{i \in Ion} \int_{D(\boldsymbol{g})} \frac{|g_i - g_i^{k,\delta}|}{|g_i|} \times 100\%. \tag{16}$$

where $D(\boldsymbol{g})$ denotes the domain where $\boldsymbol{g}$ is defined. In applications, only the residual Res_k is available, and that is all that the Algorithm 1 uses.

Remark 5. *In practice, after discretizing the equations and the unknown functions, only nodal values are known. Consider the space-time discretization $t_n = (n-1)T/(N-1)$ for $n = 1, 2\cdots, N$ and $x_j = (j-1)L/(J-1)$ for $j = 1, 2\cdots, J$. Thus, the relative error introduced above relates to the* the mean absolute percentage error

$$Error_k = \frac{1}{N_{ion}} \frac{T}{N} \frac{L}{J} \sum_{i \in Ion} \sum_{n=1}^{J} \sum_{j=1}^{N} \left| \frac{g_i(t_n, x_j) - g_i^{k,\delta}(t_n, x_j)}{g_i(t_n, x_j)} \right| \times 100\%. \tag{17}$$

Whenever $\boldsymbol{g}$ is time independent, and in this case we write $\boldsymbol{g}(t_n, x_j) = \boldsymbol{g}(x_j)$, the mean absolute percentage error is defined by

$$Error_k = \frac{1}{N_{ion}} \frac{L}{J} \sum_{i \in Ion} \sum_{n=1}^{J} \left| \frac{g_i(x_j) - g_i^{k,\delta}(x_j)}{g_i(x_j)} \right| \times 100\%. \tag{18}$$

Similar remark holds for other norms, e.g., $\|f\|_{L^2(\Gamma)}$ is to be replaced by $\|f\|_{l^2(\Gamma)}$, where

$$\|f\|^2_{l^2(\Gamma)} = \frac{T}{N} \frac{L}{J} \sum_{(t_n, x_j) \in \Gamma} |V(t_n, x_j)|^2. \tag{19}$$

We present four numerical tests. In the first three examples the geometry is defined by a segment, and in the fourth example is given by a tree. The first example considers only one ion (Ion $= \{\text{K}\}$), with $\boldsymbol{g}(x) = g_{\text{K}}(x)$ dependent only the spatial variable, and the voltage is known at $\Gamma = [0, T] \times \{0, L\}$, i.e., at all times but only at the end-points. In the second example, still with one ion (Ion = {K}), the conductance depends on the temporal and spatial variables (t, x) and measured voltage is known at $\Gamma = [0, T] \times [0, L]$, i.e., all the time and at all points. In the third example, we consider two ions (Ion = {K, Na}), where $\boldsymbol{g}(x) = (g_{\mathrm{K}}(x), g_{\mathrm{Na}}(x))$ depends only on the spatial variable and the data is again known at $\Gamma = [0, T] \times [0, L]$, i.e., all the time for all points. Finally, in the fourth example we consider the case where the geometry is defined by a tree, with the conductance being time independent under the presence of one ion, and the voltage data being known at all the time and all the points.

Example 3.1. *Consider a particular instance from Eq.* (3)*, where* $N_{ion} = 1$ *(*$Ion = \{K\}$*),* $c = 1\ [\Omega F/cm^2]$*,* $E_K = 0\ [mV]$*,* $L = 1\ [cm]$*,* $T = 1\ [ms]$*,* $g_i(t, x) = g_K(x)$ *and*

$$r(x) = 2.5 \times \tan(x), \qquad p(t) = \exp(-t), \qquad q(t) = 2\exp(-t).$$

In this test, we consider $\Gamma = [0, T] \times \{0, L\}$ *and* $N = J = 50$*. The goal is to find* $g_K(x) = \sec(x)$ *given* $V^\delta|_\Gamma$*,* $g_K^{1,\delta}(x) = 0$ *and* $\tau = 2.01$*.*

In Table 2 we present the results for various levels of noise. Note that for smaller amount of noise, more steps are required. That is due to the discrepancy principle (7) *and the relation* (15)*. At each line of the table the noise is reduced by a factor of five, and that leads to a similar reduction of the residual. The same cannot be stated about the approximation error, exposing the instability of the problem.*

In Figures 2, 3 and 4, we plot results for $\Delta = 5\%$ *of noise (see Table 2, line 4). In Figure 2 we display the exact and noisy voltages on the left, and the exact and approximate solutions and the initial guess on the right. In Figure 3 we show the error and residual functions. Finally, Figure 4 displays the error and residual as function of the iteration number.*

Example 3.2. *In this example, we consider* $g(t, x)$ *as depending on time and space. The values for equation* (3) *are:* $N_{ion} = 1$ *(*$Ion = \{K\}$*),* $c = 1\ [\Omega F/cm^2]$*,* $E_K = 1\ [mV]$*,* $L = 1\ [cm]$*,* $T = 1\ [ms]$*,* $g_i(t, x) = g_K(t, x)$ *and*

$$r(x) = \sin(x), \qquad p(t) = \exp(t), \qquad q(t) = 0.$$

Let $\Gamma = [0, T] \times [0, L]$ *and* $N = J = 50$*. The goal is to find*

$$g_K(t, x) = \frac{1}{2} \times \frac{\exp(8x - 4) - 1}{\exp(8x - 4) + 1} + t + 1,$$

given $V^\delta|_\Gamma$*,* $g_K^{1,\delta}(t, x) = 0$ *and* $\tau = 2.01$*.*

This example is harder than the previous one since now the conductance depends on two variables. In Table 3 we present the results for various levels of noise, and the same comments

Δ	k_*	$Error_{k_*}$	Res_{k_*}
125%	*1*	*100 %*	2×10^0
25%	*2*	*46 %*	5×10^{-1}
5%	*5*	*17 %*	2×10^{-1}
1%	*9*	*5.3%*	3×10^{-2}
0.2%	*18*	*4.3 %*	8×10^{-3}
0.04%	*70*	*2.5 %*	1×10^{-3}
0.008%	*1297*	*1.8 %*	3×10^{-4}

TABLE 2. Numerical results for Example 3.1. The first column describes the noise level Δ, as in Eq. (14). The second column contains the number of iterations according to Eq. (7). The third column lists the error according to Eq. (18). Finally, the fourth column presents the residual as in Eq. (16) in the sense of Eq. (19). Note that the residual decreases roughly as the noise. However, the error does not decrease at the same rate, a behavior that is typical of inverse problems.

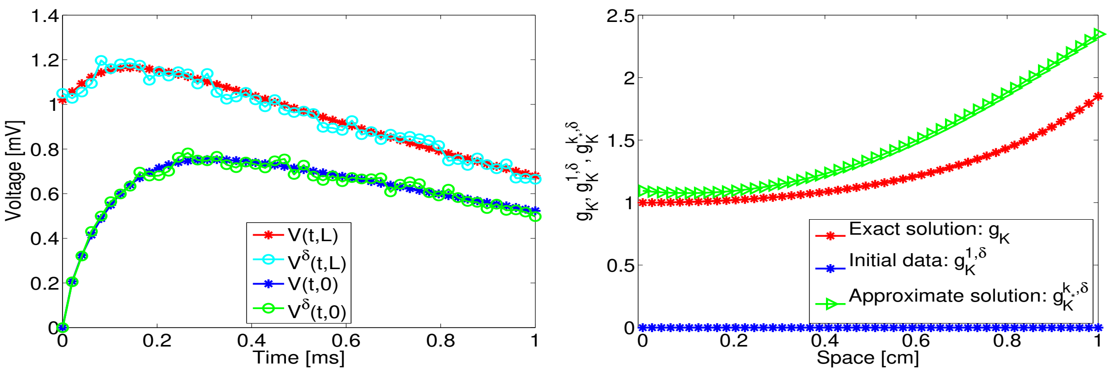

FIGURE 2. Result for Example 3.1 with $\Delta = 5\%$ noise. The plot on the left shows the exact membrane potential $V|_\Gamma$ and its measurement $V|_\Gamma^\delta$, where the dark blue and green lines are the exact and noisy data at $x = 0$. The red and light blue curves are the exact and noisy voltage at $x = L$. The plot to the right presents the exact solution (red line), the approximated solution (green line), and the initial guess (blue line).

of Example 3.1 apply. In Figures 5, 6 and 7, we plot numerical results for $\Delta = 1\%$ *(see Table 3, line 5). Observe that the data for both* $V^\delta|_\Gamma$ *and* g, g_K *depend on time and space.*

Example 3.3. *Consider now two different ions, Na and K, where* $N_{ion} = 2$ $(Ion = \{K, Na\})$, $c = 1\ [\Omega F/cm^2]$, $E_K = 0\ [mV]$, $E_{Na} = 1\ [mV]$, $L = 1\ [cm]$, $T = 1\ [ms]$, *and*

$$r(x) = 4 \times \cos(x), \qquad p(t) = \exp(-t)/2, \qquad q(t) = 0.$$

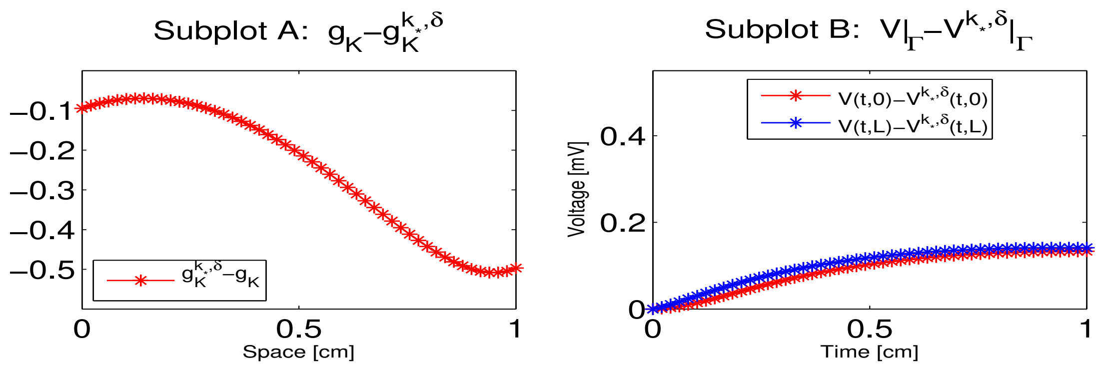

FIGURE 3. Result for Example 3.1. Subplot A presents the difference between g_K and its approximation, and subplot B shows the difference between $V|_\Gamma$ and its approximation, for $\Delta = 5\%$ of noise.

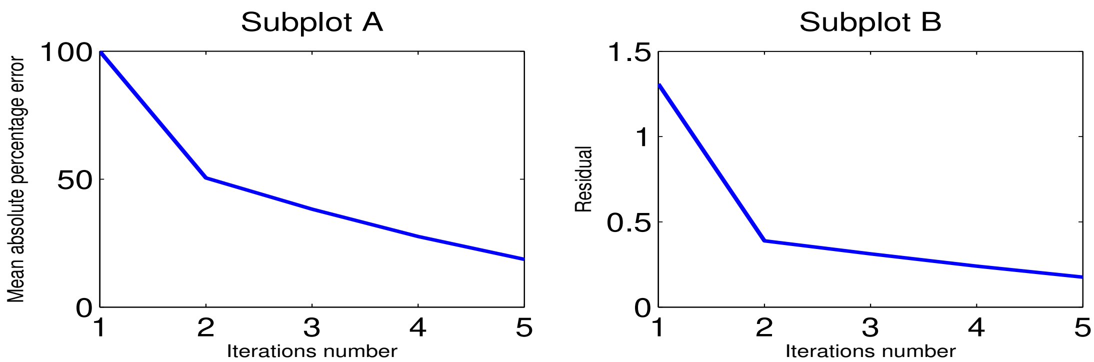

FIGURE 4. Convergence results for Example 3.1 with $\Delta = 5\%$. The plot on the left displays the mean absolute percentage error between $\boldsymbol{g}$ and $\boldsymbol{g}^{k,\delta}$ as a function of the iteration k. The plot on the right displays the residual, i.e., the difference between V and V^K again as a function of k.

Δ	k_*	$Error_{k_*}$	Res_{k_*}
125%	*1*	*100 %*	6×10^{-1}
25%	*2*	*54 %*	1×10^{-1}
5%	*26*	*35 %*	4×10^{-2}
1%	*433*	*10%*	7×10^{-3}
0.2%	*1618*	*5 %*	1×10^{-3}
0.04%	*8499*	*2%*	3×10^{-4}
0.008%	*37274*	*1%*	6×10^{-5}

TABLE 3. Numerical results for Example 3.2. See Table 2 for a description of the contents.

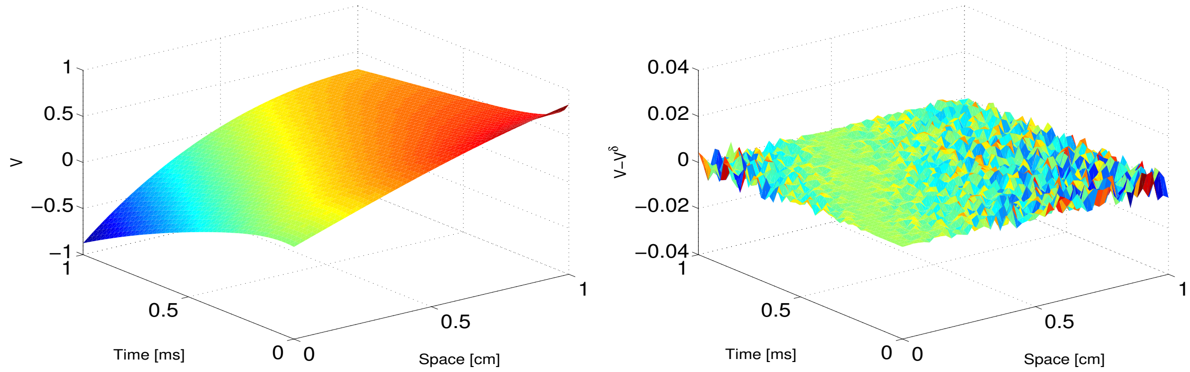

FIGURE 5. For Example 3.2 with $\Delta = 1\%$. The plot on the left shows the membrane potential. The plot on the right presents the difference between the membrane potential V and its perturbation V^δ.

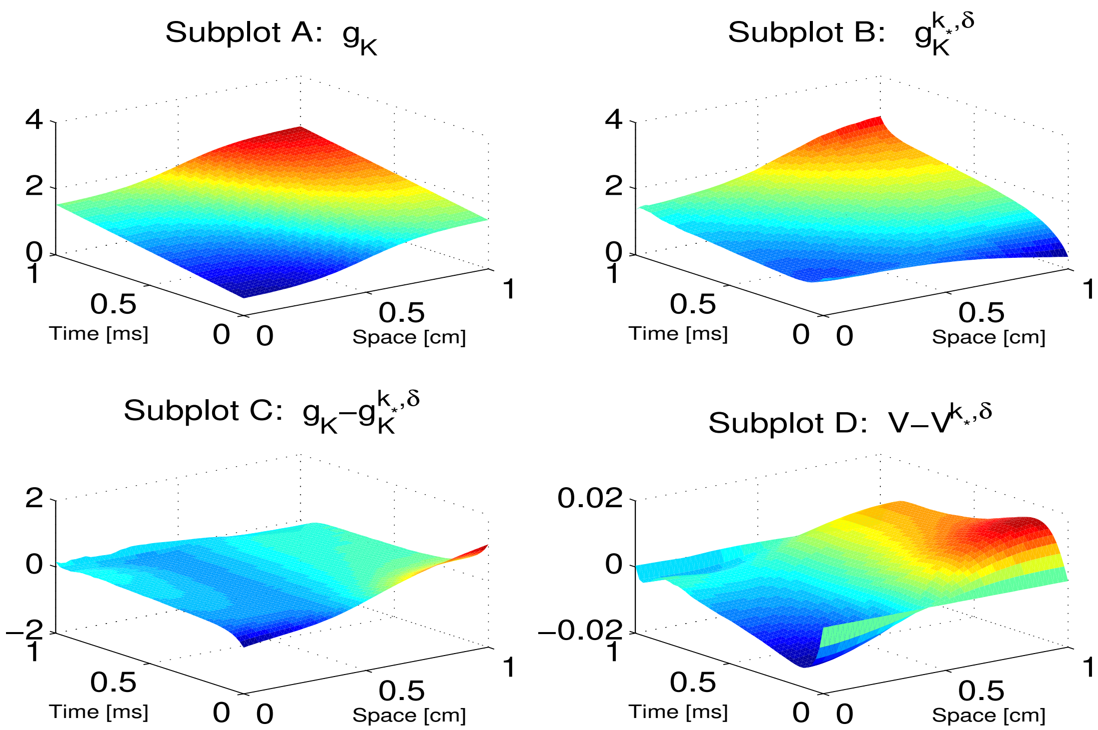

FIGURE 6. Plots for Example 3.2. The Subplots A and B are the exact solution g_K and its approximation for $\Delta = 1\%$ of noise. In Subplot C presents the difference between g_K and its approximation. Finally, in D we display the difference between the membrane potential and its approximation.

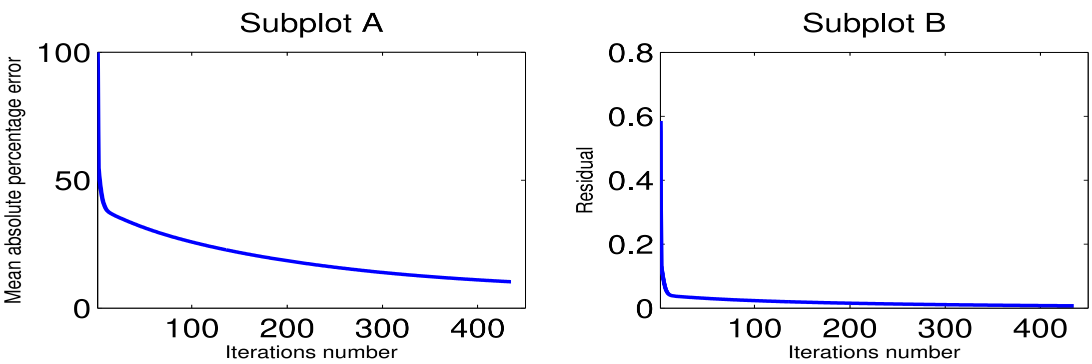

FIGURE 7. Convergence results for Example 3.2 with $\Delta = 1\%$. The Subplot A, displays the mean absolute percentage error between $\boldsymbol{g}$ and $\boldsymbol{g}^{k,\delta}$ as a function of the iteration k. The Subplot B, displays the residual, i.e., the difference between V and V^k again as a function of k.

Δ	k_*	$Error_{k_*}$	Res_{k_*}
10%	*1*	*349 %*	3×10^{-1}
1%	*157*	*28 %*	3×10^{-2}
0.1%	*1013*	*14 %*	3×10^{-3}
0.01%	*6720*	*4 %*	3×10^{-4}
0.001%	*69462*	*0.6 %*	3×10^{-5}
0.0001%	*275124*	*0.2 %*	3×10^{-6}

TABLE 4. Numerical results for Example 3.3. See Table 2 for a description of the contents.

Let $\Gamma = [0, T] \times [0, L]$ *and* $N = J = 50$. *The goal is to approximate*

$$g_K(x) = 2 \times \frac{\exp(8x-4)-1}{\exp(8x-4)+1} + 2 \quad \textit{and} \quad g_{Na}(x) = \frac{\exp(6x-3)-1}{\exp(6x-3)+1} + 1,$$

given $V^\delta|_\Gamma$, $g_K^{1,\delta}(x) = 2$, $g_{Na}^{1,\delta}(x) = 2$ *and* $\tau = 2.01$.

The extra difficulty in this lies on the fact that there are two conductance functions to be discovered. In Table 4 we present the results for various levels of noise. In Figures 8, 9, 10 and 11, we plot results for $\Delta = 1\%$ *of noise (see Table 3, line 3). Note that now there are two conductances,one related to Na and the other to* K.

Example 3.4. *As our final example, we consider the domain defined by a tree, as discussed in Section 2.1, in particular Eq.* (12). *The geometry of the tree is as depicted in Figure 1. Let* $\mathcal{E} = \{e_1, e_2, e_3\}$ *be the set of edges,* $\mathcal{V} = \{\nu_1, \nu_2, \nu_3, \nu_4\}$ *be the set of vertices with* $\partial\Theta = \{\gamma_1 = \nu_1, \gamma_2 = \nu_3, \gamma_3 = \nu_4\}$ *as the border points and with the bifurcation node* ν_2. *The edge* e_1 *has vertices* ν_1 *and* ν_2, *the edge* e_2 *has vertices* ν_2 *and* ν_3, *finally the edge* e_3 *has vertices*

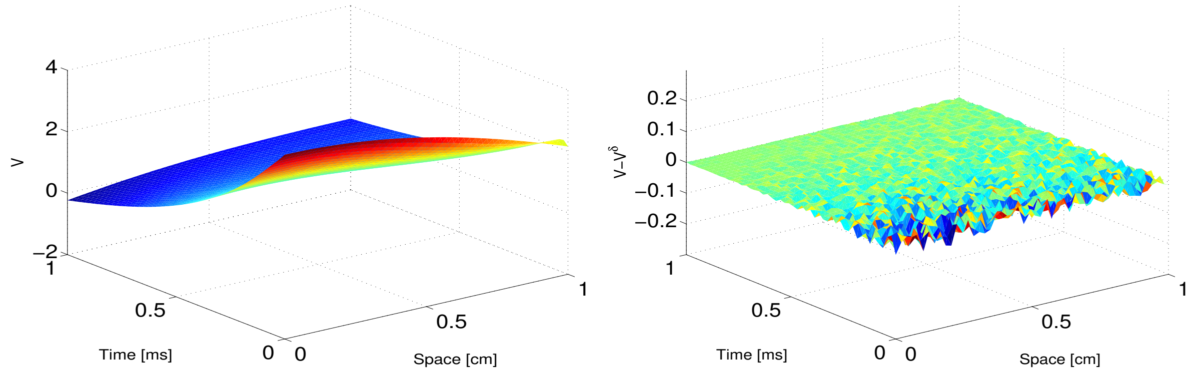

FIGURE 8. For Example 3.3 with $\Delta = 1\%$. See Figure 5 for the subplots description.

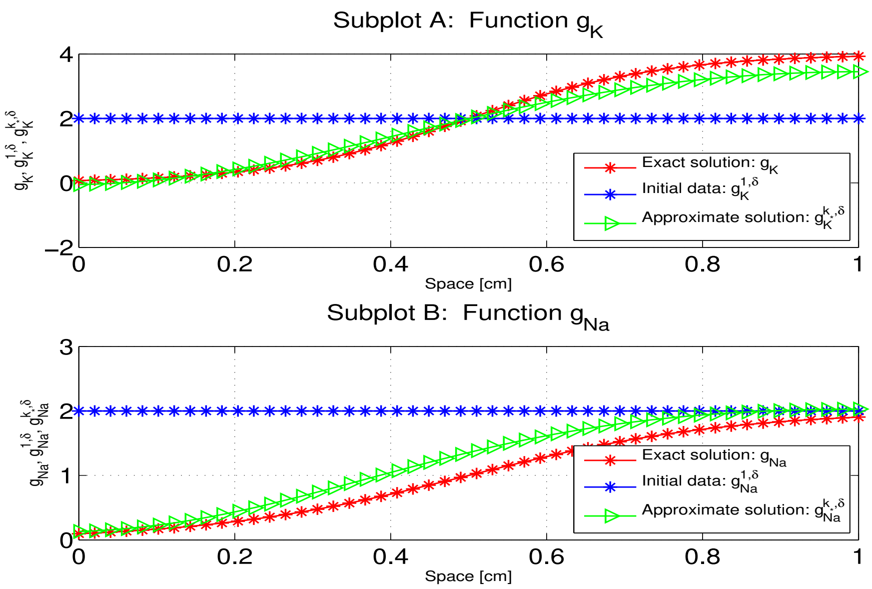

FIGURE 9. Results for Example 3.3. The Subplot A is related to g_K, and the Subplot B to g_{Na}. The red lines are the exact solutions, the blue lines are the initial guesses and the green lines are the approximations for $\Delta = 1\%$ of noise.

ν_2 *and* ν_4. *The length of the edges are:* $|e_1| = 1$, $|e_2| = 1$ *e* $|e_3| = 2$. *We consider,* $N_{ion} = 1$ $(Ion = \{K\})$, $E_K = 2\ [mV]$, $c = 2\ [\Omega F/cm^2]$, $T = 1\ [ms]$, $N = 300$, $g_i(t,x) = g_K(x)$. *The initial condition* $V(0,x) = r(\boldsymbol{x}) = 0$ *at all points* $\boldsymbol{x} \in \Theta$. *The boundary conditions are:* $V_x(t,\gamma_1) = 2t$, $V_x(t,\gamma_2) = \cos(t)$ *and* $V_x(t,\gamma_3) = 0$. *The condition at the bifurcation point* $x = \nu_2$ *(see the fourth equation from* (12)*) is*

$$V_1'(t,\nu_2) - V_2'(t,\nu_2) - V_3'(t,\nu_2) = 0.$$

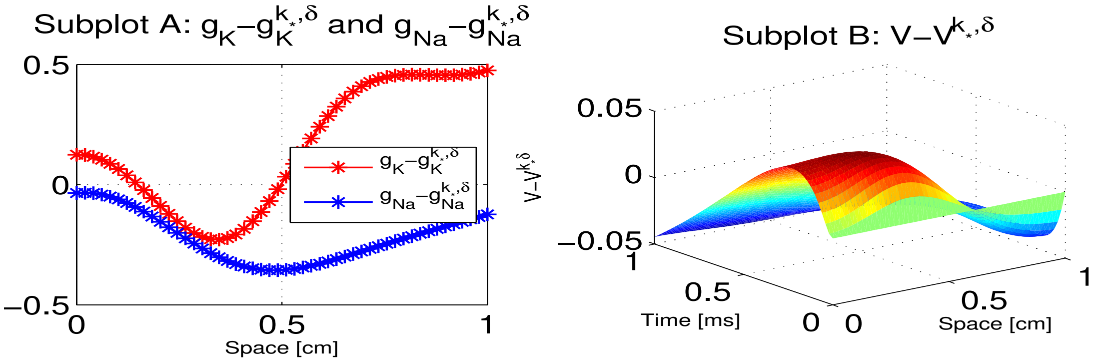

FIGURE 10. Results for Example 3.3 with $\Delta = 1\%$ of noise. See Figure 3 for the subplots description.

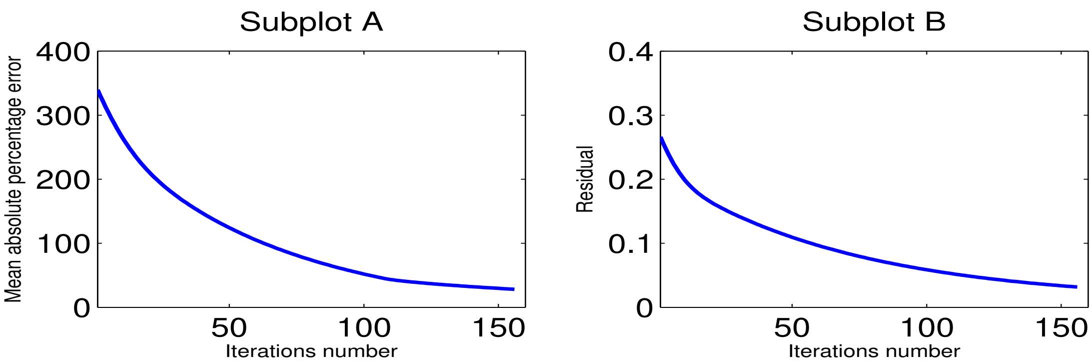

FIGURE 11. Convergence results for Example 3.3. For a description see Figure 7.

The goal of this example, given $V^\delta(t,x)$ *in all* $(t,x) \in (0,T) \times \Theta$*, is to estimate*

$$g(\boldsymbol{x}) = \begin{cases} \exp\big(\operatorname{dist}(\boldsymbol{x},\nu_1)\big) & \text{if } \boldsymbol{x} \in e_1, \\ \exp\big(1 + \operatorname{dist}(\boldsymbol{x},\nu_2)\big) & \text{if } \boldsymbol{x} \in e_2 \cup e_3, \end{cases}$$

where $\operatorname{dist}(a,b)$ *denotes the distance between the points* a *and* b*. We consider the initial guess* $g^{1,\delta}(t,x) = 0$ *and* $\tau = 2.01$*. In this example, we discretize the edges* e_1*,* e_2 *and* e_3 *using 16, 16 and 32 points* ($J = 64$)*. In Table 5 we present the results for various levels of noise. In figures 12–13, we plot numerical result for* $\Delta = 1\%$*.*

4. CONCLUSIONS

The inverse problem of finding conductances from voltage data for a given neuron model is important and difficult, and in this paper we present and test a way to approximate them, the Landweber iterative method, applied to a passive cable model. Although the scheme has a somewhat straightforward description, it is not practical in its original formulation since

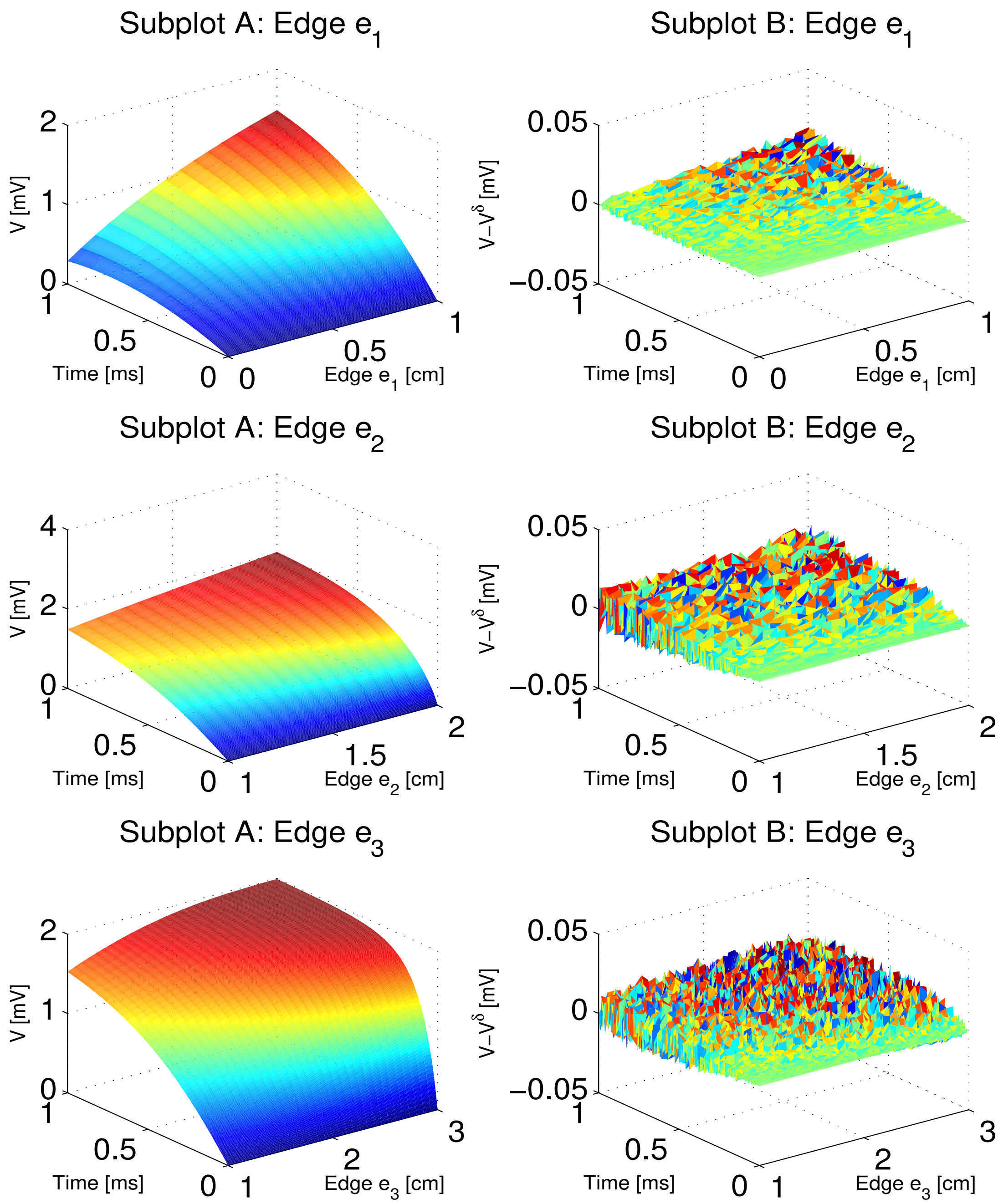

FIGURE 12. Exact potentials V and their noisy versions with noise at $\Delta = 1\%$, for Example 3.4. The subplots A on the left show the membrane electrical potential V for the three edges, and the subplots B display the difference between the membrane potential V an its perturbation V^{δ}.

Δ	k_*	$Error_{k_*}$	Res_{k_*}
125%	*1*	*100 %*	3×10^0
25%	*6*	*54 %*	1×10^0
5%	*128*	*17 %*	2×10^{-1}
1%	*1291*	*5%*	5×10^{-2}
0.2%	*5827*	*2 %*	1×10^{-2}
0.04%	*22088*	*0.8%*	2×10^{-3}
0.008%	*99326*	*0.3%*	4×10^{-4}

TABLE 5. Numerical results for Example 3.4. See Table 2 for a description of the contents.

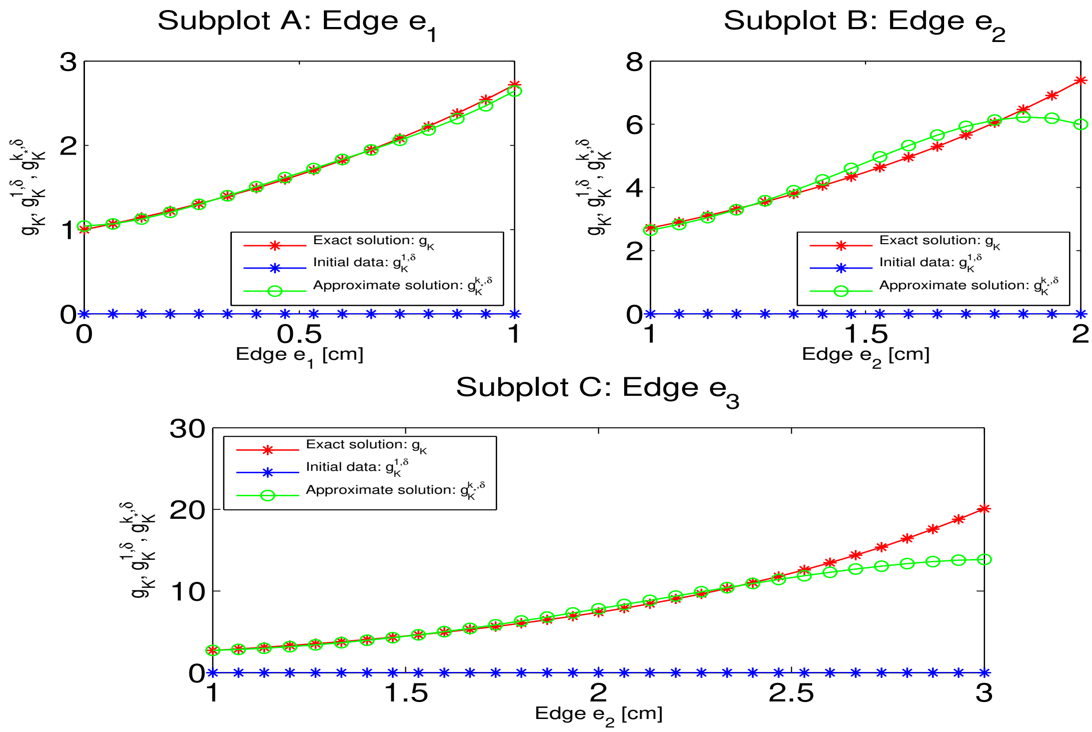

FIGURE 13. For Example 3.4, in all the Subplots, the red line is the exact solution, the blue line is the initial guess, and the green line is the approximate solution for $\Delta = 1\%$ of noise, these figures shows the conductances as functions of the spatial variable. The subplots A, B, and C correspond to the edges e_1, e_2 and e_3.

computing the adjoint of the Gâteux derivative seems unfeasible in general. The development of auxiliary equations to overcome such hurdle is more art than science, and is done in a case-by-case basis.

Certainly, the method has limitations, and is no panacea. How well the method performs depend on the noise, on how close to the solution is the initial guess, the amount of data, and

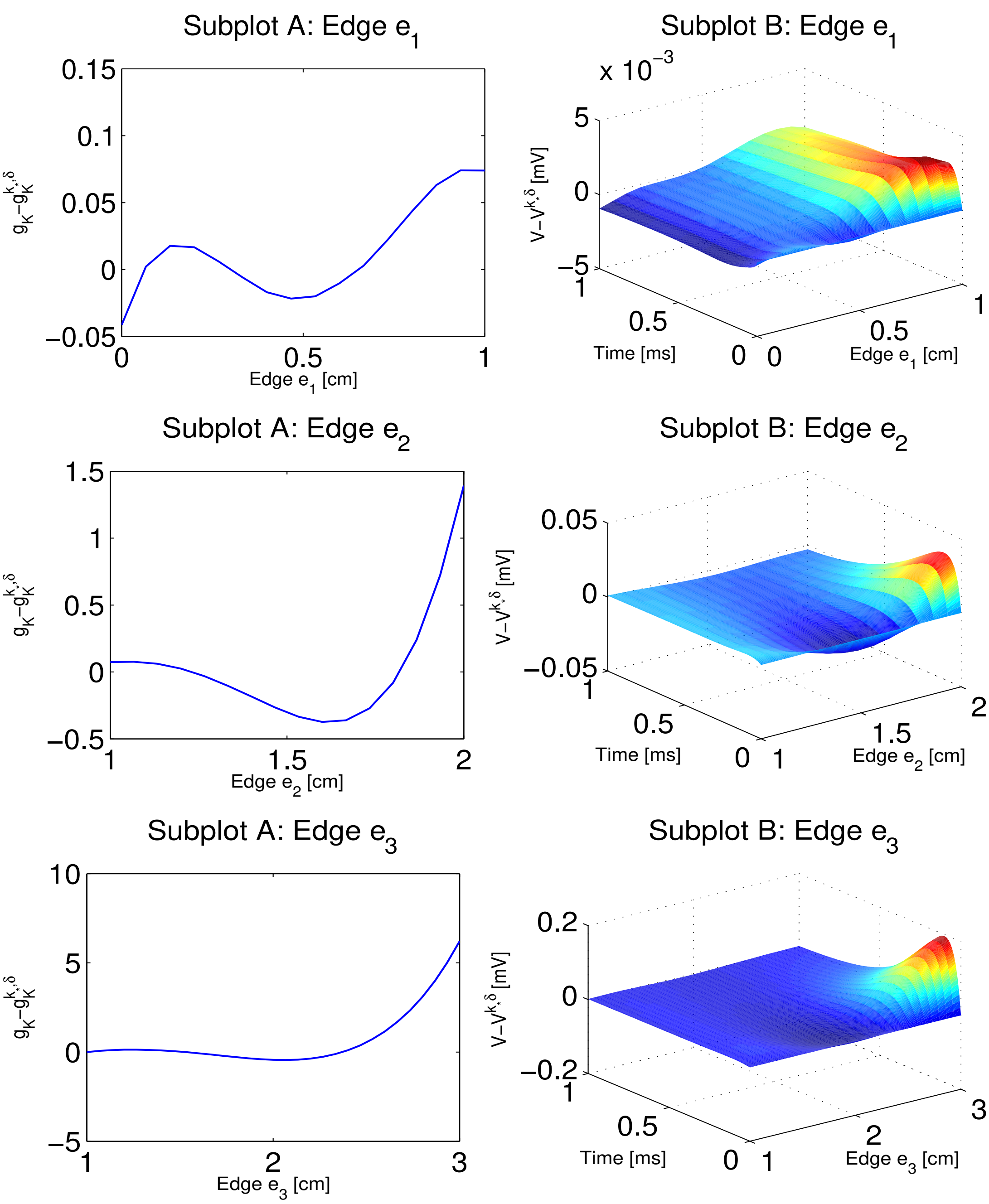

FIGURE 14. For Example 3.4 with noise at $\Delta = 1\%$, we plot on the left (subplots A) the differences between g_K and the approximations $g_K^{k_*,\delta}$, for the various edges. On the left (subplots B), we plot the difference between V and the resulting approximations.

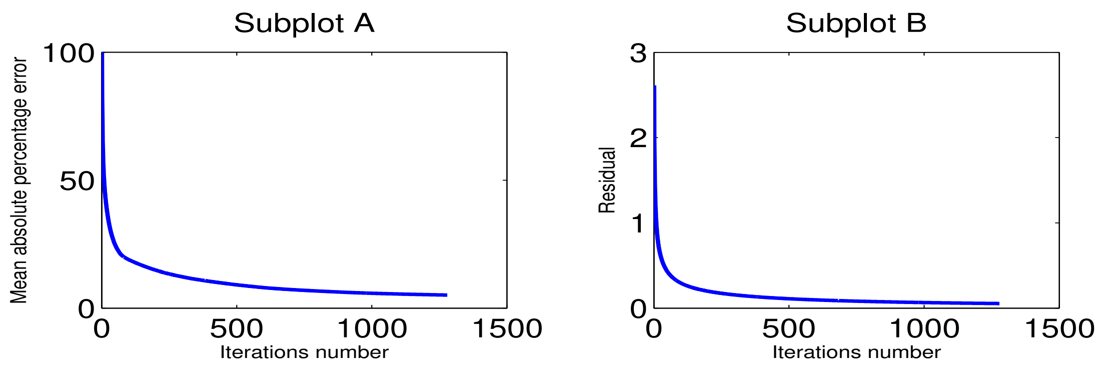

FIGURE 15. For Example 3.4, with noise at $\Delta = 1\%$. For a description see Figure 7.

on how hard the problem is. There is a nontrivial interplay between all those conditions. For instance, determining two conductances is harder than determining one, finding conductances that depend on time and space is harder than finding conductances that depend on space only. Also, having data at all points is better than if the data is available at isolated points only.

Our examples display some of these features. For some of them the method performs nicely, capturing the correct conductances. If the level of noise increases, the method delivers reasonable approximations, but these approximations cannot be qualitatively better than the available data, specially for inverse problems. Inverse problems are unstable, and thus not well posed, and difficult to solve in general. Even when the method does not do a good job in capturing the correct conductance, the computed residual is small. Whenever the residual is of the same order as the noise, there is no point in iterating further.

Under reasonable conditions, the method yields good results even in the presence of noise, as shown here. It is also general enough to accommodate for different geometries (straight cables and trees), and different measured data (end point, whole cable). The scheme showed promising results, and the even harder problem of determining the conductances of "real" (i.e., nonlinear) neurons is currently under investigation.

We believe that methods that are capable of inferring spatial properties of neurons are in demand and will grow in importance, in particular due to new imagining techniques such as VSDI. Regularizing methods for inverse problems are applied in several research fields and we think that they can also contribute in Neuroscience.

Appendix A. Abstract Formulation

In practice, $V|_\Gamma$ *is the data, and given such information and under the assumption that Eq.* (3) *holds, the inverse problem under consideration is to recover or approximate the* *conductances. The lack of stability, characteristic of ill-posed problems can be tamed by regularization methods* [18, 25, 27]*, in particular by the Landweber method.*

Consider for simplicity $T > 0$*. Let* $\Omega = \{(t, x); 0 \le t \le T, 0 \le x \le L\}$*, and*

$$H(F) = \big(L^2(\Omega)\big)^{N_{ion}} = \Big\{ f : \Omega \to \mathbb{R}^{N_{ion}};\ \int_\Omega |f(\xi)|^2 d\,\xi < \infty \Big\},$$

$$R(F) = L^2(\Gamma) = \Big\{ f : \Gamma \to \mathbb{R};\ \int_\Gamma |f(\xi)|^2 d\,\xi < \infty \Big\}$$

It is well-known that $H(F)$ *and* $R(F)$ *become Hilbert spaces under the inner products*

$$\langle f, h\rangle_{H(F)} = \int_\Omega f(\xi)h(\xi)d\xi, \qquad \langle f, h\rangle_{R(F)} = \int_\Gamma f(\xi)h(\xi)d\xi,.$$

and the associated norms $\|f\|_{H(F)} = \langle f, f\rangle^{1/2}_{H(F)}$*,* $\|f\|_{R(F)} = \langle f, f\rangle^{1/2}_{R(F)}$*. Note that the inner product on* $R(F)$ *depends on* Γ *(see Table 1) as follows:*

(20)
$$\langle f, h\rangle_{R(F)} = \alpha_1 \int_0^L \int_0^T f(t, x)h(t, x)\, dt\, dx + \alpha_2 \int_0^T f(t, 0)h(t, 0)dt + \alpha_2 \int_0^T f(t, L)g(t, L)\, dt,$$

where α_1*,* α_2 *are as in Eq.* (10)*.*

The set $D(F) = L^\infty(\Omega) \subset H(F)$ *is the Banach space of "essentially" bounded functions (see* [29] *for precise definitions). Consider the operator* $F : D(F) \subset H(F) \to R(F)$ *defined by* $F(\boldsymbol{g}) = V|_\Gamma$*. Our goal is to find an approximation for* $\boldsymbol{g}$ *using the Landweber iteration defined by Eq.* (6)*.*

In the next Theorem we show how to obtain Eq. (8) *from Eq.* (6)*.*

Theorem A.1. *Consider the iteration in Eq.* (6)*. Then Eq.* (8) *holds*

Proof. Given $\boldsymbol{g}^{k,\delta} \in D(F)$ and $\boldsymbol{\theta} = (\theta_1, \dots, \theta_{N_{\text{ion}}}) \in \big(L^\infty(\Omega)\big)^{N_{ion}}$, the Gâteux derivative of F at $\boldsymbol{g}^{k,\delta}$ in the direction $\boldsymbol{\theta}$ is given by

$$F'(\boldsymbol{g}^{k,\delta})(\boldsymbol{\theta}) = \lim_{\lambda \to 0} \frac{F(\boldsymbol{g}^{k,\delta} + \lambda\boldsymbol{\theta}) - F(\boldsymbol{g}^{k,\delta})}{\lambda} = W^k|_\Gamma, \tag{21}$$

where W^k solves

$$\begin{aligned} &W^k_{xx}(t, x) - cW^k_t(t, x) - \sum_{i\in\text{Ion}} g_i^{k,\delta}(t, x)W^k(t, x) = \sum_{i\in\text{Ion}} \theta_i(V^{k,\delta}(t, x) - E_i) \quad \text{in } \Omega,\\ &W^k(0, x) = 0 \quad \text{for } 0 < x < L, \qquad W^k_x(t, 0) = W^k_x(t, L) = 0 \quad \text{for } 0 < t < T, \end{aligned} \tag{22}$$

and $V^{k,\delta}$ solves Eq. (3) with g_i replaced by $g_i^{k,\delta}$. To obtain Eq. (22) from Eq. (21), it is enough to consider the difference between problem in Eq. (3) with coefficients $\boldsymbol{g}^{k,\delta} + \lambda\boldsymbol{\theta}$ and $\boldsymbol{g}^{k,\delta}$, divide by λ and take the limit $\lambda \to 0$.

Let $V^{k,\delta}|_\Gamma = F(\boldsymbol{g}^{k,\delta})$. From the Landweber iteration in Eq. (6), we gather that

$$\begin{aligned}\langle \boldsymbol{g}^{k+1,\delta} - \boldsymbol{g}^{k,\delta}, \boldsymbol{\theta}\rangle_{H(F)} &= \langle F'(\boldsymbol{g}^{k,\delta})^*(V^\delta|_\Gamma - F(\boldsymbol{g}^{k,\delta})), \boldsymbol{\theta}\rangle_{H(F)} \\ &= \langle F'(\boldsymbol{g}^{k,\delta})^*(V^\delta|_\Gamma - V^{k,\delta}|_\Gamma), \boldsymbol{\theta}\rangle_{H(F)}.\end{aligned}$$

By definition of adjoint operator,

$$\langle \boldsymbol{g}^{k+1,\delta} - \boldsymbol{g}^{k,\delta}, \boldsymbol{\theta}\rangle_{H(F)} = \langle V^\delta|_\Gamma - V^{k,\delta}|_\Gamma, F'(\boldsymbol{g}^{k,\delta})(\boldsymbol{\theta})\rangle_{R(F)} = \langle V^\delta|_\Gamma - V^{k,\delta}|_\Gamma, W^k|_\Gamma\rangle_{R(F)}, \tag{23}$$

from Eq. (21).

Although Eq. (23) yields an interesting relation, it carries an impeding dependence on $\boldsymbol{\theta}$ through W^k. It is possible to avoid that by performing some "trick" manipulations.

Multiplying the first equation of (9) by $-W^k$, and integrating in the intervals $[0, T]$ and $[0, L]$ we gather that

$$\begin{aligned}\int_0^L\int_0^T U^k_{xx}(t,x)W^k(t,x)\,dt\,dx + \int_0^L\int_0^T c\,U^k_t(t,x)W^k(t,x)\,dt\,dx \\ - \int_0^L\int_0^T \sum_{i\in ion} g_i^{k,\delta}(t,x)\,U^k(t,x)W^k(t,x)\,dt\,dx = \\ -\alpha_1\int_0^L\int_0^T \big(V^\delta(t,x) - V^{k,\delta}(t,x)\big)\,W^k(t,x)\,dt\,dx.\end{aligned} \tag{24}$$

Integrating by parts twice the first term from Eq. (24) with respect to the space variable, and using the boundary conditions for W^k we have

$$\int_0^L\int_0^T U^k_{xx}(t,x)W^k(t,x)\,dt\,dx = \int_0^L\int_0^T U^k(t,x)W^k_{xx}(t,x)\,dt\,dx + \int_0^T U^k_x(t,x)W^k(t,x)|_0^L\,dt, \tag{25}$$

where we denote $U^k_x(t,x)W^k(t,x)|_0^L = U^k(t,L)W^k(t,L) - U^k(t,0)W^k(t,0)$. Similarly, integrating by parts the second term of Eq. (24) with respect to time and using the initial condition of W^k and the final condition of U^k, we gather that

$$\int_0^L\int_0^T c\,U^k_t(t,x)W^k(t,x)\,dt\,dx = -\int_0^L\int_0^T cU^k(t,x)W^k_t(t,x)\,dt\,dx. \tag{26}$$

Substituting Eqs. (25) and (26) in Eq. (24), it follows that

$$\begin{aligned}\int_0^L\int_0^T \big(W^k_{xx}(t,x) - cW^k_t(t,x) - \sum_{i\in ion} g_i^{k,\delta}(t,x)W^k(t,x)\big)U^k(t,x)\,dtdx = \\ -\alpha_1\int_0^L\int_0^T \big(V^\delta(t,x) - V^{k,\delta}(t,x)\big)W^k(t,x)\,dt\,dx - \int_0^T U^k_x(t,x)W^k(t,x)|_0^L\,dt.\end{aligned}$$

Substituting the first equation of (22) in the previous equation, we obtain

$$\int_0^L \int_0^T \sum_{i \in ion} \theta_i (V^{k,\delta}(t,x) - E_i) U^k(t,x)\, dt\, dx$$
$$= -\alpha_1 \int_0^L \int_0^T \left(V^\delta(t,x) - V^{k,\delta}(t,x)\right) W^k(t,x)\, dtdx - \int_0^T U_x^k(t,x) W^k(t,x)|_0^L\, dt.$$

From the boundary conditions of Eq. (9), the following expression holds:

$$\int_0^L \int_0^T \sum_{i \in ion} \theta_i (V^{k,\delta}(t,x) - E_i) U^k(t,x)\, dtdx$$
$$= -\alpha_1 \int_0^L \int_0^T \left(V^\delta(t,x) - V^{k,\delta}(t,x)\right) W^k(t,x)\, dtdx$$
$$- \alpha_2 \int_0^T \left(V^\delta(t,0) - V^{k,\delta}(t,0)\right) W^k(t,0) - \alpha_2 \int_0^T \left(V^\delta(t,L) - V^{k,\delta}(t,L)\right) W^k(t,L)\, dt.$$

From the previous equation and the definition of the inner product in Eq. (20), we have

$$\int_0^L \int_0^T \sum_{i \in ion} \theta_i (V^{k,\delta}(t,x) - E_i) U^k(t,x)\, dtdx = -\langle V^\delta|_\Gamma - V^{k,\delta}|_\Gamma, W^k|_\Gamma \rangle_{R(F)}. \tag{27}$$

From Eqs. (23) and (27) we have

$$\int_0^L \int_0^T \sum_{i \in \mathrm{Ion}} \theta_i \left(g_i^{k+1,\delta}(t,x) - g_i^{k,\delta}(t,x)\right)\, dtdx$$
$$= - \int_0^L \int_0^T \sum_{i \in \mathrm{Ion}} \theta_i (V^{k,\delta}(t,x) - E_i) U^k(t,x)\, dtdx.$$

Since $\boldsymbol{\theta} \in \left(L^\infty(\Omega)\right)^{N_{ion}}$ is arbitrary and $L^\infty(\Omega)$ is dense in $L^2(\Omega)$, we gather that the following iteration holds:

$$g_i^{k+1,\delta}(t,x) = g_i^{k,\delta}(t,x) - (V^{k,\delta}(t,x) - E_i) U^k(t,x) \quad \text{for all } i \in \mathrm{Ion}.$$

□

References

[1] Avdonin, S., and Bell, J. Determining a distributed parameter in a neural cable model via a boundary control method. *Journal of mathematical biology 67*, 1 (2013), 123–141.

[2] Avdonin, S., and Bell, J. Determining a distributed conductance parameter for a neuronal cable model defined on a tree graph. *Journal of Inverse Problems and Imaging 9* (2015), 645–659.

[3] Bédard, C., Béhuret, S., Deleuze, C., Bal, T., and Destexhe, A. Oversampling method to extract excitatory and inhibitory conductances from single-trial membrane potential recordings. *Journal of neuroscience methods 210*, 1 (2012), 3–14.

[4] Bell, J. Introduction to theoretical neurobiology. volume 1: Linear cable theory and dendritic structure. volume 2: Nonlinear and stochastic theories (henry c. tuckwell). *SIAM Review 32*, 1 (1990), 158–160.

[5] Bell, J., and Craciun, G. A distributed parameter identification problem in neuronal cable theory models. *Mathematical biosciences 194*, 1 (2005), 1–19.

[6] Binder, A., Hanke, M., and Scherzer, O. On the landweber iteration for nonlinear ill-posed problems. *Journal of Inverse and Ill-posed Problems 4*, 5 (1996), 381–390.

[7] Brown, T. H., Fricke, R. A., and Perkel, D. H. Passive electrical constants in three classes of hippocampal neurons. *Journal of Neurophysiology 46*, 4 (1981), 812–827.

[8] Casale, A. E., Foust, A. J., Bal, T., and McCormick, D. A. Cortical interneuron subtypes vary in their axonal action potential properties. *Journal of Neuroscience 35*, 47 (2015), 15555–15567.

[9] Chapko, R., and Kügler, P. A comparison of the landweber method and the gauss–newton method for an inverse parabolic boundary value problem. *Journal of computational and applied mathematics 169*, 1 (2004), 183–196.

[10] Cox, S. J. A new method for extracting cable parameters from input impedance data. *Mathematical biosciences 153*, 1 (1998), 1–12.

[11] Cox, S. J. An adjoint method for channel localization. *Mathematical Medicine and Biology 23*, 2 (2006), 139–152.

[12] Cox, S. J., and Griffith, B. E. Recovering quasi-active properties of dendritic neurons from dual potential recordings. *Journal of computational neuroscience 11*, 2 (2001), 95–110.

[13] Cox, S. J., and Ji, L. Identification of the cable parameters in the somatic shunt model. *Biological cybernetics 83*, 2 (2000), 151–159.

[14] Cox, S. J., and Ji, L. Discerning ionic currents and their kinetics from input impedance data. *Bulletin of mathematical biology 63*, 5 (2001), 909–932.

[15] Cox, S. J., and Raol, J. H. Recovering the passive properties of tapered dendrites from single and dual potential recordings. *Mathematical biosciences 190*, 1 (2004), 9–37.

[16] D'Aguanno, A., Bardakjian, B. L., and Carlen, P. L. Passive neuronal membrane parameters: comparison of optimization and peeling methods. *IEEE transactions on biomedical engineering 33*, 12 (1986), 1188–1196.

[17] Durand, D., Carlen, P., Gurevich, N., Ho, A., and Kunov, H. Electrotonic parameters of rat dentate granule cells measured using short current pulses and hrp staining. *Journal of neurophysiology 50*, 5 (1983), 1080–1097.

[18] Engl, H. W., Hanke, M., and Neubauer, A. *Regularization of inverse problems*, vol. 375. Springer Science & Business Media, 1996.

[19] Ermentrout, G. B., and Terman, D. H. *Mathematical foundations of neuroscience*, vol. 35. Springer Science & Business Media, 2010.

[20] Grinvald, A., and Hildesheim, R. Vsdi: a new era in functional imaging of cortical dynamics. *Nature Reviews Neuroscience 5* (2004), 874–885.

[21] Hanke, M., Neubauer, A., and Scherzer, O. A convergence analysis of the landweber iteration for nonlinear ill-posed problems. *Numerische Mathematik 72*, 1 (1995), 21–37.

[22] Hodgkin, A. L., and Huxley, A. F. A quantitative description of membrane current and its application to conduction and excitation in nerve. *The Journal of physiology 117*, 4 (1952), 500–544.

[23] Holmes, W. R., and Rall, W. Estimating the electrotonic structure of neurons with compartmental models. *Journal of Neurophysiology 68*, 4 (1992), 1438–1452.

[24] Jack, J., and Redman, S. An electrical description of the motoneurone, and its application to the analysis of synaptic potentials. *The Journal of physiology 215*, 2 (1971), 321.

[25] Kaltenbacher, B., Neubauer, A., and Scherzer, O. *Iterative regularization methods for nonlinear ill-posed problems*, vol. 6. Walter de Gruyter, 2008.

[26] Kawato, M. Cable properties of a neuron model with non-uniform membrane resistivity. *Journal of theoretical biology 111*, 1 (1984), 149–169.

[27] Kirsch, A. *An introduction to the mathematical theory of inverse problems*, vol. 120. Springer Science & Business Media, 2011.

[28] Kobayashi, R., Shinomoto, S., and Lansky, P. Estimation of time-dependent input from neuronal membrane potential. *Neural Computation 23*, 12 (2011), 3070–3093.

[29] Kreyszig, E. *Introductory functional analysis with applications*, vol. 1. wiley New York, 1978.

[30] Landweber, L. An iteration formula for fredholm integral equations of the first kind. *American journal of mathematics 73*, 3 (1951), 615–624.

[31] Nayak, A. A new parameter-free regularization method for inverse problems. *arXiv e-prints* (Mar 2019), arXiv:1903.03130.

[32] Neubauer, A. On landweber iteration for nonlinear ill-posed problems in hilbert scales. *Numerische Mathematik 85*, 2 (2000), 309–328.

[33] Pierce, A. Unique identification of eigenvalues and coefficients in a parabolic problem. *SIAM Journal on Control and Optimization 17*, 4 (1979), 494–499.

[34] Rall, W. Branching dendritic trees and motoneuron membrane resistivity. *Experimental neurology 1*, 5 (1959), 491–527.

[35] Rall, W. Membrane potential transients and membrane time constant of motoneurons. *Experimental neurology 2*, 5 (1960), 503–532.

[36] Rall, W. Theory of physiological properties of dendrites. *Annals of the New York Academy of Sciences 96*, 4 (1962), 1071–1092.

[37] Rall, W. Core conductor theory and cable properties of neurons. *Comprehensive Physiology 1* (1977), 39–97.

[38] Rall, W., Burke, R., Holmes, W., Jack, J., Redman, S., and Segev, I. Matching dendritic neuron models to experimental data. *Physiological Reviews 72*, 4 (1992), S159–S186.

[39] Schierwagen, A. Identification problems in distributed parameter neuron models. *Automatica 26*, 4 (1990), 739–755.

[40] Schutter, E. D. *Computational modeling methods for neuroscientists.* The MIT Press, 2009.

[41] Stuart, G., and Spruston, N. Determinants of voltage attenuation in neocortical pyramidal neuron dendrites. *Journal of Neuroscience 18*, 10 (1998), 3501–3510.

[42] Tadi, M., Klibanov, M. V., and Cai, W. An inversion method for parabolic equations based on quasireversibility. *Computers & Mathematics with Applications 43*, 8 (2002), 927–941.

[43] Vich, C., Berg, R. W., Guillamon, A., and Ditlevsen, S. Estimation of synaptic conductances in presence of nonlinear effects caused by subthreshold ionic currents. *Frontiers in computational neuroscience 11* (2017), 69.

[44] Vich, C., and Guillamon, A. Dissecting estimation of conductances in subthreshold regimes. *Journal of computational neuroscience 39*, 3 (2015), 271–287.

[45] White, J. A., Manis, P. B., and Young, E. D. The parameter identification problem for the somatic shunt model. *Biological cybernetics 66*, 4 (1992), 307–318.

[46] Willms, A. R., Baro, D. J., Harris-Warrick, R. M., and Guckenheimer, J. An improved parameter estimation method for hodgkin-huxley models. *Journal of Computational Neuroscience 6*, 2 (1999), 145–168.

[47] Yaşar, T. B., Wright, N. C., and Wessel, R. Inferring presynaptic population spiking from single-trial membrane potential recordings. *Journal of neuroscience methods 259* (2016), 13–21.

[48] Zerlaut, Y., and Destexhe, A. Heterogeneous firing responses predict diverse couplings to presynaptic activity in mice layer v pyramidal neurons. *PLoS computational biology 13*, 4 (2017), e1005452.

Departamento de Modelagem Computacional, Laboratrio Nacional de Computao Cientfica, Av. Getlio Vargas 333, 25651-070 Petrpolis, RJ, Brazil

APPENDIX B – Paper 2

Parameter Identification Problem in the Hodgkin-Huxley Model

PARAMETER IDENTIFICATION PROBLEM IN THE HODGKIN-HUXLEY MODEL

JEMY A. MANDUJANO VALLE, ALEXANDRE L. MADUREIRA

Abstract. The Hodgkin-Huxley (H-H) model is a nonlinear system of four equations that describes how action potentials in neurons are initiated and propagated. This model represents a significant advance in the understanding of nerve cells. However, some of the parameters are obtained through a tedious combination of experiments and data tuning. In this paper, we propose the use of an iterative method (Minimal error iteration) to estimate some of the parameters in the H-H model, given the membrane potential. We provide numerical results showing that the approach can capture the correct parameters using the measured voltage as data, even in the presence of noise.

1. Introduction.

In 1952 Hodgkin and Huxley [15] used voltage-clamp technique to extract the parameters of the ionic channel model of the squid giant axon. In the space-clamped version of the H-H model, the membrane electrical potential $V : [0, T] \to \mathbb{R}$ solves

$$C_M \dot{V}(t) = I_{\text{ext}} + I_{\text{ion}}(t) \quad \text{in } (0, T], \tag{1}$$

where C_M is the specific membrane capacitance, V is the membrane potential, $\dot{V} = dV/dt$ is the rate of voltage change (dots denote time derivatives), I_{ext} is the specific external current applied on the membrane. The specific ionic current $I_{\text{ion}}(t)$ is the sum of three currents ($I_{\text{ion}}(t) = I_{\text{Na}}(t) + I_{\text{K}}(t) + I_L(t)$), potassium, sodium and leak currents, satisfying:

$$I_{\text{Na}}(t) = G_{\text{Na}}\, m^a(V,t)\, h^b(V,t)\, (V(t) - E_{\text{Na}}); \tag{2}$$

$$I_{\text{K}}(t) = G_{\text{K}}\, n^c(V,t)\, (V(t) - E_{\text{K}}); \tag{3}$$

$$I_L(t) = G_L\, (V(t) - E_L). \tag{4}$$

The constants G_{Na}, G_{K} and G_L are the maximal specific conductance for Na^+, K^+ and leakage channels, and E_{Na}, E_{K}, E_L are the Nernst equilibrium potentials. The functions m and h are the activation and inactivation variables for Na^+, and n is the activation function for K^+. These functions are unitless gating variables that take values between 0 and 1. Also,

Date: October 18, 2018.

The second author acknowledges the financial support of the Brazilian funding agency CNPq.

the exponents a, b and c are positive numbers. The units of the other parameters are in Table 1.

Parameters	**Units**	**Units name**
C_M	$\mu F/cm^2$	microfarad per square centimeter
V	mV	millivolt
$\dot{V}$	V/s	volts per second
I_{ext}, I_{ion}	$\mu A/cm^2$	microampere per square centimeter
G_{Na}, G_{K}, G_L	mS/cm^2	millisiemens per square centimeter
E_{Na}, E_{K}, E_L	mV	millivolt
t	ms	milliseconds

TABLE 1. Units of the parameters; see [15], Table 3.

The experiments performed by Hodgkin and Huxley [15] suggest that m, h and n are functions that depend on time and the membrane potential. The exponent c models the number of gating particles on the channel. In the case of active Na currents, experiments suggest that two types of independent gating particles are involved, a activation gates m, and b inactivation gates h [12]. In addition, m n and h satisfy the differential equations:

$$\dot{\mathcal{X}}(V,t) = \alpha_{\mathcal{X}}(V)(1-\mathcal{X}(V,t)) - \beta_{\mathcal{X}}(V)\mathcal{X}(V,t) \quad \text{where } \mathcal{X} = m,n,h. \tag{5}$$

The functions $\alpha_{\mathcal{X}}$ and $\beta_{\mathcal{X}}$ depend on the membrane potential and are given by

$$\begin{aligned} \alpha_m(V) &= \frac{(25-V)/10}{\exp((25-V)/10)-1}, & \beta_m(V) &= 4\exp(-V/18), \\ \alpha_n(V) &= \frac{(10-V)/100}{\exp((10-V)/10)-1}, & \beta_n(V) &= 0.125\exp(-V/80), \\ \alpha_h(V) &= 0.07\exp(-V/20), & \beta_h(V) &= \frac{1}{\exp((30-V)/10)+1}. \end{aligned} \tag{6}$$

To equation (1) we add the initial conditions

$$V(0) = V_0, \quad m(0) = m_0, \quad n(0) = n_0, \quad h(0) = h_0. \tag{7}$$

Thus, (1-7) yield the following system of ordinary differential equation (ODE):Lima, Sbado 18 de mayo del 2019 Edificio Empresarial Narciso Calle Narciso de la Colina 421, Miraflores, Sala 403 Esquina Colina con Paseo de la Repblica (Cda. 53). Estacin Ricardo Palma del

Metropolitano.

$$
(8) \quad \begin{cases} C_M \dot{V} = I_{\text{ext}} - G_{\text{Na}} m^a h^b (V - E_{\text{Na}}) - G_{\text{K}} n^c (V - E_{\text{K}}) - G_L (V - E_L) & \text{for } t \in (0, T] \\ \dot{\mathcal{X}} = (1 - \mathcal{X}) \alpha_{\mathcal{X}}(V) - \mathcal{X} \beta_{\mathcal{X}}(V) \quad \text{where } \mathcal{X} = m, n, h \text{ and } t \in (0, T] \\ V(0) = V_0, \quad m(0) = m_0, \quad n(0) = n_0, \quad h(0) = h_0, \end{cases}
$$

and C_M, I_{ext}, E_{Na}, E_{K}, E_L, m_0, n_0 and h_0 are known.

Given all the parameters, it is possible to find a (theoretical or numerical) solution for (8). That is the *direct problem.* In *inverse problems*, one is given the voltage V and has to compute one or more parameters. In this work, we consider two different *inverse* problems. The first one is to obtain the maximum conductances G_{Na}, G_{K} and G_L given the measurement of the membrane potential. For the second problem, the goal is to obtain the exponents a, b and c, again given the measurement of the membrane potential.

Using experimental data from the squid neuron, Hodgkin and Huxley obtained the parameters $a = 3$, $b = 4$ and $c = 1$. Note, however, that other neurons may produce different parameters.

Besides the Hodgkin and Huxley model, there are simplified models such as the cable equation, FitzHugh-Nagumo, and Morris-Lecar models. Wilfrid Rall [21, 22] developed the use of cable theory in computational neuroscience, as well as passive and active compartmental modeling of the neuron. In a previous paper [26], the authors determine conductances with nonuniform distribution in the equation of the cable with and without branches, using the minimal error iterative method. See also [24, 3, 1, 2], for identification of parameters in the cable equation, and [11, 10, 19, 8, 18, 25] for investigations on inverse problems in FitzHugh-Nagumo and Morris-Lecar models. In [20, 23, 27] the authors obtained approximately time-dependent but voltage-independent conductances, given the membrane potential, in a system of three ordinary differential equations (passive membrane equation). For the Hodgkin and Huxley model, the parameters of ionic channels are estimated in [5, 6] using evolutionary algorithms.

Inverse problems are said to be *ill-posed.* A problem is ill-posed in the sense of Hadamard [13] if any of the following conditions are not satisfied: there is a solution; the solution is unique; the solution has a continuous dependence on the input data (stability). Here we admit the existence of a single solution to the problem. However, stability is not guaranteed. Stability is necessary if we want to ensure that small variations in the data lead to small changes in the solution. Problems of instability can be controlled by regularization methods, in particular the minimal error iterative scheme [4, 7, 14, 17].

We now describe the contents of the present paper briefly. Section 2 presents our inverse problems for the H-H model along with some theoretical results, and in Section 3 we show numerical results to describe the effectiveness of our strategy. Finally, we include in the Appendices some more technical arguments.

2. Inverse Problem in the H-H model

In what follows, we describe an abstract formulation of the minimal error method or minimal error iteration [16].

Consider (8) and let $x = (G_{\mathrm{Na}}, G_{\mathrm{K}}, G_L) \in \mathbb{R}^3$ or $x = (a, b, c) \in \mathbb{R}^3$. Consider also the set of function $L^2[0,T]$, and the nonlinear operator

$$F : \mathbb{R}^3 \to L^2[0,T], \tag{9}$$

defined by $F(x) = V$, where V solves (8). In practical terms, the data V are obtained by measurements. Therefore, we denote the measurements by V^δ, of the which we assume to know the noise level δ, satisfying

$$\|V - V^\delta\|^2_{L^2[0,T]} = \int_0^T |V(t) - V^\delta(t)|^2 \, dt \leq \delta. \tag{10}$$

To obtain an approximation of x, given V^δ, we used the minimal error iteration

$$x^{k+1,\delta} = x^{k,\delta} + w^{k,\delta} F'(x^{k,\delta})^*(V^\delta - F(x^{k,\delta})), \tag{11}$$

where $F'(x^{k,\delta})$ is the Gateaux-derivative of F computed at $x^{k,\delta}$, and $F'(x^{k,\delta})^*$ is its adjoint. We also define

$$w^{k,\delta} = \frac{\|V^\delta - F(x^{k,\delta})\|^2_{L^2[0,T]}}{\|F'(x^{k,\delta})^*(V^\delta - F(x^{k,\delta}))\|^2_{\mathbb{R}^3}}.$$

The iteration (11) begins with a guess $x^{1,\delta}$ and stops at the minimum $k_* = k(\delta, V^\delta)$, such that, for a given $\tau > 2$ (see [16], equation (2.14)),

$$\|V^\delta - F(x^{k_*,\delta})\|_{L^2[0,T]} \leq \tau\delta. \tag{12}$$

It is possible to show that, under certain conditions (we assume that is the case), $x^{k_*,\delta}$ converges to a solution of $F(x) = V$ as $\delta \to 0$; see [16] Theorem 3.22.

2.1. **Inverse Problem to obtain conductances in the H-H model.** The present goal is to estimate the maximum conductances G_{Na}, G_{K} and G_L while assuming that (8) holds. We assume that the exponents are $a = 3$, $b = 1$, and $c = 4$.

We denote our unknown parameters such as $x = \boldsymbol{G} = (G_{\mathrm{Na}}, G_{\mathrm{K}}, G_L)$, then from iteration (11) we have

$$\boldsymbol{G}^{k+1,\delta} = \boldsymbol{G}^{k,\delta} + w^{k,\delta} F'(\boldsymbol{G}^{k,\delta})^*(V^\delta - F(\boldsymbol{G}^{k,\delta})). \tag{13}$$

Given an initial approximation $\boldsymbol{G}^{1,\delta}$ and V^δ, we obtain a regularizing approximation $\boldsymbol{G}^{k_*,\delta}$ for $\boldsymbol{G}$, from minimal error iteration (13). We denote $\boldsymbol{G}^{k,\delta} = (G^{k,\delta}_{\mathrm{Na}}, G^{k,\delta}_{\mathrm{K}}, G^{k,\delta}_L)$.

In the next theorem, we compute the adjoint of the Gateaux derivative $F'(\boldsymbol{G}^{k,\delta})^*$ to optimize from (13).

Theorem 2.1. *It follows from* (13) *that*

$$\left(G^{k+1,\delta}_{Na}, G^{k+1,\delta}_{K}, G^{k+1,\delta}_{L}\right) = \left(G^{k,\delta}_{Na}, G^{k,\delta}_{K}, G^{k,\delta}_{L}\right) + w^{k,\delta}\left(X^{k,\delta}_{Na}, X^{k,\delta}_{K}, X^{k,\delta}_{L}\right), \tag{14}$$

where

$$w^{k,\delta} = \frac{\|V^\delta - V^{k,\delta}\|^2_{L^2[0,T]}}{\left\|\left(X^{k,\delta}_{Na}, X^{k,\delta}_{K}, X^{k,\delta}_{L}\right)\right\|^2_{\mathbb{R}^3}},$$

and

$$X^{k,\delta}_{Na} = \int_0^T \left(m^{k,\delta}\right)^a \left(h^{k,\delta}\right)^b (V^{k,\delta} - E_{Na}) U^{k,\delta}\, dt, \tag{15}$$

$$X^{k,\delta}_{K} = \int_0^T \left(n^{k,\delta}\right)^c (V^{k,\delta} - E_{K}) U^{k,\delta}\, dt, \tag{16}$$

$$X^{k,\delta}_{L} = \int_0^T \left(n^{k,\delta}\right)^c (V^{k,\delta} - E_{K}) U^{k,\delta}\, dt. \tag{17}$$

The functions $m^{k,\delta}$, $n^{k,\delta}$, $h^{k,\delta}$ and $V^{k,\delta}$ solve, given $G^{k,\delta}_{Na}$, $G^{k,\delta}_{K}$ and $G^{k,\delta}_{L}$,

$$\begin{cases} C_M \dot{V}^{k,\delta} = I_{ext} - G^{k,\delta}_{Na}\left(m^{k,\delta}\right)^a \left(h^{k,\delta}\right)^b (V^{k,\delta} - E_{Na}) - G^{k,\delta}_{K}\left(n^{k,\delta}\right)^c (V^{k,\delta} - E_K) \\ \qquad -G^{k,\delta}_{L}(V^{k,\delta} - E_L), \\ \dot{\mathcal{X}} = (1 - \mathcal{X})\alpha_{\mathcal{X}}(V^{k,\delta}) - \mathcal{X}\beta_{\mathcal{X}}(V^{k,\delta}) \quad \textit{for } \mathcal{X} = m^{k,\delta}, n^{k,\delta}, h^{k,\delta}, \\ V^{k,\delta}(0) = V_0, \quad m^{k,\delta}(0) = m_0, \quad n^{k,\delta}(0) = n_0, \quad h^{k,\delta}(0) = h_0, \end{cases} \tag{18}$$

and $\alpha_{\mathcal{X}}$, $\beta_{\mathcal{X}}$ are defined by (6). Finally, $U^{k,\delta}$ solve, given $m^{k,\delta}$, $n^{k,\delta}$, $h^{k,\delta}$ and $V^{k,\delta}$,

$$
\left\{
\begin{aligned}
&C_M\dot{U}^{k,\delta} - \Big(G_{Na}^{k,\delta}\big(m^{k,\delta}\big)^a\big(h^{k,\delta}\big)^b + G_K^{k,\delta}\big(n^{k,\delta}\big)^c + G_L^{k,\delta}\Big)\,U^{k,\delta}\\
&-[(1-m^{k,\delta})\alpha'_{m^{k,\delta}}(V^{k,\delta}) - m^{k,\delta}\beta'_{m^{k,\delta}}(V^{k,\delta})]P^{k,\delta}\\
&-[(1-n^{k,\delta})\alpha'_{n^{k,\delta}}(V^{k,\delta}) - n^{k,\delta}\beta'_{n^{k,\delta}}(V^{k,\delta})]Q^{k,\delta}\\
&-[(1-h^{k,\delta})\alpha'_{h^{k,\delta}}(V^{k,\delta}) - h^{k,\delta}\beta'_{h^{k,\delta}}(V^{k,\delta})]R^{k,\delta} = V^\delta - V^{k,\delta},\\
&\dot{P}^{k,\delta} - [\alpha_{m^{k,\delta}}(V^{k,\delta}) + \beta_{m^{k,\delta}}(V^{k,\delta})]P^{k,\delta} = -aG_{Na}^{k,\delta}\big(m^{k,\delta}\big)^{a-1}\big(h^{k,\delta}\big)^b(V^{k,\delta} - E_{Na})U^{k,\delta},\\
&\dot{Q}^{k,\delta} - [\alpha_{n^{k,\delta}}(V^{k,\delta}) + \beta_{n^{k,\delta}}(V^{k,\delta})]Q^{k,\delta} = -cG_K^{k,\delta}\big(n^{k,\delta}\big)^{c-1}(V^{k,\delta} - E_K)U^{k,\delta},\\
&\dot{R}^{k,\delta} - [\alpha_{h^{k,\delta}}(V^{k,\delta}) + \beta_{h^{k,\delta}}(V^{k,\delta})]R^{k,\delta} = -bG_{Na}^{k,\delta}\big(m^{k,\delta}\big)^{a}\big(h^{k,\delta}\big)^{b-1}(V^{k,\delta} - E_{Na})U^{k,\delta},\\
&U^{k,\delta}(T)=0,\quad P^{k,\delta}(T)=0,\quad Q^{k,\delta}(T)=0,\quad R^{k,\delta}(T)=0.
\end{aligned}
\right.
\tag{19}
$$

As previously mentioned, we assume that the constants a, b, c, E_{Na} ,E_K, E_L, C_M, I_{ext}, m_0, n_0 and h_0 are known data.

Proof. See Appendix A. ☐

We next describe the computational scheme.

Data: V^δ, δ and τ

Result: Compute an approximation for $\boldsymbol{G}$ using minimal error iteration Scheme

Choose $\boldsymbol{G}^{1,\delta}$ as an initial approximation for $\boldsymbol{G}$;

Compute $m^{1,\delta}$, $n^{1,\delta}$, $h^{1,\delta}$ and $V^{1,\delta}$ from (18), replacing $\boldsymbol{G}^{k,\delta}$ by $\boldsymbol{G}^{1,\delta}$;

k=1;

while $\tau\delta \le \|V^\delta - V^{k,\delta}\|_{L^2[0,T]}$ **do**

  Compute $U^{k,\delta}$ from (19);

  Compute $\boldsymbol{G}^{k+1,\delta}$ using (14);

  Compute $m^{k+1,\delta}$, $n^{k+1,\delta}$, $h^{k+1,\delta}$ and $V^{k+1,\delta}$ from (18), replacing $\boldsymbol{G}^{k,\delta}$ by $\boldsymbol{G}^{k+1,\delta}$;

  $k \leftarrow k+1$;

end

Algorithm 1: Minimal error iteration to obtain maximal conductances

2.2. **Inverse Problem to obtain exponents in the H-H model.** Assume again that (8) holds and that G_{Na}, G_{K} and G_L are known. The goal of this subsection is to estimate the exponents a, b and c. Denoting the unknown parameters by $x = \boldsymbol{a} = (a,b,c)$ it follows from iteration (11) that

$$\boldsymbol{a}^{k+1,\delta} = \boldsymbol{a}^{k,\delta} + w^{k,\delta}F'(\boldsymbol{a}^{k,\delta})^*(V^\delta - F(\boldsymbol{a}^{k,\delta})). \tag{20}$$

Given an initial approximation $\boldsymbol{a}^{1,\delta}$ and the data V^δ, we obtain a regularizing approximation $\boldsymbol{a}^{k_*,\delta}$ for $\boldsymbol{a}$, from the minimal error iteration (20). Denote $\boldsymbol{a}^{k,\delta} = (a^{k,\delta}, b^{k,\delta}, c^{k,\delta})$.

In the next Theorem, we compute the adjoint of the Gateaux derivative $F'(\boldsymbol{a}^{k,\delta})^*$ from (20).

Theorem 2.2. *Consider the iteration* (20). *It follows then that*

$$\left(a^{k+1,\delta}, b^{k+1,\delta}, c^{k+1,\delta}\right) = \left(a^{k,\delta}, b^{k,\delta}, c^{k,\delta}\right) + w^{k,\delta}\left(X_a^{k,\delta}, X_b^{k,\delta}, X_c^{k,\delta}\right), \tag{21}$$

where $w^{k,\delta}$ *satisfies*

$$w^{k,\delta} = \frac{\|V^\delta - V^{k,\delta}\|^2_{L^2[0,T]}}{\left\|\left(X_a^{k,\delta}, X_b^{k,\delta}, X_c^{k,\delta}\right)\right\|^2_{\mathbb{R}^3}},$$

and

$$\begin{aligned}
X_a^{k,\delta} &= \int_0^T G_{Na}(V^{k,\delta} - E_{Na})\left(m^{k,\delta}\right)^{a^{k,\delta}}\left(h^{k,\delta}\right)^{b^{k,\delta}} U^{k,\delta}\ln(m^{k,\delta})\,dt,\\
X_b^{k,\delta} &= \int_0^T G_{Na}(V^{k,\delta} - E_{Na})\left(m^{k,\delta}\right)^{a^{k,\delta}}\left(h^{k,\delta}\right)^{b^{k,\delta}} U^{k,\delta}\ln(h^{k,\delta})\,dt,\\
X_c^{k,\delta} &= \int_0^T G_K(V^{k,\delta} - E_K)\left(n^{k,\delta}\right)^{c^{k,\delta}} U^{k,\delta}\ln(n^{k,\delta})\,dt.
\end{aligned}$$

The functions $m^{k,\delta}$, $n^{k,\delta}$, $h^{k,\delta}$ *and* $V^{k,\delta}$ *solve*

$$\begin{cases}
C_M\dot{V}^{k,\delta} = I_{ext} - G_{Na}\left(m^{k,\delta}\right)^{a^{k,\delta}}\left(h^{k,\delta}\right)^{b^{k,\delta}}(V^{k,\delta} - E_{Na}) - G_K\left(n^{k,\delta}\right)^{c^{k,\delta}}(V^{k,\delta} - E_K)\\
\qquad\qquad -G_L(V^{k,\delta} - E_L),\\
\dot{\mathcal{X}} = (1-\mathcal{X})\alpha_{\mathcal{X}}(V^{k,\delta}) - \mathcal{X}\beta_{\mathcal{X}}(V^{k,\delta}); \quad \mathcal{X} = m^{k,\delta}, n^{k,\delta}, h^{k,\delta},\\
V^{k,\delta}(0) = V_0; \quad m^{k,\delta}(0) = m_0; \quad n^{k,\delta}(0) = n_0; \quad h^{k,\delta}(0) = h_0,
\end{cases} \tag{22}$$

where $a^{k,\delta}$, $b^{k,\delta}$ *and* $c^{k,\delta}$ *are given. Also,* $U^{k,\delta}$ *solve*

$$\left\{\begin{array}{l} C_M\dot{U}^{k,\delta}-\Big(G_{Na}\big(m^{k,\delta}\big)^{a^{k,\delta}}\big(h^{k,\delta}\big)^{b^{k,\delta}}+G_K\big(n^{k,\delta}\big)^{c^{k,\delta}}+G_L\Big)U^{k,\delta} \\ \qquad -[(1-m^{k,\delta})\alpha'_{m^{k,\delta}}(V^{k,\delta})-m^{k,\delta}\beta'_{m^{k,\delta}}(V^{k,\delta})]P^{k,\delta} \\ \qquad -[(1-n^{k,\delta})\alpha'_{n^{k,\delta}}(V^{k,\delta})-n^{k,\delta}\beta'_{n^{k,\delta}}(V^{k,\delta})]Q^{k,\delta} \\ \qquad -[(1-h^{k,\delta})\alpha'_{h^{k,\delta}}(V^{k,\delta})-h^{k,\delta}\beta'_{h^{k,\delta}}(V^{k,\delta})]R^{k,\delta}=V^{\delta}-V^{k,\delta}, \\ \dot{P}^{k,\delta}-[\alpha_{m^{k,\delta}}(V^{k,\delta})+\beta_{m^{k,\delta}}(V^{k,\delta})]P^{k,\delta}= \\ \qquad -a^{k,\delta}G_{Na}\big(m^{k,\delta}\big)^{a^{k,\delta}-1}\big(h^{k,\delta}\big)^{b^{k,\delta}}(V^{k,\delta}-E_{Na})U^{k,\delta}, \\ \dot{Q}^{k,\delta}-[\alpha_{n^{k,\delta}}(V^{k,\delta})+\beta_{n^{k,\delta}}(V^{k,\delta})]Q^{k,\delta}= \\ \qquad -c^{k,\delta}G_K\big(n^{k,\delta}\big)^{c^{k,\delta}-1}(V^{k,\delta}-E_K)U^{k,\delta}, \\ \dot{R}^{k,\delta}-[\alpha_{h^{k,\delta}}(V^{k,\delta})+\beta_{h^{k,\delta}}(V^{k,\delta})]R^{k,\delta}= \\ \qquad -b^{k,\delta}G_{Na}\big(m^{k,\delta}\big)^{a^{k,\delta}}\big(h^{k,\delta}\big)^{b^{k,\delta}-1}(V^{k,\delta}-E_{Na})U^{k,\delta}, \\ U^{k,\delta}(T)=0; \quad P^{k,\delta}(T)=0; \quad R^{k,\delta}(T)=0; \quad Q^{k,\delta}(T)=0, \end{array}\right. \tag{23}$$

given $m^{k,\delta}$, $n^{k,\delta}$, $h^{k,\delta}$ *and* $V^{k,\delta}$. *The constants* G_{Na}, G_K, E_{Na} ,E_K, E_L, C_M, I_{ext}, m_0, n_0 *and* h_0 *are given data.*

Proof. See Appendix (B). ☐

We next describe the computational scheme.

Data: V^{δ}, δ and τ

Result: Compute an approximation for $\boldsymbol{a}$ using minimal error iteration Scheme

Choose $\boldsymbol{a}^{1,\delta}$ as an initial approximation for $\boldsymbol{a}$;

Compute $m^{1,\delta}$, $n^{1,\delta}$, $h^{1,\delta}$ and $V^{1,\delta}$ from (22), replacing $\boldsymbol{a}^{k,\delta}$ by $\boldsymbol{a}^{1,\delta}$;

k=1;

while $\tau\delta \leq \|V^{\delta}-V^{k,\delta}\|_{L^2[0,T]}$ **do**

  Compute $U^{k,\delta}$ from (23);

  Compute $\boldsymbol{a}^{k+1,\delta}$ using (21);

  Compute $m^{k+1,\delta}$, $n^{k+1,\delta}$, $h^{k+1,\delta}$ and $V^{k+1,\delta}$ from (22), replacing $\boldsymbol{a}^{k,\delta}$ by $\boldsymbol{a}^{k+1,\delta}$;

  $k \leftarrow k+1$;

end

Algorithm 2: Minimal error iteration to obtain exponents.

3. Numerical simulation

To design our numerical experiments, we first choose x ($x = \boldsymbol{G}$ or $x = \boldsymbol{a}$) and compute V from (8). Of course, in practice, the values of V are given by some experimental measurements, and thus subject to experimental/measurement errors. In our examples, for a given δ, the noisy V^δ is obtained from

$$V^\delta(t) = V(t) + V(t)\text{rand}_\varepsilon(t), \quad \text{for all } t \in [0, T] \tag{24}$$

where $\text{rand}_\varepsilon(t)$ is a uniformly distributed random variable taking values in the range $[-\varepsilon, \varepsilon]$, and $\varepsilon = \delta/\|V\|_{L^2[0,T]}$.

Next, given the initial guess $x^{1,\delta}$ and the data V^δ and δ, we start to recover x using Algorithm 1 (for $x = \boldsymbol{G}$) or Algorithm 2 (for $x = \boldsymbol{a}$). Note that we have the exact x, and we use that to gauge the algorithm performance.

The absolute error of V^δ and its approximation $V^{k,\delta}$ defines the residual from

$$\text{Res}_k = \|V^\delta - V^{k,\delta}\|_{L^2[0,T]} = \sqrt{\int_0^T \left(V^\delta(t) - V^{k,\delta}(t)\right)^2 dt}, \quad k = 1, 2, \cdots, k_*. \tag{25}$$

The percent error of vector $x \in \mathbb{R}^3$ is defined by

$$\text{Error}_k^x = \frac{\|x - x^{k,\delta}\|_{\mathbb{R}^3}}{\|x\|_{\mathbb{R}^3}} \times 100\%, \quad k = 1, 2, \cdots, k_*. \tag{26}$$

Each step of Algorithm 1 and Algorithm 2 involves solving two ODEs. Of course, there is no analytical solution for those equations, and the use of numerical methods is necessary. We use explicit Euler with a fixed time step Δt.

In this section we will present two numerical simulations. In Example 3.1 we estimate the conductances G_{Na}, G_{K} and G_L, and in Example 3.2 we estimate the exponents a, b and c. Our simulation were computed with Matlab R2012b on a Dell PC, running on a Intel(R) Core(TM) i7-4790 CPU @ 3.60GHz with 32 GB of RAM.

See the code in the URL:`https://github.com/MandujanoValle/Conductances-HH`, to estimate the conductances G_{Na}, G_{K} and G_L, and URL:`https://github.com/MandujanoValle/Exponents-HH`, to estimate the exponents a, b and c.

Example 3.1. *This example is a particular case from* (8)*, with values* (*see* [9]*, page 586*)*:* $C_M = 1$ $[\mu F/cm^2]$, $E_{Na} = 115$ $[mV]$, $E_K = -12$ $[mV]$, $E_L = 10.598$ $[mV]$, $G_{Na} = 120$ $[mS/cm^2]$, $G_K = 36$ $[mS/cm^2]$, $G_L = 0.3$ $[mS/cm^2]$, $I_{ext} = 0$ $[\mu A/cm^2]$, $a = 3$, $b = 1$ *and* $c = 4$. *Let the initial conditions* $V(0) = -25$ $[mV]$, $m(0) = 0.5$, $n(0) = 0.4$ *and* $h(0) = 0.4$. *We consider* $T = 10$ $[ms]$ *and* $\Delta t = 0.02$. *Given* V^δ*, the goal of this example is to approximate* $\boldsymbol{G} = (G_{Na}, G_K, G_L)$ $[mS/cm^2]$.

First, given $\boldsymbol{G} = (120, 36, 0.3)$ $[mS/cm^2]$*, we compute* V *from* (8)*. Then, we calculate* V^δ *from* (24) *given* ε *(see table 2). Next, we consider* V *and* $\boldsymbol{G}$ *as unknowns.*

In this test we consider the initial guess $\boldsymbol{G}^{1,\delta} = (0, 0, 0)$ $[mS/cm^2]$ *and* $\tau = 2.01$*. Table 2 presents the results for various levels of noise. When* ε *decreases, the number of iterations grow resulting in a better approximation for* $\boldsymbol{G} = (G_{Na}, G_K, G_L)$ $[mS/cm^2]$ *and smaller residuals. As expected, the result of the last column is close to* $\tau\delta$*, related to the stopping criteria* (12)*.*

In Figures 1, 2 and 3, we plot some results for $\varepsilon = 5\%$ *(Table 2, line 4).*

ε	k_*	$G_{Na}^{k_*,\delta}$	$G_K^{k_*,\delta}$	$G_L^{k_*,\delta}$	$Error_{k_*}^x$	Res_{k_*}
125%	1	0	0	0	100 %	161
25%	19303	114.08	28.49	8.1727	9.9 %	49
5%	25012	115.07	30.59	0.7938	5.8 %	10
1%	33419	119.10	34.16	0.3221	1.6 %	2
0.2%	48642	119.82	35.62	0.3043	0.3 %	0.4

TABLE 2. Numerical results for Example 3.1 for various values of ε, as in (24). The second column contains the number of iterations according to (12). The third, fourth and fifth columns are the approximations for G_{Na}, G_{K} and G_L respectively. The sixth column is the percent error between $x = \boldsymbol{G}$ and $x^{k,\delta} = \boldsymbol{G}^{k,\delta}$ according to (26). The last column is the residue, see (25).

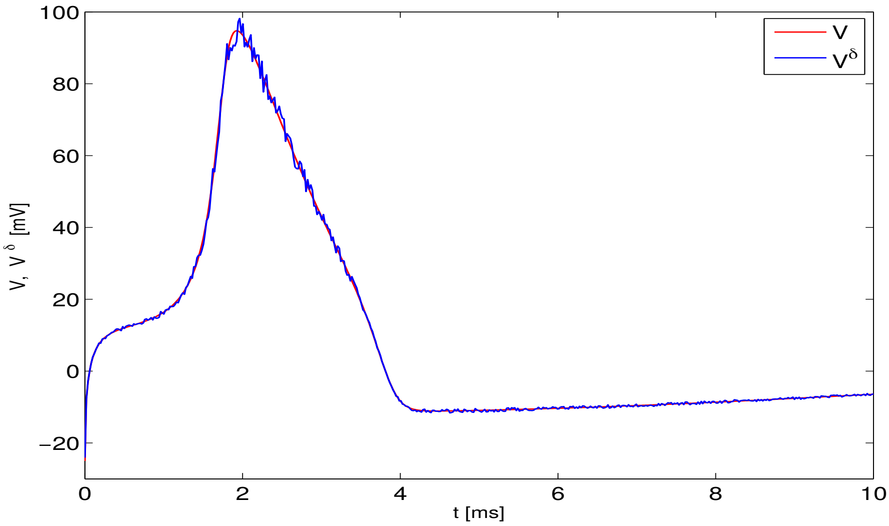

FIGURE 1. For Example 3.1. The red line (V) is the exact membrane potential and blue line (V^δ) is the membrane potential measurement; in this case $\varepsilon = 5\%$.

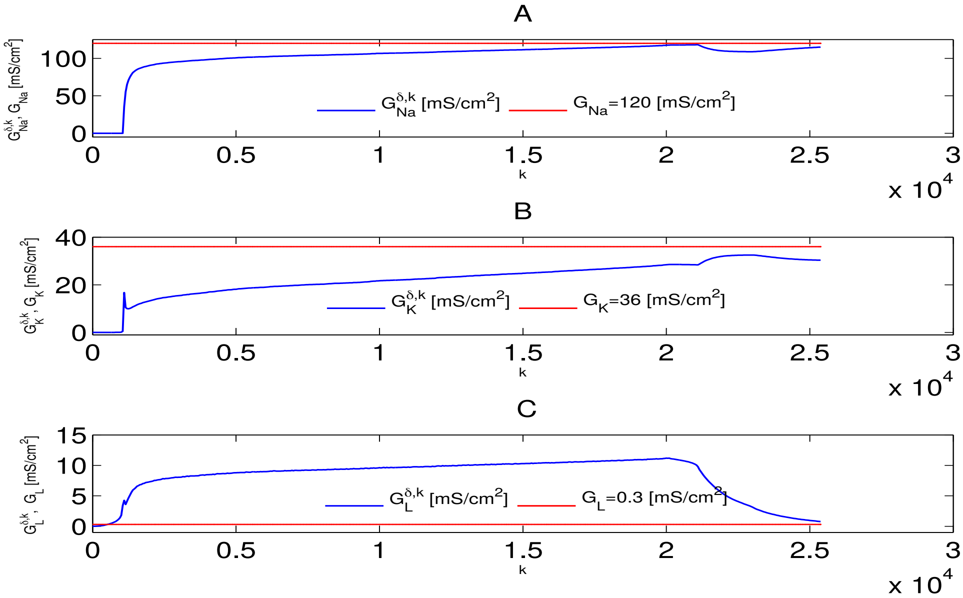

FIGURE 2. Figures for Example 3.1 (estimation of the conductances) with $\varepsilon = 5\%$. The x-axis gives the number of iterations (k) and the y-axis gives the conductance. The red lines are the exact solutions, and blue lines are the approximations. The figures 2-A, 2-B and 2-C display the estimates of the maximum conductances of sodium, potassium and leakage, respectively.

Example 3.2. *This example is another particular case from* (8) *with values (see* [9], *page 586):* $C_M = 1$ $[\mu F/cm^2]$, $E_{Na} = 115$ $[mV]$, $E_K = -12$ $[mV]$, $E_L = 10.598$ $[mV]$, $G_{Na} = 120$ $[mS/cm^2]$, $G_K = 36$ $[mS/cm^2]$, $G_L = 0.3$ $[mS/cm^2]$, $I_{ext} = 0$ $[\mu A/cm^2]$, $a = 3$, $b = 1$ *and* $c = 4$. *Let the initial conditions* $V(0) = -25$ $[mV]$, $m(0) = 0.5$, $n(0) = 0.4$ *and* $h(0) = 0.4$. *We consider the time* $T = 5$ $[ms]$ *with* $\Delta t = 0.02$. *Given* V^δ, *our goal is to approximate* $\boldsymbol{a} = (a, b, c) = (3, 1, 4)$.

First we calculate V *from* (8) *given* $\boldsymbol{a} = (3, 1, 4)$. *Then, we calculate* V^δ *from* (24) *given* ε *(see table 2). We then consider* V *and* $\boldsymbol{a}$ *unknown.*

In this example we consider the initial guess $\boldsymbol{a}^{1,\delta} = (0, 0, 0)$ *and* $\tau = 2.01$. *Table 3 presents the results for various levels of noise. In figures 4, 5 and 6, we plot some results for a level of noise* $\varepsilon = 1\%$ *(Table 3, line 5).*

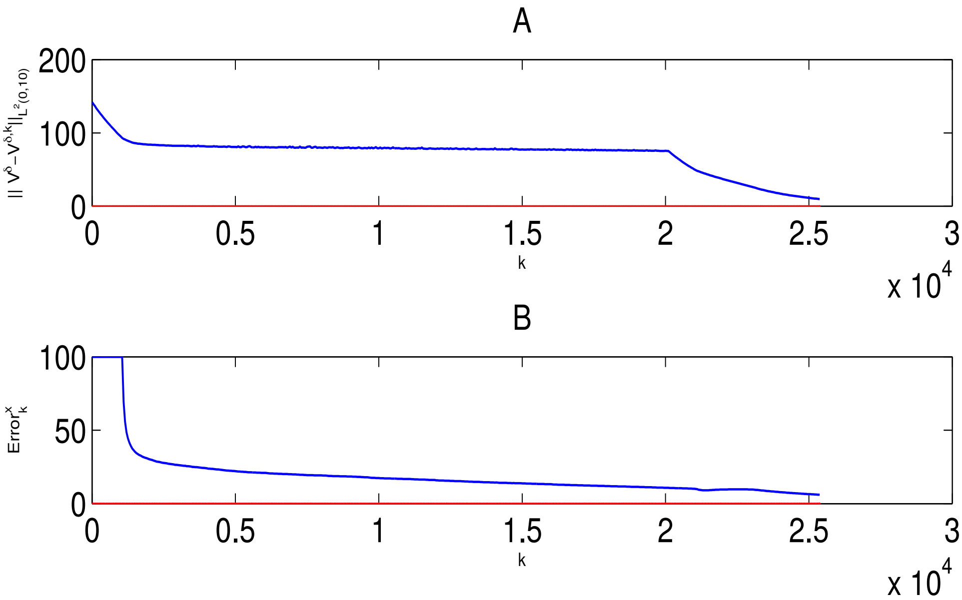

FIGURE 3. Example 3.1 with $\varepsilon = 5\%$. The x-axis indicates the number of iterations (k). The y-axis, in the figures A and B are the residual (25) and error (26), respectively.

ε	k_*	$a^{k_*,\delta}$	$b^{k_*,\delta}$	$c^{k_*,\delta}$	$Error^x_{k_*}$	Res_{k_*}
125 %	1	0	0	0	100 %	170
25 %	11681	1.572	0.496	-0.300	89 %	48
5 %	95605	2.970	0.807	2.626	27 %	9.7
1 %	188827	3.008	0.954	3.674	6 %	1.9
0.2 %	283487	3.002	0.990	3.930	1.4 %	0.4

TABLE 3. Numerical results for Example 3.2. See Table 2 for a description of the contents.

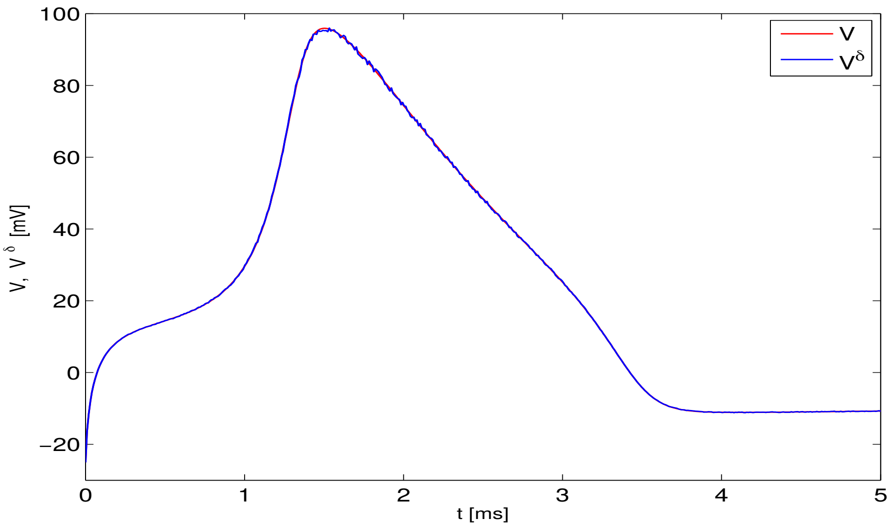

FIGURE 4. For Example 3.2 and $\varepsilon = 1\%$. The red line (V) is the exact membrane potential and blue line (V^δ) is the membrane potential measurement.

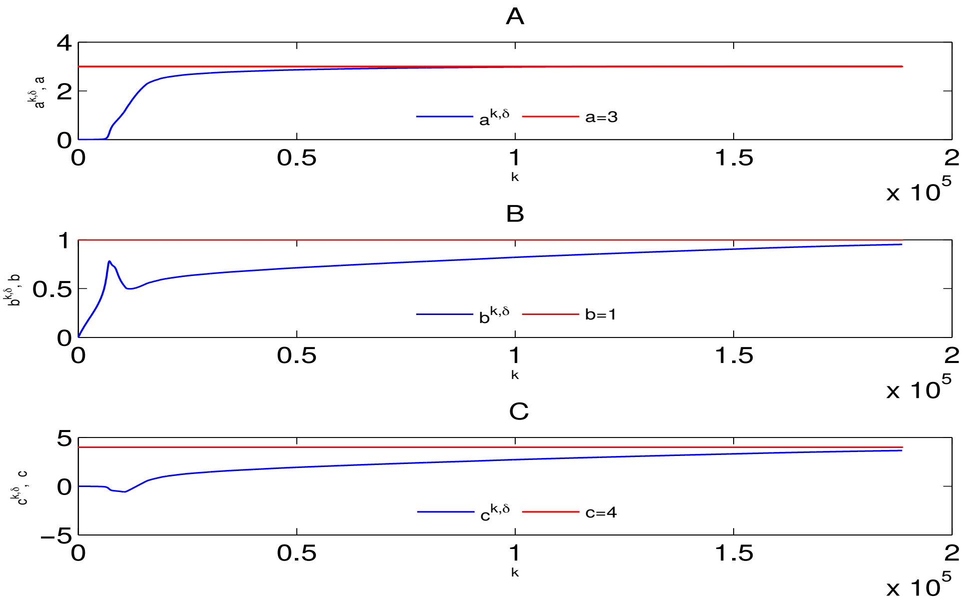

FIGURE 5. For Example 3.2 and $\varepsilon = 1\%$. The x-axis is the number of iterations (k). In y-axis, the red lines are the exact solutions, and blue lines are the approximations. The figures 5-A, 5-B and 5-C are the estimates of a, b and c, respectively.

.

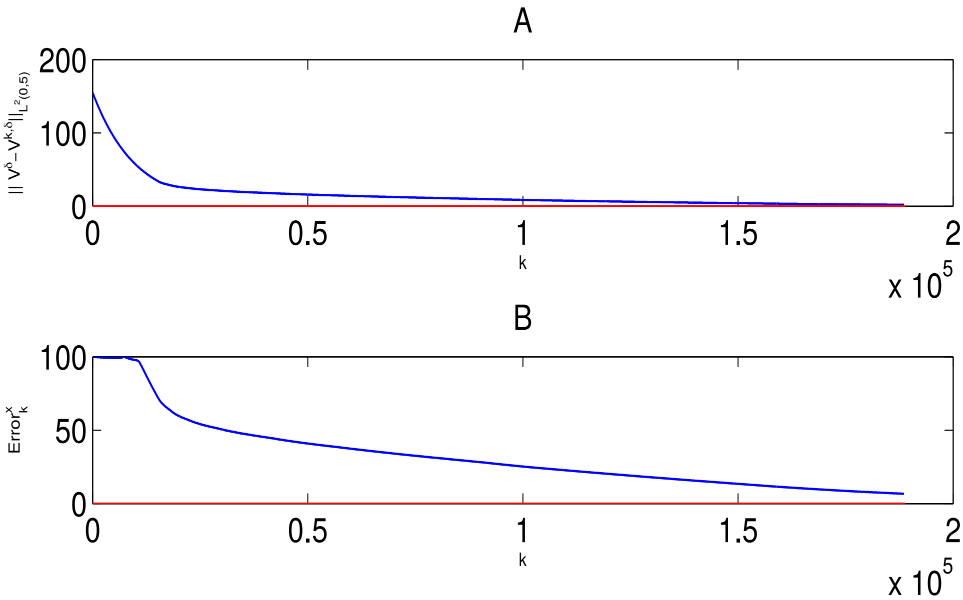

FIGURE 6. For Example 3.2 and $\varepsilon = 1\%$. The x-axis is the number of iterations (k). The y-axis, in the figures A and B are the residual (25) and error (26), respectively.

APPENDIX A. PROOF OF THEOREM 2.1

In this Appendix, we show Theorem 2.1.

Proof. Consider the operator F defined in (9). Evaluating $\boldsymbol{G}^{k,\delta}$ in F , we have $F(\boldsymbol{G}^{k,\delta}) = V^{k,\delta}$, where $V^{k,\delta}$, $m^{k,\delta}$, $n^{k,\delta}$ and $h^{k,\delta}$ solve the ODE (18).

Let vector $\boldsymbol{\theta} = (\theta_{\mathrm{Na}}, \theta_{\mathrm{K}}, \theta_L) \in \mathbb{R}^3$ and $\lambda \in \mathbb{R}$, then evaluating $\boldsymbol{G}^{k,\delta} + \lambda\boldsymbol{\theta}$ in the operator F, we have $F(\boldsymbol{G}^{k,\delta} + \lambda\boldsymbol{\theta}) = V^{k,\delta}_\lambda$, where $V^{k,\delta}_\lambda$, $m^{k,\delta}_\lambda$, $n^{k,\delta}_\lambda$ and $h^{k,\delta}_\lambda$ solve

$$
\begin{cases}
C_M \dot{V}^{k,\delta}_\lambda = I_{\mathrm{ext}} - \left(G^{k,\delta}_{\mathrm{Na}} + \lambda\theta_{\mathrm{Na}}\right)\left(m^{k,\delta}_\lambda\right)^a \left(h^{k,\delta}_\lambda\right)^b \left(V^{k,\delta}_\lambda - E_{\mathrm{Na}}\right) \\
\qquad - \left(G^{k,\delta}_{\mathrm{K}} + \lambda\theta_K\right)\left(n^{k,\delta}_\lambda\right)^c \left(V^{k,\delta}_\lambda - E_{\mathrm{K}}\right) - \left(G^{k,\delta}_L + \lambda\theta_L\right)\left(V^{k,\delta}_\lambda - E_L\right), \\
\dot{\mathcal{X}} = (1-\mathcal{X})\alpha_{\mathcal{X}}(V^{k,\delta}) - \mathcal{X}\beta_{\mathcal{X}}(V^{k,\delta}); \qquad \mathcal{X} = m^{k,\delta}_\lambda, n^{k,\delta}_\lambda, h^{k,\delta}_\lambda, \\
V^{k,\delta}_\lambda(0) = V_0; \quad m^{k,\delta}_\lambda(0) = m_0; \quad n^{k,\delta}_\lambda(0) = n_0; \quad n^{k,\delta}_\lambda(0) = n_0.
\end{cases}
\tag{27}
$$

The Gateaux derivative of F at $\boldsymbol{G}^{k,\delta}$ in the direction $\boldsymbol{\theta}$ is given by

$$
W^{k,\delta} = F'(\boldsymbol{G}^{k,\delta})(\boldsymbol{\theta}) = \lim_{\lambda\to 0} \frac{F(\boldsymbol{G}^{k,\delta} + \lambda\boldsymbol{\theta}) - F(\boldsymbol{G}^{k,\delta})}{\lambda}.
\tag{28}
$$

Also, we denote the following limits

$$
M^{k,\delta} = \lim_{\lambda\to 0} \frac{m^{k,\delta}_\lambda - m^{k,\delta}}{\lambda}, \qquad N^{k,\delta} = \lim_{\lambda\to 0} \frac{n^{k,\delta}_\lambda - n^{k,\delta}}{\lambda}, \qquad H^{k,\delta} = \lim_{\lambda\to 0} \frac{h^{k,\delta}_\lambda - h^{k,\delta}}{\lambda},
\tag{29}
$$

where $M^{k,\delta}$, $N^{k,\delta}$ and $H^{k,\delta}$ are the Gateaux derivatives of $m^{k,\delta}$, $n^{k,\delta}$ and $h^{k,\delta}$, respectively.

Considering the difference between ODEs (27) and (18), dividing by λ and taking the limit $\lambda \to 0$, we have the following ODE

$$\left\{\begin{array}{l} C_M \dot{W}^{k,\delta} + \left(G_{\text{Na}}^{k,\delta}\big(m^{k,\delta}\big)^a\big(h^{k,\delta}\big)^b + G_{\text{K}}^{k,\delta}\big(n^{k,\delta}\big)^c + G_L^{k,\delta}\right)W^{k,\delta} = \\ \qquad -aG_{\text{Na}}^{k,\delta}\big(m^{k,\delta}\big)^{a-1}M^{k,\delta}\big(h^{k,\delta}\big)^b(V^{k,\delta} - E_{\text{Na}}) \\ \qquad -bG_{\text{Na}}^{k,\delta}\big(m^{k,\delta}\big)^a\big(h^{k,\delta}\big)^{b-1}H^{k,\delta}(V^{k,\delta} - E_{\text{Na}}) - cG_{\text{K}}^{k,\delta}\big(n^{k,\delta}\big)^{c-1}N^{k,\delta}(V^{k,\delta} - E_{\text{K}}) \\ \qquad -\theta_{\text{Na}}\big(m^{k,\delta}\big)^a\big(h^{k,\delta}\big)^b(V^{k,\delta} - E_{\text{Na}}) - \theta_K\big(n^{k,\delta}\big)^c(V^{k,\delta} - E_{\text{K}}) - \theta_L(V^{k,\delta} - E_L), \\ \dot{\mathcal{X}} + [\alpha_{\mathcal{Y}}(V^{k,\delta}) + \beta_{\mathcal{Y}}(V^{k,\delta})]\mathcal{X} = [(1-\mathcal{Y})\alpha'_{\mathcal{Y}}(V^{k,\delta}) - \mathcal{Y}\beta'_{\mathcal{Y}}(V^{k,\delta})]W^{k,\delta}; \\ \ (\mathcal{X},\mathcal{Y}) = (M^{k,\delta}, m^{k,\delta}), (N^{k,\delta}, n^{k,\delta}), (H^{k,\delta}, h^{k,\delta}), \\ W^{k,\delta}(0) = 0; \quad M^{k,\delta}(0) = 0; \quad N^{k,\delta}(0) = 0; \quad H^{k,\delta}(0) = 0. \end{array}\right. \tag{30}$$

This last equation is yet another system of coupled nonlinear differential equations, depending on the parameter $\boldsymbol{\theta} = (\theta_{\text{Na}}, \theta_K, \theta_L)$, representing an arbitrary point in $\mathbb{R}^3$.

From minimal error iteration (13) and $\boldsymbol{\theta} \in \mathbb{R}^3$ arbitrary, we have

$$\begin{aligned} \langle \boldsymbol{G}^{k+1,\delta} - \boldsymbol{G}^{k,\delta}, \boldsymbol{\theta} \rangle_{\mathbb{R}^3} &= w^{k,\delta}\langle F'(\boldsymbol{G}^{k,\delta})^*(V^\delta - F(\boldsymbol{G}^{k,\delta})), \boldsymbol{\theta} \rangle_{\mathbb{R}^3}, \\ &= w^{k,\delta}\langle F'(\boldsymbol{G}^{k,\delta})^*(V^\delta - V^{k,\delta}), \boldsymbol{\theta} \rangle_{\mathbb{R}^3}. \end{aligned}$$

By definition of adjoint operator

$$\langle \boldsymbol{G}^{k+1,\delta} - \boldsymbol{G}^{k,\delta}, \boldsymbol{\theta} \rangle_{\mathbb{R}^3} = w^{k,\delta}\langle V^\delta - V^{k,\delta}, F'(x_k)(\boldsymbol{\theta}) \rangle_{L^2[0,T]},$$

where the internal product in $L^2[0,T]$ is given by $\Phi = \int_0^T (V^\delta - V^{k,\delta})W^{k,\delta}\, dt$, and from (28) and the previous equation,

$$\langle \boldsymbol{G}^{k+1,\delta} - \boldsymbol{G}^{k,\delta}, \boldsymbol{\theta} \rangle_{\mathbb{R}^3} = w^{k,\delta}\langle V^\delta - V^{k,\delta}, W^{k,\delta} \rangle_{L^2[0,T]}.$$

Denoting the last equality by Φ, we gather that

$$\Phi = \frac{\langle \boldsymbol{G}^{k+1,\delta} - \boldsymbol{G}^{k,\delta}, \boldsymbol{\theta} \rangle_{\mathbb{R}^3}}{w^{k,\delta}} = \langle V^\delta - V^{k,\delta}, W^{k,\delta} \rangle_{L^2[0,T]}. \tag{31}$$

From the previous equation and the first equality from ODE (19), we obtain

$$
\begin{aligned}
(32)\quad \Phi = &\int_0^T \left(C_M\dot{U}^{k,\delta}W^{k,\delta} - \left(G_{\mathrm{Na}}^{k,\delta}\big(m^{k,\delta}\big)^a\big(h^{k,\delta}\big)^b + G_{\mathrm{K}}^{k,\delta}\big(n^{k,\delta}\big)^c + G_L^{k,\delta}\right)U^{k,\delta}W^{k,\delta}\right)\, dt\\
&- \int_0^T \left[(1-m^{k,\delta})\alpha'_{m^{k,\delta}}(V^{k,\delta}) - m^{k,\delta}\beta'_{m^{k,\delta}}(V^{k,\delta})\right] P^{k,\delta}W^{k,\delta}\, dt\\
&- \int_0^T \left[(1-n^{k,\delta})\alpha'_{n^{k,\delta}}(V^{k,\delta}) - n^{k,\delta}\beta'_{n^{k,\delta}}(V^{k,\delta})\right] Q^{k,\delta}W^{k,\delta}\, dt\\
&- \int_0^T \left[(1-h^{k,\delta})\alpha'_{h^{k,\delta}}(V^{k,\delta}) - h^{k,\delta}\beta'_{h^{k,\delta}}(V^{k,\delta})\right] R^{k,\delta}W^{k,\delta}\, dt.
\end{aligned}
$$

Integrating the first term from (32) by parts, and from the initial ($W^{k,\delta}(0) = 0$) and final ($U^{k,\delta}(T) = 0$) conditions, we obtain

$$
(33)\qquad \int_0^T C_M\dot{U}^{k,\delta}W^{k,\delta} = -\int_0^T C_M U^{k,\delta}\dot{W}^{k,\delta}.
$$

Replacing equation (33) in (32), we have

$$
\begin{aligned}
\Phi \;=\; &-\int_0^T \left(C_M\dot{W}^{k,\delta} + \left(G_{\mathrm{Na}}^{k,\delta}\big(m^{k,\delta}\big)^a\big(h^{k,\delta}\big)^b + G_{\mathrm{K}}^{k,\delta}\big(n^{k,\delta}\big)^c + G_L^{k,\delta}\right)W^{k,\delta}\right)U^{k,\delta}\, dt\\
&- \int_0^T \left[(1-m^{k,\delta})\alpha'_{m^{k,\delta}}(V^{k,\delta}) - m^{k,\delta}\beta'_{m^{k,\delta}}(V^{k,\delta})\right] P^{k,\delta}W^{k,\delta}\, dt\\
&- \int_0^T \left[(1-n^{k,\delta})\alpha'_{n^{k,\delta}}(V^{k,\delta}) - n^{k,\delta}\beta'_{n^{k,\delta}}(V^{k,\delta})\right] Q^{k,\delta}W^{k,\delta}\, dt\\
&- \int_0^T \left[(1-h^{k,\delta})\alpha'_{h^{k,\delta}}(V^{k,\delta}) - h^{k,\delta}\beta'_{h^{k,\delta}}(V^{k,\delta})\right] R^{k,\delta}W^{k,\delta}\, dt.
\end{aligned}
$$

Replacing, the first equality from the ODE (30), in the first integral from the previous equation, we gather

$$
\begin{aligned}
(34)\quad \Phi = \int_0^T & aG_{\mathrm{Na}}^{k,\delta}(m^{k,\delta})^{a-1}M^{k,\delta}\big(h^{k,\delta}\big)^b(V^{k,\delta}-E_{\mathrm{Na}})U^{k,\delta}\,dt \\
&+\int_0^T bG_{\mathrm{Na}}^{k,\delta}\big(m^{k,\delta}\big)^a(h^{k,\delta})^{b-1}H^{k,\delta}(V^{k,\delta}-E_{\mathrm{Na}})U^{k,\delta}\,dt \\
&+\int_0^T cG_{\mathrm{K}}^{k,\delta}(n^{k,\delta})^{c-1}N^{k,\delta}(V^{k,\delta}-E_{\mathrm{K}})U^{k,\delta}\,dt \\
&+\int_0^T \big(m^{k,\delta}\big)^a\big(h^{k,\delta}\big)^b(V^{k,\delta}-E_{\mathrm{Na}})\alpha U^{k,\delta}\,dt \\
&+\int_0^T \big(n^{k,\delta}\big)^c(V^{k,\delta}-E_{\mathrm{K}})\beta U^{k,\delta}\,dt+\int_0^T (V^{k,\delta}-E_L)\gamma U^{k,\delta}\,dt \\
&-\int_0^T \big[(1-m^{k,\delta})\alpha'_{m^{k,\delta}}(V^{k,\delta})-m^{k,\delta}\beta'_{m^{k,\delta}}(V^{k,\delta})\big]\,P^{k,\delta}W^{k,\delta}\,dt \\
&-\int_0^T \big[(1-n^{k,\delta})\alpha'_{n^{k,\delta}}(V^{k,\delta})-n^{k,\delta}\beta'_{n^{k,\delta}}(V^{k,\delta})\big]\,Q^{k,\delta}W^{k,\delta}\,dt \\
&-\int_0^T \big[(1-h^{k,\delta})\alpha'_{h^{k,\delta}}(V^{k,\delta})-h^{k,\delta}\beta'_{h^{k,\delta}}(V^{k,\delta})\big]\,R^{k,\delta}W^{k,\delta}\,dt.
\end{aligned}
$$

Multiplying the second equation from (19) by $M^{k,\delta}$, and integrating in the interval $[0,T]$ it follows that

$$
\int_0^T P_t^{k,\delta}M^{k,\delta}-\big[\alpha_{m^{k,\delta}}(V^{k,\delta})+\beta_{m^{k,\delta}}(V^{k,\delta})\big]\,P^{k,\delta}M^{k,\delta}\,dt = -\int_0^T aG_{\mathrm{Na}}^{k,\delta}\big(m^{k,\delta}\big)^{a-1}\big(h^{k,\delta}\big)^b(V^{k,\delta}-E_{\mathrm{Na}})U^{k,\delta}M^{k,\delta}\,dt.
$$

Integrating by parts the first term from the previous equation, and using the initial $(M^{k,\delta}(0)=0)$ and final $(P^{k,\delta}(T)=0)$ conditions, we have

$$
\int_0^T \Big(\dot M^{k,\delta}+\big[\alpha_{m^{k,\delta}}(V^{k,\delta})+\beta_{m^{k,\delta}}(V^{k,\delta})\big]\,M^{k,\delta}\Big)\,P^{k,\delta}\,dt = \int_0^T aG_{\mathrm{Na}}^{k,\delta}\big(m^{k,\delta}\big)^{a-1}\big(h^{k,\delta}\big)^b(V^{k,\delta}-E_{\mathrm{Na}})U^{k,\delta}M^{k,\delta}\,dt.
$$

Then, from the previous equation and the second equation from ODE (30), for $(\mathcal{X},\mathcal{Y}) = (M^{k,\delta}, m^{k,\delta})$,

$$\int_0^T aG_{\mathrm{K}}^{k,\delta}\big(m^{k,\delta}\big)^{a-1}\big(h^{k,\delta}\big)^{b}(V^{k,\delta}-E_{\mathrm{Na}})U^{k,\delta}M^{k,\delta}\,dt = \int_0^T \big[(1-m^{k,\delta})\alpha'_{m^{k,\delta}}(V^{k,\delta}) - m^{k,\delta}\beta'_{m^{k,\delta}}(V^{k,\delta})\big]\,W^{k,\delta}P^{k,\delta}\,dt. \tag{35}$$

Multiplying the third equation from (19) by $N^{k,\delta}$, and integrating in the interval $[0,T]$ we gather that

$$\int_0^T \dot{Q}^{k,\delta}N^{k,\delta} - \big[\alpha_{n^{k,\delta}}(V^{k,\delta}) + \beta_{n^{k,\delta}}(V^{k,\delta})\big]\,Q^{k,\delta}N^{k,\delta}\,dt = -\int_0^T cG_{\mathrm{K}}^{k,\delta}\big(n^{k,\delta}\big)^{c-1}(V^{k,\delta}-E_{\mathrm{K}})U^{k,\delta}\,dt.$$

Integrating by parts the first term from previous equation, and using the initial $(N^{k,\delta}(0) = 0)$ and final $(Q^{k,\delta}(T) = 0)$ conditions, we have

$$\int_0^T \Big(\dot{N}^{k,\delta} + \big[\alpha_{n^{k,\delta}}(V^{k,\delta}) + \beta_{n^{k,\delta}}(V^{k,\delta})\big]\,N^{k,\delta}\Big)\,Q^{k,\delta}\,dt = \int_0^T cG_{\mathrm{K}}^{k,\delta}\big(n^{k,\delta}\big)^{c-1}(V^{k,\delta}-E_{\mathrm{K}})U^{k,\delta}\,dt.$$

Then, from the previous equation and the second equation from ODE (30), for $(\mathcal{X},\mathcal{Y}) = (N^{k,\delta}, n^{k,\delta})$, we have

$$\int_0^T cG_{\mathrm{K}}^{k,\delta}\big(n^{k,\delta}\big)^{c-1}(V^{k,\delta}-E_{\mathrm{K}})U^{k,\delta}\,dt = \int_0^T \big[(1-n^{k,\delta})\alpha a'_{n^{k,\delta}}(V^{k,\delta}) - n^{k,\delta}\beta'_{n^{k,\delta}}(V^{k,\delta})\big]\,WQ^{k,\delta}\,dt. \tag{36}$$

Multiplying the fourth equation from (19) by $H^{k,\delta}$, and integrating in the interval $[0,T]$ we gather that

$$\int_0^T \dot{R}^{k,\delta}H^{k,\delta} - \big[\alpha_{h^{k,\delta}}(V^{k,\delta}) + \beta_{h^{k,\delta}}(V^{k,\delta})\big]\,R^{k,\delta}H^{k,\delta}\,dt = -\int_0^T bG_{\mathrm{Na}}^{k,\delta}\big(m^{k,\delta}\big)^{a}\big(h^{k,\delta}\big)^{b-1}(V^{k,\delta}-E_{\mathrm{Na}})U^{k,\delta}\,dt.$$

Integrating by parts the first term from the previous equation, and using the initial ($H^{k,\delta}(0) = 0$) and final ($R^{k,\delta}(T) = 0$) conditions, we have

$$\int_0^T \left(\dot{H}^{k,\delta} + \left[\alpha_{h^{k,\delta}}(V^{k,\delta}) + \beta_{h^{k,\delta}}(V^{k,\delta})\right] H^{k,\delta}\right) R^{k,\delta}\, dt = \int_0^T bG_{\mathrm{Na}}^{k,\delta}\big(m^{k,\delta}\big)^a \big(h^{k,\delta}\big)^{b-1}(V^{k,\delta} - E_{\mathrm{Na}})U^{k,\delta}\, dt.$$

Then, from the previous equation and the second equation from ODE (30), for $(\mathcal{X}, \mathcal{Y}) = (H^{k,\delta}, h^{k,\delta})$, we have

$$\int_0^T bG_{\mathrm{Na}}^{k,\delta}\big(m^{k,\delta}\big)^a \big(h^{k,\delta}\big)^{b-1}(V^{k,\delta} - E_{\mathrm{Na}})U^{k,\delta}\, dt = \int_0^T \left[(1 - h^{k,\delta})\alpha'_{h^{k,\delta}}(V^{k,\delta}) - h^{k,\delta}\beta'_{h^{k,\delta}}(V^{k,\delta})\right] W^{k,\delta} R^{k,\delta}\, dt. \tag{37}$$

Substituting equations (35), (36), and (37) in (34), we have

$$\Phi = \int_0^T \big(m^{k,\delta}\big)^a \big(h^{k,\delta}\big)^b (V^{k,\delta} - E_{\mathrm{Na}})\theta_{\mathrm{Na}} U^{k,\delta}\, dt + \int_0^T \big(n^{k,\delta}\big)^c (V^{k,\delta} - E_{\mathrm{K}})\theta_{\mathrm{K}} U^{k,\delta}\, dt + \int_0^T (V^{k,\delta} - E_L)\theta_L U^{k,\delta}\, dt. \tag{38}$$

Substituting equations (15), (16) and (17) in equation (38) we gather that

$$\Phi = X_{\mathrm{Na}}^{k,\delta}\, \theta_{\mathrm{Na}} + X_K^{k,\delta}\, \theta_{\mathrm{K}} + X_L^{k,\delta}\, \theta_L = \left\langle \left(X_{\mathrm{Na}}^{k,\delta}, X_K^{k,\delta}, X_L^{k,\delta}\right), (\theta_{\mathrm{Na}}, \theta_{\mathrm{K}}, \theta_L)\right\rangle_{\mathbb{R}^3}. \tag{39}$$

From (31) and (39)

$$\frac{\langle \boldsymbol{G}^{k+1,\delta} - \boldsymbol{G}^{k,\delta}, \boldsymbol{\theta}\, \rangle_{\mathbb{R}^3}}{w^{k,\delta}} = \left\langle \left(X_{\mathrm{Na}}^{k,\delta}, X_K^{k,\delta}, X_L^{k,\delta}\right), \boldsymbol{\theta}\right\rangle_{\mathbb{R}^3}.$$

Since $\boldsymbol{\theta} \in \mathbb{R}^3$ is arbitrary, we obtain (14). □

Appendix B. Proof of Theorem 2.2

In what follows we prove Theorem 2.2.

Proof. Consider the operator F defined in (9). Evaluating $\boldsymbol{a}^{k,\delta}$ in F, we have $F(\boldsymbol{a}^{k,\delta}) = V^{k,\delta}$, where $V^{k,\delta}$, $m^{k,\delta}$, $n^{k,\delta}$ and $h^{k,\delta}$ solve ODE (22). Let $\boldsymbol{\theta} = (\theta_a, \theta_b, \theta_c) \in \mathbb{R}^3$ and $\lambda \in \mathbb{R}$, then

$F(\boldsymbol{a}^{k,\delta}+\lambda\boldsymbol{\theta}) = V_\lambda^{k,\delta}$, where $V_\lambda^{k,\delta}$, $m_\lambda^{k,\delta}$, $n_\lambda^{k,\delta}$ and $h_\lambda^{k,\delta}$ solve

$$(40)\quad \begin{cases} C_M \dot{V}_\lambda^{k,\delta} = I_{\text{ext}} - G_{\text{Na}}\Big(m_\lambda^{k,\delta}\Big)^{a^{k,\delta}+\lambda\theta_a}\Big(h_\lambda^{k,\delta}\Big)^{b^{k,\delta}+\lambda\theta_b}\Big(V_\lambda^{k,\delta}-E_{\text{Na}}\Big) \\ \quad -G_{\text{K}}^{k,\delta}\Big(n_\lambda^{k,\delta}\Big)^{c^{k,\delta}+\lambda\theta_c}\Big(V_\lambda^{k,\delta}-E_{\text{K}}\Big) - G_L\Big(V_\lambda^{k,\delta}-E_L\Big), \\ \dot{\mathcal{X}} = (1-\mathcal{X})\alpha_{\mathcal{X}}(V^{k,\delta}) - \mathcal{X}\beta_{\mathcal{X}}(V^{k,\delta}), \quad \text{for } \mathcal{X} = m_\lambda^{k,\delta}, n_\lambda^{k,\delta}, h_\lambda^{k,\delta}, \\ V_\lambda^{k,\delta}(0) = V_0, \quad m_\lambda^{k,\delta}(0) = m_0, \quad n_\lambda^{k,\delta}(0) = n_0, \quad n_\lambda^{k,\delta}(0) = n_0. \end{cases}$$

Considering the difference between the ODEs (40) and (22), dividing by λ and taking the limit $\lambda \to 0$, we have the ODE

$$(41)\quad \begin{cases} C_M \dot{W}^{k,\delta} + \Big(G_{\text{Na}}\big(m^{k,\delta}\big)^{a^{k,\delta}}\big(h^{k,\delta}\big)^{b^{k,\delta}} + G_{\text{K}}\big(n^{k,\delta}\big)^{c^{k,\delta}} + G_L\Big)W^{k,\delta} = \\ \quad -a^{k,\delta}G_{\text{Na}}\big(m^{k,\delta}\big)^{a^{k,\delta}-1}M^{k,\delta}\big(h^{k,\delta}\big)^{b^{k,\delta}}(V^{k,\delta}-E_{\text{Na}}) \\ \quad -\mathsf{b}G_{\text{Na}}\big(m^{k,\delta}\big)^{a^{k,\delta}}\big(h^{k,\delta}\big)^{b^{k,\delta}-1}H^{k,\delta}(V^{k,\delta}-E_{\text{Na}}) \\ \quad -c^{k,\delta}G_{\text{K}}\big(n^{k,\delta}\big)^{c^{k,\delta}-1}N^{k,\delta}(V^{k,\delta}-E_{\text{K}}) \\ \quad -G_{\text{Na}}\big(m^{k,\delta}\big)^{a^{k,\delta}}\ln(m^{k,\delta})\big(h^{k,\delta}\big)^{b^{k,\delta}}(V^{k,\delta}-E_{\text{Na}})\theta_a \\ \quad -G_{\text{Na}}\big(m^{k,\delta}\big)^{a^{k,\delta}}\big(h^{k,\delta}\big)^{b^{k,\delta}}\ln(h^{k,\delta})(V^{k,\delta}-E_{\text{Na}})\theta_b \\ \quad -G_k\big(n^{k,\delta}\big)^{\mathsf{c}}\ln(n^{k,\delta})(V^{k,\delta}-E_{\text{K}})\theta_c, \\ \dot{\mathcal{X}} + [\alpha_{\mathcal{Y}}(V^{k,\delta}) + \beta_{\mathcal{Y}}(V^{k,\delta})]\mathcal{X} = [(1-\mathcal{Y})\alpha'_{\mathcal{Y}}(V^{k,\delta}) - \mathcal{Y}\beta'_{\mathcal{Y}}(V^{k,\delta})]W^{k,\delta}, \\ \quad (\mathcal{X},\mathcal{Y}) = (M^{k,\delta}, m^{k,\delta}), (N^{k,\delta}, n^{k,\delta}), (H^{k,\delta}, h^{k,\delta}), \\ W^{k,\delta}(0) = 0, \quad M^{k,\delta}(0) = 0, \quad N^{k,\delta}(0) = 0, \quad H^{k,\delta}(0) = 0. \end{cases}$$

where $W^{k,\delta}$ is defined in equation (28) by replacing $\boldsymbol{G}^{k,\delta}$ by $\boldsymbol{a}^{k,\delta}$. Also, $M^{k,\delta}$, $N^{k,\delta}$ and $H^{k,\delta}$ are defined in equation (29).

This last equation is again a system of coupled nonlinear differential equations, parametrized by $\boldsymbol{\theta} = (\theta_a, \theta_b, \theta_c)$, where $\boldsymbol{\theta} \in \mathbb{R}^3$ is arbitrary. Considering (23), and proceeding as in Appendix A, we gather (21). □

References

[1] Avdonin, S., and Bell, J. Determining a distributed parameter in a neural cable model via a boundary control method. *Journal of mathematical biology 67*, 1 (2013), 123–141.

[2] Avdonin, S., and Bell, J. Determining a distributed conductance parameter for a neuronal cable model defined on a tree graph. *Journal of Inverse Problems and Imaging 9* (2015), 645–659.

[3] Bell, J., and Craciun, G. A distributed parameter identification problem in neuronal cable theory models. *Mathematical biosciences 194*, 1 (2005), 1–19.

[4] Binder, A., Hanke, M., and Scherzer, O. On the Landweber iteration for nonlinear ill-posed problems. *Journal of Inverse and Ill-posed Problems 4*, 5 (1996), 381–390.

[5] Buhry, L., Grassia, F., Giremus, A., Grivel, E., Renaud, S., and Saïghi, S. Automated parameter estimation of the Hodgkin–Huxley model using the differential evolution algorithm: application to neuromimetic analog integrated circuits. *Neural computation 23*, 10 (2011), 2599–2625.

[6] Buhry, L., Pace, M., and Saïghi, S. Global parameter estimation of an Hodgkin–Huxley formalism using membrane voltage recordings: Application to neuro-mimetic analog integrated circuits. *Neurocomputing 81* (2012), 75–85.

[7] Chapko, R., and Kügler, P. A comparison of the Landweber method and the Gauss–Newton method for an inverse parabolic boundary value problem. *Journal of computational and applied mathematics 169*, 1 (2004), 183–196.

[8] Che, Y., Geng, L.-H., Han, C., Cui, S., and Wang, J. Parameter estimation of the Fitzhugh–Nagumo model using noisy measurements for membrane potential. *Chaos: An Interdisciplinary Journal of Nonlinear Science 22*, 2 (2012), 023139.

[9] Cooley, J., and Dodge Jr, F. Digital computer solutions for excitation and propagation of the nerve impulse. *Biophysical journal 6*, 5 (1966), 583.

[10] Cox, S., and Wagner, A. Lateral overdetermination of the Fitzhugh–Nagumo system. *Inverse Problems 20*, 5 (2004), 1639.

[11] Cox, S. J., and Ji, L. Discerning ionic currents and their kinetics from input impedance data. *Bulletin of mathematical biology 63*, 5 (2001), 909–932.

[12] Gutkin, B., Pinto, D., and Ermentrout, B. Mathematical neuroscience: from neurons to circuits to systems. *Journal of Physiology-Paris 97*, 2-3 (2003), 209–219.

[13] Hadamard, J. *Lectures on Cauchy's problem in linear partial differential equations.* Courier Corporation, 2014.

[14] Hanke, M., Neubauer, A., and Scherzer, O. A convergence analysis of the Landweber iteration for nonlinear ill-posed problems. *Numerische Mathematik 72*, 1 (1995), 21–37.

[15] Hodgkin, A. L., and Huxley, A. F. A quantitative description of membrane current and its application to conduction and excitation in nerve. *The Journal of physiology 117*, 4 (1952), 500–544.

[16] Kaltenbacher, B., Neubauer, A., and Scherzer, O. *Iterative regularization methods for nonlinear ill-posed problems*, vol. 6. Walter de Gruyter, 2008.

[17] Neubauer, A. On Landweber iteration for nonlinear ill-posed problems in hilbert scales. *Numerische Mathematik 85*, 2 (2000), 309–328.

[18] Pavel'chak, I. Numerical solution method for the source reconstruction problem in the Fitzhugh–Nagumo model. *Computational Mathematics and Modeling 1*, 24 (2013), 22–30.

[19] Pavel'chak, I., and Tuikina, S. Numerical solution method for the inverse problem of the modified Fitzhugh–Nagumo model. *Computational Mathematics and Modeling 23*, 2 (2012), 208–215.

[20] Pospischil, M., Piwkowska, Z., Rudolph, M., Bal, T., and Destexhe, A. Calculating event-triggered average synaptic conductances from the membrane potential. *Journal of Neurophysiology 97*, 3 (2007), 2544–2552.

[21] Rall, W. Core conductor theory and cable properties of neurons. *Comprehensive Physiology 1* (1977), 39–97.

[22] Rall, W., Burke, R., Holmes, W., Jack, J., Redman, S., and Segev, I. Matching dendritic neuron models to experimental data. *Physiological Reviews 72*, 4 (1992), S159–S186.

[23] Rudolph, M., Piwkowska, Z., Badoual, M., Bal, T., and Destexhe, A. A method to estimate synaptic conductances from membrane potential fluctuations. *Journal of neurophysiology 91*, 6 (2004), 2884–2896.

[24] Tadi, M., Klibanov, M. V., and Cai, W. An inversion method for parabolic equations based on quasireversibility. *Computers & Mathematics with Applications 43*, 8 (2002), 927–941.

[25] Tuikina, S., and Solov'eva, S. Numerical method of determining the excitation source for the Fitzhugh–Nagumo mathematical model. *Computational Mathematics and Modeling 28*, 3 (2017), 301–309.

[26] Valle, J. A. M., Madureira, A. L., and Leitão, A. A computational approach for the inverse problem of neuronal conductances determination. *arXiv preprint arXiv:1810.05887* (2018).

[27] Vich, C., Berg, R. W., Guillamon, A., and Ditlevsen, S. Estimation of synaptic conductances in presence of nonlinear effects caused by subthreshold ionic currents. *Frontiers in computational neuroscience 11* (2017), 69.

Departamento de Modelagem Computacional, Laboratrio Nacional de Computao Cientfica, Av. Getlio Vargas 333, 25651-070 Petrpolis, RJ, Brazil

APPENDIX C – Paper 3

Estimation of distributed parameters from membrane potential measurement

ESTIMATION OF DISTRIBUTED PARAMETERS FROM MEMBRANE POTENTIAL MEASUREMENT

JEMY A. MANDUJANO VALLE, ALEXANDRE L. MADUREIRA

ABSTRACT. Alan Hodgkin and Andrew Huxley formed one of the most productive and influential collaborations in the history of physiology. Based on a series of voltage-clamp experiments, they developed a detailed mathematical model, which describes how action potentials are initiated and propagated. To obtain this model the authors used the squid giant neuron of the genus Loligo. The FitzHugh-Nagumo model is a simpler version of the Hodgkin-Huxley model. Here, we propose the minimal error method to estimate parameters with a non-uniform distribution in the models. Our approach estimates the unknown data given the measurement of membrane potential.

1. Introduction.

Hodgkin and Huxley (H-H) performed experiments on the squid giant axon and created a model of four mathematical equations that describes how action potentials in neurons are initiated and propagated [11]. In the H-H model, the membrane potential $V : [0, T] \to \mathbb{R}$ solves

$$C_M \dot{V}(t) = I_{\text{ext}} + I_{Na}(t) + I_K(t) + I_L(t), \quad t \in (0, T], \tag{1}$$

where the membrane capacitance C_M is in microfarad per square centimeter $[\mu F/cm^2]$, the membrane potential V in millivolt $[mV]$, the external membrane current I_{ext} is in microampere per square centimeter $[\mu A/cm^2]$. The parameters I_{Na}, I_K and I_L, in microampere per square centimeter $[\mu A/cm^2]$, are the sodium, potassium and leakage ionic currents, respectively. The time t in milliseconds $[ms]$. Also, $\dot{V} = dV/dt$ is the derivative of the voltage variable V with respect to time t.

In the paper [10], Hodgking and Huxley showed that the ionic currents can be expressed in terms of ionic conductances (g_{Na}, g_K and g_L)

$$I_{Na}(t) = g_{Na}(V(t), t)(V(t) - E_{Na}); \qquad I_K(t) = g_K(V(t), t)(V(t) - E_K); \qquad I_L(t) = G_L; \tag{2}$$

where g_{Na}, g_K and g_L, in millisiemens per square centimeter $[mS/cm^2]$, are the sodium, potassium and leak current conductances, respectively. The equilibrium potential of sodium,

Date: October 10, 2018.

potassium and leak current, in millivolt $[mV]$, is represented by E_{Na}, E_K and E_L, respectively.

Using voltage-clamp data, Hodgkin and Huxley derived expressions for K^+ and Na^+ conductances. They proposed that

$$g_{Na}(V(t),t) = G_{Na}n(V(t),t)^4 \quad \text{and} \quad g_K(V(t),t) = g_K m(V(t),t)^3 h(V(t),t), \tag{3}$$

where G_{Na}, G_K and G_L, in millisiemens per square centimeter $[mS/cm^2]$, are the maximal sodium, potassium and leak current conductances, respectively. The parameters m, n and h are unitless gating variables that take values between 0 and 1. Hence, n^4 represents the probability that a potassium channel is open: the potassium channel has 4 independent, and identical, components. The probability that the sodium activation gate is open is m^3 and the probability that the sodium inactivation gate is open is $1-h$. Each of the gating variables satisfies a first-order differential equation, that is, they satisfy equations of the form [9].

$$\dot{\mathcal{X}} = (1-\mathcal{X})\alpha_{\mathcal{X}}(V^{k,\delta}) - \mathcal{X}\beta_{\mathcal{X}}(V^{k,\delta}); \quad \mathcal{X} = m, n, h. \tag{4}$$

The experiments performed by Hodgkin and Huxley suggest that:

$$\begin{aligned}
\alpha_m(V) &= \frac{(25-V)/10}{\exp((25-V)/10)-1}, & \beta_m(V) &= 4\exp(-V/18),\\
\alpha_n(V) &= \frac{(10-V)/100}{\exp((10-V)/10)-1}, & \beta_n(V) &= 0.125\exp(-V/80),\\
\alpha_h(V) &= 0.07\exp(-V/20), & \beta_h(V) &= \frac{1}{\exp((30-V)/10)+1}.
\end{aligned}$$

To equation (1) we add the initial conditions

$$V(0) = V_0, \quad m(0) = m_0, \quad , n(0) = n_0, \quad h(0) = h_0. \tag{5}$$

Thus, from (1-5) we have the following ordinary differential equation (ODE):

$$\begin{cases}
C_M\dot{V} = I_{\text{ext}} - G_{Na}m^3h(V-E_{Na}) - G_Kn^4(V-E_K) - G_L(V-E_L);\\
\dot{m} = (1-m)\alpha_m(V) - m\beta_m(V);\\
\dot{n} = (1-n)\alpha_n(V) - n\beta_n(V);\\
\dot{h} = (1-h)\alpha_h(V) - h\beta_h(V);\\
V(0) = V_0, \quad m(0) = m_0, \quad , n(0) = n_0, \quad h(0) = h_0,
\end{cases} \tag{6}$$

where the parameters C_M, I_{ext}, G_{Na}, G_K, G_L, E_{Na}, E_K, E_L, m_0, n_0 and h_0 are assumed to be known.

We denote $\boldsymbol{\alpha} = (\alpha_m \circ V, \beta_m \circ V, \alpha_n \circ V, \beta_n \circ V, \alpha_h \circ V, \beta_h \circ V)$, where $(\alpha \circ V)(t) = \alpha(V(t))$. Hodgkin and Huxley obtained $\boldsymbol{\alpha}$ using experimental data from the squid neuron. However, other neurons may produce different parameters. In this context, our goal, from (6), is to obtain approximately $\boldsymbol{\alpha}$, given the measurement membrane potential.

The analysis of the Hodgkin-Huxley equation (6) is extremely difficult because of the nonlinearities and the large number of variables. The FitzHugh-Nagumo (F-N) model is a simplified version of the Hodgkin-Huxley model which models in a detailed manner activation and deactivation dynamics of a spiking neuron [21]. The FitzHugh-Nagumo equation have the form

$$\begin{cases} \dot{V} = I_{\text{ext}} + \boldsymbol{g} - \upsilon; \\ \dot{\upsilon} = bV - c\upsilon; \\ V(0) = V_0, \quad \upsilon(0) = \upsilon_0, \end{cases} \tag{7}$$

where $\boldsymbol{g} = g \circ V$, $b > 0$ and $c \geq 0$. For equation (7), V is the membrane potential, υ is the recovery variable, and I is the stimulus current. In this paper b and c are known, as in equation (6) the parameters I, V_0 and υ_0 also are known. Note that υ plays the role of all three variables m, n and h in (6). According to FitzHugh and Nagumo the function $\boldsymbol{g} = V(V-a)V$ for $a \in (0,1)$ [9]. In this paper, we consider $\boldsymbol{g}$ unknown. From (7), our goal is to estimate $\boldsymbol{g}$, given the measurement membrane potential.

After the Hodgkin-Huxley model, some other simplified models emerged, such as the cable equation, FitzHugh-Nagumo model, Morris-Lecar model, etc. Wilfrid Rall [17, 18] developed the use of cable theory in computational neuroscience, as well as passive and active compartmental modeling of the neuron. In [13], the authors determine conductances with nonuniform distribution in the cable equation with and without branches, using the non-linear Landweber iteration method to obtain the unknown parameters. Studies [20, 3, 1, 2], also address the identification of parameters in the cable equation. Works [8, 7, 15, 6, 14, 22] study the inverse problem in FitzHugh-Nagumo and Morris-Lecar models. In [19, 16] it obtains synaptic conductances, given the potential of the membrane, on the passive membrane equation. In [4, 5], authors estimate the constant parameters of an ion channel(Hodgkin and Huxley model), using a differential evolution algorithm to obtain the parameters.

2. Minimal Error Method

Consider $x = \boldsymbol{\alpha}$ (from equation (6)) or $x = \boldsymbol{g}$ (from equation (7)). In this paper, we use the minimal error method. We consider the problem of determining the physical quantity

$x \in \mathcal{H}$ from $V \in L^2[0,T]$, where $\mathcal{H}$ and $L^2[0,T]$ are Hilbert spaces with inner products $< \cdot, \cdot >$ and norms $|| \cdot ||$. We define the following operators

$$\langle V, W \rangle_{L^2[0,T]} = \int_0^T V(t)W(t)dt \; ; \quad \|V\|_{L^2[0,T]} = \sqrt{\langle V, V \rangle_{L^2[0,T]}} \qquad V, W \in L^2[0,T]. \tag{8}$$

In practical situations, we do not know the exact value. Instead, we have only approximate measured value $V^\delta \in L^2[0,T]$ satisfying

$$||V^\delta - V||_{L^2[0,T]} \leq \delta, \quad i = 1, \cdots, m \tag{9}$$

with noise level $\delta > 0$. The inverse problem is to estimate $x \in \mathcal{H}$, given V^δ, such that

$$F(x) = V, \tag{10}$$

where $F : \mathcal{H} \to L^2[0,T]$ is ill-posed operator. Note that V solves (6) or (7).

The minimal error iteration is defined by

$$x^{k+1,\delta} = x^{k,\delta} + w^{k,\delta} F'(x^{k,\delta})^* \left(V^\delta - F(x^{k,\delta})\right), \quad k \in \mathbb{N}. \tag{11}$$

where $F'(x^{k,\delta})$ is the Gateaux derivative of F in $x^{k,\delta}$ and $F'(x^{k,\delta})^*$ is its adjoint, and

$$w^{k,\delta} = \frac{\|V^\delta - F(x^{k,\delta})\|^2_{L^2[0,T]}}{\|F'(x^{k,\delta})^* \left(V^\delta - F(x^{k,\delta})\right)\|^2_{\mathcal{H}}}. \tag{12}$$

Note that the choice $y^{k,\delta} = 1$ corresponds to the Landweber iteration.

In the case of noisy data, the iteration procedure has to be combined with a stopping rule in order to act as a regularization method. We will employ the discrepancy principle, i.e., the iteration is stopped after $k_* = k(\delta, V^\delta)$ steps with

$$\|V^\delta - F(x^{k_*,\delta})\|_{L^2[0,T]} \leq \tau\delta < \|V^\delta - F(x^{k,\delta})\|_{L^2[0,T]}, \quad 0 \leq k < k_*, \tag{13}$$

where $\tau > 2$ is an appropriately chosen positive number.

It is possible to show that, under certain conditions (we assume that is the case), $x^{k_*,\delta}$ converges to a solution of $F(x) = V^\delta$ as $\delta \to 0$ (see [12], Theorem 3.22).

In the next example, we compare the methods of minimal error and Landweber.

Example 2.1. *Let $F : L^2(0, \pi/2] \to L^2(0, \pi/2]$ be an operator defined by the following equation $F(x) = V$, where it satisfies the following ODE $dV(t)/dt = x(t)$, with initial condition $V(0) = 1$.*

The goal of this example is to find approximately x given V. To compare results, we first calculate V given $x(t) = -\sin(t)$. Now, we consider x unknown.

We consider $\delta = 0$ in equation (11). Computing the adjoint of the Gateaux derivative from (11), we have

$$F'(x^k)^* \left(V - F(x^k)\right) = U^k, \tag{14}$$

where U^k solves the following ODE $dU^k(t)/dt = V(t) - V^k(t)$, with final condition $U(\pi/2) = 0$. Note that $V^k = F(x^k)$ and solves the following ODE $dV^k(t)/dt = x^k(t)$.

Thus, from (11) and (14), we obtain the following iteration

$$x^{k+1} = x^k + w^k U^k, \tag{15}$$

where $w^k = \|V - F(x^k)\|^2/\|U^k\|^2$ for the minimal error method, and for the Landweber method $w^k = 1$.

In this example, we compare the Landweber method and the minimal error method. Then, to obtain an approximation of x we use (15), given $x^1(t) = \cos(5t)$ and V.

Remark 1. *Note from (15) that x^{k+1} is* never corrected at final time $t = \pi/2$*, for every $k \in \mathbb{N}$, since $U^k(\pi/2) = 0$. To estimate x at time $t = \pi/2$, we perform the computations up to $\pi/2 + \Delta t$, for some given $\Delta t > 0$, and we consider, from iteration (15), only the values up to $\pi/2$.*

In figure 1, we plot some results to estimate x in $t \in [0, \pi/2]$. In this example, we consider 0.01972 as the minimum relative error, to get this value, the minimal error method required 316 iterations, and the Landweber iteration needed 11829 iterations. Thus, the minimal error method is considered more efficient of the two methods. In figure 2, we analyze the behavior of y^k from (15), for the two methods.

In this work, we use the minimal error iteration. Also, we consider Remark 1.

2.1. **Inverse Problem to obtain functions in the H-H model.** In this subsection, for the operator F defined in (10), the space $\mathcal{H} = \left(L^2[0,T]\right)^6$ and $x = \boldsymbol{\alpha}$. The present goal is to estimate $\boldsymbol{\alpha}$ from (6), given V^δ. From equation (11), we obtain

$$\boldsymbol{\alpha}^{k+1,\delta} = \boldsymbol{\alpha}^{k,\delta} + w^{k,\delta} F'(\boldsymbol{\alpha}^{k,\delta})^* \left(V^\delta - F(\boldsymbol{\alpha}^{k,\delta})\right), \tag{16}$$

where $\boldsymbol{\alpha}^{1,k}$ is know and $w^{k,\delta}$ is defined in (12). We denote $\boldsymbol{\alpha}^{k,\delta} = (\alpha_{m^{k,\delta}} \circ V^{k,\delta}, \beta_{m^{k,\delta}} \circ V^{k,\delta}, \alpha_{n^{k,\delta}} \circ V^{k,\delta}, \beta_{n^{k,\delta}} \circ V^{k,\delta}, \alpha_{h^{k,\delta}} \circ V^{k,\delta}, \beta_{h^{k,\delta}} \circ V^{k,\delta})$.

For $\boldsymbol{a} = (a_1, a_2, a_3, a_4, a_5, a_6)$ and $\boldsymbol{b} = (b_1, b_2, b_3, b_4, b_5, b_6) \in \mathcal{H}$, we define the following operators,

$$\langle \boldsymbol{a}, \boldsymbol{b} \rangle_{\mathcal{H}} = \sum_{i=1}^{6} \int_0^T a_i(t) b_i(t) dt \;; \quad \|\boldsymbol{\alpha}\|_{\mathcal{H}} = \sqrt{\langle \boldsymbol{a}, \boldsymbol{a} \rangle_{\mathcal{H}}}. \tag{17}$$

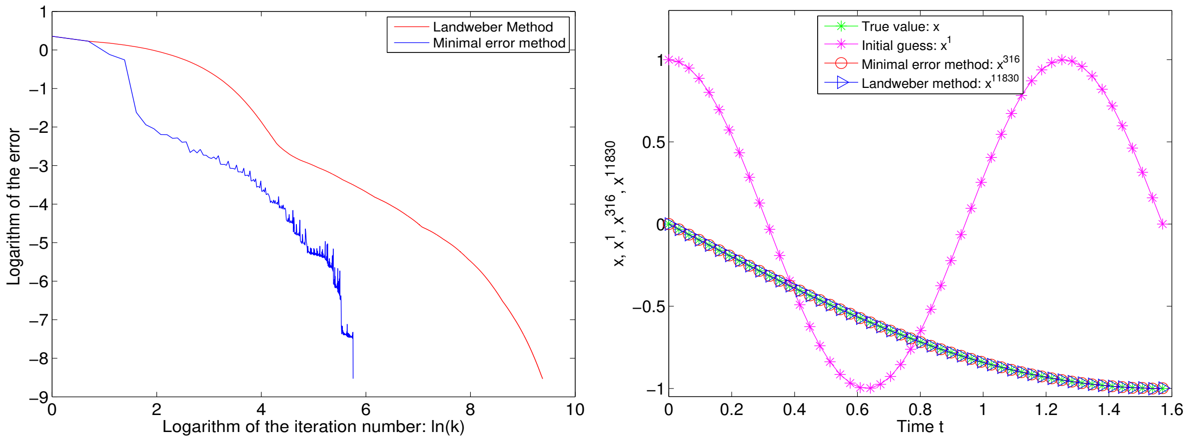

FIGURE 1. For Example 2.1. The plot on the left, the blue and red lines represent the relative errors using the minimal error and Landweber method. The figure on the right, the functions x, x^1, x^{316} and x^{11830} depending on the variable t. The green, pink, red and blue lines are the exact solution, the initial guess, the x approach using the minimal error method and the x approach using the Landweber method, respectively.

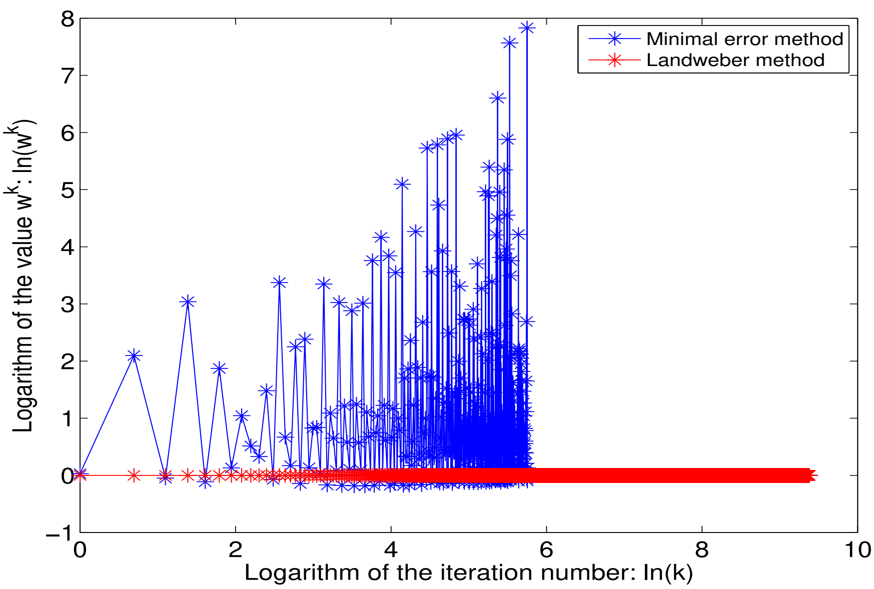

FIGURE 2. For Example 2.1. The blue line is the parameter w^k for the minimal error method. The line red is the parameter $w^k = 1$ for the Landweber iteration.

In the next theorem, from (16), we compute the adjoint of the Gateaux derivative $F'(\boldsymbol{\alpha}^{k,\delta})^*$.

Given V^δ, τ and an initial approximation $\boldsymbol{\alpha}^{1,\delta}$, we obtain a regularizing approximation $\boldsymbol{\alpha}^{k_*,\delta}$ for $\boldsymbol{\alpha}$, through iteration (18).

Theorem 2.1. *Consider the iteration* (16)*. It follows then that*

$$\boldsymbol{\alpha}^{k+1,\delta} = \boldsymbol{\alpha}^{k,\delta} + w^{k,\delta}\left(X^{k,\delta}_{\alpha_m}, X^{k,\delta}_{\beta_m}, X^{k,\delta}_{\alpha_n}, X^{k,\delta}_{\beta_n}, X^{k,\delta}_{\alpha_h}, X^{k,\delta}_{\beta_h}\right) \tag{18}$$

where $w^{k,\delta}$ *satisfies*

$$w^{k,\delta} = \frac{\|V^\delta - V^{k,\delta}\|^2_{L^2[0,T]}}{\left\|\left(X^{k,\delta}_{\alpha_m}, X^{k,\delta}_{\beta_m}, X^{k,\delta}_{\alpha_n}, X^{k,\delta}_{\beta_n}, X^{k,\delta}_{\alpha_h}, X^{k,\delta}_{\beta_h}\right)\right\|^2_{\mathcal{H}}},$$

and

$$X^{k,\delta}_{\alpha_m} = \left(1 - m^{k,\delta}\right) P^{k,\delta} \quad ; \quad X^{k,\delta}_{\beta_m} = -m^{k,\delta} P^{k,\delta}; \tag{19}$$

$$X^{k,\delta}_{\alpha_n} = \left(1 - n^{k,\delta}\right) Q^{k,\delta} \quad ; \quad X^{k,\delta}_{\beta_n} = -n^{k,\delta} Q^{k,\delta}; \tag{20}$$

$$X^{k,\delta}_{\alpha_h} = \left(1 - h^{k,\delta}\right) R^{k,\delta} \quad ; \quad X^{k,\delta}_{\beta_h} = -h^{k,\delta} R^{k,\delta}. \tag{21}$$

Given $\alpha_{\mathcal{X}}(V^{k,\delta})$ *and* $\beta_{\mathcal{X}}(V^{k,\delta})$ *for* $\mathcal{X} = m^{k,\delta}, n^{k,\delta}, h^{k,\delta}$*, the functions* $m^{k,\delta}$*,* $n^{k,\delta}$ *and* $h^{k,\delta}$ *solve*

$$\begin{cases} C_M \dot{V}^{k,\delta} = I_{ext} - G_{Na}\big(m^{k,\delta}\big)^3\big(h^{k,\delta}\big)(V^{k,\delta} - E_{Na}) - G_K\big(n^{k,\delta}\big)^4(V^{k,\delta} - E_K) \\ \qquad -G_L(V^{k,\delta} - E_L), \\ \dot{\mathcal{X}} = (1 - \mathcal{X})\alpha_{\mathcal{X}}(V^{k,\delta}) - \mathcal{X}\beta_{\mathcal{X}}(V^{k,\delta}) \quad \textit{for } \mathcal{X} = m^{k,\delta}, n^{k,\delta}, h^{k,\delta}, \\ V^{k,\delta}(0) = V_0, \quad m^{k,\delta}(0) = m_0, \quad n^{k,\delta}(0) = n_0, \quad h^{k,\delta}(0) = h_0. \end{cases} \tag{22}$$

Finally, the functions $P^{k,\delta}$*,* $Q^{k,\delta}$ *and* $R^{k,\delta}$ *solve, given* $m^{k,\delta}$*,* $n^{k,\delta}$*,* $h^{k,\delta}$ *and* $V^{k,\delta}$*,*

$$\begin{cases} C_M \dot{U}^{k,\delta} - \Big(G_{Na}\big(m^{k,\delta}\big)^3\big(h^{k,\delta}\big) + G_K\big(n^{k,\delta}\big)^4 + G_L\Big) U^{k,\delta} \\ -[(1 - m^{k,\delta})\alpha'_{m^{k,\delta}}(V^{k,\delta}) - m^{k,\delta}\beta'_{m^{k,\delta}}(V^{k,\delta})]P^{k,\delta} \\ -[(1 - n^{k,\delta})\alpha'_{n^{k,\delta}}(V^{k,\delta}) - n^{k,\delta}\beta'_{n^{k,\delta}}(V^{k,\delta})]Q^{k,\delta} \\ -[(1 - h^{k,\delta})\alpha'_{h^{k,\delta}}(V^{k,\delta}) - h^{k,\delta}\beta'_{h^{k,\delta}}(V^{k,\delta})]R^{k,\delta} = V^\delta - V^{k,\delta}, \\ \dot{P}^{k,\delta} - [\alpha_{m^{k,\delta}}(V^{k,\delta}) + \beta_{m^{k,\delta}}(V^{k,\delta})]P^{k,\delta} = -3G_{Na}\big(m^{k,\delta}\big)^2\big(h^{k,\delta}\big)(V^{k,\delta} - E_{Na})U^{k,\delta}, \\ \dot{Q}^{k,\delta} - [\alpha_{n^{k,\delta}}(V^{k,\delta}) + \beta_{n^{k,\delta}}(V^{k,\delta})]Q^{k,\delta} = -4G_K\big(n^{k,\delta}\big)^3(V^{k,\delta} - E_K)U^{k,\delta}, \\ \dot{R}^{k,\delta} - [\alpha_{h^{k,\delta}}(V^{k,\delta}) + \beta_{h^{k,\delta}}(V^{k,\delta})]R^{k,\delta} = -G_{Na}\big(m^{k,\delta}\big)^3(V^{k,\delta} - E_{Na})U^{k,\delta}, \\ U^{k,\delta}(T) = 0, \quad P^{k,\delta}(T) = 0, \quad Q^{k,\delta}(T) = 0, \quad R^{k,\delta}(T) = 0. \end{cases} \tag{23}$$

As previously mentioned, we assume that the constants C_M, I_{ext}, m_0, n_0, h_0, G_{Na}, G_K, G_L, E_{Na} ,E_K and E_L are known data. Note that $\alpha'_m(V)$ is the derivative of α_m with respect to voltage V.

Proof. See Appendix A. □

We next describe the computational scheme.

Data: V^δ, δ and τ

Result: Compute an approximation for $\boldsymbol{\alpha}$ using Iteration Scheme (18)

Choose $\boldsymbol{\alpha}^{1,\delta}$ as an initial approximation for $\boldsymbol{\alpha}$;

Compute $m^{1,\delta}$, $n^{1,\delta}$, $h^{1,\delta}$ and $V^{1,\delta}$ from (22), replacing $\boldsymbol{\alpha}^{k,\delta}$ by $\boldsymbol{\alpha}^{1,\delta}$;

k=1;

while $\tau\delta \leq \|V^\delta - V^{k,\delta}\|_{L^2[0,T]}$ **do**

  Compute $P^{k,\delta}$, $Q^{k,\delta}$ and $R^{k,\delta}$ from (23);

  Compute $\boldsymbol{\alpha}^{k+1,\delta}$ using (18);

  Compute $m^{k+1,\delta}$, $n^{k+1,\delta}$, $h^{k+1,\delta}$ and $V^{k+1,\delta}$ from (22), replacing $\boldsymbol{\alpha}^{k,\delta}$ by $\boldsymbol{\alpha}^{k+1,\delta}$;

  $k \leftarrow k+1$;

end

Algorithm 1: Minimal error iteration to obtain functions in the H-H model

2.2. **Inverse Problem to obtain one function in the F-N model.** In this subsection, for the operator F is defined in (10), the space $\mathcal{H} = L^2[0,T]$ and $x = \boldsymbol{g}$. The present goal is to estimate $\boldsymbol{g}$ from (7), given V^δ. From equation (11), we obtain

$$\boldsymbol{g}^{k+1,\delta} = \boldsymbol{g}^{k,\delta} + w^{k,\delta} F'(\boldsymbol{g}^{k,\delta})^* \left(V^\delta - F(\boldsymbol{g}^{k,\delta})\right), \tag{24}$$

where $\boldsymbol{g}^{1,k}$ is know and $w^{k,\delta}$ is defined in (12). Note that $\boldsymbol{g}^{k,\delta} = g^{k,\delta}(V^{k,\delta})$.

For $\boldsymbol{a}$, $\boldsymbol{b} \in L^2[0,T]$, we define

$$\langle \boldsymbol{a}, \boldsymbol{b}\rangle_{L^2[0,T]} = \int_0^T \boldsymbol{a}(t)\boldsymbol{b}(t)dt\ ; \quad \|\boldsymbol{a}\|_{L^2[0,T]} = \sqrt{\langle \boldsymbol{a}, \boldsymbol{a}\rangle_{L^2[0,T]}}. \tag{25}$$

In the next theorem, from (24), we compute the adjoint of the Gateaux derivative $F'(\boldsymbol{g}^{k,\delta})^*$.

Given V^δ, τ and an initial approximation $\boldsymbol{g}^{1,\delta}$, we obtain a regularizing approximation $\boldsymbol{g}^{k_*,\delta}$ for $\boldsymbol{g}$, through iteration (26).

Theorem 2.2. *Consider the iteration* (24)*. It follows then that*

$$\boldsymbol{g}^{k+1,\delta} = \boldsymbol{g}^{k,\delta} - w^{k,\delta} U^{k,\delta}, \tag{26}$$

where $w^{k,\delta} = \|V^\delta - V^{k,\delta}\|^2_{L^2[0,T]} / \|U^{k,\delta}\|^2_{L^2[0,T]}$.

Given $g^{k,\delta}(V^{k,\delta})$, the functions $V^{k,\delta}$ and $\upsilon^{k,\delta}$ solve

$$\begin{cases} \dot{V}^{k,\delta} = I + g^{k,\delta}(V^{k,\delta}) - \upsilon^{k,\delta}; \\ \dot{\upsilon}^{k,\delta} = bV^{k,\delta} - c\upsilon^{k,\delta}; \\ V(0) = V_0, \quad \upsilon(0) = \upsilon_0. \end{cases} \tag{27}$$

Finally, $U^{k,\delta}$ solve, given $V^{k,\delta}$ and $g^{k,\delta}(V^{k,\delta})$,

$$\begin{cases} \dot{U}^{k,\delta} + g^{k,\delta\prime}(V^{k,\delta})U^{k,\delta} - bP^{k,\delta} = V^{\delta} - V^{k,\delta}, \\ \dot{P}^{k,\delta} - cP^{k,\delta} = -U^{k,\delta}, \\ U^{k,\delta}(T) = 0; \quad P^{k,\delta}(T) = 0, \end{cases} \tag{28}$$

where $g^{k,\delta\prime}(V^{k,\delta})$ is the derivative of $g^{k,\delta}$ with respect to $V^{k,\delta.}$.

As previously mentioned, we assume that the constants b, c, V_0, υ_0 and I are known data.

Proof. See Appendix B. □

We next describe the computational scheme.

Data: V^{δ}, δ and τ
Result: Compute an approximation for $\boldsymbol{g}$ using Iteration Scheme (26)
Choose $\boldsymbol{g}^{1,\delta}$ as an initial approximation for $\boldsymbol{g}$;
Compute $r^{1,\delta}$ and $V^{1,\delta}$ from (27), replacing $\boldsymbol{g}^{k,\delta}$ by $\boldsymbol{g}^{1,\delta}$;
k=1;
while $\tau\delta \leq \|V^{\delta} - V^{k,\delta}\|_{L^2[0,T]}$ **do**
    Compute $U^{k,\delta}$ from (28);
    Compute $\boldsymbol{g}^{k+1,\delta}$ using (26);
    Compute $r^{k+1,\delta}$ and $V^{k+1,\delta}$ from (27), replacing $\boldsymbol{g}^{k,\delta}$ by $\boldsymbol{g}^{k+1,\delta}$;
    $k \leftarrow k+1$;
end

Algorithm 2: Minimal error iteration to obtain one function in the F-N model

3. Numerical simulation

In Subsection 2.1, we consider and obtain analytical results for six unknown functions. In computational experiments, we estimate only one function $\boldsymbol{\alpha} = \alpha_n(V)$ (from equation (6)).

In this subsection, we consider two examples. The first one is to estimate $x = \boldsymbol{\alpha}$ from (6), given V^{δ}. For the second example, the goal is to estimate $x = \boldsymbol{g}$ from (7), given V^{δ}.

To design our numerical experiments, we first choose x ($x = \boldsymbol{\alpha}$ or $x = \boldsymbol{g}$) and compute V from (6) or (7), obtaining then V. Of course, in practice, the values of V are given by some experimental measurements, and thus subject to experimental/measurement errors. In our examples, for a given δ, the noisy V^δ is obtained by

$$V^\delta(t) = V(t) + V(t)\text{rand}_\varepsilon(t), \quad \text{for all } t \in [0, T] \tag{29}$$

where $\text{rand}_\varepsilon(t)$ is a uniformly distributed random variable in the interval $[-\varepsilon, \varepsilon]$, and $\varepsilon = \delta/\|V\|_{L^2[0,T]}$. Now, we consider V and x unknown.

Next, given the initial guess $x^{1,\delta}$, V^δ and δ, we start to recover x using Algorithm 1 (for $x = \boldsymbol{\alpha}$) or Algorithm 2 (for $x = \boldsymbol{g}$).

The absolute error of V^δ and its approximation $V^{k,\delta}$ is called the residual. We define this term by the following equation,

$$\text{Res}_k = \|V^\delta - V^{k,\delta}\|_{L^2[0,T]} = \sqrt{\int_0^T (V^\delta(t) - V^{k,\delta}(t))^2\, dt}, \quad k = 1, 2, \cdots, k_*. \tag{30}$$

In practice, after discretizing the equations and the unknown functions, only nodal values are know. Consider the space-time discretization $t_n = (n-1)T/(N-1)$ for $n = 1, 2, \cdots, N$. Thus, the relative error introduced above relates to the the mean absolute percentage error

$$Error_k = \frac{1}{N-1}\sum_{n=1}^{N}\left|\frac{x(t_n) - x^{k,\delta}(t_n)}{x(t_n)}\right| \times 100\%, \quad k = 1, 2 \cdots, k_*. \tag{31}$$

For the discrete case, we define the residual (30) as

$$Res_k = \sqrt{\frac{T}{N-1}\sum_{n=1}^{N}(V^\delta(t_n) - V^{k,\delta}(t_n))^2 dt}, \quad k = 1, 2, \cdots, k_*. \tag{32}$$

In this section, we will present two numerical simulations. In Example 3.1 we estimate one function in the H-H model, and in Example 3.2 also we find approximately one function in F-N model.

Our simulation was computed with Matlab R2012b on a Dell PC, running on an Intel(R) Core(TM) i7-4790 CPU @ 3.60GHz with 32 GB of RAM.

Example 3.1. *This example is a particular case from* (6)*, where the fixed parameters are:* $T = 4$ $[ms]$, $C = 1$ $[\mu F/cm^2]$, $I_{ext} = 5$ $[\mu A/cm^2]$, $E_{Na} = 115$ $[mV]$, $E_K = -12$ $[mV]$, $E_L = 10.6$ $[mV]$, $G_{Na} = 120$ $[mS/cm^2]$, $G_K = 36$ $[mS/cm^2]$, $G_L = 0.3$ $[mS/cm^2]$ *and* $N = 100$. *The initial conditions are:* $V(0) = -20$ $[mV]$, $m(0) = 0.1$, $n(0) = 0.3$ *and* $h(0) = 0.5$. *Given* V^δ*, the goal of this example is to estimate*

$$\alpha_n(V) = \frac{(10 - V)/100}{\exp((10 - V)/10) - 1}.$$

In this test, we consider the initial guess $\alpha_n^{1,\delta}(V) = 0$ *and* $\tau = 2.01$*. Table 1 presents the results for various levels of noise. In Figures* (3)*,* (4)*,* (5) *and* (6)*, we plot results for* $\epsilon = 0.001\%$ *level of noise (Table 2, line 7).*

ε	k_*	$Error^x_{k_*}$	Res_{k_*}
100%	2	55 %	11.5×10^0
10%	4	41 %	1.4×10^0
1%	17	33 %	2.9×10^{-1}
0.1%	107	13 %	2.9×10^{-2}
0.01%	497	5.2 %	2.9×10^{-3}
0.001%	2532	1.8 %	2.9×10^{-4}
0.0001%	30916	0.4 %	2.9×10^{-5}

TABLE 1. For Example 3.1. Numerical results for various values of ε, as in (29). The second column contains the number of iterations according to (13). The third column is the mean absolute percentage error of $x = \boldsymbol{\alpha}$ according to (31). The last column is the residue, see (32).

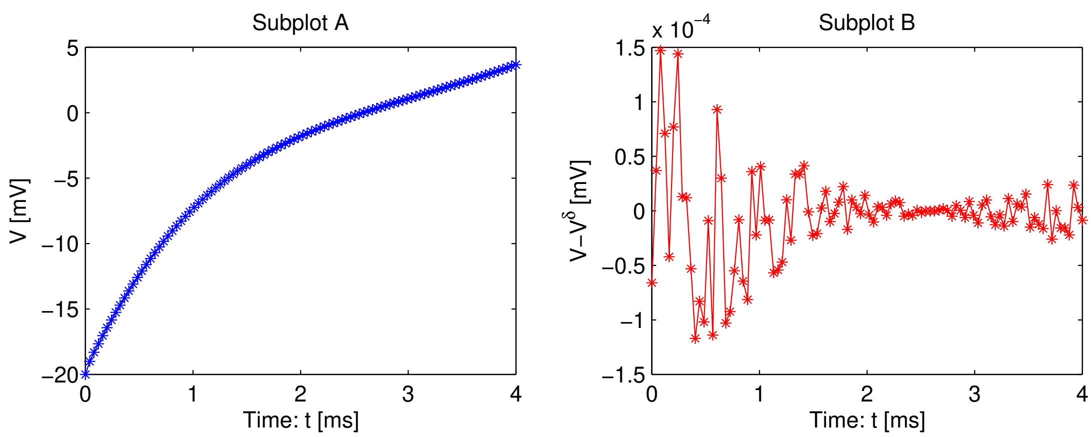

FIGURE 3. For Example 3.1. In Subplot A we present the membrane potential (V), and in B displays the difference between V and its perturbation V^δ.

Example 3.2. *This example is a particular case from* (7)*, where the fixed parameters are:* $T = 10$*,* $N = 100$*,* $I_{ext} = 0.01$*,* $b = 0.01$ *and* $c = 0.02$*. The initial conditions are:* $V(0) = -0.5$ *and* $v(0) = 0.02$*. Given* V^δ*, the goal of this example is to find* $\boldsymbol{g} = V(a - V)(V - 1)$ *for* $a = 0.01$*.*

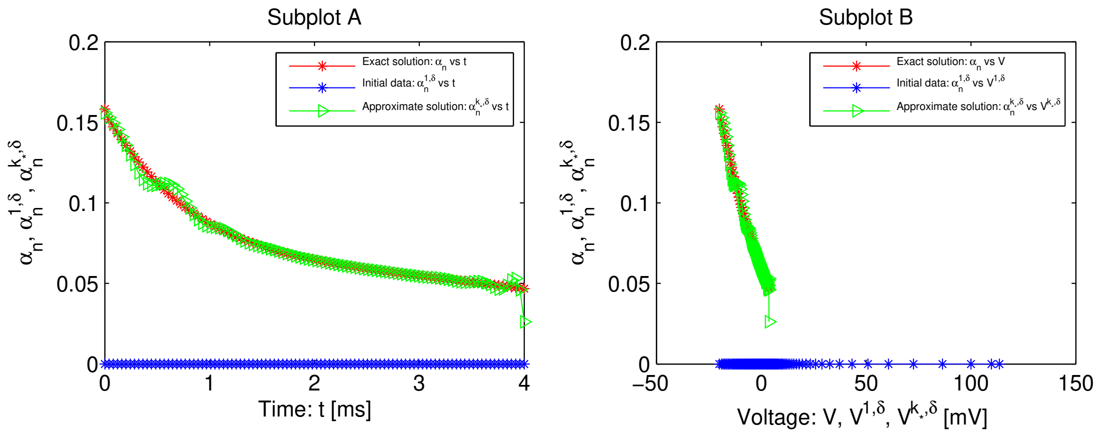

FIGURE 4. Figures for Example 3.1. For the Subplots A and B, the red lines are the exact solution, the blue lines are the initial guesses and the green lines are the approximation for $\varepsilon = 0.001\%$. In Subplot A, we present the parameters $\boldsymbol{\alpha}_n$, $\boldsymbol{\alpha}_n^{1,\delta}$ and $\boldsymbol{\alpha}_n^{k_*,\delta}$ as a function of time. In Subplot B, we show the parameters $\boldsymbol{\alpha}_n$, $\boldsymbol{\alpha}_n^{1,\delta}$ and $\boldsymbol{\alpha}_n^{k_*,\delta}$ as a function of V, $V^{1,\delta}$ and $V^{k_*,\delta}$, respectively.

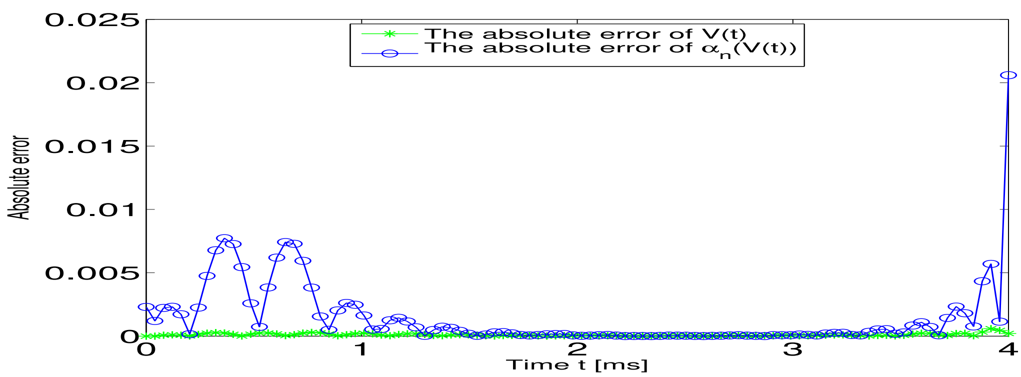

FIGURE 5. For Example 3.1. The green line is the absolute error of V ans its approximation $V^{k_*,\delta}$, for $\varepsilon = 0.001\%$. The blue line is absolute error of the true value $\alpha_n(V)$ and its approximation, for $\varepsilon = 0.001\%$.

In this test, we consider the initial guess $\boldsymbol{g}^{1,\delta} = 0$ *and* $\tau = 2.01$. *Table 2 presents the results for various levels of noise. In Figures* (7), (8), (9) *and* (10), *we plot results for* $\epsilon = 1\%$ *of noise (Table 2, line 5).*

4. CONCLUSIONS

In this work, we estimate parameters in Hodgkin-Huxley and FitzHugh-Nagumo models from membrane potential measurement. To obtain approximately the unknown parameters,

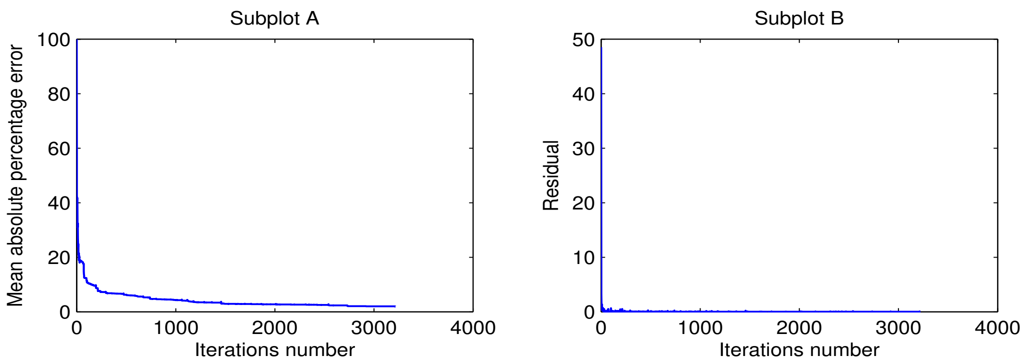

FIGURE 6. Convergence results for Example 3.1. The Subplot A, displays the mean absolute percentage error between $\boldsymbol{\alpha}$ and $\boldsymbol{\alpha}^k$ as a function of the iteration k. The Subplot B, displays the residual, i.e., the difference between V and V^k again as a function of k.

ε	k_*	$Error^x_{k_*}$	Res_{k_*}
125%	1	100 %	1.1437
25%	4	75 %	0.1595
5%	12	18 %	0.0387
1%	33	6.3 %	0.0082
0.2%	84	2.4 %	0.0018
0.04%	151	0.9 %	0.0003

TABLE 2. Numerical results for Example 3.2. See Table 1 for a description of the contents.

we apply the minimal error method. This iteration is more efficient than the Landweber method (see Example 2.1).

In the whole iterative process, the iteration of Landweber considers $y_k = 1$, and this makes the method does not converge when $y_k << 1$. In this work, in most numerical tests $y_k << 1$, then the Landweber iteration diverges, as particular cases are Examples 3.1 and 3.2. In contrast, the minimal error method considers that this term $(0 < y_k)$ vary in each iteration; this makes the technique converge for the solution when the noise level goes to zero. The minimal error method applied in this article is more efficient than the Landweber method by the same observation mentioned above.

Indeed, the methods (Landweber and minimal error) has limitations; in this work, they do not computationally estimate more than one function. For the H-H model, we obtain analytical results for six unknown functions, but in the numerical tests, we consider only

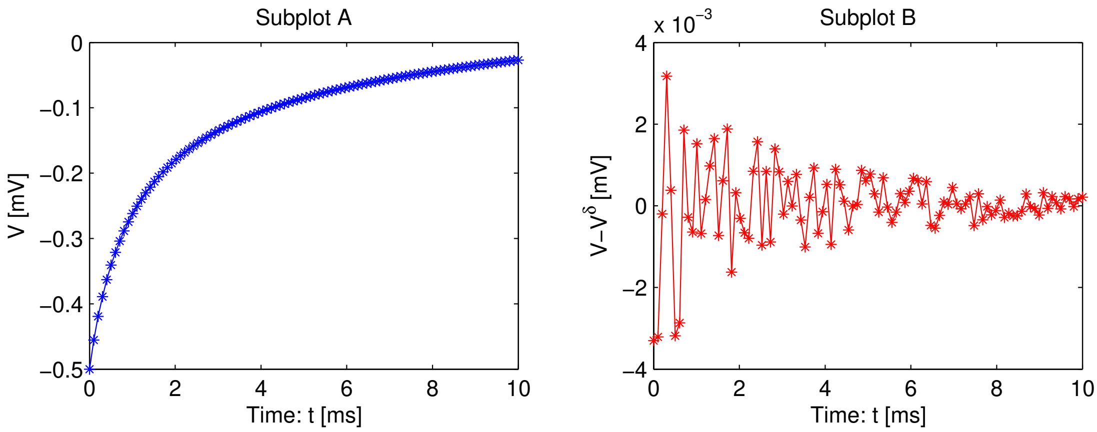

FIGURE 7. For Example 3.2. In Subplot A, we present the membrane potential (V), and in B displays the difference between V and its perturbation V^{δ}.

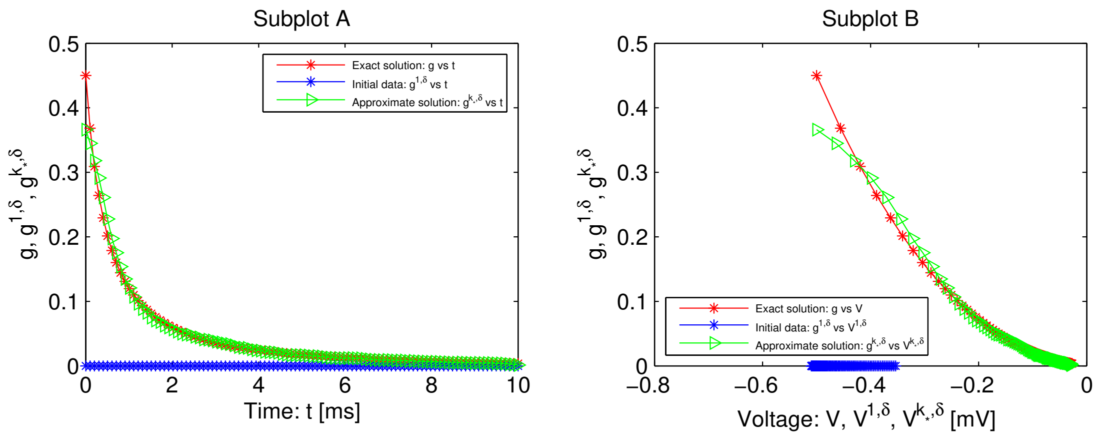

FIGURE 8. Figures for Example 3.2. For the Subplots A and B, the red lines are the exact solution, the blue lines are the initial guesses and the green lines are the approximation for $\varepsilon = 1\%$. In Subplot A, we present the parameters $\boldsymbol{g}$, $\boldsymbol{g}^{1,\delta}$ and $\boldsymbol{g}^{k_*,\delta}$ as a function of time. In Subplot B, we show the parameters $\boldsymbol{g}$, $\boldsymbol{g}^{1,\delta}$ and $\boldsymbol{g}^{k_*,\delta}$ as a function of V, $V^{1,\delta}$ and $V^{k_*,\delta}$, respectively.

one unknown function. The analytical results, obtained in this work, are significant contributions for future works where other iterative methods of regularization are applied. One of these methods is the Landweber-Kaczmarz iteration, and possibly this approach obtains approximately more than one unknown function. However, our method numerically estimates problems where it has one unknown function as in the case of the F-N model.

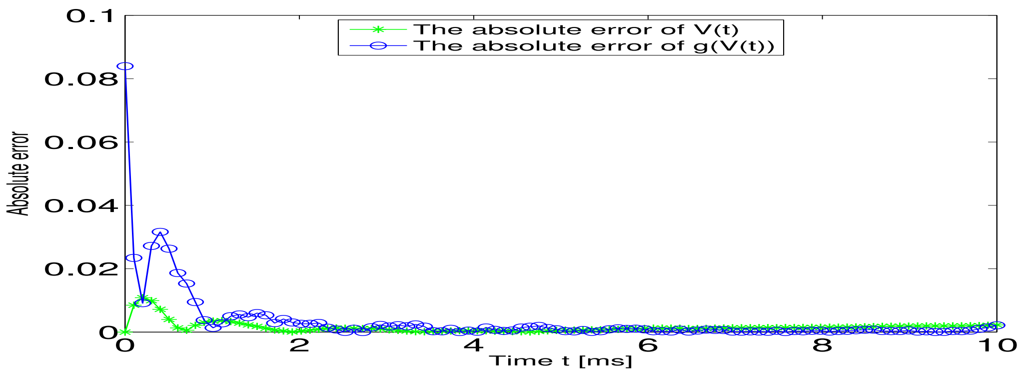

FIGURE 9. For Example 3.2. The green line is the absolute error of V ans its approximation $V^{k_*,\delta}$, for $\varepsilon = 0.001\%$. The blue line is absolute error of the true value $g(V)$ and its approximation, for $\varepsilon = 0.001\%$.

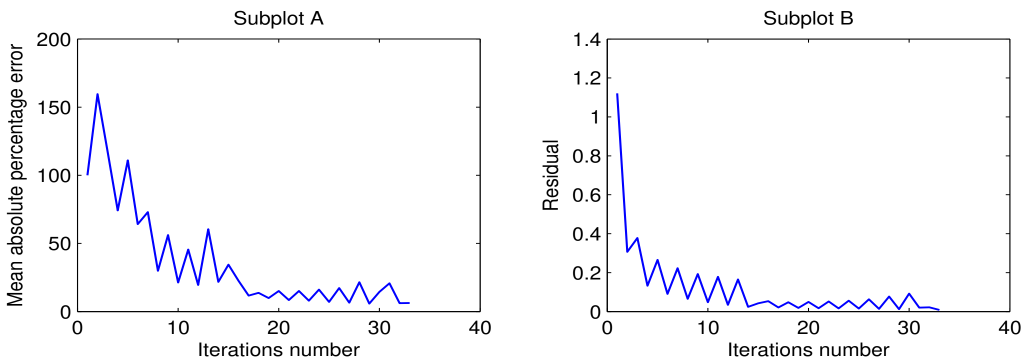

FIGURE 10. Convergence results for Example 3.2. The Subplot A, displays the mean absolute percentage error between $\boldsymbol{g}$ and $\boldsymbol{g}^k$ as a function of the iteration k. The Subplot B, displays the residual, i.e., the difference between V and V^k again as a function of k

Appendix A. Proof of Theorem 2.1

This Appendix, we show Theorem 2.1.

Proof. Consider the operator F defined in (10), $\mathcal{H} = (L^2[0,T])^6$ and $x = \boldsymbol{\alpha}$. Evaluating $\boldsymbol{\alpha}^{k,\delta}$ in F, we have $F(\boldsymbol{\alpha}^{k,\delta}) = V^{k,\delta}$, where $V^{k,\delta}$, $m^{k,\delta}$, $n^{k,\delta}$ and $h^{k,\delta}$ solve the ODE (22).

Let the vector $\boldsymbol{\theta} = (\theta_{\alpha_m}, \theta_{\beta_m}, \theta_{\alpha_n}, \theta_{\beta_n}, \theta_{\alpha_h}, \theta_{\beta_h}) \in \left(L^2[0,T]\right)^6$ and $\lambda \in \mathbb{R}$, then evaluating $\boldsymbol{\alpha} + \lambda\boldsymbol{\theta}$ in the operator F, we have $F(\boldsymbol{\alpha} + \lambda\boldsymbol{\theta}) = V_\lambda^{k,\delta}$, where $V_\lambda^{k,\delta}$ solves

$$\begin{cases} C\dot{V}_\lambda^{k,\delta} = I_{ext} - G_{Na}\left(m_\lambda^{k,\delta}\right)^3\left(h_\lambda^{k,\delta}\right)(V_\lambda^{k,\delta} - E_{Na}) \\ \qquad\qquad -G_K\left(n_\lambda^{k,\delta}\right)^4(V_\lambda^{k,\delta} - E_K) - G_L(V_\lambda^{k,\delta} - E_L), \\ \dot{m}_\lambda^{k,\delta} = (1 - m_\lambda^{k,\delta})\left[\alpha_{m_\lambda^{k,\delta}}(V_\lambda^{k,\delta}) + \lambda\theta_{\alpha_m}\right] - \left[m_\lambda^{k,\delta}\beta_{m_\lambda^{k,\delta}}(V_\lambda^{k,\delta}) + \lambda\theta_{\beta_m}\right], \\ \dot{n}_\lambda^{k,\delta} = (1 - n_\lambda^{k,\delta})\left[\alpha_{n_\lambda^{k,\delta}}(V_\lambda^{k,\delta}) + \lambda\theta_{\alpha_n}\right] - \left[n_\lambda^{k,\delta}\beta_{n_\lambda^{k,\delta}}(V_\lambda^{k,\delta}) + \lambda\theta_{\beta_n}\right], \\ \dot{h}_\lambda^{k,\delta} = (1 - h_\lambda^{k,\delta})\left[\alpha_{h_\lambda^{k,\delta}}(V_\lambda^{k,\delta}) + \lambda\theta_{\alpha_h}\right] - \left[h_\lambda^{k,\delta}\beta_{h_\lambda^{k,\delta}}(V_\lambda^{k,\delta}) + \lambda\theta_{\beta_h}\right], \\ V_\lambda^{k,\delta}(0) = V_0; \quad m_\lambda^{k,\delta}(0) = m_0; \quad n_\lambda^{k,\delta}(0) = n_0; \quad h_\lambda^{k,\delta}(0) = h_0. \end{cases} \tag{33}$$

The Gateaux derivative of F at $\boldsymbol{\alpha}^{k,\delta}$ in the direction $\boldsymbol{\theta}$ is given by

$$F'(\boldsymbol{\alpha}^{k,\delta})(\boldsymbol{\theta}) = \lim_{\lambda\to 0}\frac{F(\boldsymbol{\alpha}^{k,\delta} + \lambda\boldsymbol{\theta}) - F(\boldsymbol{\alpha}^{k,\delta})}{\lambda} = W^{k,\delta}. \tag{34}$$

Also, we denote the following limits

$$M^{k,\delta} = \lim_{\lambda\to 0}\frac{m_\lambda^{k,\delta} - m^{k,\delta}}{\lambda}, \quad N^{k,\delta} = \lim_{\lambda\to 0}\frac{n_\lambda^{k,\delta} - n^{k,\delta}}{\lambda}, \quad H^{k,\delta} = \lim_{\lambda\to 0}\frac{h_\lambda^{k,\delta} - h^{k,\delta}}{\lambda}, \tag{35}$$

where $M^{k,\delta}$, $N^{k,\delta}$ and $H^{k,\delta}$ are the Gateaux derivatives of $m^{k,\delta}$, $n^{k,\delta}$ and $h^{k,\delta}$, respectively.

Considering the difference between the ODEs (33) and (22), dividing by λ and taking the limit $\lambda \to 0$, we have the following ODE

$$\begin{cases} C\dot{W}^{k,\delta} + \left(G_{Na}\left(m^{k,\delta}\right)^3\left(h^{k,\delta}\right) + G_K\left(n^{k,\delta}\right)^4 + G_L\right)W^{k,\delta} = \\ \qquad -3G_{Na}\left(m^{k,\delta}\right)^2 M^{k,\delta}h^{k,\delta}(V^{k,\delta} - E_{Na}) \\ \qquad -G_{Na}\left(m^{k,\delta}\right)^3 H^{k,\delta}(V^{k,\delta} - E_{Na}) \\ \qquad -4G_K\left(n^{k,\delta}\right)^3 N^{k,\delta}(V^{k,\delta} - E_K), \\ \dot{M}^{k,\delta} + [\alpha_{m^{k,\delta}}(V^{k,\delta}) + \beta_{m^{k,\delta}}(V^{k,\delta})]M^{k,\delta} = \\ \left[(1 - m^{k,\delta})\alpha'_{m^{k,\delta}}(V^{k,\delta}) - m^{k,\delta}\beta'_{m^{k,\delta}}(V^{k,\delta})\right]W^{k,\delta} + (1 - m^{k,\delta})\theta_{\alpha_m} - m^{k,\delta}\theta_{\beta_m}, \\ \dot{N}^{k,\delta} + [\alpha_{n^{k,\delta}}(V^{k,\delta}) + \beta_{n^{k,\delta}}(V^{k,\delta})]N^{k,\delta} = \\ \left[(1 - n^{k,\delta})\alpha'_{n^{k,\delta}}(V^{k,\delta}) - n^{k,\delta}\beta'_{n^{k,\delta}}(V^{k,\delta})\right]W^{k,\delta} + (1 - n^{k,\delta})\theta_{\alpha_n} - n^{k,\delta}\theta_{\beta_n}, \\ \dot{H}^{k,\delta} + [\alpha_{h^{k,\delta}}(V^{k,\delta}) + \beta_{h^{k,\delta}}(V^{k,\delta})]H^{k,\delta} = \\ \left[(1 - h^{k,\delta})\alpha'_{h^{k,\delta}}(V^{k,\delta}) - h^{k,\delta}\beta'_{h^{k,\delta}}(V^{k,\delta})\right]W^{k,\delta} + (1 - h^{k,\delta})\theta_{\alpha_h} - h^{k,\delta}\theta_{\beta_h}, \\ W^{k,\delta}(0) = 0; \quad M^{k,\delta}(0) = 0; \quad N^{k,\delta}(0) = 0; \quad H^{k,\delta}(0) = 0. \end{cases} \tag{36}$$

This last equation is yet another system of coupled nonlinear differential equations, depending on the parameter $\boldsymbol{\theta}$. Note that the variable $\boldsymbol{\theta}$ represent any point in space $(L^2[0,T])^6$.

From Landweber iteration (16) and $\boldsymbol{\theta} \in (L^2[0,T])^6$ arbitrary, we have

$$\begin{aligned} \langle \boldsymbol{\alpha}^{k+1,\delta} - \boldsymbol{\alpha}^{k,\delta}, \boldsymbol{\theta} \rangle_{(L^2[0,T])^6} &= w^{k,\delta} \langle F'(\boldsymbol{\alpha}^{k,\delta})^* (V^\delta - F(\boldsymbol{\alpha}^{k,\delta})), \boldsymbol{\theta} \rangle_{(L^2[0,T])^6}, \\ &= w^{k,\delta} \langle F'(\boldsymbol{\alpha}^{k,\delta})^* (V^\delta - V^{k,\delta}), \boldsymbol{\theta} \rangle_{(L^2[0,T])^6}. \end{aligned}$$

By the definition of adjunct operator

$$\langle \boldsymbol{\alpha}^{k+1,\delta} - \boldsymbol{\alpha}^{k,\delta}, \boldsymbol{\theta} \rangle_{(L^2[0,T])^6} = w^{k,\delta} \langle V^\delta - V^{k,\delta}, F'(\boldsymbol{\alpha}^{k,\delta}).(\boldsymbol{\theta}) \rangle_{L^2[0,T]}.$$

From (34) and the previous equation,

$$\langle \boldsymbol{\alpha}^{k+1,\delta} - \boldsymbol{\alpha}^{k,\delta}, \boldsymbol{\theta} \rangle_{(L^2[0,T])^6} = w^{k,\delta} \langle V^\delta - V^{k,\delta}, W^{k,\delta} \rangle_{L^2[0,T]}.$$

We denote the last equality by Φ, then

$$\Phi = \frac{\langle \boldsymbol{\alpha}^{k+1,\delta} - \boldsymbol{\alpha}^{k,\delta}, \boldsymbol{\theta} \rangle_{(L^2[0,T])^6}}{w^{k,\delta}} = \langle V^\delta - V^{k,\delta}, W^{k,\delta} \rangle_{L^2[0,T]}. \tag{37}$$

By the definition of inner product in $L^2[0,T]$

$$\Phi = \int_0^T (V^\delta - V^{k,\delta}) W^{k,\delta} \, dt.$$

From the previous equation and the first equality from ODE (23), we obtain the following expression

$$\begin{aligned} \Phi &= \int_0^T \left(C_M \dot{U}^{k,\delta} W^{k,\delta} - \left(G_{Na} (m^{k,\delta})^3 \, (h^{k,\delta}) + G_K (n^{k,\delta})^4 + G_L \right) U^{k,\delta} W^{k,\delta} \right) \, dt \\ &- \int_0^T \left[(1 - m^{k,\delta}) \alpha'_{m^{k,\delta}}(V^{k,\delta}) - m^{k,\delta} \beta'_{m^{k,\delta}}(V^{k,\delta}) \right] P^{k,\delta} W^{k,\delta} \, dt \\ &- \int_0^T \left[(1 - n^{k,\delta}) \alpha'_{n^{k,\delta}}(V^{k,\delta}) - n^{k,\delta} \beta'_{n^{k,\delta}}(V^{k,\delta}) \right] Q^{k,\delta} W^{k,\delta} \, dt \\ &- \int_0^T \left[(1 - h^{k,\delta}) \alpha'_{h^{k,\delta}}(V^{k,\delta}) - h^{k,\delta} \beta'_{h^{k,\delta}}(V^{k,\delta}) \right] R^{k,\delta} W^{k,\delta} \, dt. \end{aligned} \tag{38}$$

Integrating by parts the first term from equation (38), and initial (see (36), $W^{k,\delta}(0) = 0$) and final (see (23), $U^{k,\delta}(T) = 0$) conditions, we obtain

$$\int_0^T C_M \dot{U}^{k,\delta} W^{k,\delta} dt = - \int_0^T C_M U^{k,\delta} \dot{W}^{k,\delta} dt. \tag{39}$$

Replacing equation (39) in (38), we have the following equality

$$\begin{aligned}\Phi &= -\int_0^T \Big(C\dot{W}^{k,\delta} + \Big(G_{Na}\big(m^{k,\delta}\big)^3\big(h^{k,\delta}\big) + G_K\big(n^{k,\delta}\big)^4 + G_L\Big)W^{k,\delta}\Big)U^{k,\delta}\,dt\\ &\quad -\int_0^T \big[(1-m^{k,\delta})\alpha'_{m^{k,\delta}}(V^{k,\delta}) - m^{k,\delta}\beta'_{m^{k,\delta}}(V^{k,\delta})\big]P^{k,\delta}W^{k,\delta}\,dt\\ &\quad -\int_0^T \big[(1-n^{k,\delta})\alpha'_{n^{k,\delta}}(V^{k,\delta}) - n^{k,\delta}\beta'_{n^{k,\delta}}(V^{k,\delta})\big]Q^{k,\delta}W^{k,\delta}\,dt\\ &\quad -\int_0^T \big[(1-h^{k,\delta})\alpha'_{h^{k,\delta}}(V^{k,\delta}) - h^{k,\delta}\beta'_{h^{k,\delta}}(V^{k,\delta})\big]R^{k,\delta}W^{k,\delta}\,dt.\end{aligned}$$

Replacing the first equality from ODE (36) in the first integral from the previous equation, we obtain

$$\begin{aligned}\Phi &= \int_0^T 3G_{Na}\big(m^{k,\delta}\big)^2M^{k,\delta}\big(h^{k,\delta}\big)(V^{k,\delta}-E_{Na})U^{k,\delta}\,dt\\ &\quad +\int_0^T G_{Na}\big(m^{k,\delta}\big)^3H^{k,\delta}(V^{k,\delta}-E_{Na})U^{k,\delta}\,dt\\ &\quad +\int_0^T 4G_K\big(n^{k,\delta}\big)^3N^{k,\delta}(V^{k,\delta}-E_K)U^{k,\delta}\,dt\\ &\quad -\int_0^T \big[(1-m^{k,\delta})\alpha'_{m^{k,\delta}}(V^{k,\delta}) - m^{k,\delta}\beta'_{m^{k,\delta}}(V^{k,\delta})\big]P^{k,\delta}W^{k,\delta}\,dt\\ &\quad -\int_0^T \big[(1-n^{k,\delta})\alpha'_{n^{k,\delta}}(V^{k,\delta}) - n^{k,\delta}\beta'_{n^{k,\delta}}(V^{k,\delta})\big]Q^{k,\delta}W^{k,\delta}\,dt\\ &\quad -\int_0^T \big[(1-h^{k,\delta})\alpha'_{h^{k,\delta}}(V^{k,\delta}) - h^{k,\delta}\beta'_{h^{k,\delta}}(V^{k,\delta})\big]R^{k,\delta}W^{k,\delta}\,dt.\end{aligned} \tag{40}$$

Multiplying the second equation from (23) by $M^{k,\delta}$, and integrating in the interval $[0,T]$ we gather that

$$\int_0^T \Big(\dot{P}^{k,\delta}M^{k,\delta} - \big[\alpha_{m^{k,\delta}}(V^{k,\delta}) + \beta_{m^{k,\delta}}(V^{k,\delta})\big]P^{k,\delta}M^{k,\delta}\Big)\,dt = \\ -\int_0^T \Big(3G_{Na}\big(m^{k,\delta}\big)^2\big(h^{k,\delta}\big)(V^{k,\delta}-E_{Na})U^{k,\delta}M^{k,\delta}\Big)\,dt.$$

Integrating by parts the first term from the previous equation, and initial (see (36), $M^{k,\delta}(0)=0$) and final (see (23), $P^{k,\delta}(T)=0$) conditions, we have

$$\int_0^T \Big(\dot{M}^{k,\delta} + \big[\alpha_{m^{k,\delta}}(V^{k,\delta}) + \beta_{m^{k,\delta}}(V^{k,\delta})\big]M^{k,\delta}\Big)P^{k,\delta}\,dt = \\ \int_0^T 3G_{Na}\big(m^{k,\delta}\big)^2\big(h^{k,\delta}\big)(V^{k,\delta}-E_{Na})U^{k,\delta}M^{k,\delta}\,dt,$$

Then, from the previous equation and the second equation from ODE (36), we have

$$\begin{aligned}(41)\quad \int_0^T 3G_{Na}\big(m^{k,\delta}\big)^2\left(h^{k,\delta}\right)(V^{k,\delta}-E_{Na})U^{k,\delta}M^{k,\delta}\,dt = \\ \int_0^T \left[(1-m^{k,\delta})\alpha'_{m^{k,\delta}}(V^{k,\delta}) - m^{k,\delta}\beta'_{m^{k,\delta}}(V^{k,\delta})\right]W^{k,\delta}P^{k,\delta}\,dt \\ + \int_0^T (1-m^{k,\delta})\theta_{\alpha_m}P^{k,\delta}dt - \int_0^T m^{k,\delta}\theta_{\beta_m}P^{k,\delta}dt.\end{aligned}$$

Multiplying the third equation from (23) by $N^{k,\delta}$, and integrating in the interval $[0,T]$ we gather that

$$\begin{aligned}\int_0^T \dot{Q}^{k,\delta}N^{k,\delta} - \left[\alpha_{n^{k,\delta}}(V^{k,\delta}) + \beta_{n^{k,\delta}}(V^{k,\delta})\right]Q^{k,\delta}N^{k,\delta}\,dt = \\ -\int_0^T 4G_K\big(n^{k,\delta}\big)^3(V^{k,\delta}-E_K)U^{k,\delta}N^{k,\delta}\,dt.\end{aligned}$$

Integrating for parts the first term of the previous equation, and initial (see (36), $N^{k,\delta}(0) = 0$) and final (see (23), $Q^{k,\delta}(T) = 0$) conditions, we have

$$\begin{aligned}\int_0^T \left(\dot{N}^{k,\delta} + \left[\alpha_{n^{k,\delta}}(V^{k,\delta}) + \beta_{n^{k,\delta}}(V^{k,\delta})\right]N^{k,\delta}\right)Q^{k,\delta}\,dt = \\ \int_0^T 4G_K\big(n^{k,\delta}\big)^3(V^{k,\delta}-E_K)U^{k,\delta}\,dt\end{aligned}$$

Then, from the previous equation and the third equation from ODE (36), we gather

$$\begin{aligned}(42)\quad \int_0^T 4G_K\big(n^{k,\delta}\big)^3(V^{k,\delta}-E_K)U^{k,\delta}\,dt = \\ \int_0^T \left[(1-n^{k,\delta})\alpha'_{n^{k,\delta}}(V^{k,\delta}) - n^{k,\delta}\beta'_{n^{k,\delta}}(V^{k,\delta})\right]WQ^{k,\delta}\,dt. \\ + \int_0^T (1-n^{k,\delta})\theta_{\alpha_n}Q^{k,\delta}dt - \int_0^T n^{k,\delta}\theta_{\beta_n}Q^{k,\delta}dt.\end{aligned}$$

Multiplying the fourth equation from (23) by $H^{k,\delta}$, and integrating in the interval $[0,T]$ we gather that

$$\begin{aligned}\int_0^T \dot{R}^{k,\delta}H^{k,\delta} - \left[\alpha_{h^{k,\delta}}(V^{k,\delta}) + \beta_{h^{k,\delta}}(V^{k,\delta})\right]R^{k,\delta}H^{k,\delta}\,dt = \\ -\int_0^T G_{Na}^{k,\delta}\big(m^{k,\delta}\big)^3(V^{k,\delta}-E_{Na})U^{k,\delta}\,dt\end{aligned}$$

Integrating for parts the first term of the previous equation, and using the initial conditions $H^{k,\delta}(0)=0$ and $R^{k,\delta}(0)=0$ we have,

$$\int_0^T \Big(\dot{H}^{k,\delta} + \big[\alpha_{h^{k,\delta}}(V^{k,\delta}) + \beta_{h^{k,\delta}}(V^{k,\delta})\big]\, H^{k,\delta}\Big)\, R^{k,\delta}\; dt = \int_0^T G_{Na}\big(m^{k,\delta}\big)^3 (V^{k,\delta} - E_{Na}) U^{k,\delta}\; dt,$$

Then, from the previous equation and the fourth equation from ODE (36), we have

$$\begin{aligned}\int_0^T G_{Na}\big(m^{k,\delta}\big)^3 (V^{k,\delta} - E_{Na}) U^{k,\delta}\; dt = &\int_0^T \big[(1-h^{k,\delta})\alpha'_{h^{k,\delta}}(V^{k,\delta}) - h^{k,\delta}\beta'_{h^{k,\delta}}(V^{k,\delta})\big]\, W^{k,\delta} R^{k,\delta}\; dt.\\ &+ \int_0^T (1-h^{k,\delta})\theta_{\alpha_h} R^{k,\delta} dt - \int_0^T h^{k,\delta}\theta_{\beta_h} R^{k,\delta} dt.\end{aligned} \tag{43}$$

Substituting the equations (41), (42), and (43) in the equation (40), leads to

$$\begin{aligned}\Phi = &\int_0^T (1-m^{k,\delta})\theta_{\alpha_m} P^{k,\delta} dt - \int_0^T m^{k,\delta}\theta_{\beta_m} P^{k,\delta} dt\\ &+ \int_0^T (1-n^{k,\delta})\theta_{\alpha_n} Q^{k,\delta} dt - \int_0^T n^{k,\delta}\theta_{\beta_n} Q^{k,\delta} dt\\ &+ \int_0^T (1-h^{k,\delta})\theta_{\alpha_h} R^{k,\delta} dt - \int_0^T h^{k,\delta}\theta_{\beta_h} R^{k,\delta} dt.\end{aligned} \tag{44}$$

Replacing equations (19), (20) and (21) into (44) we gather that

$$\begin{aligned}\Phi = &\int_0^T X^{k,\delta}_{\alpha_m}\theta_{\alpha_m} dt + \int_0^T X^{k,\delta}_{\beta_m}\theta_{\beta_m} dt + \int_0^T X^{k,\delta}_{\alpha_n}\theta_{\alpha_n} dt + \int_0^T X^{k,\delta}_{\beta_n}\theta_{\beta_n} dt\\ &+ \int_0^T X^{k,\delta}_{\alpha_h}\theta_{\alpha_h} dt + \int_0^T X^{k,\delta}_{\beta_h}\theta_{\beta_h} dt.\end{aligned}$$

Then from previous equation, we have

$$\Phi = \Big\langle \Big(X^{k,\delta}_{\alpha_m}, X^{k,\delta}_{\beta_m}, X^{k,\delta}_{\alpha_n}, X^{k,\delta}_{\beta_n}, X^{k,\delta}_{\alpha_h}, X^{k,\delta}_{\beta_h}\Big), \boldsymbol{\theta} \Big\rangle_{(L^2[0,T])^6}. \tag{45}$$

From (37) and (45)

$$\frac{\langle \boldsymbol{\alpha}^{k+1,\delta} - \boldsymbol{\alpha}^{k,\delta}, \boldsymbol{\theta}\, \rangle_{(L^2[0,T])^6}}{w^{k,\delta}} = \Big\langle \Big(X^{k,\delta}_{\alpha_m}, X^{k,\delta}_{\beta_m}, X^{k,\delta}_{\alpha_n}, X^{k,\delta}_{\beta_n}, X^{k,\delta}_{\alpha_h}, X^{k,\delta}_{\beta_h}\Big), \boldsymbol{\theta} \Big\rangle_{(L^2[0,T])^6}.$$

Since $\theta \in \left(L^2[0,T]\right)^6$ is arbitrary, we have (18) $\square$

Appendix B. Proof of Theorem 2.2

In what follows we prove Theorem 2.2.

Proof. As in Subsection 2.2, the operator F is defined in (10), $\mathcal{H} = L^2[0,T]$ and $x = \boldsymbol{g}$. Evaluating $\boldsymbol{g}^{k,\delta}$ in F, we have $F(\boldsymbol{g}^{k,\delta}) = V^{k,\delta}$, where $V^{k,\delta}$ and $\upsilon^{k,\delta}$ solve ODE (27). Let $\boldsymbol{\theta} \in L^2[0,T]$ and $\lambda \in \mathbb{R}$, then $F(\boldsymbol{g}^{k,\delta} + \lambda\boldsymbol{\theta}) = V_\lambda^{k,\delta}$, where $V_\lambda^{k,\delta}$ and $\upsilon_\lambda^{k,\delta}$ solve

$$
\begin{cases}
\dot{V}_\lambda^{k,\delta} = I_{ext} + g^{k,\delta}(V_\lambda^{k,\delta}) + \lambda\boldsymbol{\theta} - \upsilon_\lambda^{k,\delta}, \\
\dot{\upsilon}_\lambda^{k,\delta} = bV_\lambda^{k,\delta} - c\upsilon_\lambda^{k,\delta}, \\
V_\lambda^{k,\delta}(0) = V_0; \quad \upsilon_\lambda^{k,\delta}(0) = \upsilon_0.
\end{cases} \tag{46}
$$

The Gateaux derivative of F at $\boldsymbol{g}^{k,\delta}$ in the direction $\boldsymbol{\theta}$ is given by

$$
W^{k,\delta} = F'(\boldsymbol{g}^{k,\delta})(\boldsymbol{\theta}) = \lim_{\lambda\to 0} \frac{F(\boldsymbol{g}^{k,\delta} + \lambda\boldsymbol{\theta}) - F(\boldsymbol{g}^{k,\delta})}{\lambda}. \tag{47}
$$

Also, we denote the following limit

$$
R^{k,\delta} = \lim_{\lambda\to 0} \frac{\upsilon_\lambda^{k,\delta} - \upsilon^{k,\delta}}{\lambda}, \tag{48}
$$

where $R^{k,\delta}$ is the Gateaux derivative of $\upsilon^{k,\delta}$.

Considering the difference between ODEs (46) and (27), dividing by λ and taking the limit $\lambda \to 0$, we have the following ODE

$$
\begin{cases}
\dot{W}^{k,\delta} - g^{k,\delta\prime}(V^{k,\delta})W^{k,\delta} = \boldsymbol{\theta} - R^{k,\delta}, \\
\dot{R}^{k,\delta} + cR^{k,\delta} = bW^{k,\delta}, \\
W^{k,\delta}(0) = 0; \quad R^{k,\delta}(0) = 0.
\end{cases} \tag{49}
$$

This last equation is yet another system of coupled nonlinear differential equations, depending on the parameter $\boldsymbol{\theta}$, representing an arbitrary function in $L^2[0,T]$.

From Landweber iteration (24) and $\boldsymbol{\theta} \in L^2[0,T]$ arbitrary, we have

$$
\begin{aligned}
\langle \boldsymbol{g}^{k+1,\delta} - \boldsymbol{g}^{k,\delta}, \boldsymbol{\theta} \rangle_{L^2[0,T]} &= w^{k,\delta} \langle F'(\boldsymbol{g}^{k,\delta})^*(V^\delta - F(\boldsymbol{g}^{k,\delta})), \boldsymbol{\theta} \rangle_{L^2[0,T]}, \\
&= w^{k,\delta} \langle F'(\boldsymbol{g}^{k,\delta})^*(V^\delta - V^{k,\delta}), \boldsymbol{\theta} \rangle_{L^2[0,T]}.
\end{aligned}
$$

By the definition of adjoint operator

$$
\langle \boldsymbol{g}^{k+1,\delta} - \boldsymbol{g}^{k,\delta}, \boldsymbol{\theta} \rangle_{L^2[0,T]} = w^{k,\delta} \langle V^\delta - V^{k,\delta}, F'(x_k)(\boldsymbol{\theta}) \rangle_{L^2[0,T]},
$$

Combining the previous equation and (47) gives

$$
\langle \boldsymbol{g}^{k+1,\delta} - \boldsymbol{g}^{k,\delta}, \boldsymbol{\theta} \rangle_{L^2[0,T]} = w^{k,\delta} \langle V^\delta - V^{k,\delta}, W^{k,\delta} \rangle_{L^2[0,T]}.
$$

We denote the last equality by Φ, then

$$\Phi = \frac{\langle \boldsymbol{g}^{k+1,\delta} - \boldsymbol{g}^{k,\delta}, \boldsymbol{\theta} \rangle_{L^2[0,T]}}{w^{k,\delta}} = \langle V^\delta - V^{k,\delta}, W^{k,\delta} \rangle_{L^2[0,T]}. \tag{50}$$

By the definition of internal product in $L^2[0,T]$

$$\Phi = \int_0^T (V^\delta - V^{k,\delta}) W^{k,\delta} dt.$$

From the previous equation and the first equality from ODE (28), we obtain

$$\Phi = \int_0^T \left(\dot{U}^{k,\delta} W^{k,\delta} + g'(V^{k,\delta}) U^{k,\delta} W^{k,\delta} - b P^{k,\delta} W^{k,\delta} \right) dt. \tag{51}$$

Integrating by parts the first term from equation (51), and from initial (see (49), $W^{k,\delta}(0) = 0$) and final (see (28), $U^{k,\delta}(T) = 0$) conditions, we obtain

$$\int_0^T \dot{U}^{k,\delta} W^{k,\delta} dt = - \int_0^T \dot{W}^{k,\delta} U^{k,\delta} dt. \tag{52}$$

Replacing equation (52) into (51), we have

$$\Phi = - \int_0^T \left(\dot{W}^{k,\delta} - g'(V^{k,\delta}) W^{k,\delta} \right) U^{k,\delta} dt - \int_0^T b P^{k,\delta} W^{k,\delta} dt.$$

Replacing, the first equality from ODE (49), in the first integral from the previous equation, we gather

$$\Phi = - \int_0^T \boldsymbol{\theta} U^{k,\delta} dt + \int_0^T R^{k,\delta} U^{k,\delta} dt - \int_0^T b P^{k,\delta} W^{k,\delta} dt. \tag{53}$$

Multiplying the second equation from (28) by $R^{k,\delta}$, and integrating in the interval $[0,T]$ we gather that

$$\int_0^T \dot{P}^{k,\delta} R^{k,\delta} dt - \int_0^T c P^{k,\delta} R^{k,\delta} dt = - \int_0^T U^{k,\delta} R^{k,\delta} dt.$$

Integrating by parts the first term from the previous equation, and from initial (see (49), $M^{k,\delta}(0) = 0$) and final (see (28), $P^{k,\delta}(T) = 0$) conditions, we obtain

$$\int_0^T \left(\dot{R}^{k,\delta} + c R^{k,\delta} \right) P^{k,\delta} dt = \int_0^T U^{k,\delta} R^{k,\delta} dt.$$

Then, from the previous equation and the second equation from ODE (49)

$$\int_0^T b P^{k,\delta} W^{k,\delta} dt = \int_0^T U^{k,\delta} R^{k,\delta} dt. \tag{54}$$

Substituting equation (54) into (53), we gather

$$\Phi = - \int_0^T \boldsymbol{\theta} U^{k,\delta} dt = - \left\langle U^{k,\delta}, \boldsymbol{\theta} \right\rangle_{L^2[0,T]}.$$

Combining the previous equation and (50), we obtain

$$\frac{\left\langle \boldsymbol{g}^{k+1,\delta} - \boldsymbol{g}^{k,\delta}, \boldsymbol{\theta} \right\rangle_{L^2[0,T]}}{w^{k,\delta}} = -\left\langle U^{k,\delta}, \boldsymbol{\theta} \right\rangle_{L^2[0,T]}.$$

Since $\boldsymbol{\theta} \in L^2[0,T]$ is arbitrary, we have (26). $\square$

References

[1] Avdonin, S., and Bell, J. Determining a distributed parameter in a neural cable model via a boundary control method. *Journal of mathematical biology 67*, 1 (2013), 123–141.

[2] Avdonin, S., and Bell, J. Determining a distributed conductance parameter for a neuronal cable model defined on a tree graph. *Journal of Inverse Problems and Imaging 9* (2015), 645–659.

[3] Bell, J., and Craciun, G. A distributed parameter identification problem in neuronal cable theory models. *Mathematical biosciences 194*, 1 (2005), 1–19.

[4] Buhry, L., Grassia, F., Giremus, A., Grivel, E., Renaud, S., and Saïghi, S. Automated parameter estimation of the hodgkin-huxley model using the differential evolution algorithm: application to neuromimetic analog integrated circuits. *Neural computation 23*, 10 (2011), 2599–2625.

[5] Buhry, L., Pace, M., and Saïghi, S. Global parameter estimation of an hodgkin–huxley formalism using membrane voltage recordings: Application to neuro-mimetic analog integrated circuits. *Neurocomputing 81* (2012), 75–85.

[6] Che, Y., Geng, L.-H., Han, C., Cui, S., and Wang, J. Parameter estimation of the fitzhugh-nagumo model using noisy measurements for membrane potential. *Chaos: An Interdisciplinary Journal of Nonlinear Science 22*, 2 (2012), 023139.

[7] Cox, S., and Wagner, A. Lateral overdetermination of the fitzhugh–nagumo system. *Inverse Problems 20*, 5 (2004), 1639.

[8] Cox, S. J., and Ji, L. Discerning ionic currents and their kinetics from input impedance data. *Bulletin of mathematical biology 63*, 5 (2001), 909–932.

[9] Ermentrout, G. B., and Terman, D. H. *Mathematical foundations of neuroscience*, vol. 35. Springer Science & Business Media, 2010.

[10] Hodgkin, A. L., and Huxley, A. F. The components of membrane conductance in the giant axon of loligo. *The Journal of physiology 116*, 4 (1952), 473–496.

[11] Hodgkin, A. L., and Huxley, A. F. A quantitative description of membrane current and its application to conduction and excitation in nerve. *The Journal of physiology 117*, 4 (1952), 500–544.

[12] Kaltenbacher, B., Neubauer, A., and Scherzer, O. *Iterative regularization methods for nonlinear ill-posed problems*, vol. 6. Walter de Gruyter, 2008.

[13] Mandujano, J., Madureira, A., and Leitão, A. A computational approach for the inverse problem of neuronal conductances determination. *Journal of Computational Neuroscience 9* (2018), 1–20.

[14] Pavel'chak, I. Numerical solution method for the source reconstruction problem in the fitzhugh–nagumo model. *Computational Mathematics and Modeling 1*, 24 (2013), 22–30.

[15] Pavel'chak, I., and Tuikina, S. Numerical solution method for the inverse problem of the modified fitzhugh–nagumo model. *Computational Mathematics and Modeling 23*, 2 (2012), 208–215.

[16] Pospischil, M., Piwkowska, Z., Rudolph, M., Bal, T., and Destexhe, A. Calculating event-triggered average synaptic conductances from the membrane potential. *Journal of Neurophysiology 97*, 3 (2007), 2544–2552.

[17] Rall, W. Core conductor theory and cable properties of neurons. *Comprehensive Physiology 1* (1977), 39–97.

[18] Rall, W., Burke, R., Holmes, W., Jack, J., Redman, S., and Segev, I. Matching dendritic neuron models to experimental data. *Physiological Reviews 72*, 4 (1992), S159–S186.

[19] Rudolph, M., Piwkowska, Z., Badoual, M., Bal, T., and Destexhe, A. A method to estimate synaptic conductances from membrane potential fluctuations. *Journal of neurophysiology 91*, 6 (2004), 2884–2896.

[20] Tadi, M., Klibanov, M. V., and Cai, W. An inversion method for parabolic equations based on quasireversibility. *Computers & Mathematics with Applications 43*, 8 (2002), 927–941.

[21] Tuckwell, H. C. *Introduction to theoretical neurobiology: volume 2, nonlinear and stochastic theories*, vol. 8. Cambridge University Press, 1988.

[22] Tuikina, S., and Solov'eva, S. Numerical method of determining the excitation source for the fitzhugh–nagumo mathematical model. *Computational Mathematics and Modeling 28*, 3 (2017), 301–309.

Departamento de Modelagem Computacional, Laboratório Nacional de Computação Científica, Av. Getúlio Vargas 333, 25651-070 Petrópolis, RJ, Brazil

APPENDIX D – Full Papers

Full paper 1

Discrete Inverse Problem in the Hodgkin-Huxley Model

Full paper 2

Discrete Inverse Problem in the Neuronal Cable Model

DISCRETE INVERSE PROBLEM IN THE HODGKIN AND HUXLEY MODEL

Jemy Alex Mandujano Valle - jhimyunac@gmail.com
National Laboratory of Scientific Computation (LNCC), Brazil.

Abstract. *The Hodgkin–Huxley (H-H) model is a system of ordinary differential equations (ODE) that describes the action potential behavior in the squid neuron. In this work, we propose the Landweber iteration to solve the inverse problem, that is, the estimation of maximum conductances in the discrete H-H model. To obtain the discrete model, we apply the finite differences method in the continuous H-H model.*

Keywords: *Hodgkin and Huxley model, Finite differences method, Inverse problems, Landweber Iteration.*

1. INTRODUCTION

In 1952, a mathematical model was developed to describe the initiation and propagation of an action potential in a neuron. Thenceforth, the then called Hodgkin-Huxley model, named after its creators, has been used vastly in the world of physiology. To obtain this model, the authors used two experimental techniques known as space clamp and voltage clamp, achieving significant progress in the understanding of nerve cells. However, while some variables, such as the membrane potential, are easily measured by voltage-clamp experiments, many parameters are obtained through a tedious combination of experiments and data tuning.

Some recent works (Sun et al. 2011 and Fang et al. 2016) estimate maximum conductances in the H-H model. Both proposed an adaptive observer to determine unknown parameters. However, the observer proposed by Fang et al. (2016) is less conservative than the observer proposed by Sun et al. (2011). Buhry at al. (2011) and (2012) estimate the constant parameters of an ion channel (H-H model) using the differential evolution algorithm. Finally, Roudolph et al. (2004) and Pospischil et al. (2007), estimate synaptic conductances, given the potential of the membrane, on the passive membrane equation.

Thereby, the goal of the present paper is to apply the *Nonlinear Landweber method* to solve the inverse problem of recovering the maximum conductances in the H-H model. Madureira et al. (2017), Valle et al. (2017) and Valle et al. (2018), also used the same method but applied to a different problem (passive cable equation).

We give a brief overview of the paper. In Section 2, we describe the continuous and discrete H-H models. In Section 3, we present the inverse problem for the discrete case and compute the adjoint operator of the Landweber iteration. Section 4, we provide the related numerical results. Finally, we discuss our findings and show some conclusions in Section 5.

2. THE HODGKIN-HUXLEY MATHEMATICAL MODEL

The H-H model with initial conditions consists of the following ODE

$$\begin{cases} C\dfrac{dV}{dt} = I_{\text{ext}} - G_{Na}m^3h(V-E_{Na}) - G_K n^4(V-E_K) - G_L(V-E_L); & t\in(0,T] \\ \dfrac{d\mathcal{X}}{dt} = (1-\mathcal{X})\alpha_{\mathcal{X}}(V) - \mathcal{X}\beta_{\mathcal{X}}(V); & \mathcal{X}=m,n,h; \quad t\in(0,T] \\ V(0)=V_0, \quad m(0)=m_0, \quad n(0)=n_0, \quad h(0)=h_0, \end{cases} \tag{1}$$

where C is the membrane capacitance, V is the membrane potential, dV/dt is the rate of change in membrane potential, I_{ext} is the membrane external current. The constants G_{Na}, G_K and G_L are the maximal conductances for Na^+, K^+ and leakage channels respectively; E_{Na}, E_K, E_L are the Nernst equilibrium potentials. The functions n, m and h represent the so-called activation term of the potassium channel and the activation and inactivation terms of the sodium channel, respectively. The terms V_0, m_0, n_0 and h_0 are the initial conditions for V, m, n and h, respectively. Also, the functions $\alpha_{\mathcal{X}}$ and $\beta_{\mathcal{X}}$ ($\mathcal{X}=m,n,h$) are written as:

$$\alpha_m = \tfrac{(25-V)/10}{\exp((25-V)/10)-1}; \quad \alpha_h = 0.07\exp(-V/20); \quad \alpha_n = \tfrac{(10-V)/100}{\exp((10-V)/10)-1};$$
$$\beta_m = 4\exp(-V/18); \quad \beta_h = \tfrac{1}{\exp((30-V)/10)+1}; \quad \beta_n = 0.125\exp(-V/80).$$

We partition the domain in time ($[0,T]$) using a mesh $t_1, t_2, \cdots, t_{nt}$. We assume a uniform partition, so the difference between two consecutive points in time will be Δt. The point U_i represents the numerical approximation of $U(t_i)$. Here $t_i = (i-1)\Delta t$ for $i = 1, \cdots, nt$ and $\Delta t = T/(nt-1)$. Applying finite differences (Forward Euler Method) in equation (1), for $i = 1, \cdots, nt-1$, we have the following Hodgkin and Huxley discrete model,

$$\begin{cases} C\dfrac{V_{i+1}-V_i}{\Delta t} = I_{\text{ext}} - G_{Na}{m_i}^3h_i(V_i-E_{Na}) - G_K n_i^4(V_i-E_K) - G_L(V_i-E_L); \\ \dfrac{\mathcal{X}_{i+1}-\mathcal{X}_i}{\Delta t} = (1-\mathcal{X}_i)\alpha_{\mathcal{X}_i}(V_i) - \mathcal{X}_i\beta_{\mathcal{X}_i}(V_i); & \mathcal{X}=m,n,h; \\ V_1=V_0, \quad m_1=m_0, \quad n_1=n_0, \quad h_1=h_0. \end{cases} \tag{2}$$

Functions $\alpha_{\mathcal{X}_i}$ and $\beta_{\mathcal{X}_i}$ satisfy the following equations:

$$\alpha_{m_i} = \tfrac{(25-V_i)/10}{\exp((25-V_i)/10)-1}; \quad \alpha_{h_i} = 0.07\exp(-V_i/20); \quad \alpha_{n_i} = \tfrac{(10-V_i)/100}{\exp((10-V_i)/10)-1};$$
$$\beta_{m_i} = 4\exp(-V_i/18); \quad \beta_{h_i} = \tfrac{1}{\exp((30-V_i)/10)+1}; \quad \beta_{n_i} = 0.125\exp(-V_i/80).$$

We denote $\boldsymbol{V} = (V_1, \cdots, V_{nt})$, $\boldsymbol{m} = (m_1, \cdots, m_{nt})$, $\boldsymbol{n} = (n_1, \cdots, n_{nt})$, $\boldsymbol{h} = (h_1, \cdots, h_{nt})$ and $\boldsymbol{G} = (G_{Na}, G_K, G_L)$.

The objective of this work is to estimate $\boldsymbol{G}$, from (2), given the potential membrane measurement.

3. DISCRETE INVERSE PROBLEM

Consider the nonlinear operator $F : \mathbb{R}^3 \to \mathbb{R}^{nt}$, defined by

$$F(\boldsymbol{G}) = \boldsymbol{V}, \tag{3}$$

where $\boldsymbol{V}$ solves (2). In practical terms, the data $\boldsymbol{V}$ are obtained by measurements. We denote such measurements by $\boldsymbol{V}^{\delta}$, where the noise level δ is assumed to be known and satisfies

$$\|\boldsymbol{V} - \boldsymbol{V}^{\delta}\|_{\mathbb{R}^{nt}} \leq \delta. \tag{4}$$

In this paper, we admit the existence of the inverse operator F^{-1}, but not its stability. To control instability, we use an iterative method of regularization (Landweber iteration).

Here, for $x = (x_1, \cdots, x_{nt})$ and $y = (y_1, \cdots, y_{nt})$, the inner product and the norm are defined by the following equations,

$$\langle x, y\rangle = \Delta t^3 \sum_{i=1}^{nt} x_i y_i \quad \text{and} \quad \|x\| = \sqrt{\Delta t^3 \sum_{i=1}^{nt} |x_i|^2}. \tag{5}$$

From the system of equations (2), we consider the inverse problem of finding an approximation for $\boldsymbol{G}$, given the noisy data $\boldsymbol{V}^{\delta}$.

Given the initial guess $\boldsymbol{G}^{1,\delta}$, the Landweber approximation (Hanke et al. 1995, Bende et al. 1996 and Neubauer 2000), to estimate $\boldsymbol{G}$, is defined as following:

$$\boldsymbol{G}^{k+1,\delta} = \boldsymbol{G}^{k,\delta} + F'(\boldsymbol{G}^{k,\delta})^*.(\boldsymbol{V}^{\delta} - F(\boldsymbol{G}^{k,\delta})), \tag{6}$$

where $\boldsymbol{G}^{k,\delta} = (G_{Na}^{k,\delta}, G_K^{k,\delta}, G_L^{k,\delta})$ and $F'(\cdot)^*(\cdot)$ is adjoint of the directional derivative.

The iteration (6) stops at the minimum $k_* = k(\delta, \boldsymbol{V}^{\delta})$, such that, for a given $\tau > 2$,

$$\|\boldsymbol{V}^{\delta} - F(\boldsymbol{G}^{k_*,\delta})\|_{\mathbb{R}^{nt}} \leq \tau\delta. \tag{7}$$

It is possible to show that, under certain conditions, $\boldsymbol{G}^{k_*,\delta}$ converges to a solution to $F(\boldsymbol{G}) = \boldsymbol{V}$ as $\delta \to 0$ (see [7], Theorem 2.6).

In the next subsection, we calculate, from (6), the adjoint of the directional derivative.

3.1 The adjoint operator

In Theorem 3.1.1, we calculate the operator $F'(\cdot)^*.(\cdot)$ from Landweber iteration (6). Then, from Theorem 3.1.1 and algorithm (6), we have the following iteration

$$\begin{cases} G_{Na}^{k+1,\delta} = G_{Na}^{k,\delta} + \Delta t^3 \sum_{i=1}^{nt} \left(m_i^{k,\delta}\right)^3 h_i^{k,\delta}(V_i^{k,\delta} - E_{Na})U_i^{k,\delta}, \\ G_K^{k+1,\delta} = G_K^{k,\delta} + \Delta t^3 \sum_{i=1}^{nt} \left(n_i^{k,\delta}\right)^4 (V_i^{k,\delta} - E_K)U_i^{k,\delta}, \\ G_L^{k+1,\delta} = G_L^{k,\delta} + \Delta t^3 \sum_{i=1}^{nt} (V_i^{k,\delta} - E_L)U_i^{k,\delta}, \end{cases} \tag{8}$$

where $\boldsymbol{V}^{k,\delta}$, $\boldsymbol{m}^{k,\delta}$, $\boldsymbol{n}^{k,\delta}$, $\boldsymbol{h}^{k,\delta}$ solve (2), replacing $\boldsymbol{G}$ by $\boldsymbol{G}^{k,\delta}$. Also, $U_i^{k,\delta}$ solves (13), replacing $\boldsymbol{G}$ by $\boldsymbol{G}^{k,\delta}$ and $\boldsymbol{V}$ by $\boldsymbol{V}^{k,\delta}$.

In this work, to obtain an approximation of $\boldsymbol{G}$, we used iteration (8).

Theorem 3.1.1. *Consider the nonlinear operator F defined in* (3)*, then*

$$F'(\boldsymbol{G})^* . \left(\boldsymbol{V}^\delta - F(\boldsymbol{G})\right) = \Delta t^3 \left(\sum_{i=1}^{nt} m_i^3 h_i (V_i - E_{Na}) U_i, \sum_{i=1}^{nt} n_i^4 (V_i - E_K) U_i, \sum_{i=1}^{nt} (V_i - E_L) U_i \right).$$

Proof. Evaluating $\boldsymbol{G}$ in the operator F and from (2) we have $\boldsymbol{V}$, $\boldsymbol{m}$, $\boldsymbol{n}$ and $\boldsymbol{h}$.

Let the vector $\boldsymbol{\theta} = (\theta_{Na}, \theta_K, \theta_L) \in \mathbb{R}^3$ and $\lambda \in \mathbb{R}$, then evaluating $\boldsymbol{G} + \lambda\boldsymbol{\theta}$ in the operator F, we have $F(\boldsymbol{G} + \lambda\boldsymbol{\theta}) = \boldsymbol{V}^\lambda$, where $\boldsymbol{V}^\lambda$, $\boldsymbol{m}^\lambda$, $\boldsymbol{n}^\lambda$ and $\boldsymbol{h}^\lambda$ solve

$$\begin{cases} C\dfrac{V_{i+1}^\lambda - V_i^\lambda}{\Delta t} = I_{ext} - (G_{Na} + \lambda\theta_{Na}) \left(m_i^\lambda\right)^3 \left(h_i^\lambda\right) \left(V_i^\lambda - E_{Na}\right) \\ \quad - (G_K + \lambda\theta_K) \left(n_i^\lambda\right)^4 \left(V_i^\lambda - E_K\right) - (G_L + \lambda\theta_L) \left(V_i^\lambda - E_L\right), \\ \dfrac{\mathcal{X}_{i+1} - \mathcal{X}_i}{\Delta t} = (1 - \mathcal{X}_i)\alpha_{\mathcal{X}_i}(V_i) - \mathcal{X}_i \beta_{\mathcal{X}_i}(V_i); \qquad \mathcal{X} = m^\lambda, n^\lambda, h^\lambda, \\ V_1^\lambda(0) = V_0; \quad m_1^\lambda(0) = m_0; \quad n_1^\lambda(0) = n_0; \quad n_1^\lambda(0) = n_0. \end{cases} \tag{9}$$

We denote $\boldsymbol{W} = (W_1, \cdots, W_{nt})$, $\boldsymbol{M} = (M_1, \cdots, M_{nt})$, $\boldsymbol{N} = (N_1, \cdots, N_{nt})$ and $\boldsymbol{H} = (H_1, \cdots, H_{nt})$. The directional derivative of F at $\boldsymbol{G}$ in the direction $\boldsymbol{\theta}$ is given by

$$\boldsymbol{W} = F'(\boldsymbol{G}).(\boldsymbol{\theta}) = \lim_{\lambda \to 0} \frac{F(\boldsymbol{G} + \lambda\boldsymbol{\theta}) - F(\boldsymbol{G})}{\lambda} = \langle \nabla F, \boldsymbol{\theta} \rangle. \tag{10}$$

Also, we denote the following limits

$$\boldsymbol{M} = \lim_{\lambda \to 0} \frac{\boldsymbol{m}^\lambda - \boldsymbol{m}}{\lambda}, \quad \boldsymbol{N} = \lim_{\lambda \to 0} \frac{\boldsymbol{n}^\lambda - \boldsymbol{n}}{\lambda}, \quad \boldsymbol{H} = \lim_{\lambda \to 0} \frac{\boldsymbol{h}^\lambda - \boldsymbol{h}}{\lambda}, \tag{11}$$

where $\boldsymbol{M}$, $\boldsymbol{N}$ and $\boldsymbol{H}$ are the directional derivatives of $\boldsymbol{m}$, $\boldsymbol{n}$ and $\boldsymbol{h}$, respectively.

Considering the difference between (2) and (9), dividing by λ and taking the limit $\lambda \to 0$, we have the following equation

$$\begin{cases} C\dfrac{W_{i+1} - W_i}{\Delta t} + \left(G_{Na} m_i^3 h_i + G_K n_i^4 + G_L\right) W_i = -3G_{Na} m_i^2 M_i h_i (V_i - E_{Na}) \\ \quad -G_{Na} m_i^3 H_i (V_i - E_{Na}) - 4G_K n_i^3 N_i (V_i - E_K) \\ \quad -\theta_{Na} m_i^3 h_i (V_i - E_{Na}) - \theta_K n_i^4 (V_i - E_K) - \theta_L (V_i - E_L), \\ \dfrac{\mathcal{Y}_{i+1} - \mathcal{Y}_i}{\Delta t} + [\alpha_{\mathcal{X}_i}(V_i) + \beta_{\mathcal{X}_i}(V_i)]\mathcal{Y}_i = [(1 - \mathcal{X}_i)\alpha'_{\mathcal{X}_i}(V_i) - \mathcal{X}_i \beta'_{\mathcal{X}_i}(V_i)] W_i; \\ (\mathcal{X}, \mathcal{Y}) = (m, M), (n, N), (h, H), \\ W_1 = 0; \quad M_1 = 0;; \quad N_1 = 0; \quad H_1 = 0. \end{cases} \tag{12}$$

This last equation is another system of coupled nonlinear differential equations, depending on the parameter $\boldsymbol{\theta} = (\theta_{Na}, \theta_K, \theta_L)$. Note that the variable $\boldsymbol{\theta}$ represents any point in space $\mathbb{R}^3$.

We define the following system of equations

$$\begin{cases} C\dfrac{U_i - U_{i-1}}{\Delta t} - \left(G_{Na}m_i^3h_i + G_K n_i^4 + G_L\right)U_i \\ -[(1-m_i)\alpha'_{m_i}(V_i) - m_i\beta'_{m_i}(V_i)]P_i \\ -[(1-n_i)\alpha'_{n_i}(V_i) - n_i\beta'_{n_i}(V_i)]Q_i \\ -[(1-h_i)\alpha'_{h_i}(V_i) - h_i\beta'_{h_i}(V_i)]R_i = V_i^\delta - V_i \\ \dfrac{P_i - P_{i-1}}{\Delta t} - [\alpha_{m_i}(V_i) + \beta_{m_i}(V_i)]P_i = -3G_{Na}m_i^2h_i(V_i - E_{Na})U_i \\ \dfrac{Q_i - Q_{i-1}}{\Delta t} - [\alpha_{n_i}(V_i) + \beta_{n_i}(V_i)]Q_i = -4G_K n_i^3(V_i - E_K)U_i \\ \dfrac{R_i - R_{i-1}}{\Delta t} - [\alpha_{h_i}(V_i) + \beta_{h_i}(V_i)]R_i = -G_{Na}m_i^3(V_i - E_{Na})U_i \\ U_{nt} = 0; \quad P_{nt} = 0; \quad Q_{nt} = 0; \quad R_{nt} = 0. \end{cases} \tag{13}$$

We denote $\boldsymbol{U} = (U_1, \cdots, U_{nt})$, $\boldsymbol{P} = (P_1, \cdots, P_{nt})$, $\boldsymbol{Q} = (Q_1, \cdots, Q_{nt})$ and $\boldsymbol{R} = (R_1, \cdots, R_{nt})$.

By the definition of adjoint operator, we have

$$\left\langle F'(\boldsymbol{G})^* \left(\boldsymbol{V}^\delta - F(\boldsymbol{G})\right), \boldsymbol{\theta}\right\rangle_{\mathbb{R}^3} = \left\langle \boldsymbol{V}^\delta - F(\boldsymbol{G})\ ,\ F'(\boldsymbol{G}).(\boldsymbol{\theta})\right\rangle_{\mathbb{R}^{nt}}.$$

Combining the previous equation and (10) gives

$$\left\langle F'(\boldsymbol{G})^* \left(\boldsymbol{V}^\delta - F(\boldsymbol{G})\right), \boldsymbol{\theta}\right\rangle_{\mathbb{R}^3} = \left\langle \boldsymbol{V}^\delta - F(\boldsymbol{G})\ ,\ \boldsymbol{W}\right\rangle_{\mathbb{R}^{nt}}.$$

By the definition of inner product (5), we have

$$\left\langle F'(\boldsymbol{G})^* \left(\boldsymbol{V}^\delta - F(\boldsymbol{G})\right), \boldsymbol{\theta}\right\rangle_{\mathbb{R}^3} = \Delta t^3 \sum_{i=1}^{nt} \left(V_i^\delta - V_i\right) W_i.$$

We denote the last equality by Φ, then

$$\Phi = \frac{1}{\Delta t^3}\left\langle F'(\boldsymbol{G})^* \left(V^\delta - F(\boldsymbol{G})\right), \boldsymbol{\theta}\right\rangle_{\mathbb{R}^3} = \sum_{i=1}^{nt} \left(V_i^\delta - V_i\right) W_i. \tag{14}$$

From the previous equation and the first equality from (13), we obtain the following expression

$$\begin{aligned} \Phi = \sum_{i=1}^{nt} C\frac{U_i - U_{i-1}}{\Delta t}W_i - \sum_{i}^{nt}\left(G_{Na}m_i^3h_i + G_K n_i^4 + G_L\right)U_iW_i \\ - \sum_{i=1}^{nt}[(1-m_i)\alpha'_{m_i}(V_i) - m_i\beta_{m_i}(V_i)]P_i - \sum_{i=1}^{nt}[(1-n_i)\alpha'_{n_i}(V_i) - n_i\beta'_{n_i}(V_i)]Q_i \\ - \sum_{i=1}^{nt}[(1-h)\alpha'_{h_i}(V_i) - h\beta'_{h_i}(V_i)]R_i. \end{aligned} \tag{15}$$

From equations (12) and (13), the vector (W_1, U_{nt}) is equal to $(0,0)$. Then, we obtain

$$\sum_{i=1}^{nt} C\frac{U_i - U_{i-1}}{\Delta t} W_i = -\sum_{i=1}^{nt} C\frac{W_{i+1} - W_i}{\Delta t} U_i. \tag{16}$$

Substituting (16) into (15), we have the following equality

$$\begin{aligned}\Phi = &-\sum_{i=1}^{nt}\left(C\frac{W_{i+1}-W_i}{\Delta t} + \left(G_{Na}m_i^3 h_i + G_K n_i^4 + G_L\right)W_i\right)U_i \\ &-\sum_{i=1}^{nt}[(1-m_i)\alpha'_{m_i}(V_i) - m_i\beta_{m_i}(V_i)]P_iW_i - \sum_{i=1}^{nt}[(1-n_i)\alpha'_{n_i}(V_i) - n_i\beta'_{n_i}(V_i)]Q_iW_i \\ &-\sum_{i=1}^{nt}[(1-h)\alpha'_{h_i}(V_i) - h\beta'_{h_i}(V_i)]R_iW_i.\end{aligned}$$

Replacing the first equality from (12) in the previous equation, leads to

$$\begin{aligned}\Phi = &\sum_{i=1}^{nt} 3G_{Na}m_i^2 M_i h_i (V_i - E_{Na})U_i + \sum_{i=1}^{nt} G_{Na}m_i^3 H_i(V_i - E_{Na})U_i \\ &+\sum_{i=1}^{nt} 4G_K n_i^3 N_i (V_i - E_K)U_i + \sum_{i=1}^{nt}\theta_{Na}m_i^3 h_i (V_i - E_{Na})U_i \\ &+\sum_{i=1}^{nt}\theta_K n_i^4 (V_i - E_K)U_i + \sum_{i=1}^{nt}\theta_L(V_i - E_L)U_i \\ &-\sum_{i=1}^{nt}[(1-m_i)\alpha'_{m_i}(V_i) - m_i\beta_{m_i}(V_i)]P_iW_i - \sum_{i=1}^{nt}[(1-n_i)\alpha'_{n_i}(V_i) - n_i\beta'_{n_i}(V_i)]Q_iW_i \\ &-\sum_{i=1}^{nt}[(1-h)\alpha'_{h_i}(V_i) - h\beta'_{h_i}(V_i)]R_iW_i.\end{aligned} \tag{17}$$

Let $(\mathcal{X}_i, \mathcal{Y}_i, \mathcal{Z}_i) \in \{(m_i, M_i, P_i), (n_i, N_i, Q_i), (h_i, H_i, R_i)\}$. Then, multiplying the second equation from (12) by $\mathcal{Z}_i$,

$$\begin{aligned}&\sum_{i=1}^{nt}\left(\frac{\mathcal{Y}_{i+1} - \mathcal{Y}_i}{\Delta t} + [\alpha_{\mathcal{X}_i}(V_i) + \beta_{\mathcal{X}_i}(V_i)]\mathcal{Y}_i\right)\mathcal{Z}_i \\ &= \sum_{i=1}^{nt}[(1-\mathcal{X}_i)\alpha'_{\mathcal{X}_i}(V_i) - \mathcal{X}_i\beta'_{\mathcal{X}_i}(V_i)]W_i\mathcal{Z}_i.\end{aligned} \tag{18}$$

From equations (12) and (13), the vector $(\mathcal{Y}_1, \mathcal{Z}_{nt}) \in \{(M_1, P_{nt}), (N_1, Q_{nt}), (H_1, R_{nt})\}$ equals $(0,0)$. Then, we have

$$\sum_{i=1}^{nt}\frac{\mathcal{Y}_{i+1} - \mathcal{Y}_i}{\Delta t}\mathcal{Z}_i = -\sum_{i=1}^{nt}\frac{\mathcal{Z}_i - \mathcal{Z}_{i-1}}{\Delta t}\mathcal{Y}_i. \tag{19}$$

Replacing equation (19) in (18), we obtain

$$-\sum_{i=1}^{nt}\left(\frac{\mathcal{Z}_i-\mathcal{Z}_{i-1}}{\Delta t}-[\alpha_{\mathcal{X}_i}(V_i)+\beta_{\mathcal{X}_i}(V_i)]\mathcal{Z}_i\right)\mathcal{X}_i = \sum_{i=1}^{nt}[(1-\mathcal{X}_i)\alpha'_{\mathcal{X}_i}(V_i)-\mathcal{X}_i\beta'_{\mathcal{X}_i}(V_i)]W_i\mathcal{Z}_i. \quad (20)$$

For $(\mathcal{X}_i,\mathcal{Y}_i,\mathcal{Z}_i)=(m_i,M_i,P_i)$ into (20), leads to

$$-\sum_{i=1}^{nt}\left(\frac{P_i-P_{i-1}}{\Delta t}-[\alpha_{m_i}(V_i)+\beta_{m_i}(V_i)]P_i\right)M_i = \sum_{i=1}^{nt}[(1-m_i)\alpha'_{m_i}(V_i)-m_i\beta'_{m_i}(V_i)]W_iP_i. \quad (21)$$

Substituting the second equation from (13) into (21),

$$\sum_{i=1}^{nt}3G_{Na}m_i^2h_i(V_i-E_{Na})U_iM_i=\sum_{i=1}^{nt}[(1-m_i)\alpha'_{m_i}(V_i)-m_i\beta'_{m_i}(V_i)]W_iP_i. \quad (22)$$

For $(\mathcal{X}_i,\mathcal{Y}_i,\mathcal{Z}_i)=(n_i,N_i,Q_i)$ into (20), we have

$$-\sum_{i=1}^{nt}\left(\frac{Q_i-Q_{i-1}}{\Delta t}-[\alpha_{n_i}(V_i)+\beta_{n_i}(V_i)]Q_i\right)N_i = \sum_{i=1}^{nt}[(1-n_i)\alpha'_{n_i}(V_i)-n_i\beta'_{n_i}(V_i)]W_iQ_i. \quad (23)$$

Substituting the third equation from (13) into (23),

$$\sum_{i=1}^{nt}4G_Kn_i^3(V_i-E_K)U_iN_i=\sum_{i=1}^{nt}[(1-n_i)\alpha'_{n_i}(V_i)-n_i\beta'_{n_i}(V_i)]W_iQ_i. \quad (24)$$

For $(\mathcal{X}_i,\mathcal{Y}_i,\mathcal{Z}_i)=(h_i,H_i,R_i)$ into (20), we obtain

$$-\sum_{i=1}^{nt}\left(\frac{R_i-R_{i-1}}{\Delta t}-[\alpha_{h_i}(V_i)+\beta_{h_i}(V_i)]R_i\right)H_i = \sum_{i=1}^{nt}[(1-h_i)\alpha'_{h_i}(V_i)-h_i\beta'_{h_i}(V_i)]W_iR_i. \quad (25)$$

Substituting the fourth equation from (13) into (25),

$$\sum_{i=1}^{nt}G_{Na}m_i^3(V_i-E_{Na})U_iH_i=\sum_{i=1}^{nt}[(1-h_i)\alpha'_{h_i}(V_i)-h_i\beta'_{h_i}(V_i)]W_iR_i. \quad (26)$$

Substituting equations (22), (24) and (26) in (17), we have

$$\Phi = \sum_{i=1}^{nt} \theta_{Na} m_i^3 h_i (V_i - E_{Na}) U_i + \sum_{i=1}^{nt} \theta_K n_i^4 (V_i - E_K) U_i + \sum_{i=1}^{nt} \theta_L (V_i - E_L) U_i.$$

By the definition of inner product

$$\Phi = \left\langle \left(\sum_{i=1}^{nt} m_i^3 h_i (V_i - E_{Na}) U_i, \sum_{i=1}^{nt} n_i^4 (V_i - E_K) U_i, \sum_{i=1}^{nt} (V_i - E_L) U_i \right), \boldsymbol{\theta} \right\rangle_{\mathbb{R}^3}. \tag{27}$$

From equations (14) and (27), since $\boldsymbol{\theta} \in \mathbb{R}^3$ is arbitrary, we obtain

$$F'(\boldsymbol{G})^* \left(\boldsymbol{V}^\delta - F(\boldsymbol{G}) \right) = \Delta t^3 \left(\sum_{i=1}^{nt} m_i^3 h_i (V_i - E_{Na}) U_i, \sum_{i=1}^{nt} n_i^4 (V_i - E_K) U_i, \sum_{i=1}^{nt} (V_i - E_L) U_i \right).$$

□

4. NUMERICAL RESULTS

In this section, we show numerical results for the discrete inverse problem using the Landweber iteration. The parameters for the H-H model (2) *are:* $\Delta t = 0.01$, $nt = 1000$, $C = 1\ [\mu F/cm^2]$, $I_{ext} = 10\ [\mu A/cm^2]$, $E_{Na} = 50\ [mV]$, $E_K = -77\ [mV]$, $E_L = -54.387\ [mV]$ $V_0 = -15\ [mV]$, $m_0 = 0.6$, $n_0 = 0.4$ *and* $h_0 = 0.4$. *The goal of this example is to find* $G_{Na} = 120\ mS/cm^2$, $G_K = 36\ mS/cm^2$ *and* $G_L = 0.3\ mS/cm^3$.

To compare the results obtained, first we calculate $\boldsymbol{V}$ *from* (2) *given* $\boldsymbol{G} = (120, 36, 0.3)$. *We obtain* $\boldsymbol{V}^\delta$*, for* $\delta = 10^{-3}$*, from the following equation*

$$\boldsymbol{V}^\delta = \boldsymbol{V} + rand_\delta \boldsymbol{V},$$

where $rand_\delta$ *generates uniformly distributed numbers in the interval* $[-\delta, \delta]$. *Now, we consider* $\boldsymbol{V}$ *and* $\boldsymbol{G}$ *unknown.*

To obtain $\boldsymbol{G}$ *we use* (8)*, given the initial guess* $\boldsymbol{G}^{1,\delta} = (0, 0, 0)$. *For* $\tau = 4$ *in the stopping criterion* (7)*, the algorithm stops when* $k_* = 853799$.

Figures 1-A, 1-B and 1-C show estimates for the maximum sodium, potassium, and leakage conductances, respectively.

Figure 2 shows the relative error between the actual and estimated values for the algorithm iterations. The relative error of $\boldsymbol{G}$ *is defined as*

$$Error_k^{\boldsymbol{G}} = \frac{\|\boldsymbol{G} - \boldsymbol{G}^{k,\delta}\|_{\mathbb{R}^3}}{\|\boldsymbol{G}\|_{\mathbb{R}^3}} \times 100\%, \quad k = 1, \cdots, 853799. \tag{28}$$

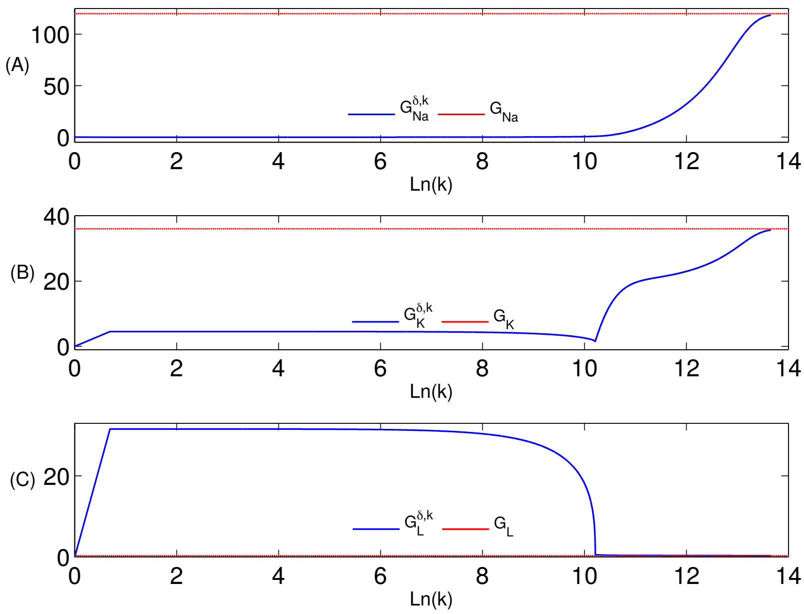

Figure 1- Estimation of the conductances G_{Na} (Subplot-A), G_K (Subplot-B) and G_L (Subplot-C).

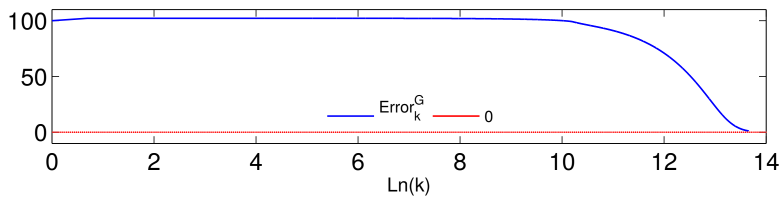

Figure 2- The relative error defined in (28).

5. CONCLUSIONS

In this work, we discretized the H-H model using the explicit Euler method. We considered the inverse problem of determining maximal conductances in the discrete model. To obtain the unknown parameters, we used the Landweber iteration. An essential contribution of the present work is the calculation of the adjoint operator of the Landweber iteration.

Compared to works Sun et al. (2011) and Fang et al. 2016., our approach has the advantage of allowing recovering the unknown parameters from noisy data. The computational results show that the method obtains a reasonable estimate for the parameters. It is important to notice that this work considers only computational data. In future studies, we plan to consider biological data as well.

Acknowledgements

The author would like to thank the support provided by CAPES.

REFERENCES

[1] Buhry, Laure et al., 2011. Automated parameter estimation of the Hodgkin-Huxley model using the differential evolution algorithm: application to neuromimetic analog integrated circuits. Neural computation*, v. 23, n. 10, p. 2599-2625.*

[2] Buhry, L., Pace, M. and Saïghi, S., 2012. Global parameter estimation of a Hodgkin–Huxley formalism using membrane voltage recordings: Application to neuro-mimetic analog integrated circuits. Neurocomputing*, v. 81, p. 75-85.*

[3] Binder, A., Hanke, M., and Scherzer, O. 1996. On the Landweber iteration for nonlinear ill-posed problems. Journal of Inverse and Ill-posed Problems*, v. 4, n. 5, p. 381-390.*

[4] Fang, L. I. A. O., and LOU, X. Y., 2016. State Estimation of Hodgkin-Huxley Model Based on Membrane Potential. DEStech Transactions on Engineering and Technology Research.

[5] Hodgkin, A. L., and Huxley, A. F. 1952. A quantitative description of membrane current and its application to conduction and excitation in nerve. The Journal of physiology*, 117(4), 500-544.*

[6] Hanke, M., Neubauer, A., and Scherzer, O., 1995. A convergence analysis of the Landweber iteration for nonlinear ill-posed problems. Numerische Mathematik*, v. 72, n. 1, p. 21-37.*

[7] Kaltenbacher, B., Neubauer, A., and Scherzer, O. 2008. Iterative regularization methods for nonlinear ill-posed problems (Vol. 6). Walter de Gruyter.

[8] Madureira, A. L. and Valle, J. A. M., 2017. Solução Númerica de um Problema Inverso em Neurociência via o Método de Landweber Não Linear. Proceeding Series of the Brazilian Society of Computational and Applied Mathematics*, v. 5, n. 1.*

[9] Neubauer, A., 2000. On Landweber iteration for nonlinear ill-posed problems in Hilbert scales. Numerische Mathematik*, v. 85, n. 2, p. 309-328.*

[10] Pospischil, M., Piwkowska, Z., Rudolph, M., Bal, T., and Destexhe, A. 2007. Calculating event-triggered average synaptic conductances from the membrane potential. Journal of Neurophysiology*, v. 97, n. 3, p. 2544-2552, 2007.*

[11] Pospischil, M, et al., 2007. Calculating event-triggered average synaptic conductances from the membrane potential. Journal of Neurophysiology*, 97(3), 2544-2552.*

[12] Rudolph, M., et al., 2004. A method to estimate synaptic conductances from membrane potential fluctuations. Journal of neurophysiology, v. 91, n. 6, p. 2884-2896.

[13] Sun, J., Deng, B., Wei, X., Jia, C., Wang, J., and Zhao, J., 2011. Parameter estimation in Hodgkin-Huxley model with adaptive method. In Biomedical Engineering and Informatics (BMEI)*, 2011 4th International Conference on (Vol. 4, pp. 1853-1857). IEEE.*

[14] Valle, J. A. M. and Madureira, A. L., 2017. Determinação de Parâmetros com Distribuição Espacial não Uniforme num Modelo de Neurociência via o Método de Landweber não Linear. X Encontro Acadêmico de Modelagem Computacional.

[15] Valle, J. A. M., Madureira, A. L., and Leitão, A., 2018. A Computational Approach for the inverse problem of neuronal conductances determination. arXiv preprint arXiv: 1810.05887.

Discrete inverse problem of neural conductances determination

Jemy A. Mandujano Valle
National Laboratory for Scientific Computing (LNCC), Brazil
E-mail: jhimyunac@gmail.com

Abstract. The neural cable model is a second order, parabolic, partial differential equation (PDE) that describes the evolution of voltage in the dendrite of a neuron. In this paper, we solve the inverse problem of recovering a single spatially distributed conductance parameter in a discrete passive cable equation through an iterative regularization method. To obtain the discrete model, we apply finite differences to the continuous model. We provide several numerical results showing that the iteration can estimate the correct parameter.

1. Introduction

The cable equation is a mathematical model derived from a circuit model of the membrane and its intracellular and extracellular space to provide a quantitative description of current flow and voltage change both within and between neurons, allowing a quantitative and qualitative understanding of how neurons function [1].

In this paper, we work with the passive cable equation; that is, the conductance is independent of the membrane potential.

From neuronal cable theory [2, 3], the membrane potential $V(t,x)$ satisfies

$$\frac{1}{R_I + R_e} V_{xx}(t,x) = C_M V_t(t,x) + G(x)(V(t,x) - E), \tag{1}$$

where the potential V is in millivolt $[mV]$; the internal and external neuronal resistance R_I, R_E are in ohm $[\Omega]$; C_M represents membrane specific capacitance in farad per square centimeter $[F/cm^2]$; the membrane specif conductance G is in siemen per square centimeter $[S/cm^2]$; the Nerst potential E is in millivolt $[mV]$. We assume that the constants R_I, R_E, C_M and E are known constants.

Consider the domain for (1) being $0 < t < T$ and $0 < x < L$, where t is in millisecond (ms) and x is in centimeters (cm). To equation (1), the boundary and initial conditions of interest are

$$V_x(t,0) = p(t) \quad , \quad V_x(t,L) = q(t), \text{ and } V(0,x) = r(x). \tag{2}$$

This work, we assume that the functions p, q and r are known.

Many of the works that estimate the conductance consider that this unknown parameter is a constant. There is not much work on spatially distributed conductance estimation.

The following papers estimate the conductance with spatial distribution: Tadi et al. [4] used an iterative method, the authors Bell and Craciun [5] presented a non-optimization approach, Cox [6] applied the adjoint method, and Avdonin and Bell [7] used the boundary control approach. They differ considerably from our procedure.

2. Statement of the discrete inverse problem

The discretization of the temporal domain [0, T] is represented by a finite number of mesh points

$$0 = t_1 < t_2 < \cdots < t_{nt-1} < t_{nt} = T.$$

Similarly, the discretization of the spatial domain $[0, L]$ is replaced by a set of mesh points

$$0 = x_1 < x_2 < \cdots < x_{nx-1} < t_{nx} = L.$$

For uniformly distributed mesh points we can introduce the constant mesh spacings Δt and Δx. We have that

$$t_n = (n-1)\Delta t, \quad n = 1, 2, \cdots, nt, \quad x_j = (j-1)\Delta x, \quad j = 1, 2, \cdots, nx.$$

We also have that $\Delta t = T/(nt-1)$ and $\Delta x = L/(nx-1)$ [8]. Applying finite differences (Forward Euler method) in equations (1) and (2), for $n = 1, \cdots nt-1$ and $j = 1, \cdots, nx$, we have the following discrete cable model

$$\begin{cases} \dfrac{1}{R_I + R_E} \dfrac{V_{j-1}^n - 2V_j^n + V_{j+1}^n}{\Delta x^2} = C_M \dfrac{V_j^{n+1} - V_j^n}{\Delta t} + G_j \left(V_j^n - E\right); \\ V_j^1 = r_j; \quad j = 1, 2, \cdots, nx, \\ \dfrac{V_1^n - V_0^n}{\Delta x} = p^n, \quad \dfrac{V_{nx+1}^n - V_{nx}^n}{\Delta x} = q^n; \quad n = 1, 2, \cdots, nt. \end{cases} \tag{3}$$

The goal of this work is to estimate G_j, from (3), given the measurement at the boundary of the membrane potential.

For simplicity we denote

$$a = \frac{\Delta t}{(R_I + R_E)\Delta x^2 C_M}, \quad b = -2a + 1 \quad \text{and} \quad g_j = \frac{G_j \Delta t}{C_M}. \tag{4}$$

Then, from (3) and (4) we have

$$\begin{cases} V_j^{n+1} = aV_{j-1}^n + bV_j^n + aV_{j+1}^n - g_j\left(V_j^n - E\right); \\ V_j^1 = r_j; \quad j = 1, 2, \cdots, nx, \\ V_0^n = V_1^n - \Delta x p^n, \quad V_{nx+1}^n = \Delta x q^n + V_{nx}^n; \quad n = 1, 2, \cdots, nt. \end{cases} \tag{5}$$

Here

$$\boldsymbol{g} = (g_1, \cdots, g_{nx}) \in \mathbb{R}^{nx}, \quad \boldsymbol{V} = \begin{bmatrix} V_1^1 & V_{nx}^1 \\ \vdots & \vdots \\ V_1^{nt} & V_{nx}^{nt} \end{bmatrix}_{\mathbb{R}^{nt\times 2}} \quad \text{and} \quad \boldsymbol{W} = \begin{bmatrix} W_1^1 & W_{nx}^1 \\ \vdots & \vdots \\ W_1^{nt} & W_{nx}^{nt} \end{bmatrix}_{\mathbb{R}^{nt\times 2}},$$

the inner product and the norm are defined by the following equations

$$\langle \boldsymbol{V}, \boldsymbol{W} \rangle_{\mathbb{R}^{nt\times 2}} = \sum_{n=1}^{nt} V_1^n W_1^n + \sum_{n=1}^{nt} V_{nx}^n W_{nx}^n \quad \text{and} \quad \|\boldsymbol{V}\|_{\mathbb{R}^{nt\times 2}} = \sqrt{\langle \boldsymbol{V}, \boldsymbol{V} \rangle_{\mathbb{R}^{nt\times 2}}}$$

Let $F : \mathbb{R}^{nt} \to \mathbb{R}^{nt\times 2}$ be a non-linear operator defined by

$$F(\boldsymbol{g}) = \boldsymbol{V}. \tag{6}$$

The inverse problem is to determinate $\boldsymbol{g}$ given $\boldsymbol{V}$. We are specially interested in the situation where the data is not exactly known, i.e., we have only an approximation $\boldsymbol{V}^\delta$ of the exact data, satisfying

$$\|\boldsymbol{V} - \boldsymbol{V}^\delta\|_{\mathbb{R}^{nt\times 2}} \le \delta,$$

of the which we assume to know the noise level $\delta > 0$.

Then, our goal is to estimate $\boldsymbol{g}$, given the noisy data $\boldsymbol{V}^\delta$. In this work, we assume that for the given exact data $\boldsymbol{V}$ there exists a unique solution $\boldsymbol{g}^* \in \mathbb{R}^{nx}$ to (6).

To solve the problem, we use an iterative regularization method (minimal error iteration). Given the initial guess $\boldsymbol{g}^{1,\delta}$, the minimal error iteration for $\boldsymbol{g}$ is defined by the sequence

$$\boldsymbol{g}^{k+1,\delta} = \boldsymbol{g}^{k,\delta} + w^{k,\delta} F'(\boldsymbol{g}^{k,\delta})^* \left(\boldsymbol{V}^\delta - F(\boldsymbol{g}^{k,\delta})\right) \tag{7}$$

where $F'(\boldsymbol{g}^{k,\delta})$ is the directional-derivative of F in $\boldsymbol{g}^{k,\delta}$ and $F'(\boldsymbol{g}^{k,\delta})^*$ is its adjoint, and

$$w^{k,\delta} = \frac{\|\boldsymbol{V}^\delta - F(\boldsymbol{g}^{k,\delta})\|^2_{\mathbb{R}^{nt\times 2}}}{\|F'(\boldsymbol{g}^{k,\delta})^* \left(\boldsymbol{V}^\delta - F(\boldsymbol{g}^{k,\delta})\right)\|^2_{\mathbb{R}^{nx}}}.$$

In the case of noisy data, the iteration procedure has to be combined with a stopping rule in order to act as a regularization method. We will employ the discrepancy principle, i.e., the iteration is stopped after $k_* = k(\delta, \boldsymbol{V}^\delta)$ steps with

$$\|\boldsymbol{V}^\delta - F(\boldsymbol{g}^{k_*,\delta})\|_{\mathbb{R}^{nt\times 2}} \le \tau\delta < \|\boldsymbol{V}^\delta - F(\boldsymbol{g}^{k,\delta})\|_{\mathbb{R}^{nt\times 2}}, \quad 0 \le k < k_*, \tag{8}$$

where $\tau > 1$ is an appropriately chosen positive number ([9], [10]).

It is possible to show that, under certain conditions (we assume that is the case), $\boldsymbol{g}^{k_*,\delta}$ converges to a solution of $F(\boldsymbol{g}) = \boldsymbol{V}^\delta$ as $\delta \to 0$ (see [9], Theorem 3.22).

In the next subsection, we calculate, from (7), the adjoint of the directional derivative.

2.1. Compute of the operator adjoint of the directional derivative

From Theorem 2.1 and algorithm (7), we obtain the following iteration

$$\boldsymbol{g}^{k+1,\delta} = \boldsymbol{g}^{k,\delta} - w^{k,\delta} \frac{1}{a\Delta x} \sum_{n=1}^{nt} \left((\mathcal{V}_1^n - E)\mathcal{U}_1^n, (\mathcal{V}_2^n - E)\mathcal{U}_2^n, \cdots, (\mathcal{V}_{nx}^n - E)\mathcal{U}_{nx}^n\right). \tag{9}$$

where $\mathcal{V}_j^n$ solves (11), given $\boldsymbol{g}^{k,\delta}$. Also, $\mathcal{U}_j^n$ solves (14), given $\boldsymbol{g}^{k,\delta}$ and $\mathcal{V}_j^n$. For iteration (9)

$$w^{k,\delta} = \frac{\|\boldsymbol{V}^\delta - F(\boldsymbol{g}^{k,\delta})\|^2_{\mathbb{R}^{nt\times 2}}}{\left\| \frac{1}{a\Delta x} \sum_{n=1}^{nt} \left((\mathcal{V}_1^n - E)\mathcal{U}_1^n, (\mathcal{V}_2^n - E)\mathcal{U}_2^n, \cdots, (\mathcal{V}_{nx}^n - E)\mathcal{U}_{nx}^n\right) \right\|^2_{\mathbb{R}^{nt\times 2}}}.$$

In this work, to obtain an approximation of $\boldsymbol{g}$ we used the iteration (9).

In the next theorem, we show how we calculate the directional derivative adjoint.

Theorem 2.1. *Consider the nonlinear operator F defined in* (6)*, then*

$$F'(\boldsymbol{g}^{k,\delta})^{*}.\left(\boldsymbol{V}^{\delta}-F(\boldsymbol{g}^{k,\delta})\right)=-\frac{1}{a\Delta x}\sum_{n=1}^{nt}\left((\mathcal{V}_1^n-E)\mathcal{U}_1^n,(\mathcal{V}_2^n-E)\mathcal{U}_2^n,\cdots,(\mathcal{V}_{nx}^n-E)\mathcal{U}_{nx}^n\right).$$

Proof. Evaluating $\boldsymbol{g}^{k,\delta}$ in the operator F, we have $F(\boldsymbol{g}^{k,\delta})=\boldsymbol{V}^{k,\delta}$, where $\left(V_j^n\right)^{k,\delta}=\mathcal{V}_j^n$ solves

$$\begin{cases}\mathcal{V}_j^{n+1}=a\mathcal{V}_{j-1}^n+b\mathcal{V}_j^n+a\mathcal{V}_{j+1}^n-g_j^{k,\delta}\left(\mathcal{V}_j^n-E\right);\\ \mathcal{V}_j^1=r_j;\quad j=1,2,\cdots,nx,\\ \mathcal{V}_0^n=\mathcal{V}_1^n-\Delta xp^n,\quad \mathcal{V}_{nx+1}^n=\Delta xq^n+\mathcal{V}_{nx}^n;\quad n=1,2,\cdots,nt.\end{cases}\tag{10}$$

We denote

$$\boldsymbol{W}=\begin{bmatrix}W_1^1 & W_{nx}^1\\ \vdots & \vdots\\ W_1^{nt} & W_{nx}^{nt}\end{bmatrix}_{\mathbb{R}^{nt\times 2}}.$$

Let the vector $\boldsymbol{\theta}=(\theta_1,\theta_1,\cdots,\theta_{nx})\in\mathbb{R}^{nx}$ and $\lambda\in\mathbb{R}$, then evaluating $\boldsymbol{g}^{k,\delta}+\lambda\boldsymbol{\theta}$ in the operator F, we have $F(\boldsymbol{g}^{k,\delta}+\lambda\boldsymbol{\theta})=\boldsymbol{V}^{k,\delta}+\lambda\boldsymbol{W}^{k,\delta}$, where $\left(V_j^n\right)^{k,\delta}+\lambda\left(W_j^n\right)^{k,\delta}={\mathcal{V}^{\lambda}}_j^n$ solves

$$\begin{cases}{\mathcal{V}^{\lambda}}_j^{n+1}=a{\mathcal{V}^{\lambda}}_{j-1}^n+b{\mathcal{V}^{\lambda}}_j^n+a{\mathcal{V}^{\lambda}}_{j+1}^n-\left(g_j^{k,\delta}+\lambda\theta_j\right)\left({\mathcal{V}^{\lambda}}_j^n-E\right);\\ {\mathcal{V}^{\lambda}}_j^1=r_j;\quad j=1,2,\cdots,nx,\\ {\mathcal{V}^{\lambda}}_0^n={\mathcal{V}^{\lambda}}_1^n-\Delta x\,p^n,\quad {\mathcal{V}^{\lambda}}_{nx+1}^n=\Delta xq^n+{\mathcal{V}^{\lambda}}_{nx}^n;\quad n=1,2,\cdots,nt.\end{cases}\tag{11}$$

The directional derivative of F at $\boldsymbol{g}^{k,\delta}$ in the direction $\boldsymbol{\theta}$ is given by

$$\boldsymbol{W}^{k,\delta}=F'(\boldsymbol{g}^{k,\delta}).(\boldsymbol{\theta})=\lim_{\lambda\to 0}\frac{F(\boldsymbol{g}^{k,\delta}+\lambda\boldsymbol{\theta})-F(\boldsymbol{g}^{k,\delta})}{\lambda}.\tag{12}$$

Considering the difference between (10) and (11), dividing by λ and taking limit $\lambda\to 0$, we have the equation (13), where $\left(W_j^n\right)^{k,\delta}=\mathcal{W}_j^n$.

$$\begin{cases}\mathcal{W}_j^{n+1}=a\mathcal{W}_{j-1}^n+b\mathcal{W}_j^n+a\mathcal{W}_{j+1}^n-g_j^{k,\delta}{\mathcal{W}_j}^n-\theta_j\left(\mathcal{V}_j^n-E\right);\\ \mathcal{W}_j^1=0;\\ {\mathcal{W}_1}^n=\mathcal{W}_0^n,\quad \mathcal{W}_{nx+1}^n=\mathcal{W}_{nx}^n.\end{cases}\tag{13}$$

Note that the variable θ_j, from (13), represents any point in $\mathbb{R}$.

We denote $\left(U_j^n\right)^{k,\delta}=\mathcal{U}_j^n$. We define the following system of equations

$$\begin{cases}\mathcal{U}_j^n=a\mathcal{U}_{j-1}^{n+1}+b\mathcal{U}_j^{n+1}+a\mathcal{U}_{j+1}^{n+1}-g_j^{k,\delta}\mathcal{U}_j^{n+1};\\ \mathcal{U}_j^{nt}=0;\\ \mathcal{U}_0^{n+1}=\mathcal{U}_1^1+\Delta x\left({V_1^{n+1}}^{\delta}-\mathcal{V}_{nx}^{n+1}\right),\quad \mathcal{U}_{nx+1}^{n+1}=\mathcal{U}_{nx}^{n+1}+\Delta x\left({V_{nx}^{n+1}}^{\delta}-\mathcal{V}_{nx}^{n+1}\right).\end{cases}\tag{14}$$

By definition of adjoint operator, we have

$$\left\langle F'(\boldsymbol{g}^{k,\delta})^{*}.\left(\boldsymbol{V}^{\delta}-F(\boldsymbol{g}^{k,\delta})\right),\boldsymbol{\theta}\right\rangle_{\mathbb{R}^{nx}}=\left\langle \boldsymbol{V}^{\delta}-F(\boldsymbol{g}^{k,\delta})\ ,\ F'(\boldsymbol{g}^{k,\delta}).(\boldsymbol{\theta})\right\rangle_{\mathbb{R}^{nx}}.$$

From the previous equation and from (12), we obtain

$$\left\langle F'(\boldsymbol{g}^{k,\delta})^{*}.\left(\boldsymbol{V}^{\delta}-F(\boldsymbol{g}^{k,\delta})\right),\boldsymbol{\theta}\right\rangle_{\mathbb{R}^{nx}}=\left\langle \boldsymbol{V}^{\delta}-\boldsymbol{V}^{k,\delta}\ ,\boldsymbol{W}^{k,\delta}\right\rangle_{\mathbb{R}^{nt\times 2}}.$$

By definition of inner product, we have

$$\left\langle F'(\boldsymbol{g}^{k,\delta})^{*}.\left(\boldsymbol{V}^{\delta}-F(\boldsymbol{g}^{k,\delta})\right),\boldsymbol{\theta}\right\rangle_{\mathbb{R}^{nx}}=\sum_{n=1}^{nt}\left(V_1^{n\delta}-V_1^{nk,\delta}\right)\mathcal{W}_1^n+\sum_{n=1}^{nt}\left(V_{nx}^{n\ \delta}-V_{nx}^{n\ k,\delta}\right)\mathcal{W}_{nx}^n. \quad (15)$$

Multiplying the first equation from (14) by $\mathcal{W}_j^{n+1}$, and summing at points $n=0,1,\cdots,nt-1$ and $j=1,2,\cdots,nx$ we gather

$$\sum_{n=0}^{nt-1}\sum_{j=1}^{nx}\mathcal{U}_j^n\mathcal{W}_j^{n+1}=\sum_{n=0}^{nt-1}\sum_{j=1}^{nx}\left(a\mathcal{U}_{j-1}^{n+1}+b\mathcal{U}_j^{n+1}+a\mathcal{U}_{j+1}^{n+1}-g_j^{k,\delta}\mathcal{U}_j^{n+1}\right)\mathcal{W}_j^{n+1}. \quad (16)$$

$$\sum_{n=0}^{nt-1}\sum_{j=1}^{nx}\mathcal{U}_j^n\mathcal{W}_j^{n+1}=\sum_{n=1}^{nt}\sum_{j=1}^{nx}\mathcal{U}_j^n\mathcal{W}_j^{n+1}. \quad (17)$$

$$\sum_{n=0}^{nt-1}\sum_{j=1}^{nx}\left(a\mathcal{U}_{j-1}^{n+1}+a\mathcal{U}_{j+1}^{n+1}\right)\mathcal{W}_j^{n+1}=\sum_{n=1}^{nt}\sum_{j=1}^{nx}\left(a\mathcal{W}_{j-1}^n+a\mathcal{W}_{j+1}^n\right)\mathcal{U}_j^n+$$
$$a\Delta x\sum_{n=1}^{nt}\left(V_1^{n\delta}-aV_1^{nk,\delta}\right)\mathcal{W}_1^n+a\Delta x\sum_{n=1}^{nt}\left(V_{nx}^{n\ \delta}-aV_{nx}^{n\ k,\delta}\right)\mathcal{W}_{nx}^n. \quad (18)$$

$$\sum_{n=0}^{nt-1}\sum_{j=1}^{nx}\left(b\mathcal{U}_j^{n+1}-g_j^{k,\delta}\mathcal{U}_j^{n+1}\right)W_j^{n+1}=\sum_{n=1}^{nt}\sum_{j=1}^{nx}\left(b\mathcal{W}_j^n-g_j^{k,\delta}\mathcal{W}_j^n\right)\mathcal{U}_j^n. \quad (19)$$

Replacing (17), (18) and (19) in (16), we have

$$\sum_{n=1}^{nt}\sum_{j=1}^{nx}\mathcal{U}_j^n\mathcal{W}_j^{n+1}=\sum_{n=1}^{nt}\sum_{j=1}^{nx}\left(a\mathcal{W}_{j-1}^n+b\mathcal{W}_j^n+a\mathcal{W}_{j+1}^n-g_j^{k,\delta}\mathcal{W}_j^n\right)\mathcal{U}_j^{n+1}+$$
$$a\Delta x\sum_{n=1}^{nt}\left(V_1^{n\delta}-aV_1^{nk,\delta}\right)\mathcal{W}_1^n+a\Delta x\sum_{n=1}^{nt}\left(V_{nx}^{n\ \delta}-V_{nx}^{n\ k,\delta}\right)\mathcal{W}_{nx}^n. \quad (20)$$

Multiplying the first equation from (13) by $\mathcal{U}_j^n$, and summing at points $n=1,2,\cdots,nt$ and $j=1,2,\cdots,nx$ we gather

$$\sum_{n=1}^{nt}\sum_{j=1}^{nx}\mathcal{W}_j^{n+1}\mathcal{U}_j^n=\sum_{n=1}^{nt}\sum_{j=1}^{nx}\left(a\mathcal{W}_{j-1}{}^n+b\mathcal{W}_j{}^n+a\mathcal{W}_{j+1}{}^n-g_j^{k,\delta}\mathcal{W}_j{}^n\right)\mathcal{U}_j^n$$
$$-\sum_{n=1}^{nt}\sum_{j=1}^{nx}\theta_j\left(\mathcal{V}_j{}^n-E\right)\mathcal{U}_j^n. \quad (21)$$

Replacing equation (21) in (20), we obtain

$$\sum_{n=1}^{nt}\left(V_1^{n\delta}-aV_1^{nk,\delta}\right)\mathcal{W}_1^n+\sum_{n=1}^{nt}\left(V_{nx}^{n\,\delta}-V_{nx}^{n\,k,\delta}\right)\mathcal{W}_{nx}^n=-\frac{1}{a\Delta x}\sum_{j=1}^{nx}\sum_{n=1}^{nt}\theta_j(\mathcal{V}_j^n-E)\mathcal{U}_j^n. \qquad (22)$$

Replacing the equation (22) in (15), we have

$$\left\langle F'(\boldsymbol{g}^{k,\delta})^*.\left(\mathcal{V}^\delta-F(\boldsymbol{g}^{k,\delta})\right),\boldsymbol{\theta}\right\rangle_{\mathbb{R}^{nx}}=-\frac{1}{a\Delta x}\sum_{j=1}^{nx}\sum_{n=1}^{nt}\theta_j(\mathcal{V}_j^n-E)\mathcal{U}_j^n.$$

From the previous equation

$$\left\langle F'(\boldsymbol{g}^{k,\delta})^*.\left(\mathcal{V}^\delta-F(\boldsymbol{g}^{k,\delta})\right),\boldsymbol{\theta}\right\rangle_{\mathbb{R}^{nx}}=$$
$$\left\langle-\frac{1}{a\Delta x}\sum_{n=1}^{nt}\left((\mathcal{V}_1^n-E)\mathcal{U}_1^n,(\mathcal{V}_2^n-E)\mathcal{U}_2^n,\cdots,(\mathcal{V}_{nx}^n-E)\mathcal{U}_{nx}^n\right),\boldsymbol{\theta}\right\rangle_{\mathbb{R}^{nx}}.$$

Since $\boldsymbol{\theta}\in\mathbb{R}^{nx}$ is arbitrary, we gather that the following equation holds:

$$F'(\boldsymbol{g}^{k,\delta})^*.\left(\mathcal{V}^\delta-F(\boldsymbol{g}^{k,\delta})\right)=-\frac{1}{a\Delta x}\sum_{n=1}^{nt}\left((\mathcal{V}_1^n-E)\mathcal{U}_1^n,(\mathcal{V}_2^n-E)\mathcal{U}_2^n,\cdots,(\mathcal{V}_{nx}^n-E)\mathcal{U}_{nx}^n\right).$$

□

3. Numerical Results

In this section, we show numerical results for the inverse problem, in the discrete cable model, using the minimal error iteration (9).

Consider equation (3), the parameters for discrete model are: $\Delta t = 5.0025\times10^{-4}$ $[ms]$, $\Delta x = 0.0345$ $[cm]$, $R_I+R_E=1$ $[\Omega]$, $C_M=1$ $[F/cm^2]$, $E=0$ $[mV]$, $r_j=0$ $[mV]$ for $j=1,2,\cdots 30$, $p^n=-\exp(-(n-1)\Delta t)$ $[mV/cm]$ and $q^n=\exp(-(n-1)\Delta t)$ $[mV/cm]$ for $n=1,2,\cdots,2000$. The goal of this section is to estimate the discontinuous conductance

$$\begin{aligned} G_j &= 1 \quad j\in\{1,2,\cdots,10\}\cup\{21,22,\cdots,30\},\\ G_j &= 2 \quad j\in\{11,12,\cdots,20\}. \end{aligned}$$

To compare the results, first we calculate $\boldsymbol{V}$ from (3) given $\boldsymbol{G}=(G_1,G_2,\cdots,G_{nx})$. We obtain $\boldsymbol{V}^\delta$, for $\delta=3.8\times10^{-6}$, from the following equation

$$\boldsymbol{V}^\delta=\boldsymbol{V}+\frac{rand_\delta}{\|\boldsymbol{V}\|_{\mathbb{R}^{nt\times2}}}\boldsymbol{V},$$

where

$$rand_\delta=\begin{bmatrix}(rand_\delta)_1^1 & (rand_\delta)_{nx}^1\\ \vdots & \vdots\\ (rand_\delta)_1^{nt} & (rand_\delta)_{nx}^{nt}\end{bmatrix}_{\mathbb{R}^{nt\times2}}.$$

For $j=1,nx$ and $n=1,2,\cdots,nt$, the uniformly distributed random variable $(rand_\delta)_j^n$ taking values in the range $[-\delta,\delta]$. Now, we consider $\boldsymbol{V}$ and $\boldsymbol{G}$ unknown.

To estimate $\boldsymbol{G}$ we use (9), given $\boldsymbol{G}^{1,\delta}=(0,0,\cdots,0)$ and $\boldsymbol{V}^\delta$. We consider $\tau=2.01$, for the stopping criterion (8).

In figure 1 shows the conductance estimation. The red line is the exact solution, and the blue line is the approximation obtained at the iteration $k^*=119374$. The green line is the initial guess of our iterative procedure.

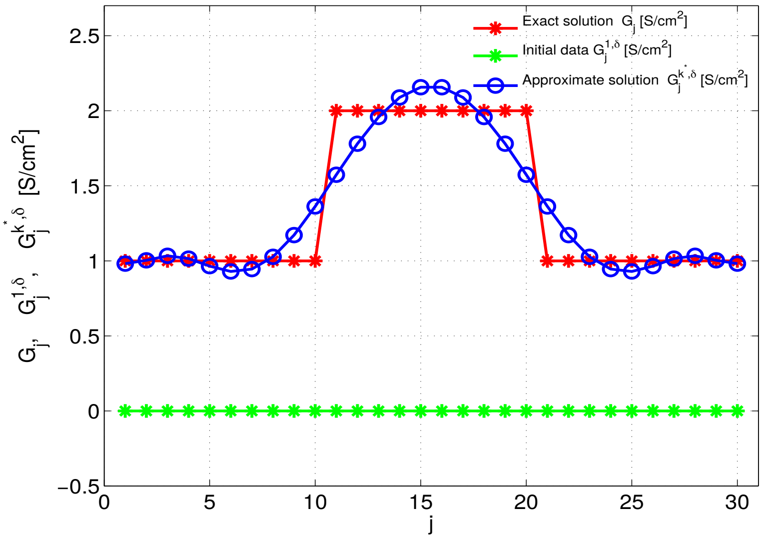

Figure 1. Estimation of the conductance $\boldsymbol{G}$.

4. Conclusion

We have presented the minimal error method to estimate the conductance $\boldsymbol{G}$ in the discrete cable model. An important contribution of the work is to calculate the adjoint operator of the method. We computed this operator to optimize computational cost. The simulation results demonstrate the effectiveness of our estimation method when the noise level is minimal.

In [5], approximate $\boldsymbol{G}$ when all points of the initial condition are nonzero, i.e. when $V_j^1 \neq 0$ for all $j = 1, 2, \cdots, nx$. In this work we obtain approximately $\boldsymbol{G}$ for any initial condition.

4.1. Acknowledgments

The author would like to thank the support through CAPES.

References

[1] Jaeger D and Jung R 2015 *Encyclopedia of computational neuroscience* (Springer Publishing Company, Incorporated)
[2] RALL W 1977 *The Neurons System* **1** 39–97
[3] Rall W, Koch C and Segev I 1989 *Koch C., Segev I*
[4] Tadi M, Klibanov M V and Cai W 2002 *Computers & Mathematics with Applications* **43** 927–941
[5] Bell J and Craciun G 2005 *Mathematical biosciences* **194** 1–19
[6] Cox S J 2006 *Mathematical medicine and biology: a journal of the IMA* **23** 139–152
[7] Avdonin S and Bell J 2013 *Journal of mathematical biology* **67** 123–141
[8] Langtangen H P and Linge S 2017 *Finite difference computing with PDEs: a modern software approach* vol 16 (Springer)
[9] Kaltenbacher B, Neubauer A and Scherzer O 2008 *Iterative regularization methods for nonlinear ill-posed problems* vol 6 (Walter de Gruyter)
[10] Vainikko G M 1980 *Avtomatika i Telemekhanika* 84–92